CANADIAN THESES ON MICROFICHE

THÈSES CANADIENNES SUR MICROFICHE

National Library of Canada
Collections Development Branch

Canadian Theses on
Microfiche Service

Ottawa, Canada
K1A 0N4

Bibliothèque nationale du Canada
Direction du développement des collections

Service des thèses canadiennes
sur microfiche

NOTICE

The quality of this microfiche is heavily dependent upon the quality of the original thesis submitted for microfilming. Every effort has been made to ensure the highest quality of reproduction possible.

If pages are missing, contact the university which granted the degree.

Some pages may have indistinct print especially if the original pages were typed with a poor typewriter ribbon or if the university sent us an inferior photocopy.

Previously copyrighted materials (journal articles, published tests, etc.) are not filmed.

Reproduction in full or in part of this film is governed by the Canadian Copyright Act, R.S.C. 1970, c. C-30. Please read the authorization forms which accompany this thesis.

AVIS

La qualité de cette microfiche dépend grandement de la qualité de la thèse soumise au microfilmage. Nous avons tout fait pour assurer une qualité supérieure de reproduction.

S'il manque des pages, veuillez communiquer avec l'université qui a conféré le grade.

La qualité d'impression de certaines pages peut laisser à désirer, surtout si les pages originales ont été dactylographiées à l'aide d'un ruban usé ou si l'université nous a fait parvenir une photocopie de qualité inférieure.

Les documents qui font déjà l'objet d'un droit d'auteur (articles de revue, examens publiés, etc.) ne sont pas microfilmés.

La reproduction, même partielle, de ce microfilm est soumise à la Loi canadienne sur le droit d'auteur, SRC 1970, c. C-30. Veuillez prendre connaissance des formules d'autorisation qui accompagnent cette thèse.

THIS DISSERTATION
HAS BEEN MICROFILMED
EXACTLY AS RECEIVED

LA THÈSE A ÉTÉ
MICROFILMÉE TELLE QUE
NOUS L'AVONS REÇUE

Canada

NL 339 (r. 85/09)

STARTUP AND STEADY STATE KINETICS OF ANAEROBIC DOWNFLOW STATIONARY FIXED FILM REACTORS

by

Kevin Joseph Kennedy

Submitted in partial fulfillment
of the requirements for the degree of
Doctor of Philosophy

Department of Civil Engineering
School of Graduate Studies
University of Ottawa
Ottawa, Canada
April, 1985

UNIVERSITÉ D'OTTAWA
UNIVERSITY OF OTTAWA

ACKNOWLEDGEMENTS

The author wishes to express his sincere appreciation and thanks to Dr. Ronald Droste for his guidance, support and stimulating discussions during the investigation and writing of this thesis. He would also like to thank Mr. Bert van den Berg for his guidance and continuous encouragement offered throughout the course of this work.

A special feeling of appreciation is extended to Milan Muzar, Ken Weymss and Karen Lamb for technical assistance and help with the manuscript.

The author would also like to thank the National Research Council of Canada for permitting him to undertake this project.

Finally, the author wishes to thank his wife, Linda, who offered encouragement, advice, and support through his entire graduate education and which without her help, would have been impossible.

ABSTRACT

A mathematical model describing the change in effectiveness factor or effective diffusivity for the intermediate substrate in sequential substrate removal reactions in fixed biofilms is presented. Typical results from the solution of the model show that production of intermediate substrate in the biofilm increases the conversion of primary substrate to ultimate product in all cases although the increase is not always significant.

Soluble influent chemical oxygen demand (COD) concentrations between 5,000 and 20,000 mg L^{-1} influence the rate of biofilm development during startup. Total biomass yields are higher and rates of biofilm accumulation faster for treatment of lower strength wastes, even though ultimate loadings are not necessarily achieved as rapidly as in reactors fed higher strength wastes. Organic loading of fixed film reactors can be increased while volatile acid (VA) concentrations are maintained between 200-1500 mg L^{-1} as long as reactor pH is maintained between 6.8-7.6. Fixed film reactors should be started with dilute wastewater.

A dynamic model based on mass balances and kinetic constants of acid forming and methane forming bacteria in the mixed liquor and biofilm is presented to describe startup. The model indicates that biomass attachment and detachment rates of 0.1-0.2 best described biomass accumulation and reactor substrate concentration during startup. The model

also predicts that under stable operating conditions, 15-20% of the total or biofilm biomass in downflow stationary fixed film (DSFF) reactors is composed of methanogenic bacteria.

Steady state reactor operation indicates that DSFF reactors successfully treat wastewater of different concentrations at high organic loading rates and short hydraulic retention times (HRT). Biofilm biomass concentration increase with increased organic loading rate and decreased HRT reaching a maximum of 8.7 kg volatile film solids (VFS) m^{-3} at a loading rate of 10 kg COD m^{-3} d^{-1}.

Reactor solid retention time (SRT) is described as a function of HRT or organic volumetric loading rate (LRT). Based on this, an empirical steady state model and concomitant kinetic coefficients are presented to predict COD removal efficiency and reactor biomass concentration. The empirical model gives a good fit to the data.

Maximum biofilm substrate utilization rates are not effected by biofilm thickness. For biofilm thicknesses up to 2.6 mm the maximum biofilm substrate utilization rate is between 1.0-1.2 kg COD kg VFS^{-1} d^{-1}. This indicates that the biofilm is completely active and substrate penetrates the complete biofilm depth with minimal diffusional resistance.

TABLE OF CONTENTS

LIST OF TABLES

LIST OF FIGURES

NOMENCLATURE

a = surface area to volume ratio, $[L^{-1}]$

A^* = rate of biomass attachment, $[T^{-1}]$

A = surface area, $[L]$

b = microbial decay rate $[T^{-1}]$

B_v = maximum volumetric loading rate, $[ML^{-3}T^{-1}]$

B_{vna} = volumetric loading rate of nonbiodegradable organics, $[ML^{-3}T^{-1}]$

B_{vs} = volumetric loading rate of biodegradable organics, $[ML^{-3}T-1]$

D = diffusivity, $[L^2T^{-1}]$

D^* = rate of biomass detachment, $[T^{-1}]$

E = COD conversion efficiency, [%]

E' = biofilm efficiency factor, [0]

f = washout factor, [0]

F = mass of substrate, [M]

k = maximum specific reaction velocity, $[T^{-1}]$

K = half velocity constant, $[ML^{-3}]$

K_i = inhibition constant, $[ML^{-3}]$

L_f = film thickness, [L]

N = mass flux, $[ML^{-2}T^{-1}]$

N_z' = actual mass flux without production of intermediate substrate, $[ML^{-2}T^{-1}]$

N_{zmax} = maximum flux at liquid-film boundary without intermediate substrate production in the film, $[ML^{-2}T^{-1}]$

N_t = total mass flux at the liquid-film interface for a single substrate, $[ML^{-2}T^{-1}]$

p = rate of production of intermediate substrate, $[ML^{-3}T^{-1}]$

P = total amount of intermediate substrate converted to product per unit surface area of film per unit surface area of film per unit time, $[ML^{-2}T^{-1}]$

Q = flow rate, $[L^{-3}T^{-1}]$

R^* = recirculation ratio of reactor, [0]

R = ratio of modified effectiveness factor with intermediate production to effectiveness factor without intermediate production, [0]

r^* = first order reaction rate, $[ML^{-3}T^{-1}]$

r_m = maximum reaction rate per unit area, $[ML^{-2}T^{-1}]$

r_m^* = maximum first order reaction rate per unit area, $[ML^{-2}T^{-1}]$

r_s = rate of substrate uptake, $[ML^{-3}T^{-1}]$

r_g = rate of microbial growth, $[ML^{-3}T^{-1}]$

S = substrate concentration, $[ML^{-3}]$

S_o = influent substrate concentration, $[ML^{-3}]$

S_b = substrate concentration at liquid-film interface, $[ML^{-3}]$

t = time, [T]

T_c = temperature, [°C]

T_k = temperature, [°K]

V = volume, $[L^3]$

x = distance, [L]

X = active microorganism concentration, $[ML^{-3}]$

X' = active microorganism concentration, $[ML^{-2}]$

y = distance, [L]

Y = acetate yield factor, [0]

Y' = net acetate yield factor, [0]

Y_m = biomass yield factor, [0]

Z^* = total mass of attached cells, [M]

z = dimensionless distance, [O]

β = yield modulus, [O]

ϵ = dimensionless substrate concentration, [O]

ϵ_2' = dimensionless concentration of intermediate substrate that occurs in the absence of production of intermediate substrate, [O]

η = effectiveness factor, [O]

η_2' = effectiveness factor for second group of microorganisms

η^* = effectiveness factor for first order reaction, [O]

K = half velocity modulus, [O]

u = specific growth rate, $[T^{-1}]$

μ^* = dynamic viscosity, $[ML^{-1}T^{-1}]$

u_m = maximum specific growth rate, $[T^{-1}]$

u_n = net specific growth rate, $[T^{-1}]$

U = specific reaction velocity, $[T^{-1}]$

ϕ = Thiele modulus, [O]

ϕ_g = general Thiele modulus, [O]

θ_c = solids retention time, [T]

θ_H = hydraulic retention time, [T]

CM = complete mixed

COD = chemical oxygen demand

CSTR = continuous stir tank reactor

DSFF = downflow stationary fixed film

HRT = hydraulic retention time

LRT = volumetric organic loading rate

NPP = needle punched polyester

SRT = solids retention time

TFS = total film solids

TSS = total suspended solids

TSFS = total suspended and film solids

VA = volatile acids

VFS = volatile film solids

VSS = volatile suspended solids

VSFS = volatile suspended and film solids

Subscripts

1 - refers to primary substrate and microorganisms associated with it

2 - refers to intermediate substrate and microorganisms associated with it

f - refers to biofilm

L - refers to mixed liquor

r - refers to recycle stream

1. INTRODUCTION

1.1 General Background

Anaerobic biological treatment processes have been used for many years to stabilize sludge solids produced by other wastewater treatment systems. This supporting rather than primary role for anaerobic digestion has stemmed from limitations associated with the process. Firstly, methanogenic bacteria have a low growth rate which requires a long solids retention time (SRT) and a long hydraulic retention time (HRT). To fulfill these conditions a large reactor volume must be used. Secondly, the process is generally considered to be unstable and susceptible to failure. The sensitivity of anaerobic digesters is due to complex interactions between acidogenic and methanogenic bacteria. Thirdly, treated effluent is high in soluble and insoluble organic material and usually requires further treatment before meeting discharge requirements.

However, anaerobic digestion has certain advantages over aerobic processes. Firstly, less energy is required than for aerobic systems because oxygen need not be supplied and secondly, methane gas is evolved. The low solubility of methane allows the gas to be used to offset system energy requirements. These advantages have led researchers to investigate ways of minimizing the limitations of anaerobic digestion. This has led to several novel reactor configura-

tions which have made anaerobic digestion a much more useful and economical wastewater treatment process.

These second generation anaerobic reactors have in common the ability to retain active microbial biomass in the reactor beyond the HRT, instead of allowing it to leave with treated effluent as in a continuous stirred tank reactor (CSTR). This enables SRT to be independent of HRT with concomitant decrease of reactor volume. Included in these novel types of anaerobic reactors are the upflow anaerobic sludge bed reactor (UASB) (Lettinga *et al.*, 1979, 1980), upflow anaerobic filter (Young, 1967; Young and McCarty, 1969), combination upflow sludge-blanket-filter (UBF), (Guiot and van den Berg, 1984), anaerobic fluidized/expanded bed reactor (Switzenbaum, 1978; Switzenbaum and Jewell, 1980), baffled reactor (Bachman *et al.*, 1983) and anaerobic downflow stationary fixed film reactor (DSFF) (van den Berg and Lentz, 1979,1980; Kennedy and van den Berg, 1981, 1982a, b). All of these anaerobic processes have been shown to successfully treat low, medium or high strength wastewaters at high organic loading rates (LRT) and short HRT. Also, these reactors have been shown to be stable, easy to operate and insensitive to adverse transient phenomena. Reactor stability is attributed to the long SRT (Young, 1980; Speece, 1981).

Anaerobic DSFF reactors are a recent addition to the family of second generation anaerobic reactors and have been

mostly used for treatment of agricultural and industrial wastewaters. Studies with DSFF reactors have emphasized waste treatability once the reactor has sufficient biomass to sustain high rate steady state operation. No results are available that relate process efficiency to parameters such as biomass concentration, microbial activity or SRT. Physical models that have been developed are descriptive both in concept and design. Despite full-scale applications of the process since its inception, the need for a rational design procedure still exists.

Little attention has been paid to parameters that affect startup of DSFF reactors. Startup of an anaerobic reactor is a critical step and the time during which the process is most prone to failure. The main objective in startup of fixed film processes is to develop, in as short a time as possible, a highly active microbial film from the seed sludge. Factors affecting accumulation of active biomass during startup have not been reported. Since properties of microbial films can be determined during their early development (Heukelekian,1956; Hartman, 1967; Bryers and Characklis, 1981, 1982; Characklis, 1973, 1981) final reactor performance may be dictated by the startup procedure. It is also not known if kinetic constants that apply to DSFF reactor biomass during startup are applicable to steady state reactor operation.

The purpose of this study was to examine effects of waste concentration on startup and steady state performance of DSFF reactors. Empirical and inductive deterministic mathematical models based on the continuous culture theory of Monod (1949) have been successfully applied to CSTR processes but not to DSFF reactors. This theory will be applied to develop models suitable for the DSFF reactor during startup and steady state operation.

Diffusion into the biofilm is a factor of primary importance in the operation of a DSFF reactor. Some studies (Williamson and McCarty, 1976a, b; Henze and Harremoes, 1982) have indicated that diffusion in anaerobic processes should not be a limiting factor. However, this has not been confirmed under typical operating conditions of DSFF reactors. Furthermore, the overall biofilm effectiveness factor is affected by sequential substrate removal which occurs in anaerobic processes due to the presence of acetogenic and methanogenic bacteria. Previous theoretical developments have not considered this phenomenon which is examined here.

Batch and continuous tests on the biofilm are the most effective means of cross-checking substrate utilization kinetic constants. These tests are to be performed along with analyses of biofilm biomass parameters, including biofilm thickness to determine if diffusion problems arise as the reactor matures. Also, kinetics of substrate utilization and biofilm growth may change as the biofilm matures from a

rapid growth startup phase to steady state operation at estimate loading rates. Steady state kinetics are to be compared to startup kinetics.

1.2 Objectives

The broad objectives of this study were to investigate startup and steady state operation of anaerobic DSFF reactors operating at 35°C and develop models to predict reactor performance. The specific objectives were to:

1. Determine the effect of substrate concentration on reactor startup and biofilm accumulation.
2. Evaluate the effect of substrate concentration on steady state reactor performance and biofilm growth.
3. Determine biofilm and liquid phase microbial activity and show the importance of the biofilm in the process.
4. Determine kinetic constants during startup and steady state reactor operation.
5. Characterize the mixing regime in the reactor.
6. Determine the capacity of the process in terms of organic mass and volumetric loading rates.
7. Present a theoretical development of the modified effectiveness factor for sequential substrate utilization in biofilms.
8. Develop models to describe steady state and dynamic DSFF reactor performance.

2. LITERATURE SURVEY

2.1 General Scheme of Anaerobic Digestion

Microbial decomposition of organic compounds involves two main metabolic processes. Dissimilation or biochemical oxidation of organic compounds yields energy which results in growth and production of new cell material. Biochemical oxidation involves the reaction between two compounds in which protons and electrons are transferred from a reduced compound (hydrogen electron donor) to a less reduced compound (hydrogen electron acceptor). Electron acceptors can be either inorganic or organic compounds. In fermentation processes, organic compounds act as electron acceptors (Fig. 2.1; Zoetemeyer, 1982). In respiration processes, the inorganic compound may be oxygen (aerobic respiration), nitrate (nitrate reduction), sulphate (sulphate reduction) or carbon dioxide (methane formation).

The transfer of electrons results in the release of chemically bound energy which is stored in microbial cells in the form of adenosine triphosphate (ATP). The energy released during aerobic decomposition of organic material is many times more than the energy released during anaerobic decomposition of the same material (Fig. 2.2). Taking glucose as a substrate, for example, approximately 75% of the energy in the glucose molecule is not used for growth of microbial cells but rather released in the form of methane.

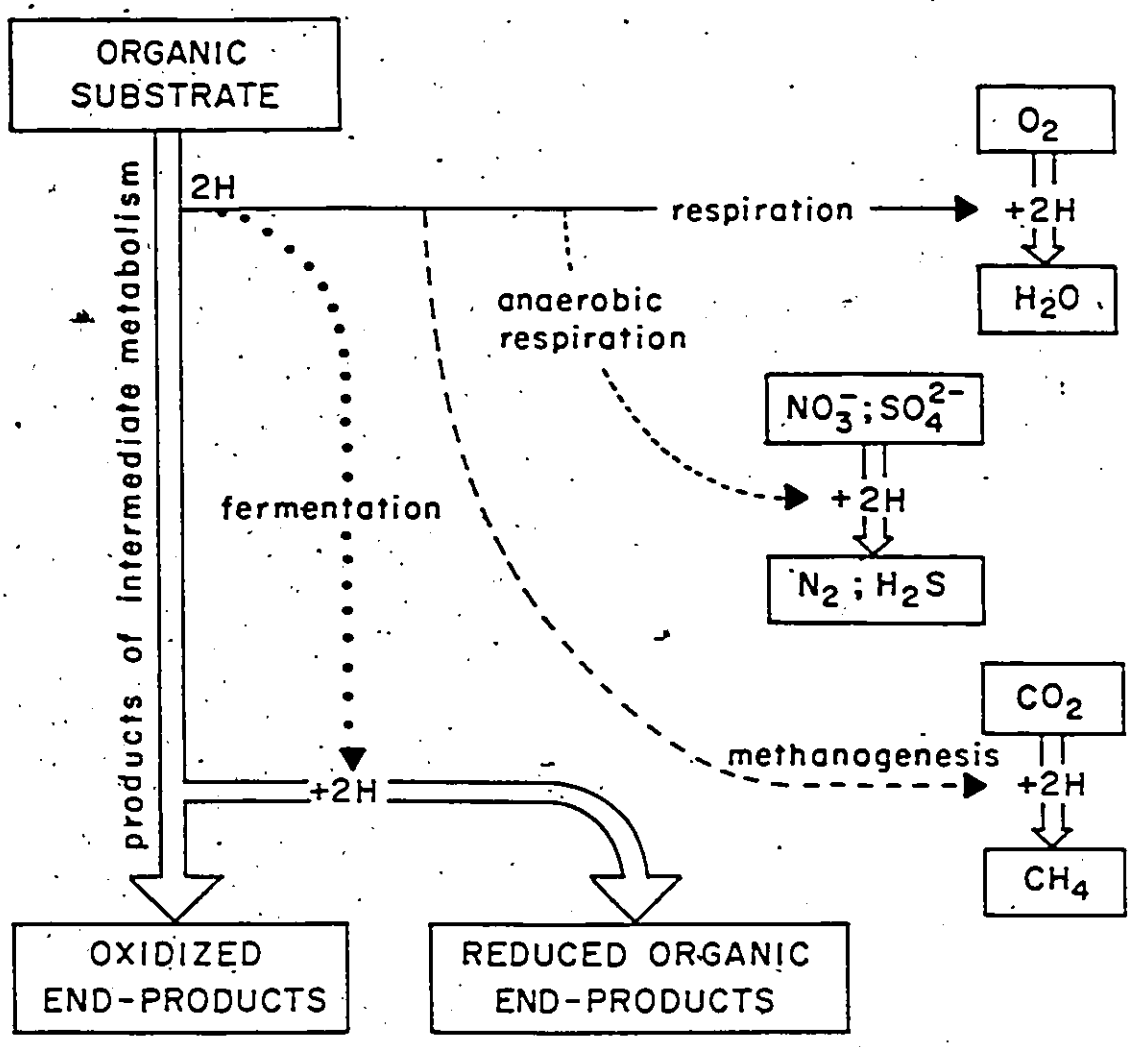

Figure 2.1 Hydrogen electron acceptors in biological systems (Zoetemeyer, 1982)

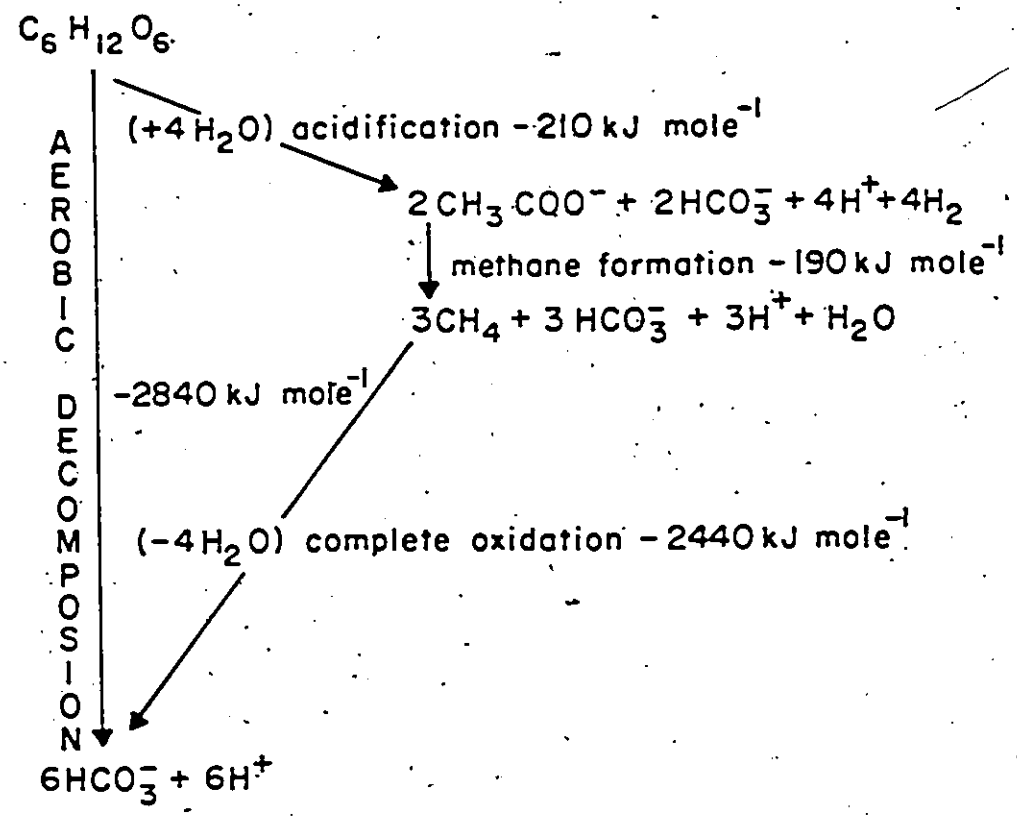

Figure 2.2 Calculation of the free formation enthalpy at pH 7 for aerobic and anaerobic decomposition of glucose to HCO_3^- and H^+ (Zoetemeyer, 1982)

From Fig. 2.2, it is apparent that anaerobic as opposed to aerobic decomposition of organic materials, results in slower microbial growth rates and production of less microbial cells per unit of substrate utilized.

The anaerobic digestion process involves a complex consortium of microorganisms which is able to metabolize complex organic material such as carbohydrates, lipids and proteins to methane, carbon dioxide and cellular material. Toerien *et al.* (1970) suggested that the biochemical processes as well as microbial species involved could be divided into three categories: 1) hydrolysis, which is the extracellular enzymatic hydrolysis of large complex soluble substrates and insoluble substrates into smaller molecules which can be transported into the cell and metabolized; 2) acetogenesis, which is the fermentation of hydrolysis end products into organic acids, hydrogen and carbon dioxide which are suitable for methanogenesis; and, 3) methanogenesis, conversion of short chain organic acids, carbon dioxide and hydrogen into methane and carbon dioxide by a group of substrate specific obligate anaerobes. A schematic representation of these reaction steps is outlined in Fig. 2.3 (Zehnder *et al.*, 1982).

2.2 Hydrolysis and Acid Formation

The first step of anaerobic waste treatment is hydrol-

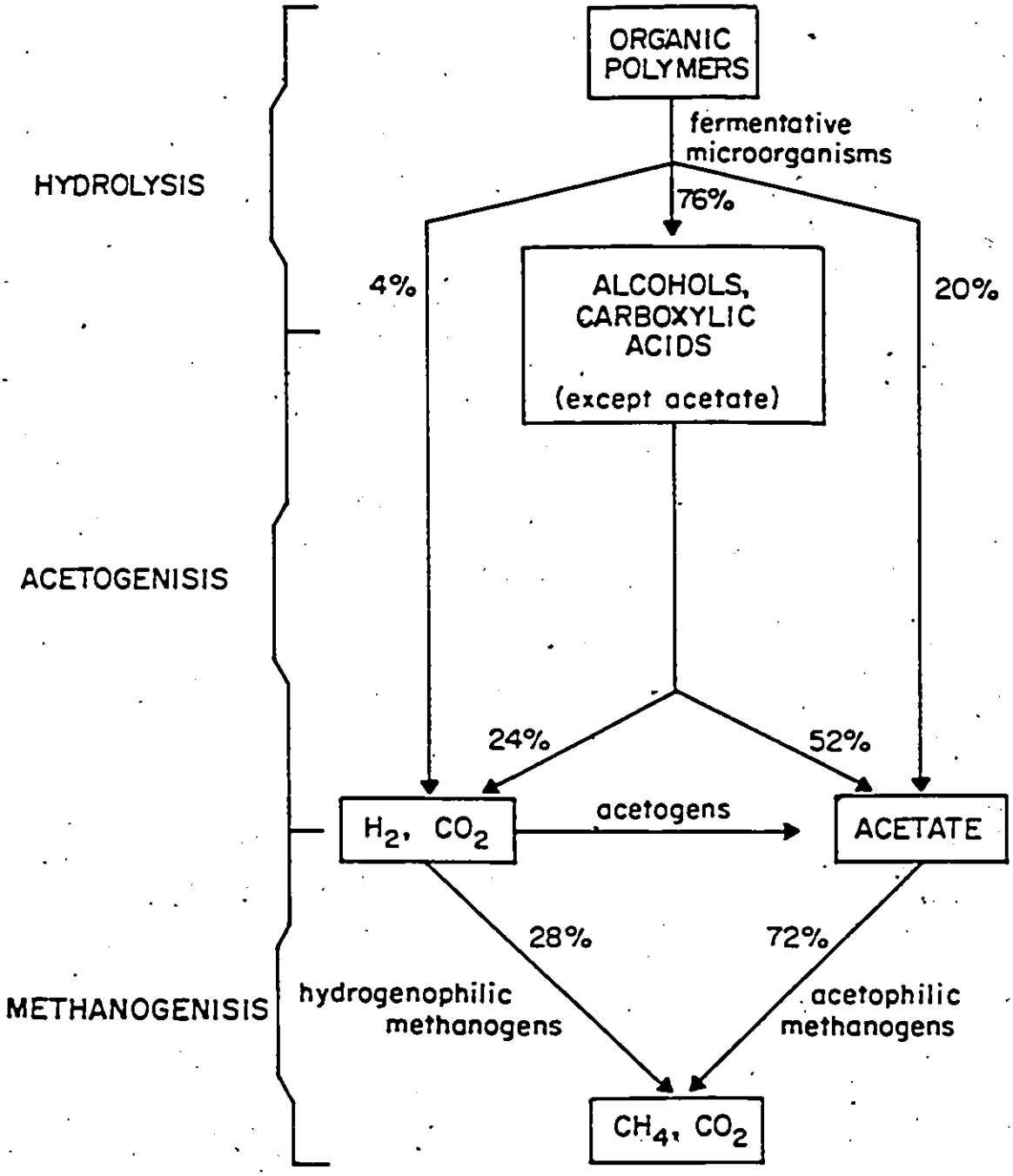

Figure 2.3 Anaerobic decomposition of organic matter. Percentages represent the flow of electrons (energy) resulting from the reduction of organic/inorganic compound.

ysis of complex soluble and insoluble organic wastes to simpler soluble organics. Reviews by Kirsch and Sykes (1971), Hobson *et al.* (1974), Mah *et al.* (1977), Zeikus (1975, 1977), Kirsop (1982), Wolfe (1979a, b, 1980) and Zinder (1984) indicate that while considerable work is being done to determine the microorganisms responsible for non-methanogenic degradation in anaerobic digesters, the amount of information is still limited.

Hydrolysis or liquefaction is brought about by excretion of extracellular microbial enzymes into the mixed liquor or by direct contact of microorganisms with a complex substrate. For wastes composed primarily of suspended solids, hydrolysis has been found to be the rate limiting step of anaerobic digestion (van Velsen, 1977; Kennedy and van den Berg, 1982a). For soluble carbohydrate wastewaters, hydrolysis and acetogenesis are very fast and methanogenesis is rate limiting (Young, 1967).

The ultimate source of energy for anaerobic microorganisms is not the hydrolysis reaction, but oxidation-reduction reactions performed on hydrolysis products. The use of hydrolysis products for production of methanogenic substrates has been reviewed by Iannotti (1973), Ferry and Wolfe (1976) and Bryant *et al.* (1968, 1979). In all cases, microbial degradation of hydrolysis products was accompanied by hydrogen production. Continued degradation of the original substrate was dependent on a secondary hydrogen-

utilizing bacteria which maintained a low hydrogen concentration in the digester. *Methanobacillus omelianskii*, which was initially thought to be a pure culture, was actually a symbiotic association of two organisms linked by interspecies hydrogen transfer (Bryant *et al.*, 1967). Dawson (1980) reported that oxalate degradation by a continuous enrichment culture was inhibited by the presence of hydrogen. The methanogenic bacteria in the enrichment culture, on the other hand, could not degrade oxalate, but were stimulated by hydrogen, indicating that oxalate degradation was dependent upon a synergistic association between hydrogen-producing and hydrogen-utilizing bacteria.

These studies have indicated the important role hydrogen plays in determining the end products of acid forming anaerobes. Cohen *et al.* (1980) stated that formation of hydrogen (Eq. 2.1) serves as an important route by which non-methanogens dispose of electrons from reduced nicotinamide adenine dinucleotide (NAD).

$$NADH + H^{+} \Longrightarrow NAD^{+} + H_2 \qquad 2.1$$

$$G_o' = +4.3 \text{ Kcal mole}^{-1}$$

Unless the partial pressure of hydrogen is very low equilibrium is in the direction of NADH, which is the case when there are no hydrogen utilizing bacteria in a culture.

Wolin (1974a) demonstrated that with decreasing hydrogen partial pressures, the free energy change of the reaction would favor oxidation of NADH. If hydrogen was not

formed from the flow of electrons, normal microbial pathways with reduced end-products would result. Wolin (1974b) reported that fermentation of glucose by *R. albus* produced ethanol as the end-product when the hydrogen partial pressure was high and acetate, a relatively more oxidized compound when hydrogen partial pressure was maintained at a low level by a hydrogen utilizing methanogen.

Non-methanogenic bacteria have also been reported to utilize hydrogen. Ohwaki and Hungate (1977) and Schoberth (1977) isolated species of *Clostridium aceticum* and *Acetobacterium woodii* respectively which were able to convert hydrogen and carbon dioxide to acetic acid. The importance of this type of bacteria to anaerobic digestion has not yet been established.

2.3 Methane Formation

It is through microbial methanogenesis that complex organic molecules, which have been previously hydrolyzed are further degraded to volatile organic acids (VA), carbon dioxide and hydrogen and are finally removed in the form of methane gas. However, relatively few reports enumerate the species of microorganisms responsible for methane formation. The reason for this is that all methanogens isolated to date, are obligate anaerobes, extremely sensitive to oxygen (Mah *et al.*, 1977, 1978; Wolfe, 1971 ,1979a, b, 1980; Smith *et al.*, 1980; Bochem *et al.*, 1982; Zinder, 1984). In addi-

tion, all are chemoautotrophic which results in low cell yields and low specific growth rates. Characteristics of various methanogenic microorganisms are summarized in Table 2.1.

Zeikus (1977) conducted a morphological analysis of methanogenic bacteria and concluded that methanogens were structurally diverse and displayed no unique features by which all species could be characterized. However, they do have some unique biochemical characteristics. First, few organic acids or other compounds are fermented whereas normal energy sources such as carbohydrates and amino acids are not metabolized. Second, peptidoglycan, a common bacterial cell wall component is not present in their cell walls (Bryant, 1979; Kandler and Hippe, 1977; Kandler and Konig, 1978). Third, nucleotide sequencing of the 16S ribosomal RNA indicates that they lack the common base sequence "TGC" (thymine - guanine - cytosine) found in all other forms of life (Balch *et al.*, 1977; Wilkinson, 1978). Fourth, methanogens contain 3 coenzymes unique to them: coenzyme 420, which takes the place of ferrodoxin in electron transfer; (Cheeseman *et al.*, 1971; Tzeng *et al.*, 1975a, b) coenzyme M, which is involved in methyl transfer (Balch and Wolfe, 1979 a, b; Shapiro and Wolfe, 1980); and Factor B which is responsible for enzymatic formation of methane from methyl-coenzyme M (McBride and Wolfe, 1971;

Table 2.1 Methanogenic Bacteria in Pure Culture

Genus	Species	Substrate					Temp.	Doubling time days	K mg acetate L^{-1}	Morphology	Reference
		H_2+CO_2	HCOOH	CH_3OH	CH_3NH_2	CH_3COOH					
Methanobacterium	formicicum	+	+				M			long rods	
	bryantii	+					M			long rods	
	thermoautotrophicum	+					T			long rods	
Methanobrevibacter	ruminantium	+	+				M			short rods	
	arboriphilus	+					M			short rods	
	smithii	+	+				M			short rods	
Methanothermus	fervidus	+					extreme T			long rods	Stetter et al (1982)
Methanoplanus	limicola	+	+				M			flat angular plates	Weidgrubber et al. (1982)
Methanococcus	vanniellii	+	+				M			coccus	
	voltae	+	+				M			coccus	
	thermolithotrophicus	+	+				T			coccus	Huser et al. (1982)
Methanomicrobium	mobile	+	+				M			short curved rod	
Methanogenium	cariaci	+	+				M			coccus	
	marisnigri	+	+				M			coccus	
Methanolobus	tendarius			+	+		M				Konig and Stetter (1982)
Methanospirillum	hungatei	+	+				M			long curved rod	
Methanosarcina	barkeri	+		+	+	+	M	3-6	150-250	coccus in pockets	Bochem (1982)
Methanothrix	soehngenii					+	M	3-6	15-40	long rods forming filaments	Huser et al. (1982)
	concilii					+	M	1-3	70-100	long rods forming filaments	Patel (1985)
	?					+	T	1-3	15-20		Zinder (1982)
Methanoplasma	elizabethii	+	+				M			mycoplasma	Rose and Birt (1981)

a. M = mesophilic, T = thermophilic

From Bochem et al. (1982) unless specified.

Zeikus, 1977). The exact enzymatic mechanisms involved are not known nor is the mechanism of ATP synthesis. However, work has been done to investigate methanogenic reactions that provide energy for the microorganisms.

Methanogens isolated to date except those of the genus *Methanothrix* (Huser *et al.*, 1982; Patel, 1985) utilize hydrogen for energy while reducing carbon dioxide to methane (Wolfe, 1971; Bryant, 1979; Smith and Mah, 1980; Schoberth, 1982). This fact was thought to be insignificant since hydrogen is seldom detected in anaerobic digesters. Considerable amounts of hydrogen are produced during digestion, and methanogens have been shown to rapidly utilize it to reduce carbon dioxide to methane, thus maintaining a very low hydrogen partial pressure in the reactor (van den Berg and Kennedy, 1982a). Pretorius (1972) reported a similar reaction for the utilization of formate by methanogens, however, this reaction may have occurred after the enzymatic breakdown of formate to carbon dioxide and hydrogen. The stoichiometry of the reactions (Eqs. 2.2 and 2.3) and resulting negative free energy changes push equilibrium to the right.

$$4H_2 + HCO_3^- + H^+ \Rightarrow CH_4 + 3H_2O \qquad 2.2$$

$$G_o' = -33.4 \text{ Kcal mole}^{-1}$$

$$HCOO^- + H_2O + H^+ \Longrightarrow CH_4 + 3HCO_3^- \qquad 2.3$$

$$G_o' = -31.2 \text{ Kcal mole}^{-1}$$

A study of hydrogen assimilation kinetics by a methanogenic enrichment culture growing on hydrogen as the only energy substrate (Shea *et al.*, 1968) indicated a maximum specific growth rate, u_{max}, of 0.04 hr^{-1} and a maximum specific hydrogen utilization rate, k, of 64.6 uM $(mg\ VSS)^{-1}hr^{-1}$.

Radioactive labeling experiments have shown that 70-80 percent of the methane produced in an anaerobic reactor comes from acetate fermentation (Kirsch and Sykes, 1971; Mah *et al.*, 1977). Only *Methanothrix soehngenii* (Huser *et al.*, 1982) and *Methanothrix concilii* (Patel, 1985) have been reported to utilize acetate alone in pure culture. *Methanosarcina barkerii* and *Methanobacterium thermoautotrophicum* utilize acetate only in the presence of hydrogen (Zeikus, 1975). Zeikus pointed out that the accepted reaction for methane formation by acetate cleavage (Eq. 2.4) yielded less energy than the 11.7 Kcal $mole^{-1}$ required for ATP formation.

$$CH_3COO^- + H_2O \Longrightarrow CH_4 + HCO_3^- \qquad 2.4$$

$$G_o' = -6.71 \text{ Kcal mole}^{-1}$$

Based on finding that both carbons from acetate were reduced to methane, Zeikus proposed a reaction of the form:

$$CH_3COO^- + 4H_2 + H^+ \Longrightarrow 2CH_4 + 2H_2O \qquad 2.5$$

$$\delta_o' = -39.0 \text{ Kcal mole}^{-1}$$

The reaction in Eq. 2.5 yields sufficient energy for growth and explains why so much methane comes from acetate. A central role for hydrogen in methanogenesis is also shown. Alternately, Lawrence and McCarty (1969), van den Berg (1977), Smith and Mah (1980), Huser (1981), Huser *et al.*, (1982) and Patel (1985) have reported growth of enrichment cultures or pure cultures on acetate alone. Contrast in these reports indicates that more work is required before all mechanisms of methane production are understood.

2.4 Anaerobic Processes

Anaerobic waste treatment processes can be divided into several categories based on reactor characteristics. These include: conventional high rate reactors, conventional high rate reactors with recycled biomass and retained biomass reactors. The final class of reactors called second generation anaerobic reactors can be further broken down to: upflow anaerobic filters (Young, 1967; Young and McCarty,

1969), UASB reactors (Lettinga, 1979; Lettinga *et al.*, 1979, 1980), UBF reactors (Guiot and van den Berg, 1984), fluidized or expanded bed reactors (Switzenbaum, 1978; Switzenbaum and Jewell, 1980) and DSFF reactors (van den Berg and Lentz, 1979,1980). Basic designs of the reactors mentioned above are shown in Fig. 2.4.

2.5 History of the DSFF Reactor

Development of DSFF reactors started in 1976 as part of a project to circumvent problems encountered with upflow anaerobic filter reactors (Young, 1967). These problems included difficulties in assessing the exact role of the packing, plugging of the packing and difficulties in using wastes containing high concentrations of suspended solids. Lettinga *et al.* (1980, 1982) avoided the first two difficulties by operating without packing, and as a result developed the UASB reactor.

The role of biofilm development on performance of anaerobic reactors was studied by van den Berg and Lentz (1979, 1980). By studying the performance of single tube glass reactors of varying inside diameters, the effect of reactor surface area to volume ratio was assessed. Tubes were set vertically to avoid settling of suspended solids on the reactor walls. Reactors were operated in the downflow mode to allow continuous removal of suspended solids as well

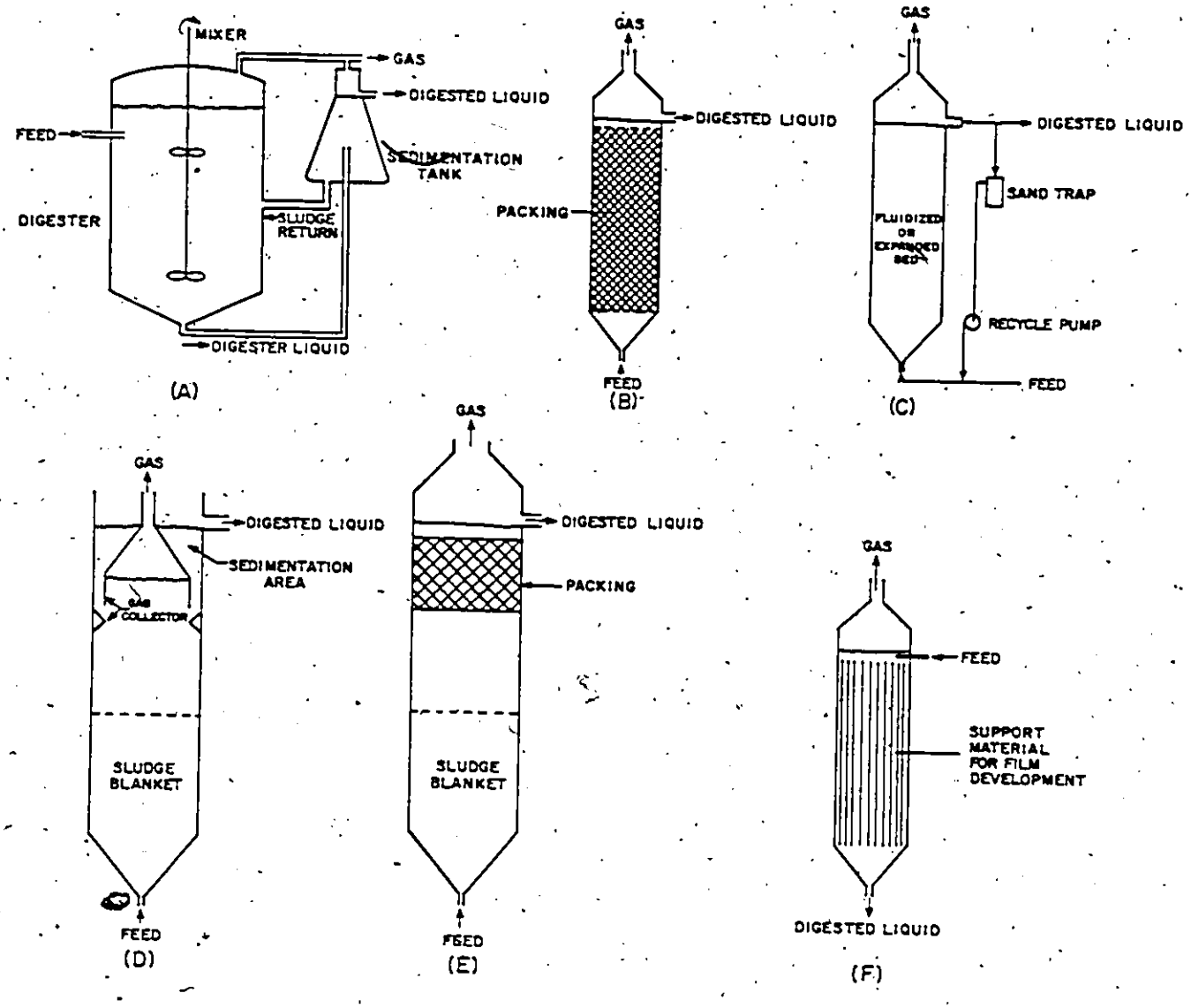

Figure 2.4 Anaerobic processes: A) anaerobic contact, B) upflow anaerobic filter, C) fluidized bed, D) UASB, E) UBF, F) DSFF

as being operated in the more customary upflow mode. This experimental setup permitted evaluation of biofilm performance as it developed.

Once the principle of DSFF reactors was established, studies were expanded to evaluate effects of factors such as waste composition (van den Berg and Kennedy 1981a, 1982b, c, d, 1983), nutrients (Murray and van den Berg 1982), temperature (Kennedy and van den Berg, 1981), reactor height and width (multichannel reactors; Kennedy and van den Berg, 1982e, Samson *et al.*, 1984) and ability to withstand adverse operating conditions such as hydraulic and organic overloading (Kennedy *et al.*, 1982b, c, 1985), intermittent loading and change in waste composition. DSFF reactors have been shown to successfully treat a large number of different wastewaters which has led to construction and operation of full-scale plants (Szendry, 1983a, b; Matt, 1983; Samson *et al.*, 1984b).

2.6 Description and Principle of Operation

As with other second generation reactor designs, enhanced performance of anaerobic DSFF reactors (Fig. 2.4) is based on maximizing the reactor biomass concentration. By immobilizing anaerobic bacteria on inert support media SRT can be maintained independent of HRT. Support media to which bacteria adhere can be made of various nontoxic, non-

biodegradable materials (van den Berg and Kennedy, 1981a; Copp and Kennedy, 1983).

Two major design and operational differences make DSFF reactors unique from other second generation anaerobic reactors. DSFF reactors use packing with an oriented geometry that forms vertical channels that run the length of the packing. Upflow anaerobic filters on the other hand, utilize a random packed media such as stones, Raschig rings or plastic biorings. The other major difference is direction of movement of wastewater through the packing. In DSFF reactors wastewater enters at the top of the reactor through a submerged distribution device and effluent is removed from the bottom. In other second generation reactors, influent is introduced at the bottom of the reactor and effluent overflows at the top (Fig. 2.4). These two factors result in major differences in reactor performance.

The downflow mode of operation in combination with oriented support media configuration allows utilization of the countercurrent interaction of mixed liquor and digester gas to enhance reactor mixing. Influent is introduced into the reactor volume where mixing is most intense thus minimizing localized areas of high VA concentrations which can decrease reactor performance. Localized areas of high VA where influent is introduced into the reactor have been reported for UASB reactors (Trudell, 1983) and upflow an-

aerobic filters (Young, 1967). The liquid volume above and below the packing in DSFF reactors also enhances inter-channel mixing while protecting the submerged biofilm and minimizing clogging in the bottom of the reactor.

Mixing studies in laboratory (Samson *et al.*, 1984a) and pilot plant DSFF reactors (Hall, 1982) have shown them to have tracer curves similar to complete mixed (CM) reactors. Combining downflow waste addition with vertically oriented packing also minimizes suspended solids accumulation in DSFF reactors. This enables DSFF reactors to treat both soluble and insoluble wastes without clogging (Kennedy and van den Berg 1982a, b; Harvey, 1984; Lo *et al.*, 1984). Wastewaters with suspended solids concentrations up to 4 percent (w/v) have been treated successfully. Other second generation reactors are limited to soluble component wastewaters.

Suspended solids lost in the effluent from DSFF reactors include not only untreated waste material but also active suspended biomass. This indicates a major role for the biofilm in the efficiency of wastewater treatment with DSFF reactors. In contrast to this, biomass profiles in upflow filter systems (Young and Dahab, 1982) have shown them to be hybrid reactors: they are combinations of a DSFF reactor and a UASB reactor. The majority of reactor biomass and waste stabilization capacity in upflow filters is found

in the interstitial spaces among packing material in the lower one-third depth of the reactor.

2.7 DSFF Reactor Performance

Studies done with anaerobic DSFF reactors have been aimed at determining treatability of a wide variety of wastes using mature DSFF reactors. Little attention has been given to developing an understanding of relationships that exist between DSFF reactor biomass and reactor performance. No design equations exist for DSFF reactors. Table 2.2 summarizes characteristics of some wastes treated with DSFF reactors, and results obtained. A wide variety of wastes (soluble-insoluble; dilute-concentrated) have been successfully treated with DSFF reactors.

2.8 Recirculation

Rich (1963) summarized the process effect of recirculation by stating that there is no theoretical basis for increased reactor efficiency but there are indirect benefits from increased hydraulic loading.

Recirculation in DSFF reactors has a number of advantages:

1. Increases mixing thereby minimizing effects of toxic and inhibitory components in a wastewater.
2. Minimizes the formation of gradients.

Table 2.2 Performance of Anaerobic DSFF Reactors with Various Substrates

Waste	Concentration Kg COD m^{-3}	Suspended COD % of total	Reactor Surface-to-volume ratio $m^2 m^{-3}$	Reactor volume m^3	HRT days	Loading rate kg COD $m^{-3}d^{-1}$	COD removal %
Bean blanch	10	10-30	157	0.035	0.85	11.6	86
Pig slurry	27-51	60-70	157	0.035	8.0 2.7 1.0	6.1 14.5 39.2	70 43 27
Pear peeling	110-140	35-50	157	0.035	17.5	6.4	58
Rum stillage	50-70	10	157	0.035	4.5	13.3	57
Thermal conditioned sludge supernatant	10	0-10	150	0.0013	0.34	29.2	70
Cheese plant waste	2-5	10-30	70 90	0.65 450	0.50 0.50	19 7	70 70 [Samson et al. (1984b)]

From van den Berg and Kennedy (1982b).

3. Minimizes excess biofilm development on the upper portion of support media where influent enters the reactor.
4. Aids in uniform deposition of inoculum on support media.
5. Suspended solids do not settle out as rapidly, minimizing plugging problems in the bottom of the reactor.

Effluent recycle in DSFF reactors has been found especially beneficial during startup and when treating wastes with a high concentration of suspended solids. Recirculation rates of 4-15 reactor volumes per day have been reported (Kennedy and van den Berg, 1982b, d; Duff and Kennedy, 1983; Szendry, 1983a, b).

2.9 Non-Steady State Reactor Performance

Non-steady state performance of anaerobic reactors has major importance in waste treatment. Industries produce widely varying quantities and strengths of wastewater. Wastewater composition can vary considerably from hour-to-hour, day-to-day or week-to-week and relatively long plant shut-down periods are not uncommon. A waste treatment system must be able to cope with all these variations and provide good treatment most of the time. The DSFF reactor has been tested for non-steady state performance.

2.9.1 Hydraulic Overloading

Mesophilic DSFF reactors are able to handle extreme hydraulic overloads and recover normal performance within a

short time. (Kennedy and van den Berg, 1981, 1982b). Ability of DSFF reactors to handle this type of shock results from bacteria being immobilized within the system and not lost in the effluent. Waste stabilization decreases with decreasing HRT due to insufficient time for bacteria-substrate contact. Methane production during extreme overloading quickly stabilizes at rates much higher than during normal operation. This new pseudo-steady state methane production rate is an indication of excess methane production capacity by methanogens. Better substrate diffusion into the biofilm could also be a factor in utilizing this excess capacity.

Hydraulic overloading often leads to sloughing of parts of the biofilm. This usually does not affect reactor performance and preshock performance is quickly restored. It is unclear whether biofilm sloughing is a result of intense biogas production in the biofilm or localized high VA concentrations and low pH in the biofilm. It is unlikely that increased liquid velocities resulting from overloading play a major role in biofilm sloughing because linear liquid flow velocities are usually low (less than 1.0 cm s^{-1}).

Thermophilic DSFF reactors do not cope with hydraulic overloads as well as their mesophilic counterparts (Duff and Kennedy, 1982). The limited number of methanogenic species that survive at thermophilic temperatures may be responsible

for the inability of DSFF reactors to respond quickly to transient changes.

2.9.2 Organic Overloading

Mesophilic DSFF reactors can tolerate sudden organic shock loads at constant hydraulic loading and recover normal performance within a few days (Kennedy *et al.*, 1985). COD removal efficiency decreases with increased loading even though actual amount of waste organics converted and methane gas produced increases. As with hydraulic overloads, increased biofilm sloughing occurs during organic shock loading.

DSFF reactors subjected to organic shockloads with poorly buffered wastewater indicated that reactor recovery was affected more by low pH than by high VA concentrations. Low reactor pH resulted in reactor failure or extended recovery periods.

Thermophilic DSFF reactors can not handle sudden organic shocks to the same extent as mesophilic reactors (Duff and Kennedy, 1982). The reason for this has been discussed in Section 2.9.1.

2.9.3 Starvation

Low decay rates for anaerobic bacteria allow DSFF reactors to stand idle for weeks or months without significant loss in microbial activity. This is particularly the case

when reactors are cooled to 5-10°C. In this respect, DSFF reactors are similar to upflow filters and UASB reactors. It has also been reported that the latter reactors are able to remain dormant for long periods and regain normal performance within a short time. This ability makes these second generation reactors ideal for wastes that are produced for only a short time during each month or year.

2.9.4 Changes in Waste Composition

DSFF reactors are able to cope with changes in waste composition. In many cases, reactor loading rates can be maintained more or less constant, although COD removal changes with waste composition (Kennedy *et al.*, 1981). Changes from one food processing waste to another, even when sodium concentration changed from 20 to 4000 mg L^{-1}, (Stevens and van den Berg, 1981) and from a sewage waste to a chemical industry waste have been reported with little or no setbacks in reactor performance.

2.10 Startup

Startup of anaerobic reactors is time-consuming and often difficult because of the slow growth rate of acetate converting methanogens. Work with DSFF reactors by van den Berg and Lentz (1978) and van den Berg and Kennedy (1981) showed startup times of up to one year were not out of the ordinary, depending on the type of support media. Switzenbaum (1978) reported that startup of anaerobic expanded bed

reactors took 9 months. Once startup was completed only 6 months were required to characterize steady state performance of the system. Although much time and effort has been spent starting anaerobic reactors, few systematic studies on startup or guidelines for startup of anaerobic reactors can be found in the literature. Kennedy and van den Berg (1985) state that the following factors have a major effect on startup of anaerobic reactors in general and on DSFF reactors in particular:

1. Quality of inoculum in terms of concentration of slow growing methanogenic bacteria adapted to the waste.
2. Rate of adaptation of methanogenic bacteria to the waste.
3. Rate of growth of methanogenic bacteria.
4. Rate of loss of methanogenic bacteria from the system.

While the four factors discussed above are rather broad, their significance can be compared to startup experiences reported in the literature.

De Zeeuw and Lettinga (1981) and Hulshoff Pol *et al.* (1982) working with UASB reactors reported that proper management of the reactor during startup was very critical to development of sludge granules. Using a VA mixture as a substrate during studies on UASB reactor startup, they established tentative guidelines designed to optimize sludge granulation. By following these guidelines, summarized in Table 2.3, they were able to cultivate a granular sludge

with good settling properties within 6 weeks from the start of the experiment. Furthermore, they determined that a surface load of approximately 1 m^3 m^{-2} d^{-1} and a minimum specific loading rate of 0.6 kg COD kg VSS^{-1} d^{-1} were required before the rate of sludge granulation became visibly pronounced.

Table 2.3 Tentative Guideline for Startup of UASB Reactors

1. Amount of seed sludge: 10-20 kg VSS m^{-3}.

2. Initial sludge load: 0.05-0.1 kg COD kg VSS^{-1} d^{-1}.

3. Organic loading rate should not be increased unless VA are well degraded (*i.e.*, less than 100 mg L^{-1}).

4. Voluminous sludge should be allowed to wash-out. The heavy part of the seed sludge should be retained.

5. Long periods of overloading or underloading with respect to specific substrate loading rate (*i.e.*, sludge loading rate) should be avoided.

Hulshoff Pol *et al.* (1982) identified three transitionary stages associated with startup of UASB reactors and the simultaneous development of sludge granules: (1) a significant washout of lighter, more flocculent, dispersed particles of sludge: (2) followed by microbial growth concentrating on heavier retained particles either organic or inorganic in nature, resulting in proliferation of sludge

granules: and, (3) gradual expansion of the sludge bed resulting from microbial growth and enhanced biogas production rates. They concluded that the basis for granulation in UASB reactors is the continuous selection of heavier sludge particles retained in the reactor, which in turn is governed by biogas production rate and hydraulic flux.

Finally, Hulshoff Pol *et al.* (1982) reported that long periods of specific organic overloading and underloading must be prevented during startup of UASB reactors. They observed that organic underloading resulted in development of a voluminous flocculent sludge which eventually was lost from the reactor. Microscopic examination of this sludge revealed that it consisted almost completely of filamentous bacteria, presumably *Methanothrix soehngenii*. Overloading also led to high rates of gas production which negatively affected sludge settlement. Van den Berg *et al.* (1981) and Hall (1982), also working with UASB reactors, and following the startup procedure described by De Zeeuw and Lettinga (1981) and Hulshoff Pol *et al.* (1982), reported that while the procedure worked for some wastewaters it did not work for others and concluded that startup of UASB reactors was also waste specific. Startup results with UASB reactors are closely related to the general guidelines given above for anaerobic reactor startup.

Young (1967) reported that startup of upflow anaerobic

filters was improved if a more concentrated inoculum was used or if multiple inoculations were carried out. Additionally, Young reported that reactors started more quickly with an adapted inoculum than with inoculum taken from a digester treating domestic sewage sludge. Although no startup data or specific guidelines for startup of anaerobic filters were presented, Young's experiences were directly related to all four general startup factors.

Van den Berg and Kennedy (1981a) report that if possible DSFF reactors should be started by completely filling the reactor with adapted inoculum. Recirculating mixed liquor at 4-8 reactor volumes per day is recommended to allow methanogenic bacteria to attach to support media. Feed is slowly added to the reactors starting at a 40-50 day HRT. Feed rates should then be increased only if the reactor VA concentration is below 500 mg L^{-1}. Although this technique fulfills the general guidelines for startup and is successful, no information is available on what physical or biological changes occur in DSFF reactors during this time.

Szendrey (1983a, b) reported that a 10,000 m^3 DSFF reactor treating rum slops (mostos) was started with seed sludge adapted to the waste to minimize acclimation problems. The inoculum was 20 percent of the reactor volume. Following inoculation, the reactor was filled with rum mostos (60,000 mg COD L^{-1}) and recirculated (15 $v \cdot v^{-1} d^{-1}$) for five weeks without further substrate addition.

After 5 weeks of recirculation, the reactor was fed rum slops at an HRT of 90 days. Further addition of rum slops was then determined by VA concentrations (not reported) in the reactor. The purpose of this procedure was to minimize the rate of loss of methanogenic bacteria in the effluent and allow sufficient time for bacterial growth.

Other than these references, no other information was found in the literature for startup of second generation anaerobic reactors.

3. THEORY

3.1 Microbial Biofilms

Bryers and Characklis (1981, 1982; Fig. 3.1) describe development of aerobic microbial biofilms in four phases. Phase one is attachment, followed by the second phase which is characterized by log growth. Phase three begins when the rate of substrate utilization becomes constant and biofilm growth is linear. The final phase is reached when newly grown bacteria do not attach to the biofilm. Most reports on growth of biological films have been done with aerobic cultures to achieve a better understanding of fixed biofilm reactors such as trickling filters and rotating biological contactors (RBC). These results are examined for their applicability to anaerobic biofilm processes.

Reports published before the development of DSFF reactors (Topiwala and Hamer, 1971; Atkinson and Davies, 1972; Howell *et al.*, 1972; Mehta and LeRoux, 1974; Atkinson and Fowler, 1974; Howell and Atkinson, 1976a, b) have shown the importance of biofilms or wall growth in prevention of washout of microorganisms in aerobic systems. This is particularly significant in an anaerobic system because of slow growth rates of methanogens. Topiwala and Hamer (1971) showed the effect of varying amounts of biofilm growth in an aerobic CSTR system. These results are reproduced in Fig. 3.2 where the parameter Z^* is a measure of total mass of attached cells. With no wall growth there was a pronounced

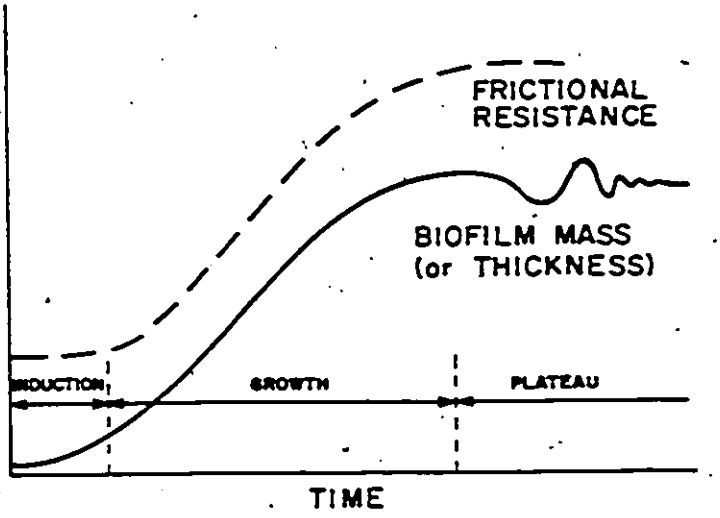

Figure 3.1a Stages of biofilm development
(Characklis, 1981)

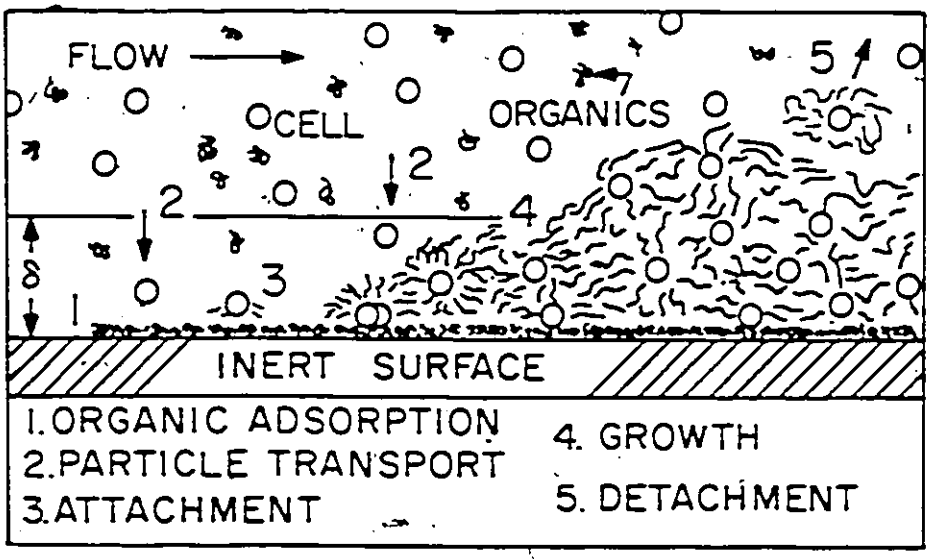

Figure 3.1b Biofilm development processes
(Characklis, 1981)

washout of organisms at an HRT of 1.25 hrs. With a small amount of wall growth ($Z^* = 0.05$) washout was significantly reduced. These results showed that wall growth effectively extended the operational range of the CSTR. Prevention of washout in anaerobic CSTR with wall growth was demonstrated by Balmer (1974), Schillinger (1975) and Gill (1978).

Another effect of wall growth discussed by Topiwala and Hamer (1971) was change in culture productivity at high growth rates (Fig. 3.3). Both maximum productivity and range of HRT possible were increased by the presence of wall growth. This effect has also been reported by Howell *et al.* (1972). Atkinson and Davies (1974) pointed out that unlike a CSTR, substrate utilization in a CSTR with wall growth is maximal at high flow rates and there is no danger of the microbial mass being washed out.

In waste treatment processes, substrate utilization by the microbial culture is the reason for employing a biological process. Maximum rates of substrate utilization occur at high specific growth rates. Unfortunately, as demonstrated by the curve for no wall growth, (Fig. 3.2) biological reactors operated at high growth rates are unstable and can fail because of microorganism washout. Consequently the economics of rapid growth rates must be sacrificed to achieve a greater degree of process stability associated with lower growth rates. Curves in Figs. 3.2 and 3.3 show however, that wall growth in a reactor allows a small reactor to be used while providing stability associated with a

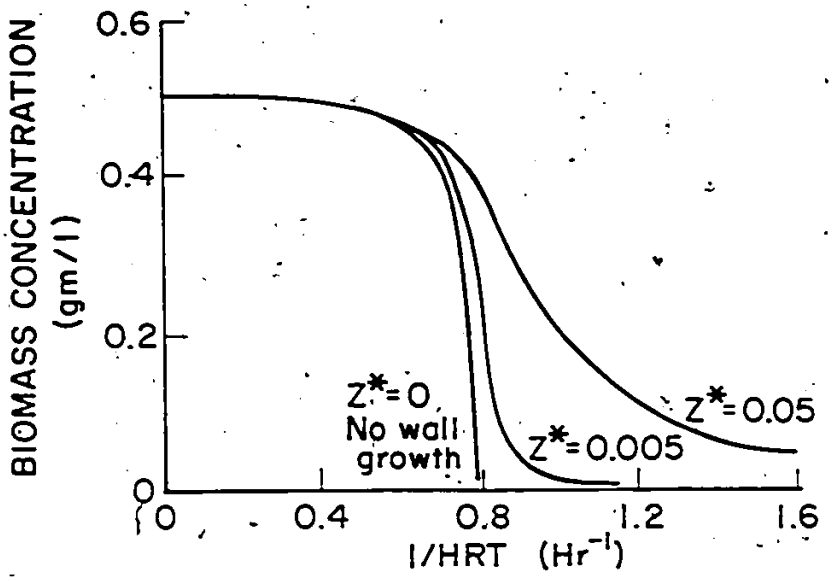

Figure 3.2 Effect of wall growth upon biomass concentration (Topiwala and Hamer, 1971)

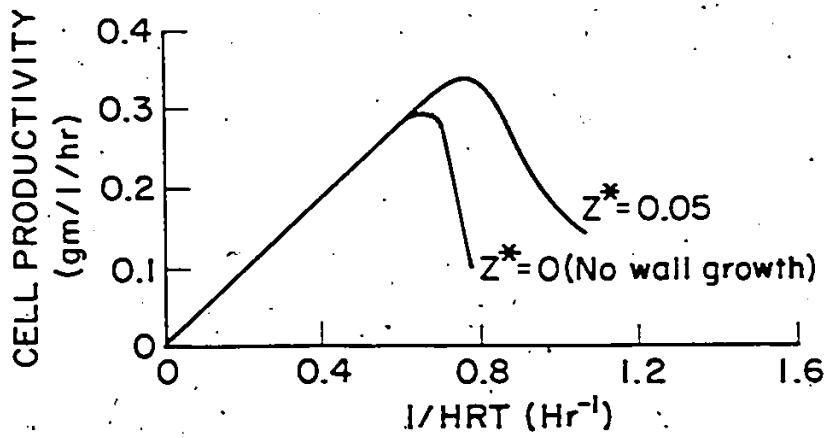

Figure 3.3 Effect of wall growth upon cell production (Topiwala and Hamer, 1971)

large reactor. These results indicate why good process stability has been observed with anaerobic DSFF reactors.

Models for wall growth within a CSTR have been proposed by Howell *et al.* (1972), Atkinson and Davies (1974) and Topiwala and Hamer (1971). These models are based upon two assumptions: (1) there is a single or predominant culture of organisms in the reactor, and (2) cells will be growing in either a monolayer or a very thin multilayer. Both of these assumptions are violated in anaerobic DSFF reactors: (1) the culture employed is complex, with many synergistic interactions, and (2) the support media contains a thick multilayer of cells. It appeared unlikely that models developed for aerobic biofilms would be entirely applicable to anaerobic biofilm reactors. Furthermore, it was apparent from the literature review that more would have to be known about the anaerobic system before reasonable modeling efforts could be made. Since nearly all work reported has been either theoretical or with aerobic cultures, and no basic work had been done on DSFF reactors, experimental work with biofilms in an anaerobic DSFF reactor was justified.

3.2 Biofilm Substrate Utilization

Microbial biofilms that develop in DSFF reactors are uncontrolled zoogloeal biofilms (Table 3.1; Kennedy and van den Berg 1981). This type of biofilm is characterized by a thick layer, indicating that bacterial cells stick to one

another. With thick biofilms, transport of nutrients to the organism may be diffusion limited. The basic concept of biofilm kinetics is that substrates diffuse into the biofilm where a reaction takes place, and that reaction products have to diffuse out. There is resistance to mass transfer in both liquid and solid phases. Overall rate of reaction depends on diffusivities and microbial reaction rates of each reactant involved.

Diffusional resistance reduces efficiency of substrate removal because substrate may not penetrate the complete biofilm depth. Howell and Atkinson (1976a) and Kornegay and Andrews (1968) discussed biofilm thickness in terms of mass transport and stated that the ideal biofilm thickness is equal to the penetration depth of the limiting substrate. Thus, ideal biofilm thickness will depend upon the nature of the rate limiting substrate. In aerobic systems, ideal biofilm thickness is determined by the transport of either oxygen or organic nutrients. For fermentation of organic wastes to methane in a biofilm, mass transfer efficiency of acetate compared to maximum reaction rate for acetate utilization in suspended culture is the only phenomenon evaluated. No other electron donors or acceptors are required.

Table 3.1 Groups of Microbial Films*

Group	Description	Thickness, mm
I	Uncontrolled zoogloeal film	0.2–4.0
II	Zoogloeal film, subject to mechanical or hydrodynamic control	0.07–0.2
III	Pure cultures in CSTR	0.001–0.01
IV	Casual deposition	0.001

* Atkinson, (1974)

The classic work of Thiele (1939) examined reaction and single substrate diffusion into a particle. Atkinson and co-workers (1968, 1974a, b, c) generalized this work to apply for groups of particles and fixed films. DeWalle and Chian (1976) used this work to develop a steady state model for a CM anaerobic filter. The model incorporated substrate diffusion and bacterial substrate utilization for each successive layer of biofilm. The main points of the development will be presented here. A definition sketch is shown in Fig. 3.4. The substrate flux in the biofilm was described by Fick's law:

$$N = - D\frac{\partial S}{\partial x} \qquad 3.1$$

Where N = mass flux ($ML^{-2}T^{-1}$);

D = diffusion coefficient (L^2T^{-1});

S = substrate concentration (ML^{-3}); and

x = distance (L).

The diffusion coefficient, D was assumed to be constant in the biofilm. Substrate uptake within the biological layer was described by Eq. 3.2 (Monod, 1949)

$$r_s = - \frac{k\, X_f\, S}{K + S} \qquad 3.2$$

Where r_s = rate of substrate uptake ($ML^{-3}T^{-1}$);

k = maximum specific reaction velocity (T^{-1});

K = half velocity constant (ML^{-3})

X_f = concentration of active microorganisms in the biofilm (ML^{-3}).

The above expression was not refined to include surface area of the microorganisms in the biofilm. This is a difficult parameter to estimate and therefore, X_f, refers to nominal concentration of active microorganisms.

A mass balance on an elemental biofilm volume lead to the governing differential equation at steady state:

$$D \frac{d^2S}{dx^2} - \frac{k\, X_f\, S}{K + S} = 0 \qquad 3.3$$

Equation 3.3 assumes that there is no variation of S in the y direction. The mixed liquor in the reactor is assumed to be CM which results in a uniform concentration of substrate at the liquid-biofilm interface. However, substrate concentration at the interface, S_b, is not the same as the sub-

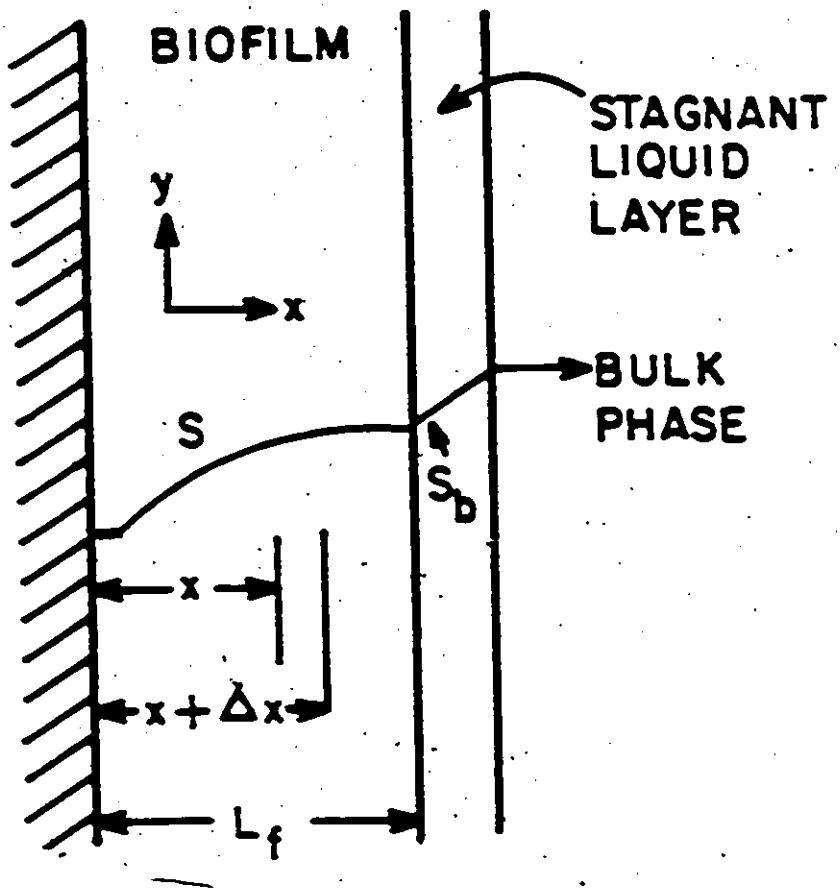

Figure 3.4 Definition sketch of biofilm

strate concentration in the bulk fluid phase, due to a stagnant liquid layer at the biofilm. This has been experimentally verified (Williamson and McCarty, 1976a) and a theoretical description of this limitation has been developed (Williamson and McCarty, 1976b; Rittmann and McCarty, 1980a, b). DeWalle and Chian (1976) neglected the presence of the stagnant liquid layer and assumed that substrate concentration at the biofilm interface was the same as the bulk liquid concentration.

When S is very large relative to K, Eq. 3.3 reduces to a zero order expression:

$$\frac{d^2S}{dx^2} = \frac{k\ X_f}{D} \qquad 3.4$$

Equation 3.4 was integrated over the cross-sectional area of the filter and the mass transfer rate at the interface expressed as:

$$\frac{dF}{dt} = k\ X_f\ L_f \qquad 3.5$$

where L_f = biofilm thickness (L);

F = substrate mass (M) ; and t = time (T)

For a given waste, k and X_f were not expected to vary significantly indicating that mass transfer rate would be independent of substrate concentration but directly proportional to biofilm thickness. In this situation DeWalle and Chian (1976) stated that a decrease in substrate concen-

tration within the biofilm is small compared to the interface concentration. Therefore, the specific substrate utilization rate is the same as if biomass solids were evenly dispersed throughout the liquid.

When S is much smaller relative to K, Eq. 3.3 reduces to a first order expression:

$$\frac{d^2S}{dx^2} = \frac{k\ X_f\ S}{D\ K} \qquad 3.6$$

Equation 3.6 was integrated over a unit cross-sectional area giving the following expression for substrate mass transfer rate at the interface.

$$\frac{dF}{dt} = S_b\left(\frac{D\ k\ X_f}{K}\right)^{1/2} \qquad 3.7$$

Since D, k, X_f and K were not expected to vary greatly with a given substrate, Eq. 3.7 indicates that the mass transfer rate is related to bulk liquid substrate concentration and is independent of biofilm thickness. Since Eqs. 3.6 and 3.7 were derived for a unit cross-sectional area, mass transfer rate is also proportional to specific surface area within the reactor.

Using sucrose as their substrate, DeWalle and Chian (1976) observed maximum removal rates of 7 kg COD $m^{-3}\ d^{-1}$ and K values of 1500 mg L^{-1}. They limited their final conclusions to the following general statement: "Comparison of the fixed biofilm model with results obtained tended to in-

dicate that substrate removal rate is affected by substrate concentration, specific surface area, flow rate and temperature."

Using general parameters of anaerobic digestion, Henze and Harremoes (1982) evaluated the significance of diffusional resistance on acetate utilization in anaerobic biofilms. Results of their analysis indicated that diffusional resistance does not become significant until biofilm thicknesses reach 1 mm. This is in part attributed to the high K of anaerobic bacteria. Williamson and McCarty (1976a, b) stated that anaerobic biofilms could be developed to any thickness without diffusional resistance problems because of the high K values associated with anaerobic digestion.

Henze and Harremoes (1982) state that diffusional resistance can result in buildup of substrate and acidity inside anaerobic biofilms. This problem is further complicated since most wastes are multi-component and complex relationships exist among substrate utilization rates and growth rates of acidogens and methanogens that coexist in anaerobic biofilms. Henze and Harremoes (1982) and Kennedy and van den Berg (1982b, 1985) have also commented that in cases where thick anaerobic biofilms exist, diffusion of methane and carbon dioxide gas bubbles out of the biofilm may cause disturbances that alter the whole diffusion pattern. Microcurrents generated by bubble movements could increase the diffusion rate and make diffusional resistance in the biofilm insignificant.

3.3 Substrate Utilization in Biofilms

For a mixed anaerobic biofilm (acidogens/methanogens), the overall rate of reaction depends on diffusivities and microbial reaction rates of each reactant involved. For a mixed biofilm culture fermenting a complex waste to methane, both mass transfer of primary substrate in the biofilm and its conversion to acetate in the biofilm along with diffusion of acetate from primary substrate conversion in the liquid will influence system efficiency. This section presents a theoretical development of the modified effectiveness factor that will result from taking into account production and diffusion of intermediate substrate in the biofilm. The analysis will be specifically related to anaerobic methane fermentation but is applicable to any situation where sequential substrate conversion is involved. It will be shown that ignoring production of intermediate substrate in the biofilm can result in significant error in some circumstances.

3.3.1 Single Substrate Removal

For single substrate removal by a biofilm, Eqs. 3.1 and 3.2, combined in a mass balance. give Eq. 3.3. Similar to the work of DeWalle and Chian (1976) the following development will neglect the resistance of the stagnant liquid boundary layer and proceed from the substrate concentration

at the biofilm interface (Fig. 3.4). The other boundary condition for Eq. 3.3 applies to the flux at the wall.

Expressions for the boundary conditions are:

$$S\Big|_{x=L_f} = S_b \qquad 3.8a$$

$$\left.\frac{dS}{dx}\right|_{x=0} = 0 \qquad 3.8b$$

It is convenient to express the above in dimensionless form. The following transformations are used:

$$z = \frac{x}{L_f} \qquad 3.9a$$

$$\epsilon = \frac{S}{S_b} \qquad 3.9b$$

Substituting Eqs. 3.9a and 3.9b into Eqs. 3.3, 3.8a and 3.8b, and rearranging, one finds

$$\frac{d^2\epsilon}{dz^2} - \frac{\phi^2\epsilon}{1+\epsilon\mathcal{K}} = 0 \qquad 3.10$$

$$\epsilon\Big|_{z=1} = 1.0 \qquad 3.11a$$

$$\left.\frac{d\epsilon}{dz}\right|_{z=0} = 0 \qquad 3.11b$$

The two terms that have arisen in Eq. 3.10 are ϕ, the Thiele modulus and $\mathcal{K}$, a parameter related to the half vel-

ocity constant. These are defined in Eqs. 3.12a and 3.12b below.

$$\phi = \left[\frac{k \times L_f^2}{DK}\right]^{1/2} \qquad 3.12a$$

$$\lambda = \frac{S_b}{K} \qquad 3.12b$$

3.3.2 Effectiveness Factor

Equation 3.10 is a nonlinear second order differential equation which must be solved by numerical methods. Equation 3.10 is most useful when integrated and used to compute the efficiency or effectiveness factor, as it is commonly known, which compares the flux to the maximum possible rate of reaction.

Total mass flux, N_L, evaluated at the interface describes the amount of substrate being converted at steady state per unit surface area of biofilm.

$$N_L = -\frac{D\,S_b}{L_f}\left.\frac{d\epsilon}{dz}\right|_{z=1} \qquad 3.13$$

Maximum reaction rate per unit area, r_m, (or maximum flux) for a given S_b is:

$$r_m = -\frac{\phi^2\,D\,S_b}{L_f(1+\lambda)} \qquad 3.14$$

The effectiveness factor, η, is defined as the ratio of Eq. 3.13 to Eq. 3.14.

$$\eta = \frac{1+K}{\phi^2} \left.\frac{d\epsilon}{dz}\right|_{z=1} \qquad 3.15$$

If S_w is small compared to K, the reaction equation can be simplified to a first order expression.

$$r^* = -\frac{k \; X \; S}{K} \qquad 3.16$$

Where r^* = first order rate of reaction ($ML^{-3}T^{-1}$).

The dimensionless differential equation that results from the mass balance using a first order reaction (Eq. 3.17a) has an analytical solution (Eq. 3.17b).

$$\frac{d^2\epsilon}{dz^2} - \phi^2\epsilon = 0 \qquad 3.17a$$

$$\epsilon = \frac{\cosh \phi z}{\cosh \phi} \qquad 3.17b$$

The maximum rate of reaction per unit area, r_m^*, in this case is:

$$r_m^* = \frac{\phi^2 D S_w}{L} \qquad 3.18$$

The effectiveness factor, η^* corresponding to this situation is the ratio of Eq. 3.13 to Eq. 3.18:

$$\eta^* = \frac{\tanh \phi}{\phi} \qquad 3.19$$

If S is large compared to K_s across the biofilm, the reaction formulation can be simplified to a zero order expression leading to another differential equation with an analytical solution.

Plots of effectiveness factor versus Thiele modulus may now be constructed. This plot can be improved by using the generalized modulus, ϕ_g, developed by Bischoff (1965).

The general modulus, ϕ_g, for Monod kinetics is:

$$\phi_g = \left(\frac{\phi K}{1+K}\right)[2K - 2\ln(1+K)]^{-1/2} \qquad 3.20$$

The general modulus corresponding to first order kinetics is the same as the Thiele modulus defined in Eq. 3.12a. The familiar plot of effectiveness factor versus generalized modulus is shown in Fig. 3.5 for Monod kinetics. As ϕ_g increases diffusion limitations become more pronounced.

3.3.3 Sequential Substrate Removal

For a mixed culture in which a portion of the microorganisms generate substrate for another group of microorganisms, application of the above will lead to erroneous results. Production of intermediate substrate in the bio-

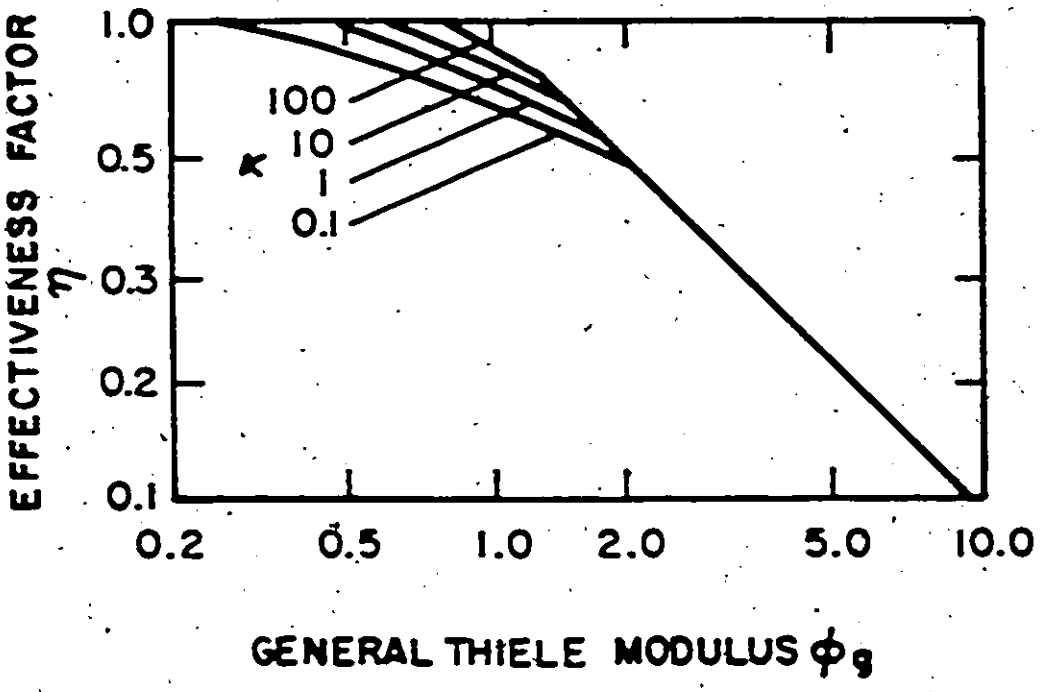

Figure 3.5 Variation in effectiveness factor with general Thiele modulus

film will in every case improve the ability of the second group of microorganisms to convert their substrate to product (assuming no intermediate substrate inhibition), although, as shown later, this improvement may be negligible.

In the developments which follow, subscript 1 will refer to parameters associated with the first group of microorganisms and subscript 2 will refer to parameters associated with the second group. Refer to Fig. 3.4 for a definition sketch. The analysis assumes that no interactions that will cause kinetic or diffusion parameters to change from values associated with individual cultures of each group occur between the two groups of microorganisms. Nominal concentrations of each group of microorganisms will be affected because of the presence of both groups. It is further assumed that the microorganisms in each group are randomly dispersed throughout the biofilm and therefore parameters are constant.

The analysis presented in the previous section applies to the first group of microorganisms. At any point x in the biofilm, production of substrate, p, for the second group of microorganisms depends on a substrate yield factor, Y, that is related to the reactions stoichiometry and primary substrate conversion rate in the biofilm, r_m, which is Eq. 3.2 applied to the first group.

$$p = - Yr_{mx} \qquad 3.21$$

A steady state mass balance over an elemental volume for intermediate substrate shows that intermediate substrate consumed by the second group of microorganisms is equal to the production of intermediate substrate plus its mass flux into the element.

$$r_{m2} = \frac{dN_2}{dx} + Yr_{m1} \qquad 3.22$$

Substituting Eqs. 3.1 and 3.2 into Eq. 3.22 with appropriate subscripts for parameters related to N_2, r_{m1} and r_{m2} respectively, and rearranging yields the governing differential Eq. 3.23.

$$D_2 \frac{d^2S_2}{dx^2} - \frac{k_2X_2S_2}{K_2+S_2} = - \frac{Yk_1X_1S_1}{K_1+S_1} \qquad 3.23$$

Boundary conditions that apply to Eq, 3.23 are similar to those used earlier.

$$S_2\Big|_{x=L_f} = S_{b2} \qquad 3.24a$$

$$\frac{dS_2}{dx}\Big|_{x=0} = 0 \qquad 3.24b$$

Transforming Eqs. 3.23 and 3.24 into dimensionless form by use of Eqs. 3.9a and 3.9b results in:

$$\frac{d^2\epsilon_2}{dz^2} - \frac{\phi_2^2\epsilon_2}{1+\beta_2\epsilon_2} = - Y \frac{S_{b1}}{S_{b2}} \frac{D_1}{D_2} \frac{\phi_1^2\epsilon_1}{1+\beta_1\epsilon_1} \qquad 3.25$$

$$\epsilon_2\Big|_{z=1} = 1.0 \qquad 3.26a$$

$$\frac{d\epsilon_2}{dz}\Big|_{z=0} = 0 \qquad 3.26b$$

The yield factor in Eq. 3.25 is dimensionless and it was grouped with the two ratios following it, resulting in a new modulus, β.

$$\beta = Y \frac{S_{w1}}{S_{w2}} \frac{D_1}{D_2} \qquad 3.27$$

The differential equation in its final form is:

$$\frac{d^2\epsilon_2}{dz^2} - \frac{\phi_2^2\epsilon_2}{1+k_2\epsilon_2} = -\beta \frac{\phi_1^2\epsilon_1}{1+k_1\epsilon_1} \qquad 3.28$$

Equation 3.28 with boundary restraints was solved by the Runge-Kutta-Gill technique in double precision for various values of the parameters. A binary search routine (Carnahan, 1969) was used to generate ϵ_1 and ϵ_2 values at the lefthand boundary. The right hand dimensionless concentration criterion allowed a maximum deviation of 0.05 % from 1.0. The program was run on a mainframe using Fortran and a copy of the listing is found in Appendix B.

If first order kinetics apply to both groups of microorganisms the resulting dimensionless differential equation is:

$$\frac{d^2\epsilon_2}{dz^2} - \phi_2^2\epsilon_2 = -\beta\,\phi_1^2\epsilon_1 \qquad 3.29$$

Substituting Eq. 3.17b for ϵ (first order kinetics), solution of this equation is

$$\epsilon_2 = \frac{\cosh \phi_2 z}{\cosh \phi_2} + \beta \left(\frac{\phi_1^2}{\phi_1^2-\phi_2^2}\right)\left(\frac{\cosh \phi_2 z}{\cosh \phi_2} - \frac{\cosh \phi_1 z}{\cosh \phi_1}\right) \qquad 3.30a$$

When $\phi_1 \neq \phi_2$

$$\epsilon_2 = \frac{\cosh \phi z}{\cosh \phi} - \frac{\beta \phi}{2\cosh \phi} z\sinh(\phi z),\ \phi_1 = \phi_2 \qquad 3.30b$$

3.3.4 Effectiveness Factor for Sequential Substrate Removal

The effectiveness factor in the case of sequential substrate removal cannot be defined on the basis of mass flux into the biofilm compared to the maximum reaction rate. In some instances intermediate substrate is actually diffusing out of the biofilm. One approach is to use an observed effectiveness factor, η_2, that is related to the effectiveness factor that would have occurred in the absence of intermediate substrate production in the biofilm without changing the values of parameters associated with the second group of microorganisms. This provides an estimation of effective increase in diffusivity of intermediate substrate.

From above, the effectiveness factor, η_2', for the second group of microorganisms that would be observed without intermediate substrate production is:

$$\eta_2' = \frac{1+\gamma_2}{\phi_2^2} \left. \frac{d\epsilon_2'}{dz} \right|_{z=1} \qquad 3.31$$

where η_2' = dimensionless concentration of intermediate substrate that occurs in the absence of production of intermediate substrate.

Dimensionless concentration, ϵ_2', and its derivative are calculated using the method for single substrate removal.

Defining N_{2max} (Eq. 3.32) as maximum flux at the liquid-biofilm boundary that occurs when the biofilm is saturated with intermediate substrate, the flux, N_2', that exists without intermediate substrate production in the biofilm, is related to N_{2max} by Eq. 3.33 below:

$$N_{2max} = \frac{\phi_2^2 D_2 S_{2b}}{L_f(1+\gamma)} \qquad 3.32$$

$$N_2' = \eta_2' N_{2max} \qquad 3.33$$

Flux in Eq. 3.33 is compared to production of ultimate product when intermediate substrate is generated in the biofilm. Total amount of intermediate substrate converted to product per unit time, P, depends on production of intermediate substrate in the biofilm and rate of external mass

transfer of intermediate substrate at the liquid-biofilm boundary.

$$P = -Y\int_0^{L_f} r_{s1}\,dx - D_2\left.\frac{dS_2}{dx}\right|_{x=L_f} \qquad 3.34$$

It should be noted that the first term (including the minus sign) on the right hand side of Eq. 3.34 is always positive while the second term may be either positive or negative.

The integral on the right hand side of Eq. 3.34 can be replaced by the flux, N_1, of S_1 into the biofilm at the liquid-biofilm boundary. The boundary flux, N_2, that actually exists with production in the biofilm along with the production can be related to N_{2max} defined above by an observed effectiveness factor, η_2.

$$\eta_2 N_{2max} = YN_1\Big|_{x=L_f} + N_2\Big|_{x=L_f} \qquad 3.35$$

The ratio, R, of Eq. 3.35 to Eq. 3.33 gives the improvement in the effectiveness factor due to production of intermediate substrate in the biofilm. Using dimensionless variables, Eq. 3.36 describes R.

$$R = \frac{\eta_2}{\eta_2'} = \frac{\beta\left.\frac{d\epsilon_1}{dz}\right|_{z=1} + \left.\frac{d\epsilon_2}{dz}\right|_{z=1}}{\left.\frac{d\epsilon_2'}{dz}\right|_{z=1}} \qquad 3.36$$

In the above equation, ϵ_2' is calculated with the same values for ϕ_2 and S_{b2} that were used to obtain ϵ_2.

The analytical expression for R that results from using first order reaction rate expressions when $\phi_1 \neq \phi_2$ is:

$$R = 1.0 + \beta\left\{\left(\frac{\phi_1}{\phi_2}\right)\tanh\phi_1 \coth\phi_2 + \left(\frac{\phi_1^2}{\phi_1^2 - \phi_2^2}\right)\left[1-\left(\frac{\phi_1}{\phi_2}\right)\tanh\phi_1 \coth\phi_2\right]\right\} \qquad 3.37$$

In Eq. 3.37, the expression within the {} brackets can be shown to be ≥ 0 for all values of ϕ_1 and ϕ_2. It is observed that improvement in the effectiveness factor is directly proportional to β at given values of ϕ_1 and ϕ_2.

For nonlinear Monod kinetics, five parameters characterize R: K_1, K_2, ϕ_{o1}, ϕ_{o2} and β. Computations have shown that R is nearly directly proportional to β if the other dimensionless variables are held constant. Maximum change in the effectiveness factor for β values of 0.10 and 0.20 was 8 and 16% respectively over the range of modified Thiele moduli examined. A few typical plots (Fig. 3.6) illustrate trends in R, ϕ_{o1} and ϕ_{o2} each vary from 0 to 4 and K_1 and K_2 each vary from 0.1 to 100 for $\beta = 0.1$.

3.3.5 Significance of Sequential Substrate Utilization in Biofilms

Production of intermediate substrate in the biofilm always increases the concentration of this substrate compared

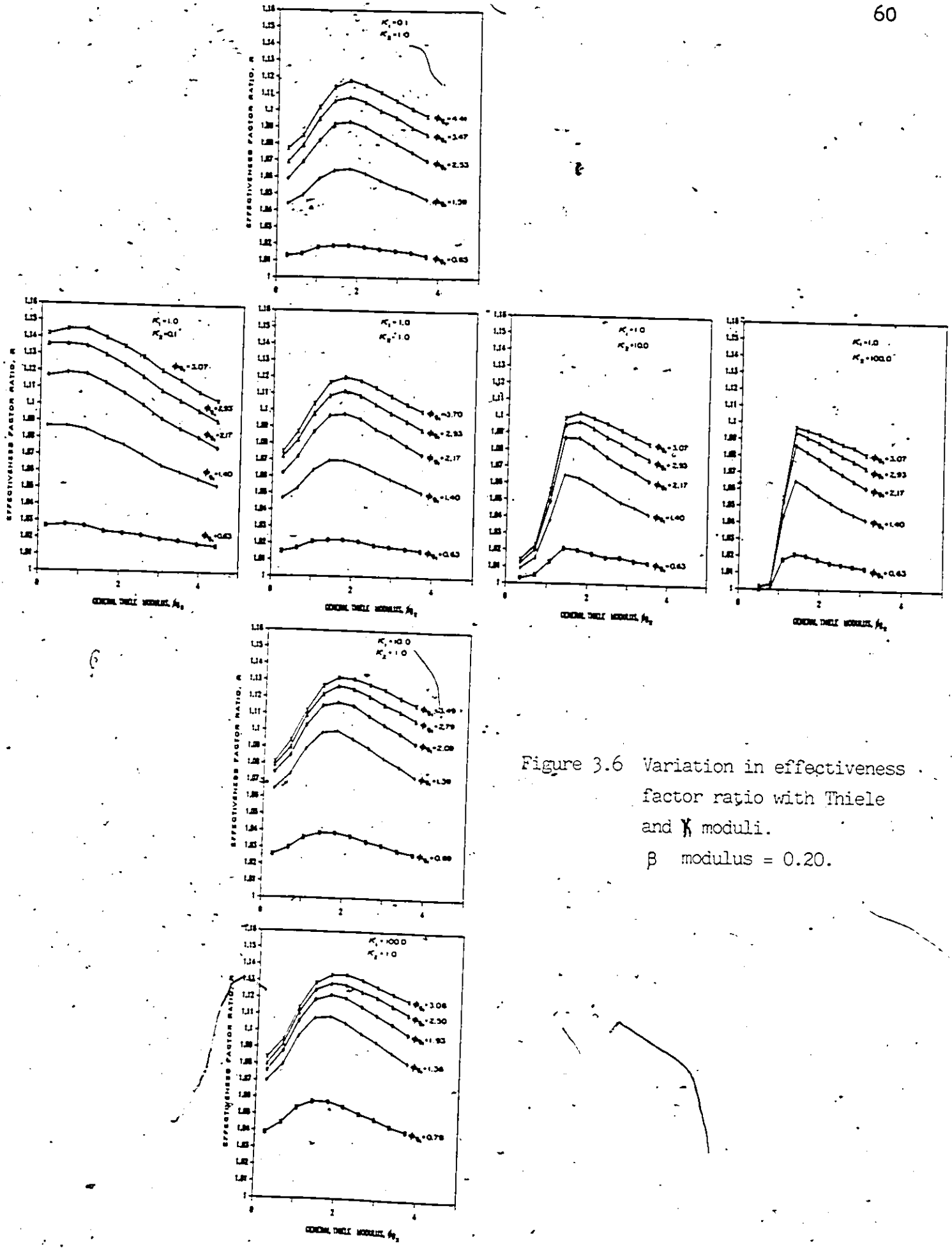

Figure 3.6 Variation in effectiveness factor ratio with Thiele and χ moduli.
β modulus = 0.20.

to the case without production and thus the reaction efficiency improves. In some instances, a portion or all of the biofilm becomes supersaturated with intermediate substrate compared to the boundary concentration of intermediate substrate. Production of intermediate substrate and its consequent rise in concentration mitigates the flux of intermediate substrate from the liquid.

Interaction of λ and ϕ_o causes distinct trends in R as observed in Fig. 3.6. In general as ϕ_{o1} increases the amount of intermediate substrate produced in the biofilm increases causing an increase in R. This is due to the increase of k which results in more primary substrate conversion by the first group of microorganisms.

As λ_2 increases, the Monod equation changes from a first order expression to a zero order expression. A zero order expression is not affected by a concentration change. At low values of ϕ_{o2} the biofilm is close to saturation when intermediate substrate production is nonexistent. Thus at low values of ϕ_{o2} and high λ_2 values there is little change in efficiency. As the biofilm length increases, which causes ϕ_{o2} to increase, the concentration of intermediate substrate in the inner depths of the biofilm falls and the reaction order rises to one. Intermediate substrate production exhibits a more dramatic effect in these circumstances until a critical maximum point is reached which depends on λ values. As ϕ_{o2} increases beyond this point, the limiting effects of diminished mass transfer of inter-

mediate substrate from the liquid become more predominant and R values decrease to 1.0.

3.3.6 Application to Anaerobic Digestion

Anaerobic wastewater treatment depends on complete conversion of initial substrate to primarily CH_4 and CO_2 which is accomplished by two groups of microorganisms: acidogens and methanogens. In this section, data pertaining to anaerobic fermentations will be summarized and used to calculate the change in effectiveness factor. The primary intermediate substrate is acetate. Tables 3.2 and 3.3 give values for k and K for the respective groups found by various researchers under different conditions. These tables are not meant to be exhaustive but instead illustrative of the variation that can be found in the parameters. Values listed in these tables are from studies in which dispersed growth or fixed films existed. Williamson and McCarty (1976a, b) demonstrated that the maximum specific rate constant, k, did not change for biofilm or dispersed growth of their culture and it is assumed here that k and K values are the same for fixed biofilm or dispersed growth of a culture.

Table 3.2 Kinetic Coefficients for Acidogens[a]

Substrate	k_1 g COD(g VSS)$^{-1}$d^{-1}	K_1 g COD L^{-1}	Reference
dextrose	173	0.024	Ghosh and Pohland (1974)
protein-carbohydrate	1.0	0.15	Mueller and Mancini[b] (1975)
sludge	9.6	37[c]	Ghosh et al. (1975)
glucose	209	2.6	Massey and Pohland (1978)
glucose	72	0.022	Zoetemeyer (1982)

[a] For temperatures in the range of 30-37°C.
[b] Based on analysis of Young and McCarty's data (1969).
[c] Assuming their sludge had a composition of $C_5H_7O_2N$.

Table 3.3 Kinetic Coefficients for Methane Formers[a]

k_z g COD(g VSS)$^{-1}$d^{-1}	K_z g COD L^{-1}	Reference
4.0		Mueller and Mancini[b] (1975)
4.0-4.5		van den Berg (1977)
5.0-8.6	0.17-0.93	Lawrence and McCarty (1969)
	0.64	Ghosh and Pohland (1975)
	0.39	Massey and Pohland (1978)
6.7	0.002	Andrews and Graef (1971)

[a] For temperatures from 25-37°C.
[b] Based on analysis of Young and McCarty's data (1969).

There is little information on the concentration of each group of microorganisms in anaerobic biofilms. A survey of microorganism concentrations in aerobic biofilms (Williamson and McCarty, 1976a) found concentrations to range from 20 to 110 kg m^{-3}. Results of this study (given later) for anaerobic DSFF reactors have shown total biofilm solids (TFS) concentrations of up to 60 kg m^{-3} of biofilm at steady state. Volatile biofilm solids were 75-80% of TFS. Biofilm thicknesses of up to 2.6 mm were achieved.

The diffusivities of sucrose, glucose and acetate in water at 25°C are shown in Table 3.4. These are common substrates used in laboratory studies. A guide to estimate diffusivities of other compounds based on molecular weight is given in Table 3.5. Williamson and McCarty (1976a) considered it adequate to estimate diffusivities in the biofilm at about 80 percent of their value in water. This estimate will be used here.

Acetate yield from various substrates was calculated from the half reactions given by Christensen and McCarty (1975) for domestic waste, protein, carbohydrate and grease (Table 3.6). The yields in Table 3.6 have been calculated ignoring the yield of microorganisms. Depending on sludge age and other system operating conditions, the yield of acidogens will vary, which, in any case, will decrease acetate yields given in Table 3.6. Reported values of the yield factor for acidogens range from 0.2 to 0.70 g microorganism COD (g substrate COD)$^{-1}$ (Henze and Harremoes,

1982), assuming microorganisms to have a COD of 1.42 g (g volatile film solids)$^{-1}$ (VFS). Net yield will be somewhat less due to endogenous decay. It is significant to note that higher yields are associated with carbohydrate wastes.

COD concentrations in the mixed liquor can vary over a wide range depending on influent COD concentrations and operating conditions. It is not only the absolute concentrations of primary and intermediate substrates existing in the liquid but their ratio that determines R. Steady state results reported later for a range of organic loading rates and HRT have shown that the ratio of VA to other soluble organic compounds averaged 3:1 on a COD basis. The ratio ranged from 1:1 to 9:1. The major component of the VA was acetic acid. Below it is assumed that soluble compounds in the liquid are degradable and of relatively low molecular weight which would result in their having diffusivities on the order of that for glucose.

It is clear from the information given above that ß and Thiele moduli can vary over a wide range at given biofilm thicknesses. Glucose will be used as the primary substrate to calculate the modified effectiveness factor that could apply to many laboratory situations. Based on information in Table 3.6 a yield factor of 0.80 will be used. This is the yield of acetate from glucose reduced by a factor of about 20 percent to account for net acidogen yield. The ratio of S_{b1} to S_{b2} is 0.33 from above and the ratio of D_1

Table 3.4 Diffusivities[a,b] of Common Substrates in Anaerobic Studies

Species	D, $cm^2 d^{-1}$
sucrose	0.48
glucose	0.60
acetic acid	1.03

[a] At 25°C, D at another temperature may be found from $D_\mu T_k$ = constant where μ is solvent viscosity and T_k temperature in °K.

[b] Perry and Chilton (1973)

Table 3.5 Guide for Diffusivities Based on Molecular Weight[a]

Molecular weight	D, $cm^2 d^{-1}$
10	1.9
100	0.61
1,000	0.22
10,000	0.095
100,000	0.043
1,000,000	0.022

[a] Perry and Chilton (1973)

to D_2 is 0.58 from Table 3.4. These numbers fix the value of the ß modulus at 0.16.

To estimate the general Thiele moduli, typical kinetic coefficients for acidogens and methanogens suggested by Henze and Harremoes (1982), will be used (Table 3.7). Diffusion limitations will not exist in thin films; therefore a biofilm thickness of 1 mm was selected. Degradable soluble effluent COD is specified at 100, 1000 and 10,000 mg L^{-1} to typify effluent from a reactor receiving low, medium or high strength influent. Active VFS concentration in the biofilm will be arbitrarily taken as 10 kg m^{-3} for each group. For these conditions improvements in the effectiveness factor, R, are listed in Table 3.8. The modified effectiveness factor is significantly different from the effectiveness factor found considering acetate alone in two cases. As biofilm thickness increases the maximum change in effectiveness factor over the range of ϕ_o considered for a ß modulus value of 0.16 is approximately 7%. Considering the range of kinetic constants in Tables 3.2 and 3.3, it is possible in some circumstances that the ratio of ϕ_{o1} to ϕ_{o2} is greater than the maximum value considered here, which would increase the upper bound of the maximum change in effectiveness factor to a value greater than 7%.

To evaluate kinetic constants, the above approach must be applied to the data that arise in each case. If

Table 3.6 Yield of Acetate from Various Substrates[a]

Substrate	Yield, Y kg acetate COD(kg substrate COD)$^{-1}$
domestic waste	0.47
protein	0.86
carbohydrate	0.98
grease	0.98

[a] Based on half reactions in Christensen and McCarty (1975).

Table 3.7 Typical Values of Kinetic Coefficients at 35°C[a]

Culture	k gCOD(gVSS)$^{-1}$d^{-1}	K gCOD L^{-1}
acidogens	10	0.2
methanogens	10	0.05

[a] Henze and Harremoes (1982)
[b] Assuming 100% active VSS; k and VSS are assumed to be directly proportional to each other.

Table 3.8 R Values for Test Situation at 35 °C

S_{b1} mg L^{-1}	S_{b2} mg L^{-1}	K_1	K_2	ϕ_{e1}	ϕ_{e2}	η_2	R
25	75	0.125	1.5	3.24	2.98	0.335	1.072
250	750	1.25	15.0	2.08	1.02	0.909	1.065
2500	7500	12.5	150.0	0.73	0.31	1.000	1.027

substrates other than simple sugars are present as in domestic or many industrial wastes, the yield factor for acetate will decrease. Also the diffusivity ratio will decrease. It is possible in some reactors operated at high rates, that the ratio of soluble primary substrate to intermediate substrate in the liquid would increase, but for reactors achieving high removals, the ratio of S_{b1} to S_{b2} used above is probably near the maximum value. If all of these factors apply, they would result in a substantial decrease in the modulus. The amount of improvement in the effectiveness factor is also sensitive to the ratio between the Thiele moduli for each group. As this ratio becomes larger, the maximum change in the effectiveness factor increases. However at extreme high or low values of ϕ_{o1} the change in the effectiveness factor is much less than the maximum change regardless of the value of ϕ_{o2}. The overall analysis also depends on activities of each group in both liquid and biofilm phases.

3.4 Design of Fixed Biofilm Reactors

There are basically two different approaches to the design of wastewater treatment reactors:

1. The traditional approach by which years of experience are synthesized into permissible loading rates on which reactor design is based and a resulting degree of purification is expected.

2. The conceptual approach by which it is attempted to simulate the processes involved to such a degree that the purification result can be predicted.

The first approach has been the technique used to date for design of DSFF reactors. But it is dangerous to extrapolate to conditions outside the range of experience. The conceptual approach strives to incorporate main features of the process to increase the generality of the design approach.

Henze and Harremoes (1982) used the concept of SRT and biomass yield to develop an equation describing maximum volumetric organic loading (based on reactor volume) in fixed biofilm reactors.

$$B_v = B_{vd} + B_{vnd} \qquad 3.38a$$

Where B_v = maximum volumetric load, $(ML^{-3}T^{-1})$;

B_{vd} = load of biodegradable organics, $(ML^{-3}T^{-1})$;

B_{vnd} = load of non-biodegradable suspended organics, $(ML^{-3}T^{-1})$.

At the maximum volumetric organic loading rate, biomass removal is equal to biomass production rate. The SRT can then be described by Eq. 3.38b.

$$\theta_m = \frac{X}{Y_m B_{vd}} \qquad 3.38b$$

where:

X = total reactor biomass concentration, (ML^{-3});

θ_m = solids retention time, (T);

Y_H = biomass yield.

Rearranging Eq. 3.38b and substituting for B_{vd} in Eq. 3.38a results in Eq. 3.38c:

$$B_v = \frac{(X/\theta_m)}{Y_H} + B_{vnd} \qquad 3.38c$$

Figure 3.7 demonstrates the influence of Y_H and reactor biomass concentration on maximum volumetric organic loading rate.

Kennedy and van den Berg (1985) modified Eq. 3.38c to incorporate the effect of surface area to reactor volume ratio. The SRT in this case can be described by Eq. 3.39a.

$$\theta_m = \frac{aX_f' + X_L}{Y_H B_{vd}} \qquad 3.39a$$

Where a = support area to reactor volume ratio, (L^{-1});

X_f' = biofilm biomass areal concentration, (ML^{-2});

X_L = mixed liquor biomass concentration, (ML^{-3}).

Assuming that biomass in the mixed liquor is negligible Eq. 3.39a can be rearranged and substituted into Eq. 3.38a to give Eq. 3.39b.

$$B_v = \frac{(aX_f'/\theta_m)}{Y_H} + B_{vnd} \qquad 3.39b$$

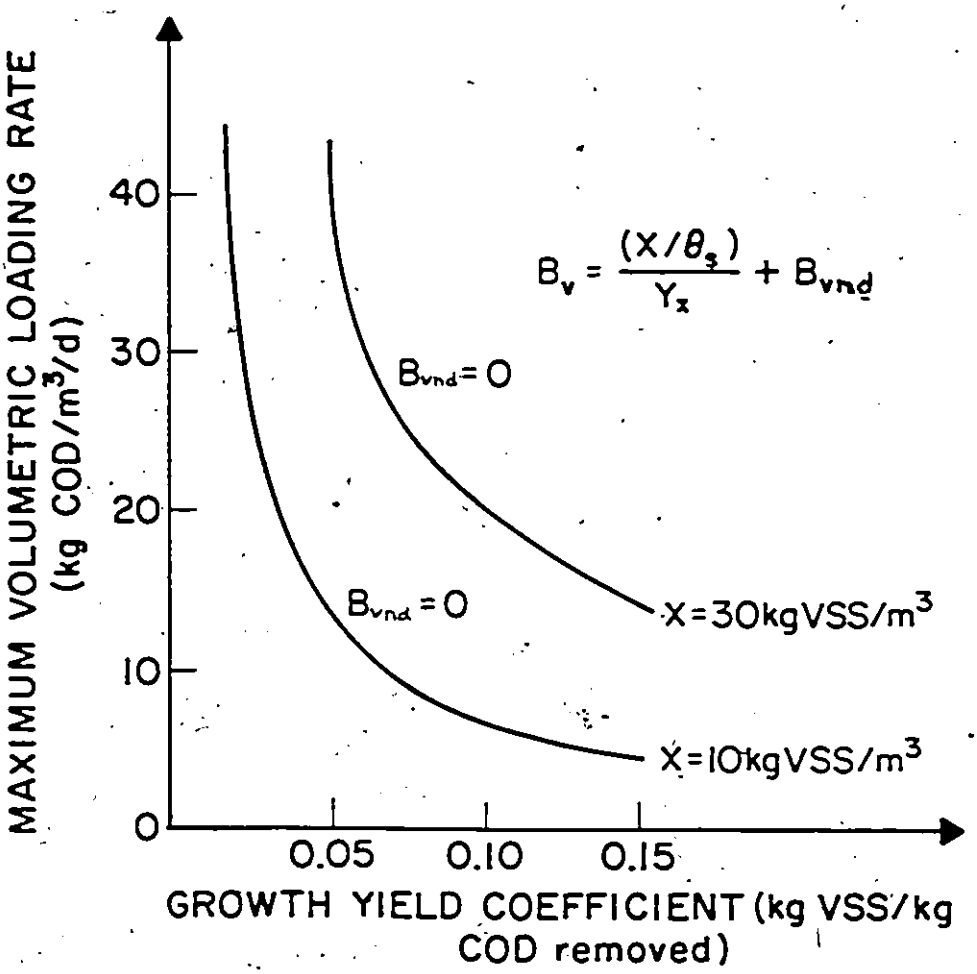

Figure 3.7 Effect of biomass yield and biomass concentration on maximum volumetric loading rate; (θ_s=20 days, B_{vnd}=0 kg COD $m^{-3}d^{-1}$) (Henze and Harremoes, 1982)

Figure 3.8 shows the effect of biomass yield and surface area to volume ratio on maximum volumetric loading rate. Equation 3.39b does not take into account physical problems that can be associated with reactors that have high surface area to volume ratios and thick biofilms. Channel diameter is important to optimize reactor performance and to avoid channel plugging. Optimum channel diameter is about 3.5 cm (van den Berg and Lentz, 1979) which corresponds to a surface area to volume ratio of approximately 100 m^2m^{-3}.

In terms of conceptual design the most relevant design and appraisal parameters are related to either unit surface of support media or to unit of sludge mass in the reactor.

If substrate only partially penetrates the biofilm or if wastewater is dominated by particulate matter that has to be adsorbed and hydrolyzed, then substrate removal has to be related to surface area of media in the reactor.

However, if substrate fully penetrates the biofilm, either because the biofilm is thin, substrate concentration is high or methane production causes an increased diffusional exchange, removal has to be related to a unit of sludge mass. This again has to be related to other design parameters that influence the sludge mass accumulated per unit surface of the media or per unit volume of reactor. The latter approach will be used to develop models describing DSFF reactor performance.

The following empirical steady state model development is based on the following assumptions:

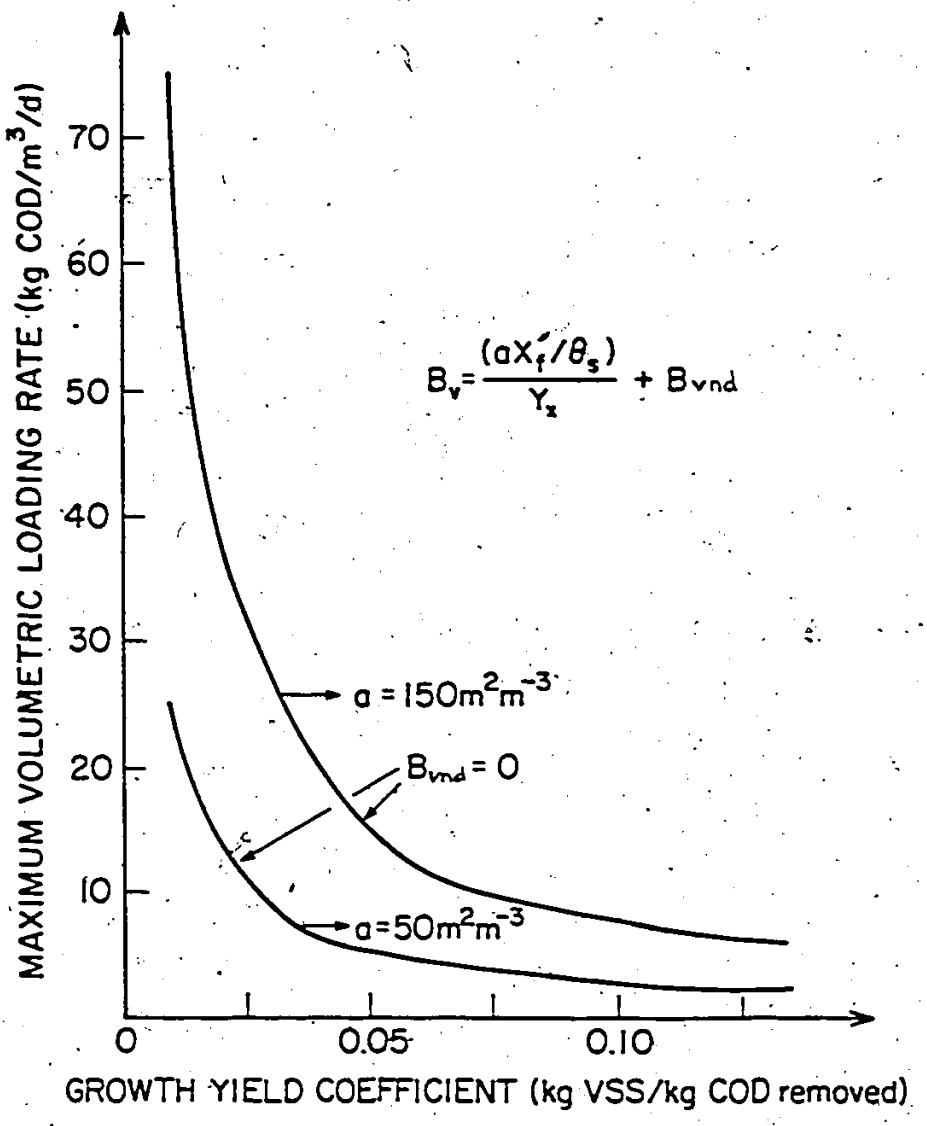

Figure 3.8. Effect of biomass yield and surface area to volume ratio on maximum volumetric loading rate; (θ_s=20 days; B_{vnd}=0 kg COD $m^{-1}d^{-1}$; X_f'=0.1 kg VSS m^{-2})

1. Anaerobic digestion is a process characterized by a heterogeneous microbial population metabolizing components of a complex waste. The rate limiting substrate is the soluble organics as determined by COD analysis.

2. Substrate completely penetrates the biofilm and no substrate gradient exists across the biofilm depth, L_f (*i.e.*, Thiele Modulus=0).

3. Biofilm accumulation rate is small and can be neglected.

4. Concentration of nonbiodegradable organic material in the reactors is small and can be neglected.

5. Reactor is completely mixed in terms of soluble substrate.

6. Relationship between biomass and substrate utilization can be described by Eq. 3.2.

7. Influent to the reactors is totally soluble and contains no biomass.

Based on the above assumptions a mass balance for substrate in the reactor gives Eq. 3.40.

$$\frac{dS}{dt} = \frac{Q}{V}(S_o - S) - \frac{u\,X}{Y_m} \qquad 3.40$$

Where S_o = influent substrate concentration, (ML^{-3});

V = reactor volume, (L^3);

Q = influent flow rate, (L^3T^{-1});

u = specific growth rate, (T^{-1}).

A mass balance for the microorganisms can be expressed as:

$$\frac{dX}{dt} = (u-b)X - \frac{Q}{V} X_L \qquad 3.41$$

Where b = decay rate, (T^{-1}).

The distribution of cell ages in a biological waste treatment process is such that significant numbers of cells are not in the log-growth phase. Eq. 3.41 incorporates a decay rate to account for endogenous bacterial respiration (Herbert, 1958).

At steady state, Eqs. 3.40 and 3.41 are written as:

$$X = Y_m (S_o - S) \frac{Q/V}{u} \qquad 3.42$$

$$u = \frac{Q\ X_L}{V\ X} + b \qquad 3.43$$

Defining the SRT or sludge age as:

$$\theta_c = \frac{V\ X}{Q\ X_L} \qquad 3.44$$

Equation 3.43 can then be written as follows:

$$u = \frac{1}{\theta_m} + b \qquad 3.45$$

Equation 3.45 can also be written as:

$$u = u_m + b \qquad 3.46$$

Where u_m = net specific growth rate, (T^{-1})

Specific growth rate of bacteria can be described by Eq. 3.47:

$$u = \frac{u_m S}{K+S} \qquad 3.47$$

Microbial substrate utilization is related to bacterial growth by Eq. 3.48:

$$U = \frac{-k\ S}{K+S} \qquad 3.48$$

Where U = specific substrate utilization rate, (T^{-1})

Equation 3.48 can be linearized using the Hanes method (Grady and Lim, 1980) to:

$$\frac{S}{U} = \frac{S}{k} + \frac{K}{k} \qquad 3.49$$

Equation 3.49 allows the kinetic parameters, k and K to be determined from routine reactor measurements.

Equations 3.46 and 3.48 can be combined and rearranged to give a linear expression for u_m:

$$u_n = -Y_n U - b \qquad 3.50$$

Equation 3.50 indicates that net specific growth rate, u_n, is directly related to specific substrate utilization rate, U. A plot of u_n versus U allows Y_n and b to be determined.

The maximum specific growth rate, u_m can be determined from Eq. 3.51:

$$u_m = Y_n k \qquad 3.51$$

These constants are valuable for kinetic analysis and allow one to determine the amount of solids which accumulate in the reactor.

If a model is to describe performance of a DSFF reactor it is important to know the relationship between HRT and SRT. In CSTR biological processes u_n and SRT^{-1} are equal to HRT^{-1} (Grady and Lim, 1980). This indicates that biomass growth and removal are dependent on the HRT of the system. In DSFF reactors biomass is attached to and growing on support media. In this case u_n and SRT^{-1} are equal to HRT^{-1} multiplied by a washout factor. Because of the difficulty in measuring film solids and consequently SRT in DSFF reactors, determination of a washout factor for individual wastes will allow reactor performance to be predicted as a function of easily measured parameters such as HRT or LRT.

If the biofilm accumulation rate is small and is neglected, then u_m for each steady state can be described by Eq. 3.52.

$$u_m = \frac{1}{\theta_m} = \frac{f}{\theta_H} \qquad 3.52$$

Where: f = washout factor, (0);

θ_H = hydraulic retention time, (T)

Implicit in the calculation of the kinetic parameters is the assumption that the system is at steady state and biomass concentration remains constant during the evaluation period. With the large biomass concentrations that exist in DSFF reactors (van den Berg *et. al.*, 1981) and low growth rates of anaerobic bacteria, biomass accumulation rates will be insignificant.

Combining and rearranging Eqs. 3.43, 3.46 3.47 and 3.52, COD removal efficiency, E, and reactor biomass concentration, X, can be predicted as a function of HRT using Eqs. 3.53 and 3.54.

$$E = \left[1 - \frac{K((f/\theta_H)+b)}{S_o(u_m-(f/\theta_H)-b)}\right] 100 \qquad 3.53$$

Where E = COD removal efficiency, (%)

$$X = \frac{Y_m(S_o-S)}{(f/\theta_H + b)\ \theta_H} \qquad 3.54$$

In Eq. 3.54, X describes the total biomass concentration in the reactor. Biofilm biomass can be determined by subtracting biomass in the mixed liquor.

3.5 Dynamic Anaerobic Reactor Models

The empirical model developed in Section 3.4 uses conventional CSTR theory and apparent kinetic constants to predict DSFF reactor efficiency and biomass concentration. This model is limited to steady state reactor operation and cannot be used to predict performance during startup or transient operation. In this section various dynamic models will be discussed leading to development of a dynamic model for DSFF reactors.

Andrews (1969) developed a deterministic one culture dynamic model to describe anaerobic treatment in a CSTR. Mass balance equations were developed that described interactions between gas, liquid and biological phases of an anaerobic CSTR system. Methanogenesis was considered to be rate limiting in the stepwise conversion of complex organics to methane and carbon dioxide. The key feature of this model was incorporation of an inhibition kinetic expression analogous to the Haldane function (Lenninger, 1975) in enzyme kinetics to describe microbial growth:

$$u = \frac{u_m}{1 + \frac{K}{S} + \frac{S}{K_i}} \qquad 3.55$$

Where K_a = inhibition constant, $(M\ L^{-3})$

The concentration of undissociated forms of short chain VA was assumed to be rate limiting and rate inhibiting. However, the concentration of undissociated acids is a function of both total concentration of acid and pH. To determine the concentration of undissociated acids, ionic equilibrium and gas transfer expressions were used to describe the carbonic acid system and the interaction between gas and liquid phases. Graef and Andrews (1974) extended this model to incorporate an expression for organism death induced by a conservative toxic agent. Buhr and Andrews (1977) employed this updated one culture model to simulate a thermophilic anaerobic CSTR. These dynamic models were tested and shown to predict fairly well the response of CSTR reactors to various transient conditions.

Massey and Pohland (1978) presented equations describing growth of microorganisms in a two phase anaerobic system. Equations for this two-culture system were derived from steady state mass balances around separate acid forming and methane forming CSTR. Although a dynamic model was not developed, this work described the separation of the two main cultures responsible for anaerobic digestion.

The steady state growth rate of acid forming bacteria was described by Eq. 3.56 assuming influent to be free of acid forming microorganisms.

$$u_1 = \frac{1+R^*_1}{\theta_{w1}} - \frac{R^*_1 X_{w1}}{\theta_{w1} X_1} + b_1 \qquad 3.56$$

Where R^* = recirculation ratio, (0);

X_{w1} = concentration of acidogens in recycle, (ML^{-3})

Subscript 1 refers to primary substrate and acidogens.

Similarly a mass balance for substrate around the acid forming reactor was described by Eq. 3.57:

$$\frac{S_{w1}}{\theta_{w1}} - \frac{S_1}{\theta_{w1}} = \frac{u_1}{Y_{w1}} X_1 \qquad 3.57$$

Combining Eqs. 3.56 and 3.57 resulted in the following steady state expression for biomass concentration in the acid forming reactor:

$$X_1 = \frac{Y_{w1}(S_{w1}-S_1)+R^* X_{w1}}{1+R^*_1+b_1\theta_{w1}} \qquad 3.58$$

Combining Eqs. 3.47, 3.56 and 3.58, substrate concentration in the acid phase reactor was described by Eq. 3.59:

$$S_1 = \frac{-g_1 \pm (g_1^2-4h_1m_1)^{1/2}}{2h_1} \qquad 3.59$$

Where $h_1 = u_{m1} - \frac{(1+R^*_1)}{\theta_{w1}} - b_1$

$$g_1 = \left(\frac{1+R^*_1}{\theta_{w1}} + b_1\right)(S_{e1}-K_1) - u_{m1}\left(S_{e1} + \frac{R^*_1 X_{R1}}{Y_{w1}}\right)$$

$$m_1 = S_{e1}K_1\left(\frac{1+R^*_1}{\theta_{w1}} + b_1\right)$$

By analogous reasoning, Eqs. 3.60, 3.61 and 3.62 were developed to describe specific growth rate, biomass concentration and substrate concentration in the methane phase reactor, respectively.

$$u_2 = \frac{1+R^*_2}{\theta_{w2}} - \frac{R^*_2 X_{R2}}{\theta_{w2} X_2} + b_2 \qquad 3.60$$

Where X_{r2} = concentration of methanogens in recycle, (ML^{-3})

Subscript 2 refers to intermediate substrate and methanogens

$$X_2 = \frac{Y_{w2}(S_{e2}-S_2) + R^*_2 X_{R2}}{1+R^*_2+b_2\theta_{w2}} \qquad 3.61$$

$$S_2 = \frac{-g_2 \pm (g_2^2 - 4h_2 m_2)^{1/2}}{2h_2} \qquad 3.62$$

Where $h_2 = u_{m2} - \frac{(1+R^*_2)}{\theta_{w2}} - b_2$

$$g_2 = \left(\frac{1+R^*_2}{\theta_{w2}} + b_2\right)(S_{e2}-K_2) - u_{m2}\left(S_{e2} + \frac{R^*_2 X_{R2}}{Y_{w2}}\right)$$

$$\mu_2 = S_{e2}K_2\left(\frac{1+R^{*}_{2}}{\theta_{c2}} + b_2\right)$$

Application of this model to two phase anaerobic digestion processes (Massey and Pohland, 1978) was found to give reasonable estimates of biomass and substrate concentrations in acid forming and methane forming CSTR.

Kleinstreuer and Poweigha (1982) combined the dynamic model of Graef and Andrews (1974) with the two culture model of Massey and Pohland (1978) and developed a dynamic model that distinguished between acid forming and methane forming bacteria coexisting in a single CSTR. This model had the capability to accommodate various substrate feeding modes, and simulated the transient physico-biochemical transport conversion processes occurring in the biological, liquid and gaseous phases. Dynamic simulations were not compared to actual reactor data because of difficulties in determining concentrations of acid forming and methane forming bacteria coexisting in a single CSTR.

In the remainder of this section, development of a dynamic DSFF reactor model will be discussed. The model will be a pseudo four-culture process that distinguishes between acid forming and methane forming bacteria in the biofilm and mixed liquor. All assumptions used for the steady state model except Number 2 will be valid. Intrinsic kinetic parameters not determined in this study but required for the model will be obtained from the literature.

Graef and Andrews (1974) and Kleinstreurer and Poweigha (1982) incorporated an inhibition function into their models to describe bacterial growth. At present there is still controversy over the exact nature of the limiting substrate and the effect on inhibition (Duarte, 1980; Zender, 1982). Additionally, DSFF reactors used in this study were heavily buffered to maintain constant pH. Therefore an inhibition function has been omitted as well as the ionic equilibrium and gas transfer equations used to determine changes in pH.

The dynamic DSFF model is based on biomass and substrate balances for acid forming bacteria and methane forming bacteria in the mixed liquor and biofilm.

Assuming that no diffusional resistance exists for biomass in suspension, growth rates of acid formers and methane formers in suspension can be described by Eqs. 3.63 and 3.64 respectively. The subscripts L and f refer to mixed liquor and biofilm respectively.

$$r_{g1L} = X_{1L}u_{1L} = \frac{u_{m1L}S_1X_{1L}}{K_{1L}+S_1} \qquad 3.63$$

$$r_{g2L} = X_{2L}u_{2L} = \frac{u_{m2L}S_2X_{2L}}{K_{2L}+S_2} \qquad 3.64$$

Where: r_{g1L} = growth rate of acid formers in suspension, $(ML^{-3}T^{-1})$;

r_{g2L} = growth rate of methane formers in suspension, $(ML^{-3}T^{-1})$.

Substrate removal for acid formers and methane formers in suspension can be described by Eqs. 3.65 and 3.66 respectively.

$$r_{s1L} = -\frac{1}{Y_{x1L}} u_{1L}X_{1L} = -\frac{u_{m1L}S_1X_{1L}}{Y_{x1L}(K_{1L} + S_1)} \qquad 3.65$$

$$r_{s2L} = -\frac{1}{Y_{x2L}} u_{2L}X_{2L} = -\frac{u_{m2L}S_2X_{2L}}{Y_{x2L}(K_{2L} + S_2)} \qquad 3.66$$

Where r_{s1L} = substrate removal rate by acid formers in suspension, $(ML^{-3}T^{-1})$;

r_{s2L} = substrate removal rate by methane formers in suspension, $(ML^{-3}T^{-1})$.

From Eqs. 3.3, 3.4 and 3.6 it has been shown that diffusion resistance can affect substrate utilization and biomass growth in biofilms. This can be taken into account by incorporating an efficiency factor into equations describing biomass growth and substrate utilization. The growth rate of acid formers and methane formers in the biofilm can be described by Eqs. 3.67 and 3.68.

$$r_{g1f} = X_{1f}u_{1f} = E'_1 \frac{u_{m1f}S_1X_{1f}}{K_{1f}+S_1} \qquad 3.67$$

$$r_{g2f} = X_{2f}u_{2f} = E'_2 \frac{u_{m2f}S_2X_{2f}}{K_{2f}+S_2} \qquad 3.68$$

Where r_{g1f} = growth rate of acid formers in biofilm, $(ML^{-3}T^{-1})$;

r_{g2f} = growth rate of methane formers in biofilm, $(ML^{-3}T^{-1})$;

E' = biofilm efficiency factor, (0).

Substrate removal for acid formers and methane formers in the biofilm can be described by Eqs. 3.69 and 3.70 respectively.

$$r_{m1f} = -\frac{1}{Y_{M1f}} u_{1f} X_{1f} = -E'_1 \frac{1}{Y_{M1f}} \frac{u_{m1f} S_1 X_{1f}}{K_{1f} + S_1} \qquad 3.69$$

$$r_{m2f} = -\frac{1}{Y_{M2f}} u_{2f} X_{2f} = -E'_2 \frac{1}{Y_{M2f}} \frac{u_{m2f} S_2 X_{2f}}{K_{2f} + S_2} \qquad 3.70$$

Where r_{m1f} = substrate removal rate by acid formers in the biofilm, $(ML^{-3}T^{-1})$;

r_{m2f} = substrate removal rate by methane formers in the biofilm, $(ML^{-3}T^{-1})$.

Biomass balances for acid forming and methane forming bacteria in the mixed liquor can be described by Eqs. 3.71 and 3.72 respectively. The biomass balances for the liquid and biofilm phases are dependent on the attachment and detachment rates of the respective groups of bacteria. First order expressions were assumed to describe these phenomena.

$$\frac{dX_{1L}}{dt} = \frac{(X_{e1}-X_{1L})}{\theta_H} + r_{e1L} - b_{1L}X_{1L} - A_1^*X_{1L} + D_1^*X_{1f} \qquad 3.71$$

Where A^* = biomass attachment rate, (T^{-1});

D^* = biofilm detachment rate, (T^{-1});

X_e = influent biomass concentration , (ML^{-3}).

$$\frac{dX_{2L}}{dt} = \left(\frac{(X_{e2}-X_{2L})}{\theta_H} + r_{e2L} - b_{2L}X_{2L} - A_2^*X_{2L} + D_2^*X_{2f}\right) \qquad 3.72$$

Equations 3.73 and 3.74 describe the concentrations of acid forming and methane forming bacteria in the biofilm respectively.

$$\frac{dX_{1f}}{dt} = A_1^*X_{1L} - D_1^*X_{1f} + r_{e1f} - b_{1f}X_{1f} \qquad 3.73$$

$$\frac{dX_{2f}}{dt} = A_2^*X_{2L} - D_2^*X_{2f} + r_{e2f} - b_{2f}X_{2f} \qquad 3.74$$

Equations 3.71, 3.72, 3.73 and 3.74 indicate that attachment and detachment rates can be different. However, there have been no studies providing evidence to suggest that attachment and detachment rates should differ between the various groups of anaerobic bacteria. If bacteria are randomly dispersed throughout the biofilm, detachment or sloughing rate would be the same for each group of bac-

teria. The most reasonable approximation for the first attempt at modeling this reactor is to use the same attachment and detachment rate coefficients respectively for each group of bacteria.

Equation 3.75 is a mass balance for primary substrate.

$$\frac{dS_1}{dt} = \frac{(S_{o1}-S_1)}{\theta_H} + (r_{m1L} - \frac{b_{1L}X_{1L}}{Y_{H1L}}) + (r_{m1\phi} - \frac{b_{1\phi}X_{1\phi}}{Y_{H1\phi}}) \qquad 3.75$$

The mass balance for intermediate substrate used for methane formation is described by Eq. 3.76. Similar to the developent in Section 3.3 a net acetate yield factor, Y_a, has also been incorporated into this development

$$\frac{dS_2}{dt} = \frac{(S_{o2}-S_2)}{\theta_H} + (r_{m2L} - \frac{b_{2L}X_{2L}}{Y_{H2L}}) + (r_{m2\phi} - \frac{b_{2\phi}X_{2\phi}}{Y_{H2\phi}})$$

$$- (r_{m1L} - \frac{b_{1L}X_{1L}}{Y_{H1L}})Y_a - (r_{m1\phi} - \frac{b_{1\phi}X_{1\phi}}{Y_{H1\phi}})Y_a \qquad 3.76$$

Equations 3.71, 3.72, 3.73, 3.74, 3.75 and 3.76 constitute a non-linear initial value problem. These first order differential equations can be solved simultaneously using the Runge Kutta technique and appropriate parameter values. A computer program solving these equations, written in Basic for an IBM personal computer is found in Appendix C. Calibration and discussion of this model will be dealt with in Chapter 5.

4. MATERIALS AND METHODS

To accomplish the objectives outlined in Chapter 1, a laboratory study was conducted over a 24 month period. In the course of this investigation a total of twelve anaerobic reactors were operated. The original anaerobic reactor was seeded with digester sludge from Greens Creek Wastewater Treatment facility, Ottawa, Canada. It was first cultured in a 100 L CSTR to allow acclimatization of the sludge to the test substrate and to wash out inorganic grit and other solids from the original sludge. Sludge from the CSTR was then used to inoculate various DSFF reactors used in this study.

4.1 Apparatus

4.1.1 Preliminary Culturing System

The CSTR used for culturing the original reactor seed was constructed using a 120 L Pyrex jar. The mouth of the jar was sealed with a 1.5 cm thick plexiglass plate fitted with a rubber gasket. Four metal rods running the length of the jar and anchored at the bottom to a wooden base plate insured that the reactor lid was secure and airtight. The plexiglass top plate had three holes bored into it. One hole opened into the headspace above the reactor liquid and served as an outlet for biogas. The two other holes had dip tubes made of 1.2 cm internal diameter (i.d.) PVC pipe

extending into the culture liquid to a depth of 20 cm to prevent air from entering the reactor. One dip tube was used for influent addition while the other was used for removing effluent.

Mixing was provided by a DC servo motor turning a stainless steel shaft with two 15 cm diameter flat blade turbine impellers at 50 rpm. To circumvent vortexing 4 equal-spaced baffles were incorporated into the reactor. Reactor biogas production was measured with a Precision Scientific wet test gas meter, then vented into a fume hood. A small glass tee fitted with a septum was placed in the gas line between the reactor and gas meter to facilitate gas sampling.

4.1.2 Startup and Steady State

Four laboratory scale DSFF reactors were constructed for use in Phases 1 (startup) and 2 (steady state) of the experimental study (Figs. 4.1 and 4.2). Each reactor consisted of a vertical tank (19.0 x 19.0 x 98.0 cm i.d.) made of 1.25 cm thick plexiglass and having an empty bed volume of 24.4 L. Each reactor was covered with a 2 cm thick removable plexiglass lid. The cover was sealed to the reactor with a rubber gasket and silicone grease. Seal integrity was maintained by pressure applied through eight bolts running through the cover plate and anchored to a 3 cm wide flange which was attached to the top of the reactor. The cover plate had two holes. One hole opened into the head

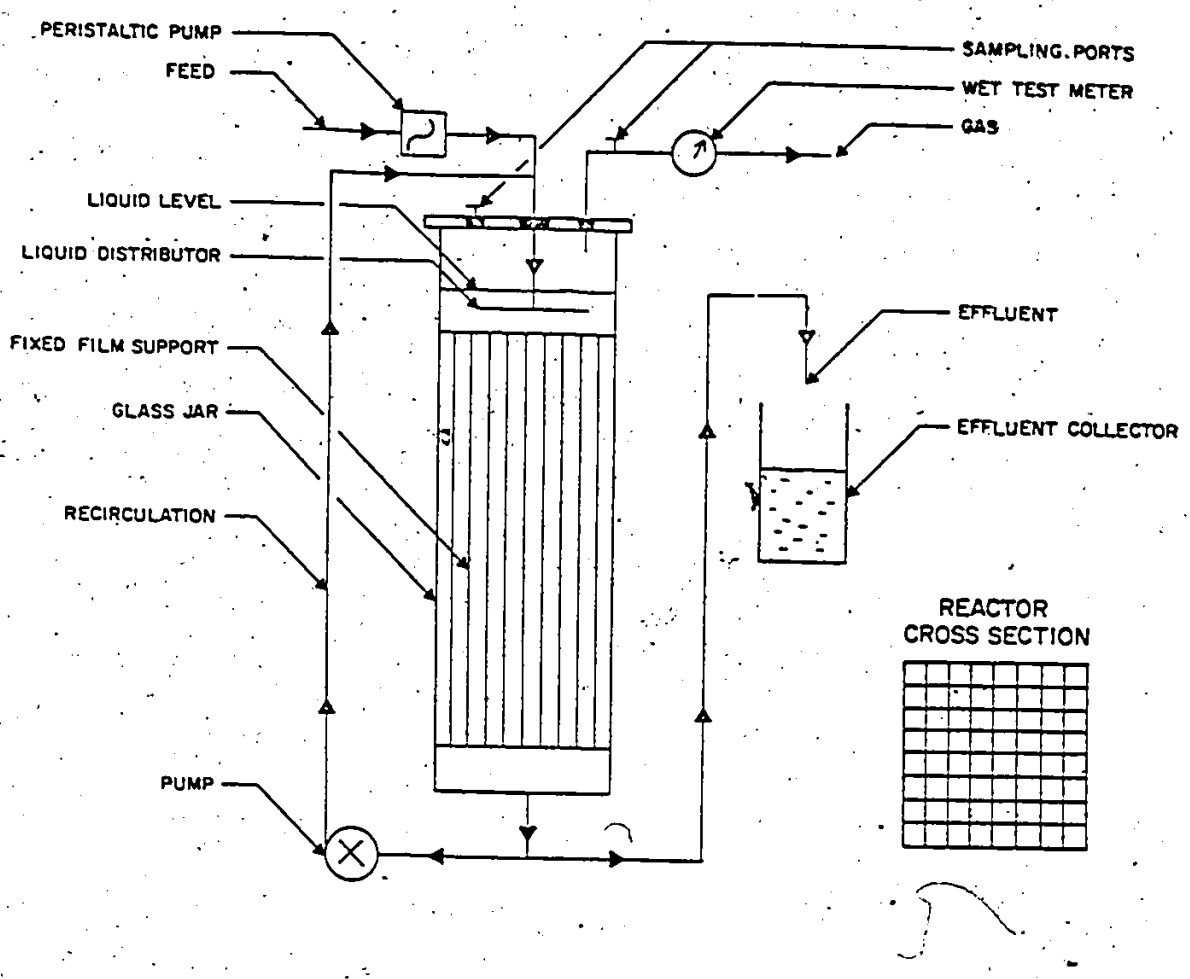

Figure 4.1 Setup of anaerobic DSFF reactor system

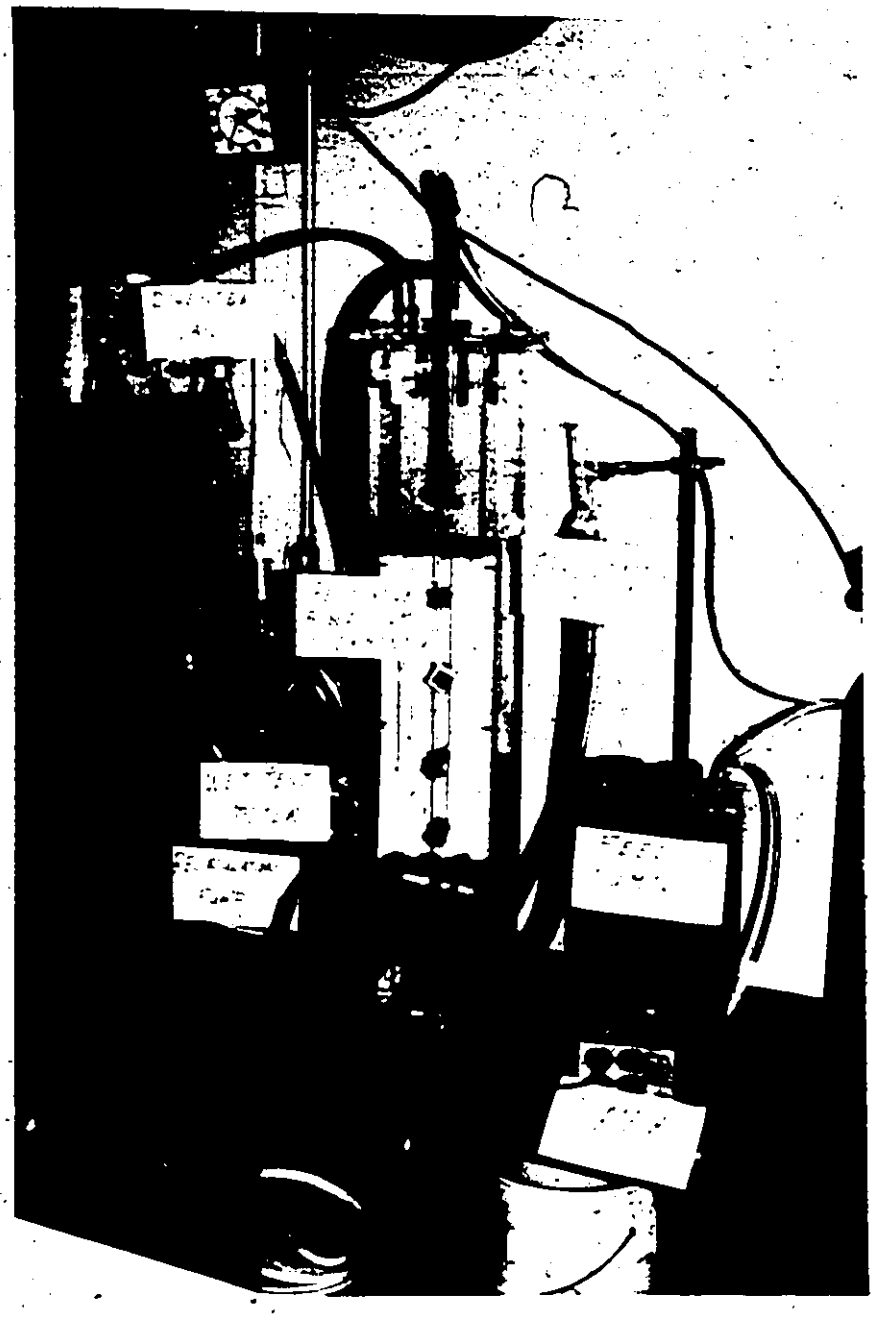

Figure 4.2 DSFF reactor setup

space and allowed biogas to escape. Biogas production was monitored with a Precision Scientific wet test gas meter then vented into a fume hood. A glass tee fitted with a septum was placed in the gas line between the reactor and the gas meter to facilitate determination of biogas quality. The second hole in the centre of the cover plate had a 1.25 cm i.d. dip tube fitted with a distribution manifold which was submerged 4 cm below the surface of the mixed liquor. Liquid was distributed horizontally at the top of the reactor through a distributor which was made from a PVC T-tube 6 cm long and 1.0 cm i.d.. The bottom of the DSFF reactor was tapered to one side at an angle of 45 degrees to minimize solids accumulation in the reactor bottom (Kennedy and van den Berg, 1981).

Effluent removal and reactor liquid level were controlled by a displacement system. Effluent was removed through a 1.3 cm i.d. hole located 4.0 cm from the bottom of the reactor and was attached by tygon tubing to a level overflow.

Internal recirculation maintained at 120 L d^{-1} was provided by a Masterflex positive displacement pump. Recirculation was taken from the bottom effluent port and returned to the top of the reactor by attaching the recirculation line to the feed line with a plastic Y connector. Influent was pumped continuously from a refrigerated reservoir (4°C) into the top of the reactor through a submerged distribution manifold with a variable

speed Harvard peristaltic pump. A glass tee fitted with a septum, for taking samples for determination of VA, was placed in the recirculation line, before the Y connector. Sampling ports were also placed at different points along the height of the reactor. Each port was 1.0 cm i.d. and extended 2.5 cm into the bulk reactor liquid to minimize any wall effects.

Each reactor was filled with oriented needle punched polyester (NPP; 3mm thick, 280 g m^{-2}; white; Texel Inc., Beauce Nord, Quebec) support material. Physical characteristics of the NPP material are summarized in Table 4.1. NPP material was selected because of the ease of construction, operation and effectiveness of DSFF reactors utilizing this support media (van den Berg and Kennedy, 1981a; Copp and Kennedy, 1983). NPP material was sewn on 316 stainless steel wire frames to make straight vertical channels 2.8 x 2.8 cm square and 61.0 cm long (Figs. 4.3 and 4.4). NPP media was supported 25.0 cm from the bottom of the reactor on a ledge 1.0 cm wide. The liquid level was maintained 5 cm above the top of the biofilm support material to protect the biofilm and to provide a volume for enhanced mixing of recirculated mixed liquor and influent. The active liquid volume was 22.4L.

Nine removable preweighed biofilm supports 61 cm long and 2.8 cm wide with a surface area of 338 cm^2 (two sides) were placed in the centre of each reactor and held in place on a plexiglass mounting rack (Figs. 4.4 and 4.5). These

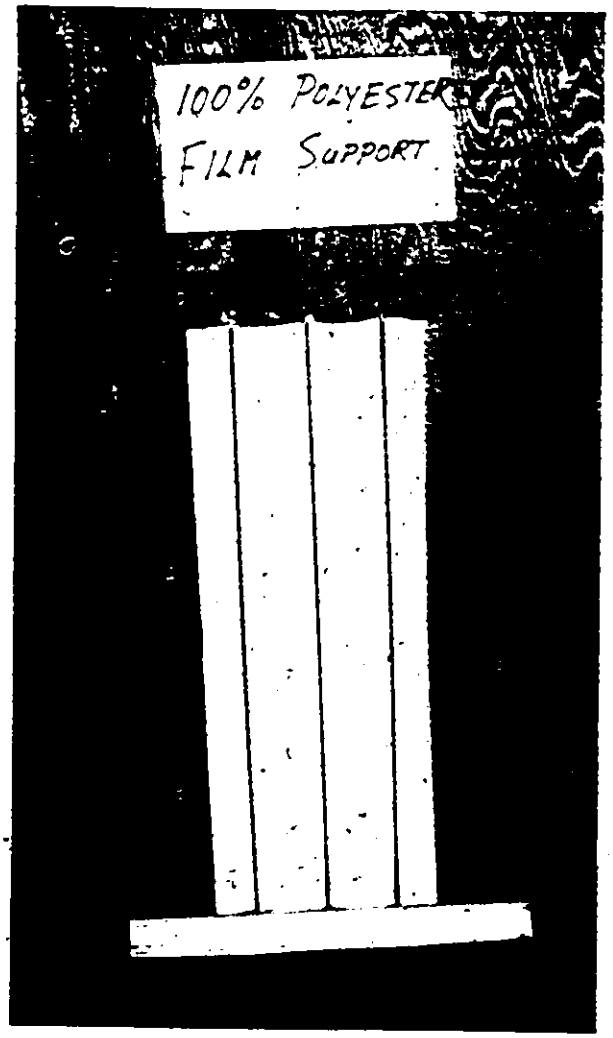

Figure 4.3 Photograph of NPP support material on stainless steel wire frame.

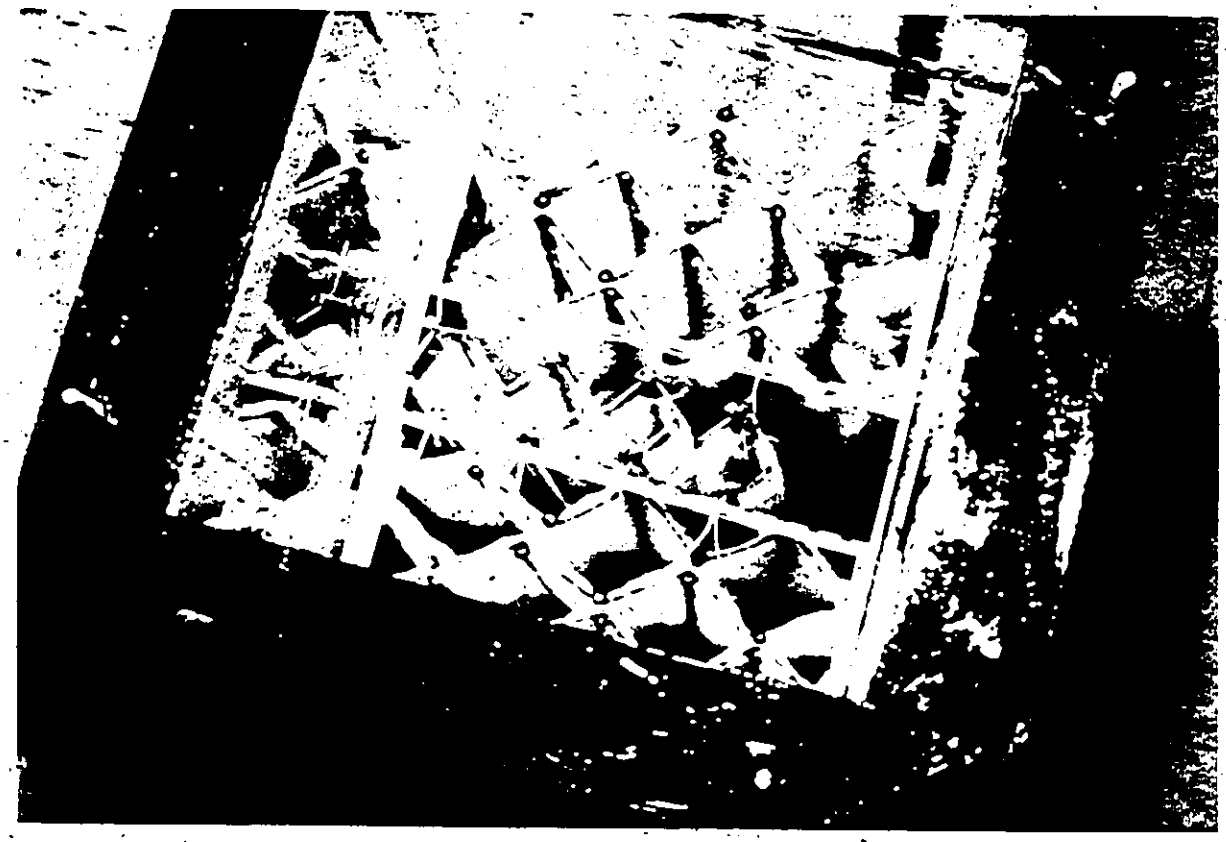

Figure 4.4 Fixed and removable NPP supports in DSFF reactor.

supports were removed at predetermined time intervals during startup (Phase 1) and after each steady state condition (Phase 2) for determination of biofilm concentration, average biofilm thickness and methanogenic or acetogenic microbial activity. Each removable biofilm support made up 2.0 % of the total biofilm surface area in the reactor and their removal and immediate replacement with a clean support would not significantly affect reactor performance.

Surface area to volume ratio was chosen based on the surface area optimization studies of van den Berg and Lentz (1979). Surface area to volume ratio was 75 $m^2\ m^{-3}$. This did not take into account the surface area of the reactor walls. Van den Berg and Lentz (1980) reported that on glass surfaces only casual biofilm deposition (Table 3.1) would occur during the time frame of these studies. Observations indicated that wall growth was negligible. Surface area to volume ratio was based on the average ratio with removable supports in place (80 $m^2\ m^{-3}$) and with removable supports absent (70 m^2/m^{-3}). Characteristics of DSFF reactors used in Phases 1 and 2 are summarized in Table 4.2. All reactors were located in a temperature controlled room maintained at 35 $\pm$ 1°C.

Table 4.1 Properties and Characteristics of NPP Material

Specific weight	1.38 g cm^{-3}
Color	white
Weight	280 g m^{-2}
Thickness	3.0 mm
Tensile strength	480 N
Tear propagation (trapezoid method)	275 N
Pore size	30–150 microns

Table 4.2 Physical Characteristics of DSFF Reactor

Parameter	
Height, cm	98.0
Inside dimensions, cm	19.0 x 19.0
Liquid volume, L	22.4
Empty bed volume, L	24.4
Surface area to volume ratio, m^2m^{-3}	75[a]
Voidage,	.92
Cross-section area of channels, cm^2	7.8

a average value (both sides of support material included)

Figure 4.5 Removable NPP support and plastic support rack.

4.2 Reactor Operation and Program of Experimentation

4.2.1 Preliminary Culturing System

The CSTR was operated in a semi-continuous fill and draw mode. At the start of each daily feeding cycle, 2.0 L of effluent was withdrawn from the reactor using a master-flex pump attached to the effluent dip tube. Effluent was then replaced by manual addition of influent through the influent dip tube. Since the working volume of the reactor was 100 L the HRT was 50 days. Culture medium (1 percent sucrose and mineral salts media; Table 4.5) was stored at 4°C until used. Total and volatile suspended solids concentration, as well as methanogenic activity of the reactor mixed liquor, was periodically checked to ensure that a healthy inoculum was maintained. The CSTR was operated in a temperature controlled room at 35 ± 1°C.

4.2.2 Startup

Three DSFF reactors were started with mixed liquor from the preliminary culturing anaerobic CSTR acclimated to sucrose wastewater. Acclimated inoculum was used rather than domestic sewage sludge to minimize any effects due to microbial adaptation. Additionally, to create a set starting point for future startup experiments methanogenic activity of the inoculum (22.4 L) was diluted to 1.5 g acetic acid utilized L^{-1} d^{-1} with tap water. This procedure standardized the inoculum and allowed startup runs conducted at

different times to be compared since effects due to quality of inoculum were eliminated. Following standardization, 22.4L of inoculum was added to each reactor (Fig. 4.6). Characteristics of the inoculum are summarized in Table 4.3.

Table 4.3 Characteristics of Inoculum (Phase 1)

Parameter	Run 1	Run 2
Waste acclimated to	1.0 %	sucrose
Total COD, g L^{-1}	5.9	6.3
Soluble COD, g L^{-1}	0.8	0.6
Suspended COD, g L^{-1}	5.1	5.7
Methanogenic activity, g acetic acid $L^{-1}d^{-1}$	1.5	1.5
Specific methanogenic activity, g acetic acid (g suspended COD)$^{-1}d^{-1}$	0.30	0.26

Following inoculation, the three DSFF reactors were initially operated at an HRT of approximately 30-40 days with sucrose wastewaters with approximate COD concentrations of 5,000, 10,000, and 20,000 mg L^{-1} (Table 4.5), respectively. The recirculation rate was 120 L d^{-1} (5.4 v v^{-1} d^{-1}).

Daily feed rates were slowly increased in increments of 5-15 % on a daily basis while maintaining VA in the mixed liquor between 200-500 mg L^{-1} (acetic acid equivalents; Run 1). Depending on the VA concentration, reactor feed rates

Figure 4.6 Inoculation of DSFF reactor.

were either increased, decreased or maintained constant. If VA were less than the preset limit, loading rates were increased 5-15 percent. When VA were above the preset limit, daily loading rates were decreased in increments of 5-20 percent until the VA concentration was within the preset limits. If VA were at the upper limit of the preset concentration range, loading rates were maintained constant until there was an increase or a decrease in the VA concentration in the reactor.

VA concentration and quality of biogas were determined from grab samples taken on a daily basis. Biogas production was also measured daily. COD's were determined 2-3 times a week on 24 hour composite samples that were not refrigerated. Volatile suspended solids (VSS) in the mixed liquor were determined assuming 1.42 g of suspended COD equals 1.0 g of VSS (Lawerence and McCarty, 1968). Alkalinity, Eh and pH were determined weekly from grab samples. Periodically samples were taken from sample ports along the height of the reactor for determination of VA or COD reactor profiles. Biofilm biomass, biofilm microbial activity and mixed liquor microbial activity were determined on a weekly basis

The second run of this experimental phase was conducted maintaining higher VA concentrations in the reactor mixed liquor during startup. The three reactors used in Run 1 were used in this run with no changes. Reactors were restarted with all conditions of startup and sample analyses similar to those discussed above except the VA concentration

of the mixed liquor was maintained between 1000-1500 mg L^{-1} (acetic acid equivalents). Higher VA concentrations in the mixed liquor were achieved by increasing the loading rate in daily increments of 5-20 % and running the DSFF reactors at higher organic and hydraulic loading rates.

4.2.3 Steady State

Effect of substrate concentration on steady state DSFF reactor performance was conducted with four reactors treating sucrose wastewater, with approximate COD concentrations of 2,500, 5,000, 10,000 and 20,000 mg L-1 (Table 4.5). Reactors were started using the technique described in Section 4.2.2. Conditions were identical to Run 1 except that removable supports were not taken out of the reactor during startup. Startup took approximately 4 months.

Following startup each reactor was to be operated at 5 different steady state HRT ranging between 0.4 and 7.0 days (starting at the longest HRT and progressing to the shortest HRT). Steady state data was obtained by operating each reactor for a minimum of 30 days at each HRT which corresponds to operation for a minimum of 8-75 HRT at each steady state condition. Complete steady state evaluation including startup took 11 months. After 30 days of operation at a particular steady state condition, samples were taken on 3 successive days and the average of the three data points reported. If a large discrepancy existed among any of the

data points the steady state period was extended and reactors resampled.

Routine reactor performance was assessed by determining influent feed rate, rate of biogas production, biogas composition and VA concentration on a daily basis while COD and pH of the influent and effluent were determined on a weekly or biweekly bases (three consecutive days during steady state evaluation).

On the final day of each steady state condition (third steady state sampling day) two removable biofilms were taken from each reactor for determination of biofilm volume, TFS and VFS. At each steady state COD and VA profiles in the reactors were determined by sampling from the side ports along the height of the reactors.

4.2.4 Microbial Activity Tests

A technique was developed for the determination of microbial activity in the mixed liquor and biofilm. On a weekly basis during startup and at the conclusion of each steady state condition, removable biofilm supports were taken from each DSFF reactor and transferred anaerobically in a bell jar (Fig. 4.7a, b) flushed with a nitrogen-carbon dioxide gas mixture (60/40) to a glass activity test chamber (Figs. 4.8 and 4.9).

The activity chamber was 63 cm long and had an internal diameter of 3.0 cm. The top of the chamber was flared to 15 cm to accommodate a number 12 stopper which was used

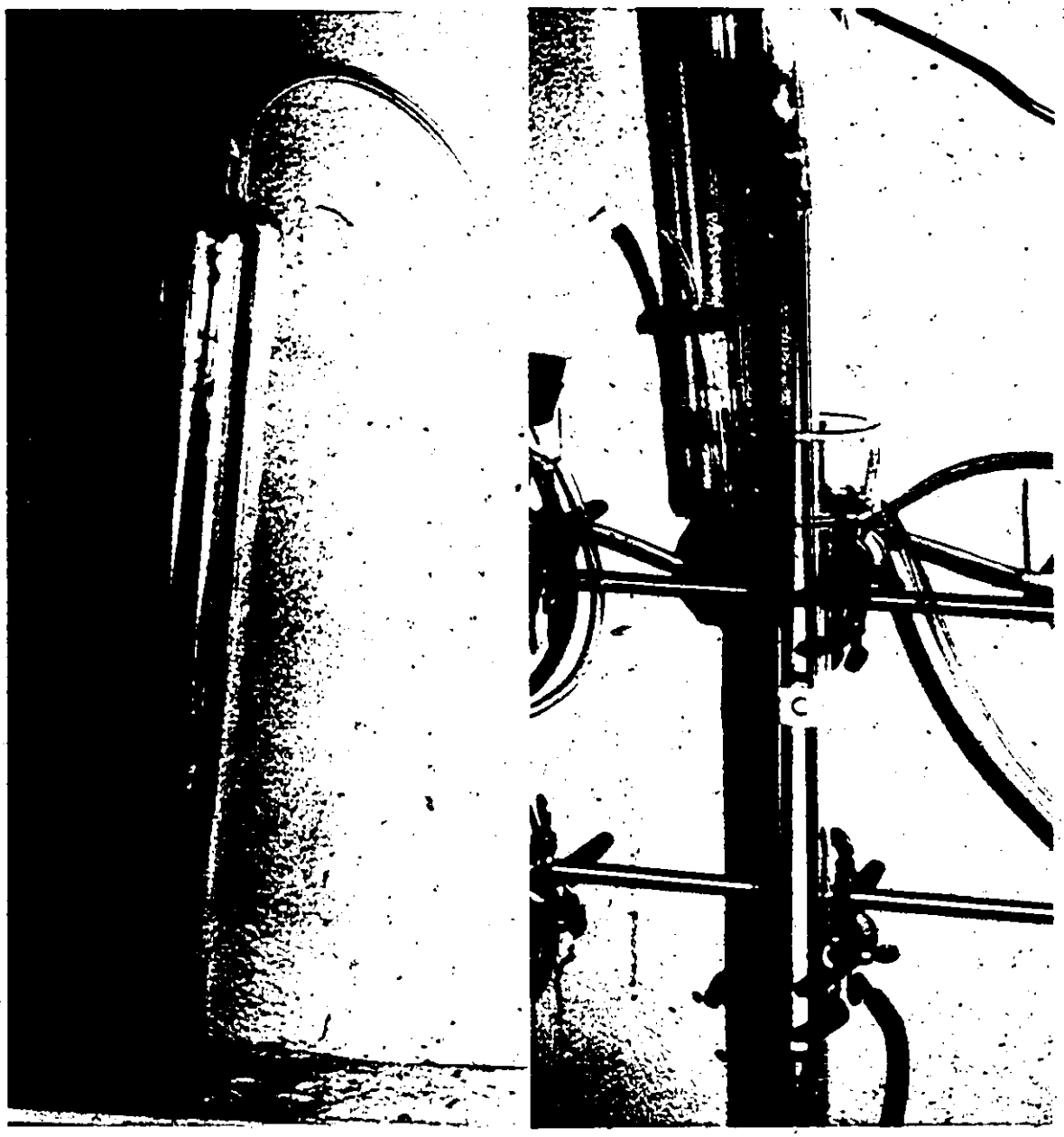

(a) (b)

Figure 4.7 Bell jar transfer chamber (a) and transfer of removable biofilm support into activity test chamber (b).

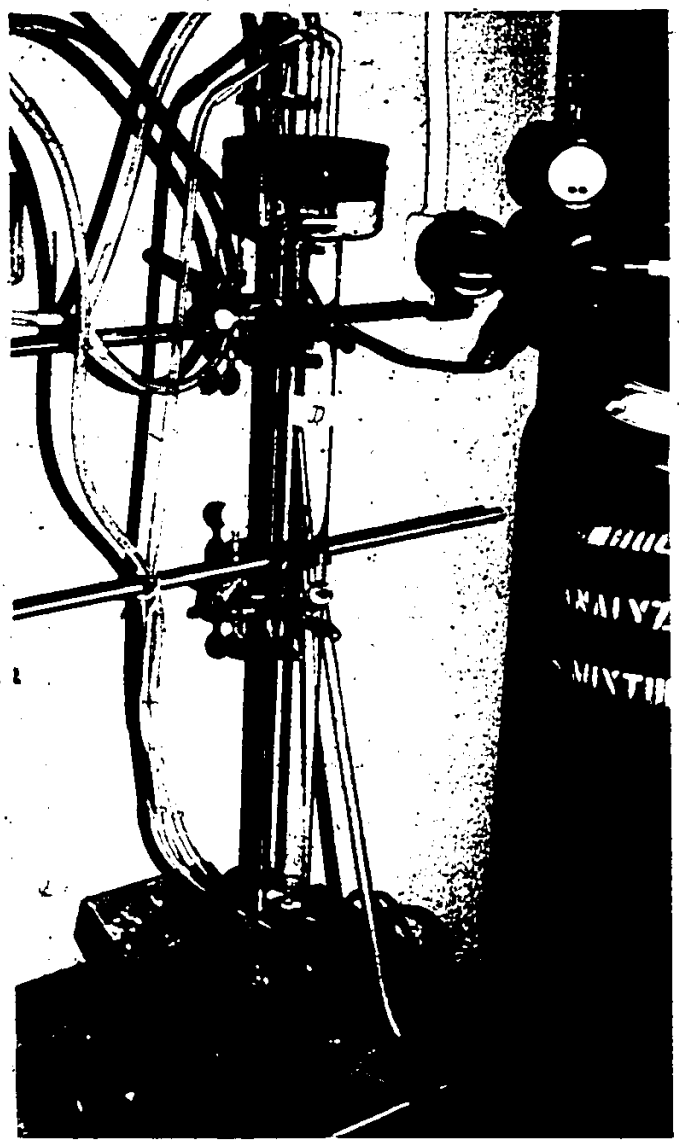

Figure 4.8 Biofilm activity chamber.

to seal the system. The stopper had two holes bored into it. One hole opened into the headspace above the reactor liquid and served as an outlet for biogas. The biogas outlet was connected by tygon tubing to a water trap before being vented to a fume hood. The other hole in the rubber stopper had a dip tube with a small plastic tee extending 1.5 cm into the mixed liquor for liquid distribution. The dip tube was connected to a 0.8 cm opening in the bottom of the test chamber with tygon tubing connected to a Masterflex pump. The Masterflex pump recirculated the reactor mixed liquor from the bottom to the top of the reactor. A septum placed 33 cm from the bottom of the test chamber was included for reactor sampling. The activity chamber setup is shown in Fig. 4.10.

Biofilm supports were immersed into 650 ml of reduced media which had the same composition as the 10,000 mg L-1 sucrose feed (Table 4.5) without the carbon source. Surface area to volume ratio of the activity test system with removable fixed films in place was 50 m^2 m^{-3}. Reactor liquid was sparged through the septum with a nitrogen-carbon dioxide mixture (60/40) to reduce the media, thus minimizing effects of oxygen on the microbes. Resazurin, which undergoes a colorimetric change at an Eh of -117 mV, was used to indicate if the liquid media was suitably reduced.

A small volume of concentrated carbon source (usually acetate, Table 4.4) was introduced into the test chamber through the septum to produce the desired initial concentra-

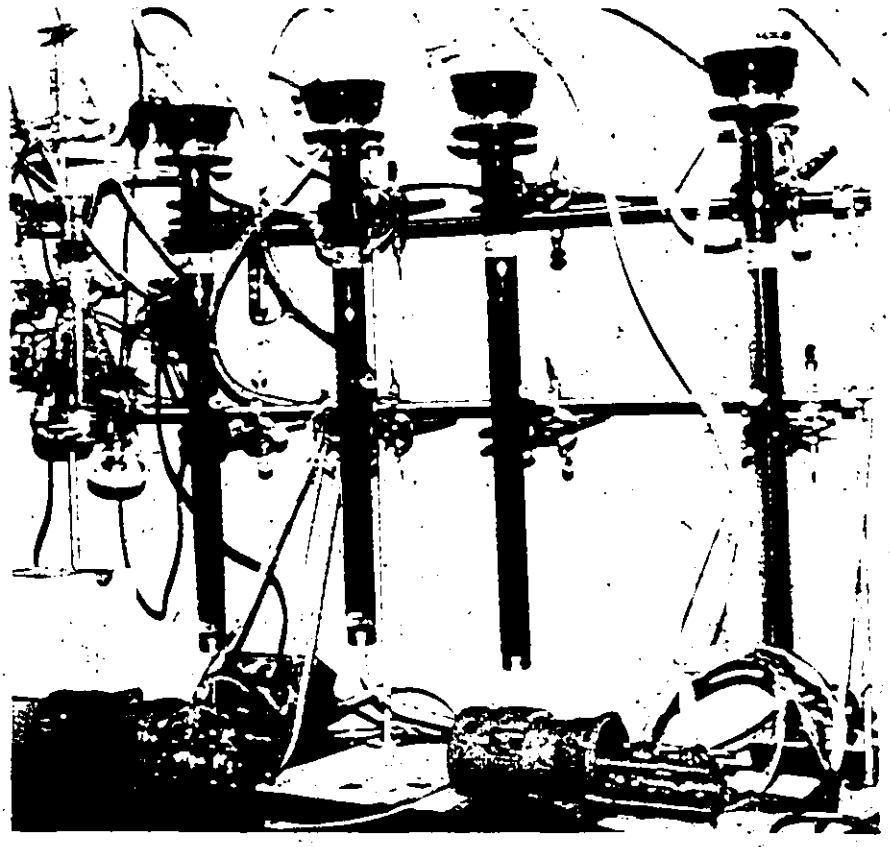

Figure 4.9 Photograph of removable biofilms in activity chamber.

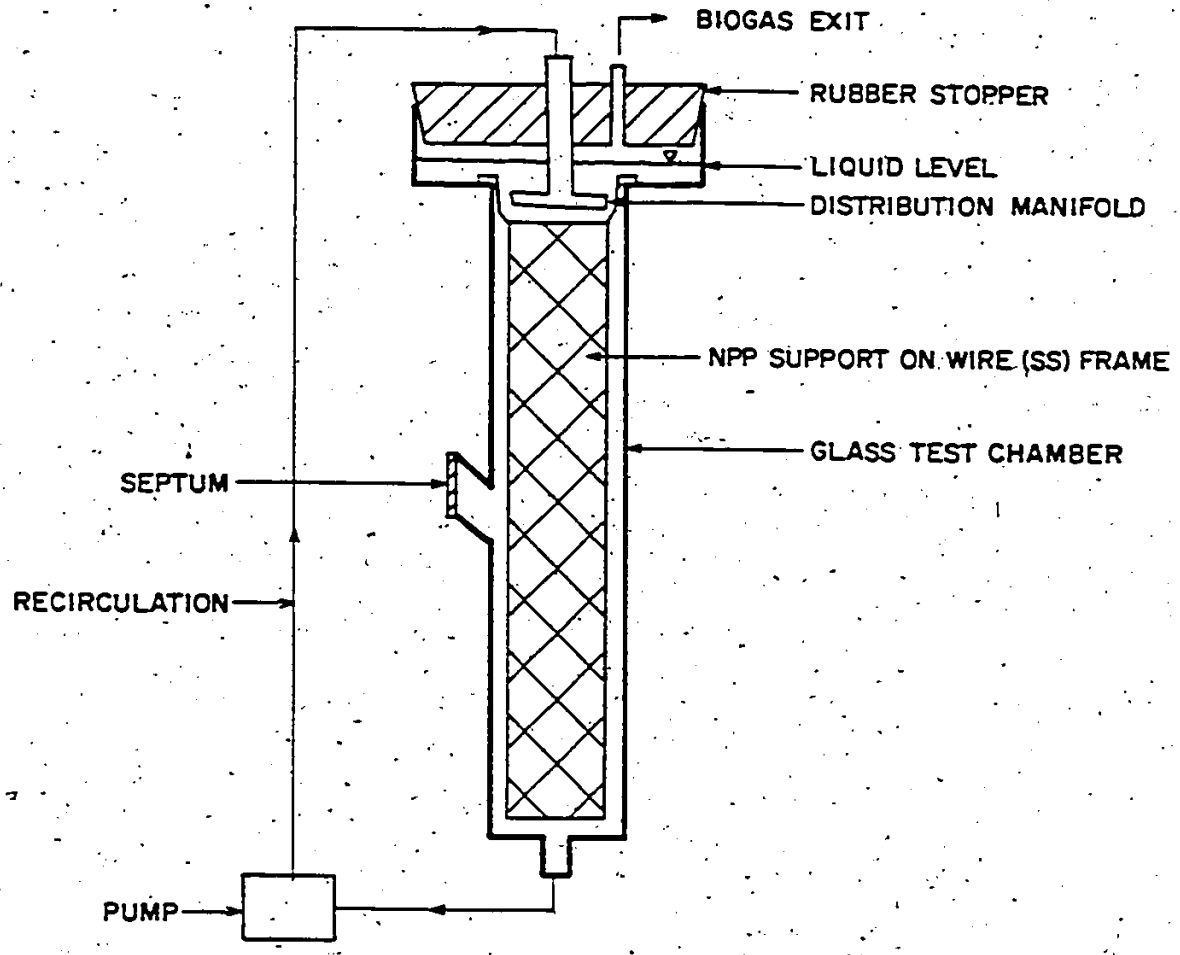

Figure 4.10 Schematic of activity chamber setup.

tion of substrate. The test chamber contents were recirculated at a rate of 200 mL min^{-1} (0.7 cm s^{-1}) to ensure complete mixed conditions and minimize external mass transfer resistance in the liquid. Grab samples were analyzed and the initial rate of substrate removal determined (Appendix F) for different substrate concentrations. Substrate utilization rates, using sucrose as the substrate, were run over a maximum time of 8 hours to minimize additional accumulation of biomass on the biofilm.

Microbial activity tests similar to those conducted on biofilm supports were also conducted on the mixed liquor. Grab samples of 40 mL were removed from the reactor recirculation line and transferred into serum vials using anaerobic techniques. A carbon source was then injected into the serum vial. Vials were placed on a New Brunswick 4556 shaker rotating at 40 rpm. Acidogenic and methanogenic activities of the mixed liquor were determined from initial sucrose or acetate utilization rates respectively. Biofilm and mixed liquor activity tests were conducted in a room maintained at 35 $\pm$ 1°C.

4.3 Biofilm Characterization

After methanogenic or acidogenic activity of the biofilm was determined, the support media was removed from the test chamber for determination of TFS (total film solids) and VFS (volatile film solids). TFS were determined by drying samples at 105°C for twentyfour hours, samples were then

Table 4.4 Acetate Media for Methanogenic Activity Tests

Solution A 12.8 g ammonia acetate

16.4 g potassium acetate

per 100 mL H_2O

Solution B 18.3 g sodium acetate

6.7 g glacial acetic acid

per 100 mL H_2O

Equal volumes of solutions A and B were added to 1.0 % mineral salts medium to give desired acetate concentration.

Table 4.5 Composition of Sucrose Wastes

	g L^{-1}	g L^{-1}	g L^{-1}	g L^{-1}
Sucrose	20.0	10.0	5.0	2.5
$(NH_4)HCO_3$	4.0	2.0	1.0	0.5
$Na(HCO_3)$	2.0	2.4	2.5	2.6
KH_2CO_3	2.0	2.6	3.1	3.6
$(NH_4)_2SO_4$	1.00	0.50	0.25	0.130
K_2HPO_4	0.52	0.26	0.13	0.065
KH_2PO_4	0.40	0.20	0.10	0.050
Yeast extract	0.020	0.10	0.05	0.025

cooled in a desiccator, and weighed. To determine VFS, dried solids were ashed at 560°C for 20 minutes, cooled in a desiccator and weighed again. A blank was carried through all steps. In the latter stages of biofilm development average biofilm thickness was also determined. Biofilms removed from the test chamber were allowed to air dry (35°C) for 5 minutes, then, by gently scraping biofilm and associated bound water into a graduated cylinder, its volume was determined. An average relationship was determined between biofilm volume and VFS (Appendix E). Knowing the flat surface area of the support material as well as the relationship between biofilm volume and VFS average biofilm thickness was calculated from Eq. 4.1:

$$L_f = \frac{V_f}{A} \qquad 4.1$$

Where V_f = volume of biofilm and bound water, (L^{-3});

A = surface area of support, (L^{-2}).

4.4 Mixing Studies

Mixing studies were run using tritium as a tracer to determine the mixing regime in the reactors. These studies were performed after startup had been completed on the reactor receiving 5,000 mg COD L^{-1} sucrose wastewater. Tracer was injected as a pulse during normal reactor operation. Effluent samples were collected with a Gilson 201 fraction collector every 15 minutes during the first 2 hours, every

30 minutes for the next 2 hours and every hour over the remaining time. Total sampling time was about three HRT.

Three individual runs at HRT of 0.9, 3.0, and 15.0 days, respectively, were made. Mixing analyses over this wide range of HRT were conducted on the DSFF reactor treating one of the most dilute wastewaters since this reactor produced the least amount of biogas for a particular HRT. Reactor mixing profiles from this reactor would be the least affected from the benefits of biogas mixing and would represent the poorest mixing regime possible for DSFF reactors used in this study. This test was conducted before the reactor treating 2,500 mg COD L^{-1} wastewater was operating.

4.5 Composition of Wastewater

The soluble carbon source was sucrose. Substrate was made by diluting a 20,000 mg L^{-1} stock sucrose solution. Reactors were operated with approximate COD concentrations of 2,500, 5,000, 10,000 and 20,000 mg L^{-1} (assuming that 1 g of sucrose equals 1 g COD; Table 4.5). Substrate was maintained at 4°C and was not preheated before being added to the reactors. To minimize degradation of substrate in the storage tanks, feed was replaced every 5 days. To maintain the same buffering capacity, additional alkalinity was added to the 0.25, 0.5 and 1.0 % feeds from an equimolar mixture of $KHCO_3$ and $NaHCO_3$.

4.6 Analytical Techniques

4.6.1 Biogas Quality

Biogas composition (methane and carbon dioxide) was determined by the gas chromatography method of van Huyssteen (1967). This technique involved using a Porapak T column (6.35 mm x 304.3 cm) on a Hewlett-Packard 5710a gas chromatograph equipped with a thermal conductivity detector and a model 3380A integrator. The column was held at 70 °C and helium flowing at a rate of 40 ml min^{-1} was used as the carrier gas.

4.6.2 VA Determinations

VA were determined by the method of Ackman (1972) using a Hewlett-Packard 5721A gas chromatograph equipped with an automatic sampler, flame ionization detector, model 3380A integrator, and Chromosorb 101 glass column (6.35 mm x 365.76 cm). The column was kept at 180 °C. Temperature of the flame ionization detector was 350 °C. Helium passing over formic acid at a flow rate of 15 ml min^{-1} was used as the carrier gas. VA samples were prepared by adding 0.5 ml of sample to 0.5 ml of an internal standard that contained 1000 mg L^{-1} of isobutyric acid. The chromatograph was calibrated with a standard that contained 1000 mg L^{-1} each of acetic, propionic, butyric, and isobutyric acids. The volume of sample injected (on the column packing) was 0.8 uL.

4.6.3 pH

The pH of grab samples was determined using a combination electrode connected to a Fisher model 620 pH meter.

4.6.4 Eh

Eh was determined by the method of Patel (1981) using a platinum electrode and Fisher model 620 pH meter.

4.6.5 Alkalinity

Alkalinity was determined by methyl orange indicator as described in APHA (1975).

4.6.6 COD

COD was determined by the colorimetric method of Knechtel (1979). For soluble COD, samples were centrifuged at 10,000 g for 20 minutes, and the supernatant used for COD analysis. Insoluble COD was determined by the difference between total COD and soluble COD.

4.6.7 Sucrose

Sucrose concentration was determined using the Phenol technique (Herbert, 1963).

5. Results and Discussion

Anaerobic DSFF reactors were operated for a period of 24 months. The first 15 months were used to evaluate start-up (Phase 1) and last 8 months to study steady state (Phase 2) reactor performance. Major parameters examined during Phases 1 and 2 were influence of influent substrate concentration, VA concentration, HRT and organic loading rate on DSFF reactor efficiency and biofilm development. Batch methanogenic activity tests were also conducted to evaluate and compare intrinsic biofilm kinetic constants, K and k during startup and steady state reactor operation.

5.1 Mixing Regime

Results from mixing studies indicated that over the range of HRT tested, multiple channel DSFF reactors had tracer curves similar to CSTR (Appendix A). Also, VA samples taken from different depths in DSFF reactors during startup and steady state operation indicated that no concentration gradients existed in the mixed liquor (discussed in Section 5.3). The complete mixed nature of DSFF reactors is attributed to the high recirculation rate and to a gas lift pump effect in which mixed liquor in some channels moved in a downward direction while liquid in other channels traveled upward (Hall, 1982; Samson *et al.*, 1984a). Measurement of

individual parameters from any point in DSFF reactors were representative of the whole reactor.

5.2 DSFF Reactor Startup

In Phase 1, reactors A, B and C refer to DSFF reactors receiving influent sucrose concentrations of 0.5, 1.0 and 2.0 percent (w/v), respectively. Results of 2 runs are discussed. Run 1 evaluates the effects of maintaining VA (acetic acid equivalents) between 200-500 mg L^{-1} while for the second run VA were maintained at 1000-1500 mg L^{-1}.

5.2.1 General Reactor Performance

Figures 5.1a, b and c show the range in which mixed liquor VA concentrations were maintained and average VA concentration for each reactor during startup (Run 1). These results demonstrate that with careful operation, controlled startup can be effected. With dilute wastewater (Fig. 5.1a) VA concentrations could be controlled more easily than with concentrated wastewater (Figs. 5.1b, c). Periodic pH and Eh measurements indicated that for the most part, all reactors operated between 6.8-7.6 and -270 to -390 mV, respectively. These are within acceptable operating limits (Grady and Lim, 1980). All reactors in Run 1 had Eh values between -170 to -190 mV for the first 20 days of operation.

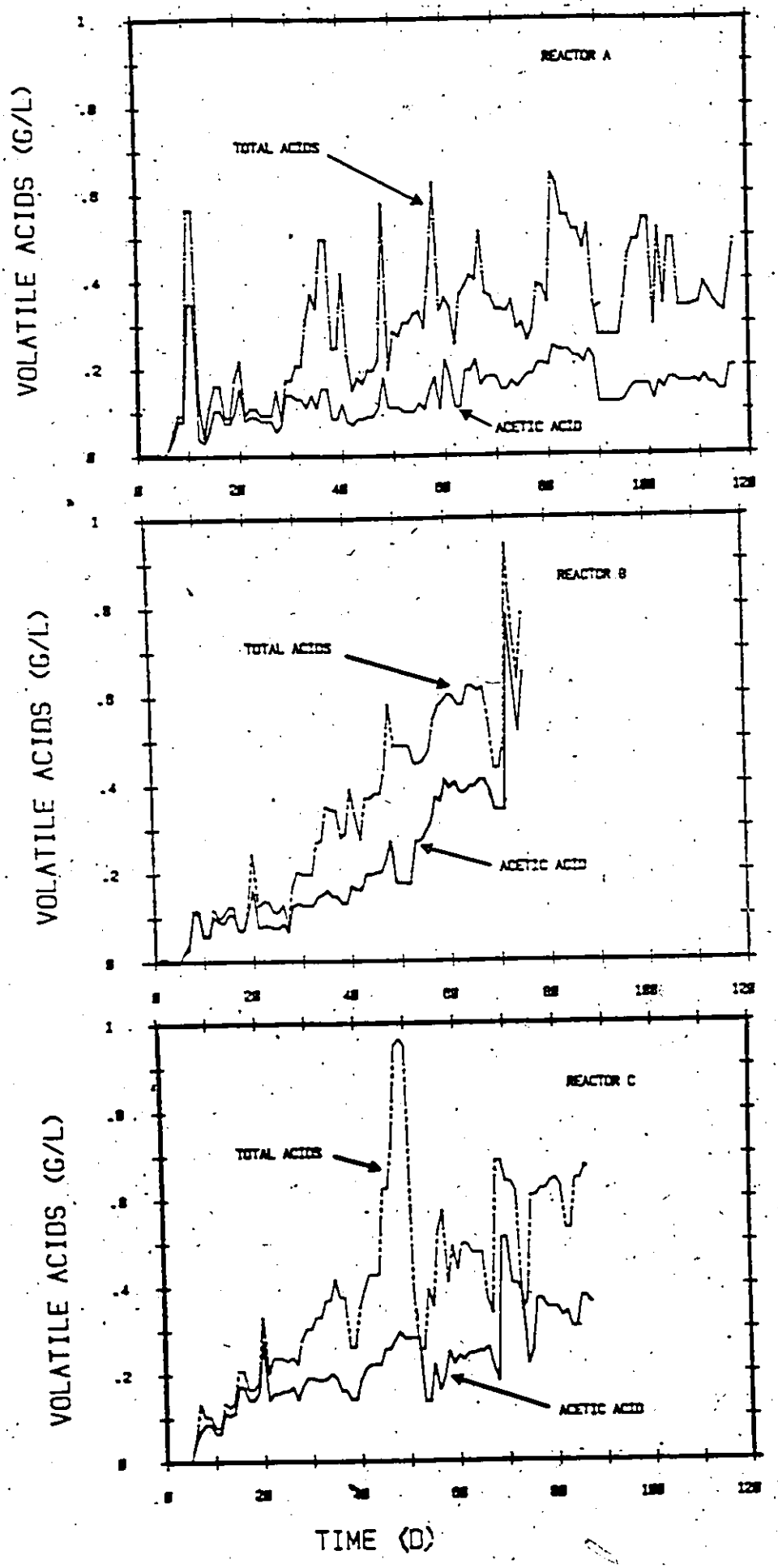

Figure 5.1 Reactor volatile acid concentrations during startup (Run 1)

Run 2 was conducted to observe the effect of higher mixed liquor VA concentrations on startup. Reactors had sufficient buffer capacity to maintain pH above 6.8. Periodic checks of Eh indicated all reactors had readings less than -350 mV. Although a mixed liquor VA concentration of 1000-1500 mg L^{-1} was desired it was difficult to obtain (Figs. 5.2a, b, c). Reactor A, treating dilute wastewater, was often unable to maintain VA concentrations this high. On the other hand, reactors treating more concentrated substrate often had VA concentrations much higher than desired. Comparison of these results with Run 1 indicates that controlled startup at high VA concentrations was more difficult to achieve.

Figures 5.3a and b and 5.4a and b show the effects influent substrate concentration had on volumetric organic loading rates and HRT for Runs 1 and 2 respectively. In Run 1 there was little difference in the final loading rates for DSFF reactors treating 0.5 and 1.0 % sucrose respectively. The final loading rate of Reactor C was lower than that obtained with reactors treating more dilute wastewater. Reactor C was characterized by development of floating biomass that began to clog reactor channels. If reactor operating conditions changed, floating biomass could be washed out of the reactor with probable adverse consequences. Since the purpose of this study was to examine biofilm development in DSFF reactors, floating biomass was removed from Reactor C.

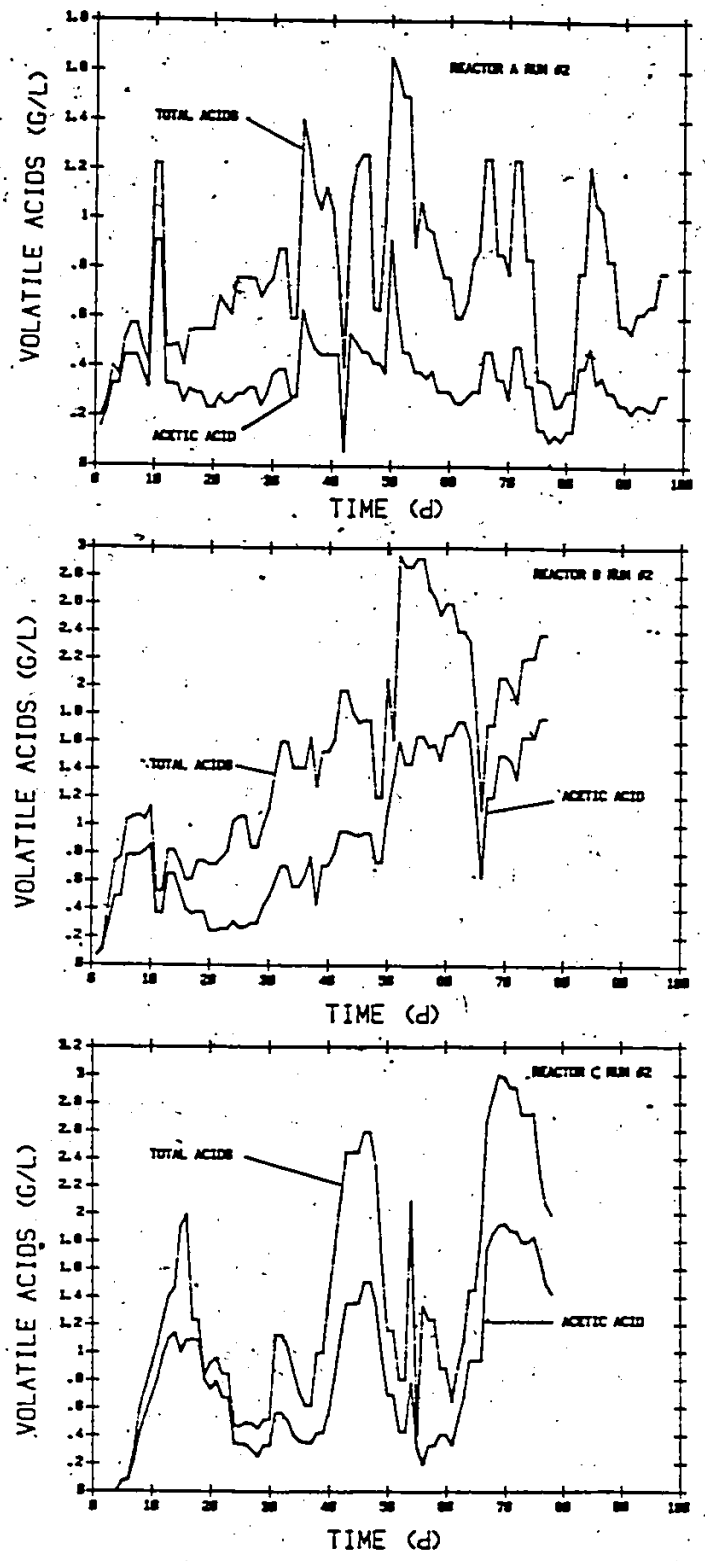

Figure 5.2 Reactor volatile acid concentrations during startup Run 2.

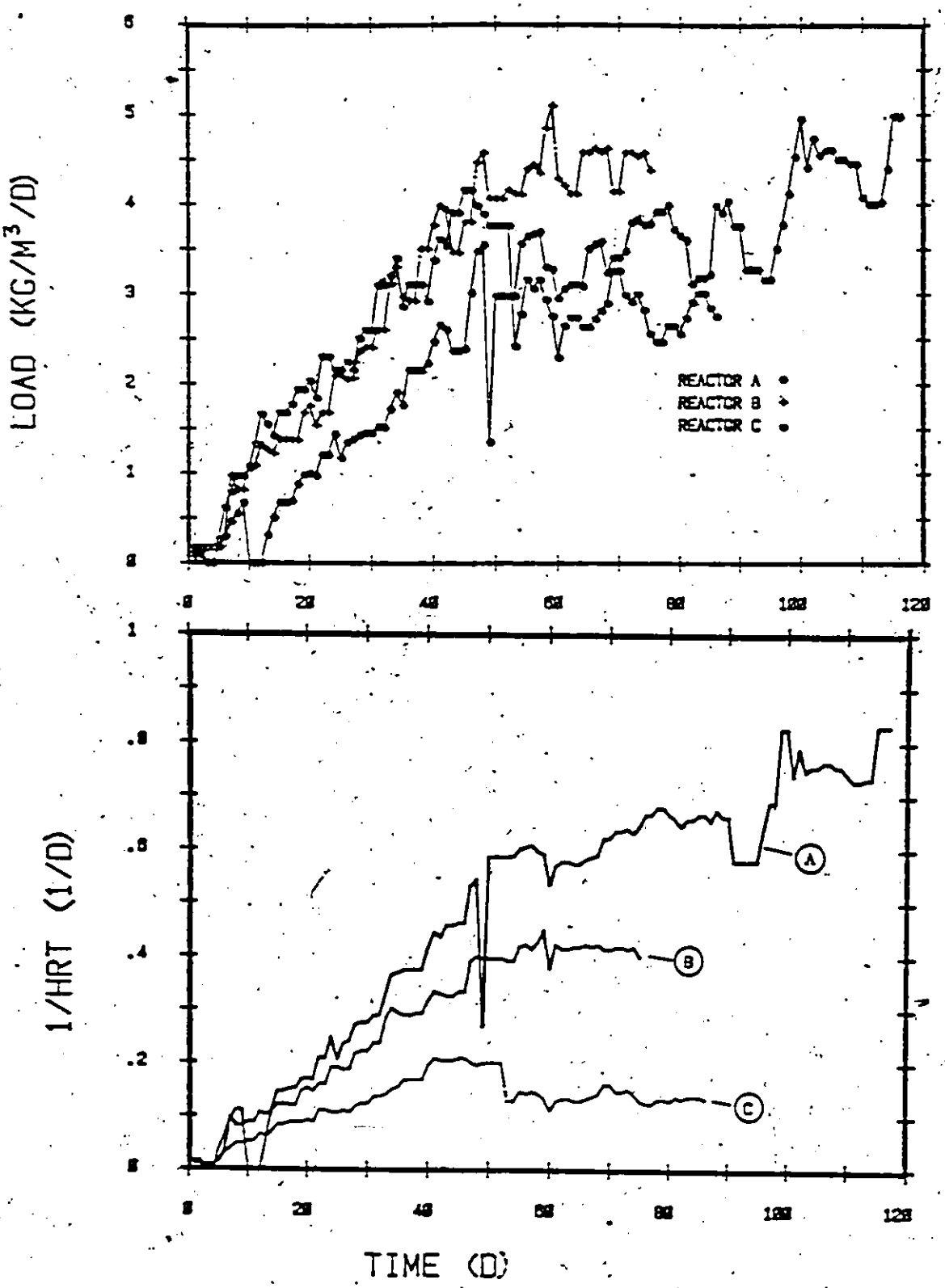

Figure 5.3 Effect of substrate concentration on organic loading rate and HRT during startup (Run 1).

Approximately 1 L (47 g VSS) of floating biomass was removed on the 52nd day of operation; consequently, Reactor C was unable to sustain its previous organic loading rate. Specific methanogenic activity of this material was in the range of 0.5-1 g COD (g VSS)$^{-1}$d^{-1}. Reactor C continued to accumulate floating biomass although at a slower rate than during initial stages of startup. Given time, the lost biomass would have been replaced and the organic loading rate would also have increased. Reactors treating less concentrated sucrose wastewater had no accumulation of biomass in the liquid above the packing. In Run 2 a gradual accumulation of floating biomass was also observed in Reactor C but not in reactors treating 0.5 and 1.0 % sucrose wastewater.

Influent substrate concentration also had an effect on the rate at which reactor loading rates (Fig. 5.3a) could be increased. In Run 1 Reactor A had the slowest rate of loading increase (0.015 d^{-1}) and required approximately 98 days to achieve its maximum steady state loading rate (Table 5.1a). On the other hand, reactor A was the most stable and easiest to operate of the three reactors. Stability is evident when one compares daily VA concentrations of Reactors A, B and C. Reactors B and C operating with more concentrated feed, had similar rates of volumetric organic load increase (0.025 d^{-1}) and achieved a maximum loading of 4.0-4.5 kg COD m^{-3}d^{-1} within 50-60 days of inoculation.

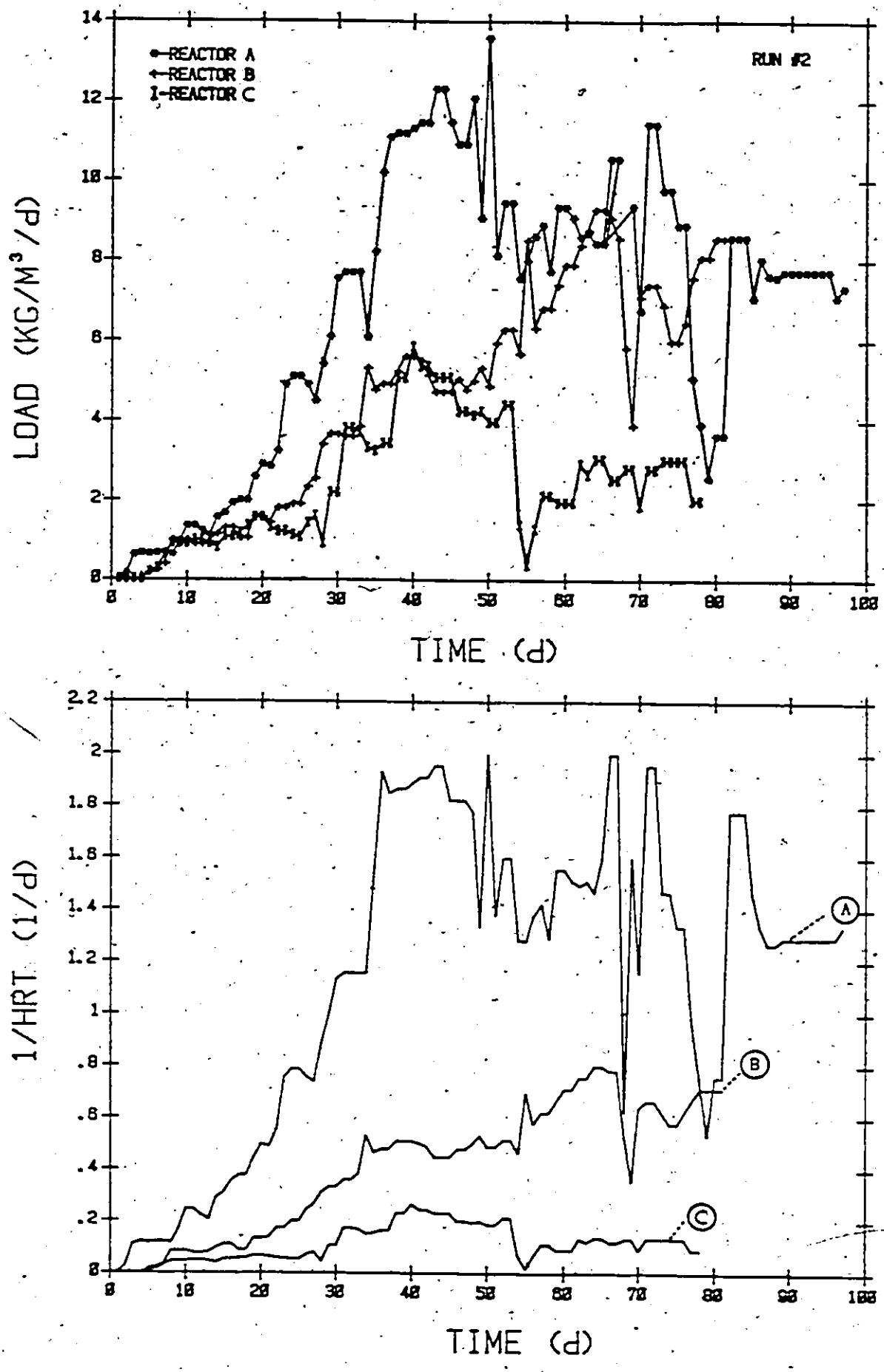

Figure 5.4 Effect of substrate concentration on organic loading rate and HRT during startup (Run 2).

Figure 5.4a indicates that the most dramatic effect of maintaining higher mixed liquor VA concentrations occurred with the least concentrated wastewater. A loading rate of 11.5 kg COD $m^{-3}d^{-1}$ and HRT of 0.5 days was achieved within 45 days of startup (Table 5.1b). Rate of startup diminished with increased substrate concentration. Rates of volumetric organic loading increase were 0.054 d^{-1} for Reactor A and 0.028 d^{-1} for Reactors B and C. Reactor C showed no better results than in Run 1. Results from Run 2 indicate that startup of DSFF reactors treating dilute sucrose wastewater can be accelerated by maintaining higher VA concentrations in the mixed liquor.

5.2.2 Cumulative Carbon Balance

Since startup of DSFF reactors is not a steady state operation, a cumulative mass balance (Appendix D) was used to assess reactor performance. Figures 5.5a and 5.5b show methane production with respect to time during startup for Runs 1 and 2' respectively. During Run 1 Fig. 5.6a shows that for a given mass of COD load, cumulative soluble COD (COD_s) in the effluent remained constant for all reactors. This was not surprising since VA, which made up the majority of effluent soluble COD, were maintained relatively constant. For a given load of COD Fig. 5.6a indicates that the

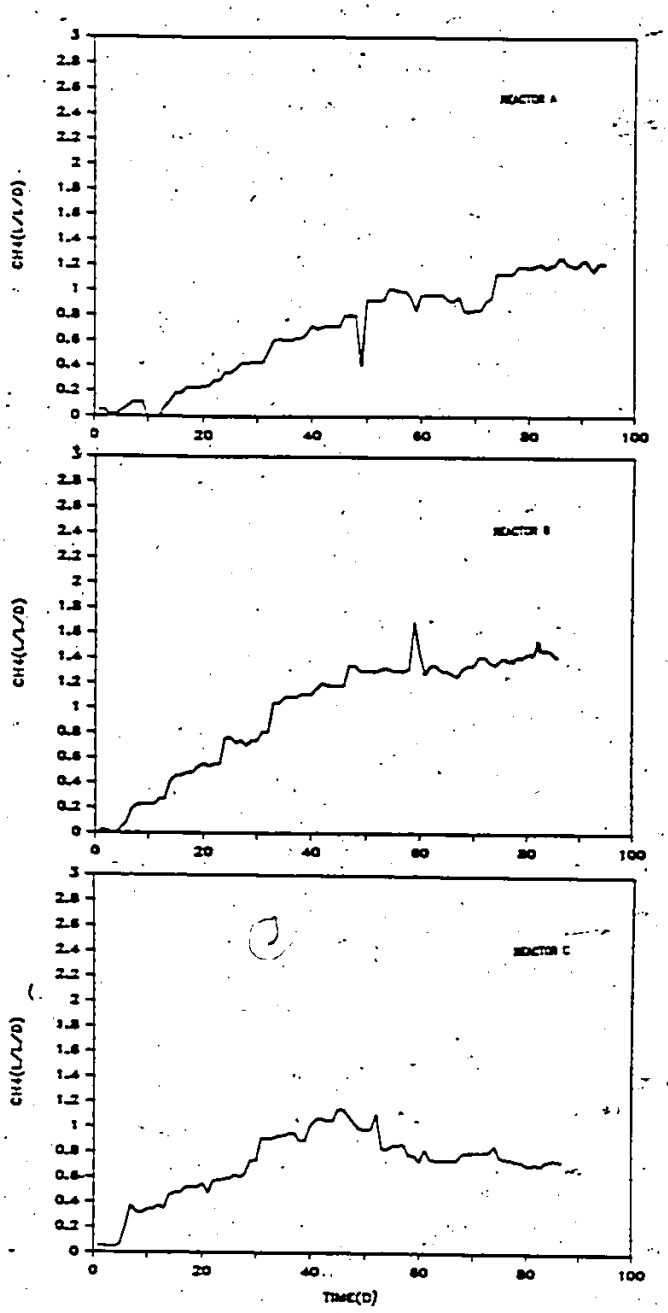

Figure 5.5a Methane gas production during startup (Run 1).

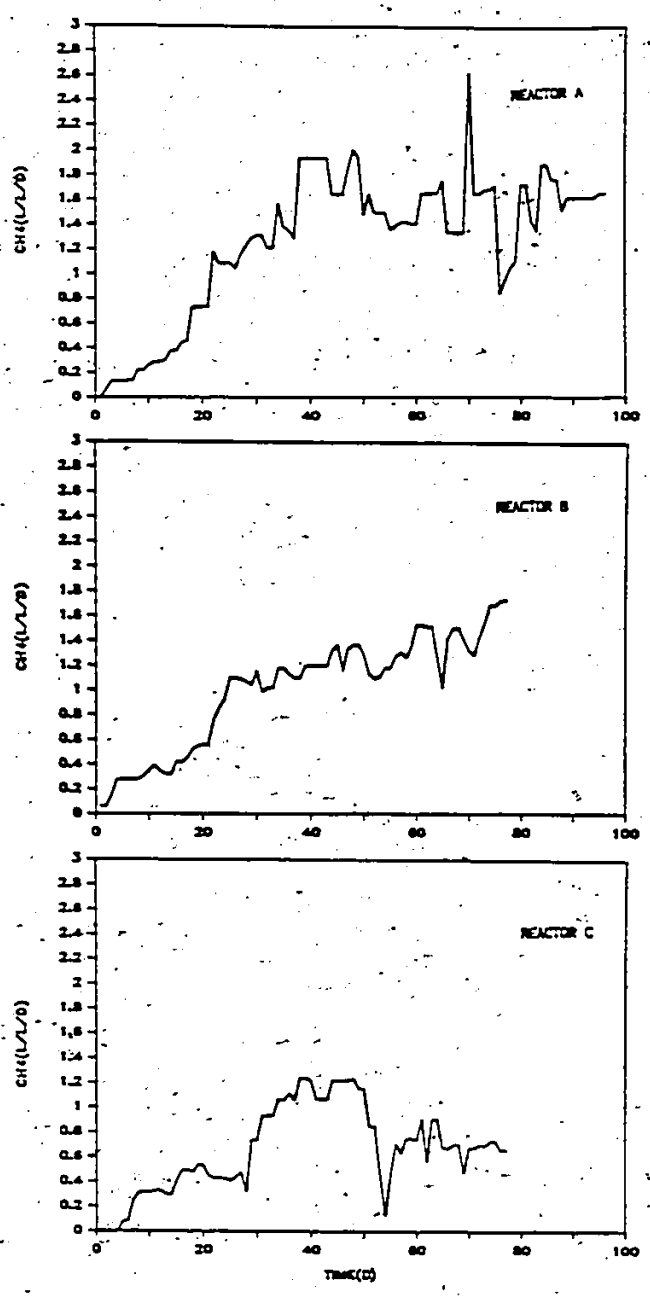

Figure 5.5b Methane gas production during startup (Run 2).

Table 5.1a Reactor Performance Summary for Startup[a] (Run 1)

Parameter	Reactor		
	A	B	C
Average VA, acetic acid equivalents, mgL^{-1}	320	330	370
Time for startup, d	98	65	52
Surface loading[b], $kgCOD\ m^{-2}d^{-1}$	0.060	0.060	0.053
Space loading[b], $kgCOD\ m^{-3}d^{-1}$	4.5	4.5	4.0
Specific biofilm loading[b], $kgCOD(kgVFS)^{-1}d^{-1}$	0.8	1.0	1.4
Specific biofilm COD removal[b], $kgCOD(kgVFS)^{-1}d^{-1}$	0.6	0.8	1.2
Cumulative COD load, $kg\ m^{-3}$	232	180	123
Cumulative COD removal, $kg\ m^{-3}$	173	145	104
Cumulative COD removal, %	74	81	85
Cumulative biogas produced, $m^3(STP)\ m^{-3}$	115	79	59
Cumulative methane produced, $m^3(STP)\ m^{-3}$	60	41	31
Biogas yield, $m^3(STP)(kgCOD\ removed)^{-1}$	0.66	0.55	0.57
Methane yield, $m^3(STP)(kgCOD\ removed)^{-1}$	0.34	0.29	0.30
Total biomass yield, $kgVSFS(kgCOD\ removed)^{-1}$ [c]	0.21	0.14	0.11
Biofilm yield, $kgVFS(kgCOD\ removed)^{-1}$	0.034	0.030	0.027
COD accounted for, %	102	89	90

[a] i) Results from day 0 - time for startup
ii) Based on 22.4 L liquid volume and 75 m^2m^{-3} surface area to volume ratio
[b] values at the end of startup
[c] VSFS - volatile suspended and film solids

Table 5.1b Reactor Performance Summary for Startup[a] (Run 2)

Parameter	Reactor		
	A	B	C
Average VA, acetic acid equivaleots, mgL^{-1}	760	1530	1120
Time for startup, d	45	65	53
Surface loading[b], $kgCOD\ m^{-2}d^{-1}$	0.15	0.12	0,061
Space loading[b], $kgCOD\ m^{-3}d^{-1}$	11.5	9.0	4.6
Specific biofilm loading[b], $kgCOD(kgVFS)^{-1}d^{-1}$	2.9	2.6	1.7
Specific biofilm COD removal[b], $kgCOD(kgVFS)^{-1}d^{-1}$	1.6	1.5	1.3
Cumulative COD load, $kg\ m^{-3}$	225	249	130
Cumulative COD removal, $kg\ m^{-3}$	126	149	102
Cumulative COD removal, %	56	60	79
Cumulative biogas produced, $m^3(STP)\ m^{-3}$	78	196	60
Cumulative methane produced, $m^3(STP)\ m^{-3}$	37	49	32
Biogas yield, $m^3(STP)(kgCOD\ removed)^{-1}$	0.62	0.71	0.59
Methane yield, $m^3(STP)(kgCOD\ removed)^{-1}$	0.30	0.33	0.31
Total biomass yield, $kgVSFS(kgCOD\ removed)^{-1}$	0.28	0.16	0.11
Biofilm yield, $kgVFS(kgCOD\ removed)^{-1}$	0.031	0.023	0.027
COD accounted for, %	93	98	94

[a] i) Results from day 0 - time for startup
ii) Based on 22.4 L liquid volume and 75 m^2m^{-3} surface area to volume ratio

[b] values at the end of startup

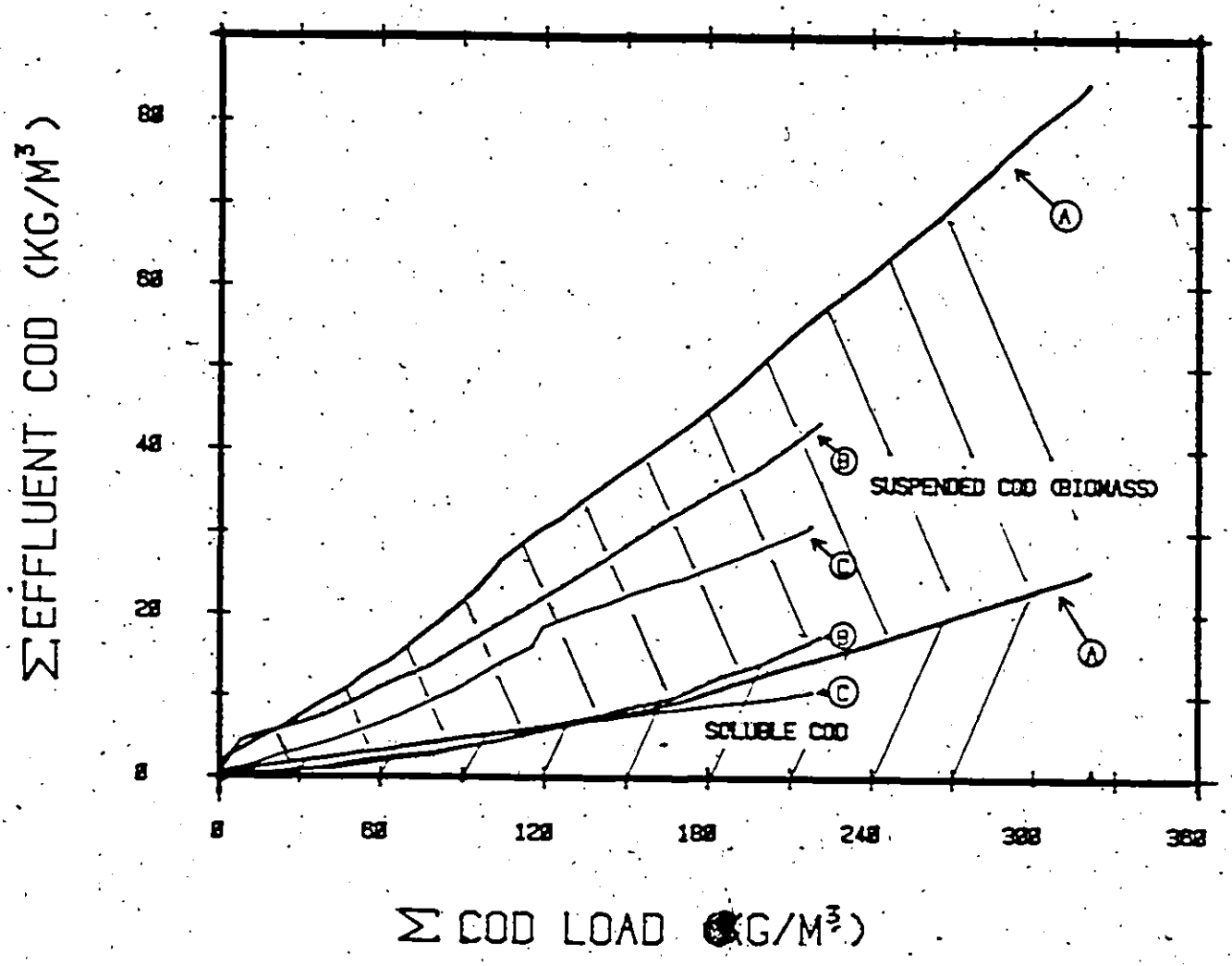

Figure 5.6a Cumulative effluent COD versus cumulative COD load for various substrate concentrations during startup (Run 1).

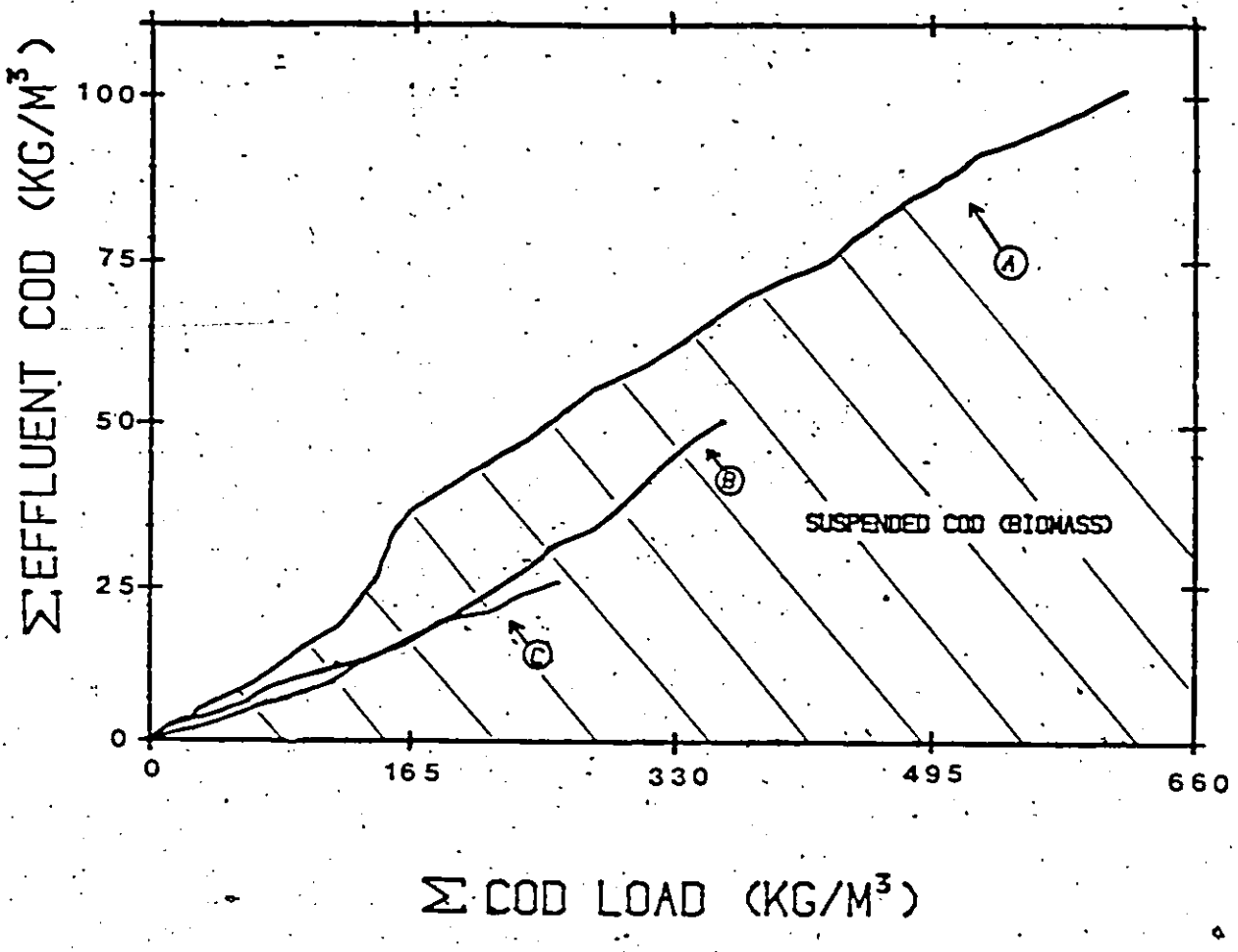

Figure 5.6b Cumulative insoluble effluent COD versus cumulative COD load for various substrate concentrations during startup (Run 2).

amount of insoluble COD, (COD_{is}) generated increased with decreasing influent concentration. Initially suspended COD in the effluent was high due to loss of original inoculum. Contribution of inoculum to effluent COD did not significantly affect the cumulative COD balance. In all reactors, total COD removal efficiency decreased with decreasing HRT. Cumulative total COD removal efficiencies for Run 1 were 74, 81 and 85 % for Reactors A, B and C, respectively (Table 5.1a).

For Run 2, cumulative soluble COD in the effluents from Reactors A, B and C for a given mass of COD load were not as uniform as during Run 1 because of an inability to control reactor VA concentrations within the desired range. Because of this variation only insoluble COD is plotted in Fig. 5.6b. However, as in Run 1 the amount of insoluble COD in the effluent for a given COD load increased with decreased substrate concentration.

Total cumulative COD removal efficiencies for Run 2 were 56, 66 and 79 % for Reactors A, B and C respectively (Table 5.1b). These results are lower than for Run 1 but this is expected since, for the majority of startup, these reactors were operated with shorter HRT and higher soluble COD concentrations (VA) in the mixed liquor. Reactor A was again the most stable. COD removal efficiency for this reactor was poor due to low operating HRT.

5.2.3 Biofilm Development

Visual inspection of the biofilm (Runs 1 and 2) indicated that early biofilm development was characterized by spotty growth on the support material (Fig. 5.7a). This was due to different rates of biomass deposition immediately following inoculation. As biofilm development progressed, support media became uniformly coated with a luxurious zoogloeal biofilm (Fig. 5.7b). A mature biofilm was a porous filamentous microbial mat with an extremely large surface area. Initial attachment of inoculum to support media followed by biofilm growth corresponds to the first stage of aerobic biofilm development described by Bryers and Characklis (1981).

In UASB systems, Hulshoff Pol *et al.*, (1982) recommend that VA concentrations during startup be less than 100 mg L^{-1} before organic loads are increased. Maintaining low VA concentrations in UASB reactors helps select granular sludge particles. Operating at higher VA concentrations in DSFF reactors selects for a filamentous sludge which is more advantageous for biofilm development. Selection of different microrganisms in UASB and DSFF reactors also explains differences in waste treatability between these two systems (van den Berg *et al.*, 1981). UASB reactors successfully treat a narrower spectrum of wastewater in comparison to DSFF reactors.

(a)

(b)

Figure 5.7 Photograph of early (a) and mature (b) biofilm development.

Figures 5.8 and 5.9 show the effect of substrate concentration on biofilm accumulation with respect to time and cumulative COD respectively for Run 1. Initial rates of biofilm accumulation were logarithmic for the first 30-35 days followed by a linear development stage. Rates of biofilm accumulation were found to decrease with increased influent substrate concentration. Results are for the biofilm only and to not take into account suspended growth. Comparison of Figs. 5.8 and 5.9 with Fig. 5.6a indicates increased biofilm accumulation was related to increased biomass in the effluent.

Logarithmic anaerobic biofilm development followed by a linear rate of development is similar to that described by Bryers and Characklis (1981) for aerobic biofilms. The reason for this is related to strict operating requirements used to maintain VA concentrations within a desired concentration range. VA concentrations maintained in the mixed liquor were sufficient to completely saturate anaerobic biofilms resulting in logarithmic growth. Complete substrate saturation of the biofilm also indicates anaerobic bacteria have a high K value. Linear growth was a result of increased biofilm detachment, incomplete substrate saturation in the biofilm or a combination of these factors.

Total biomass yield, Y_m and biofilm biomass yield, Y_{m_f} for NPP support media treating sucrose wastewater (Run 1; Table 5.1a) were 0.21, 0.14 and 0.11 g VSFS $(g\ COD)^{-1}$ removed and 0.034, 0.030 and 0.027 g VFS $(g\ COD)^{-1}$ removed for

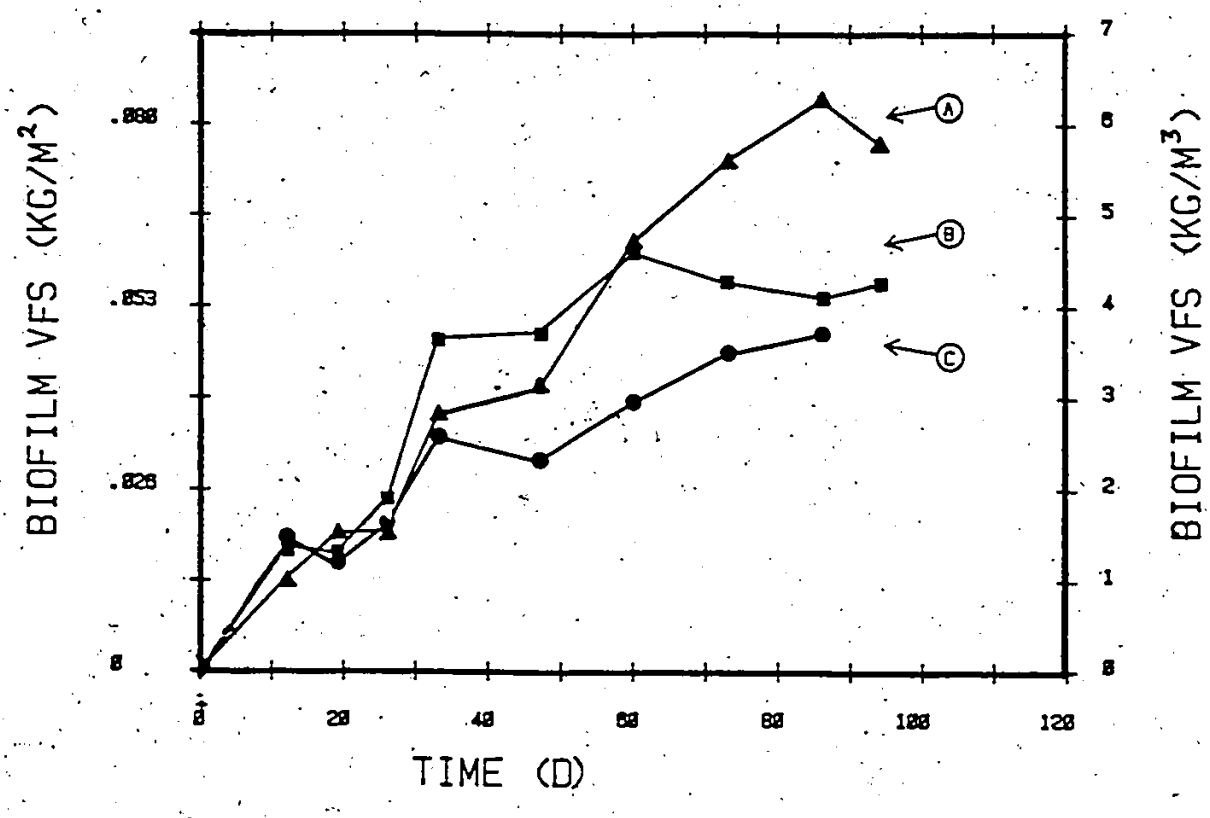

Figure 5.8 Biofilm accumulation versus time for various substrate concentrations during startup (Run 1) Reactor A (▲), Reactor B (■), and Reactor C (●).

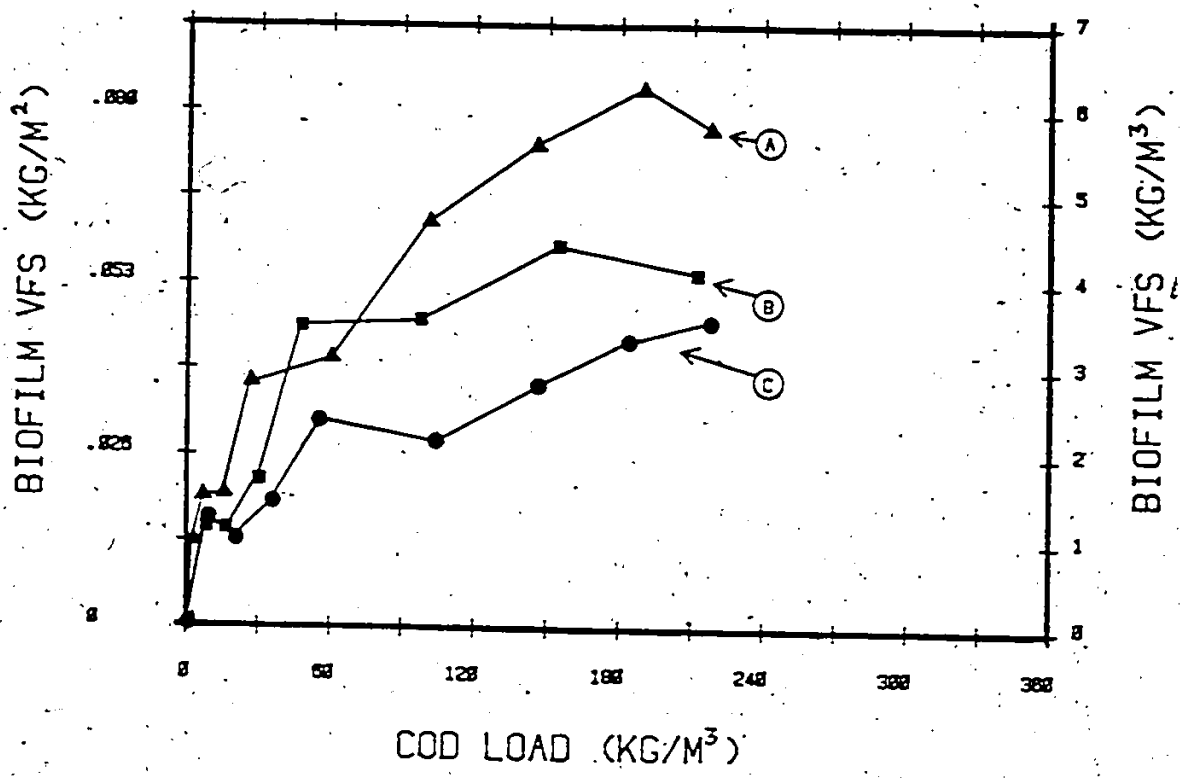

Figure 5.9 Biofilm accumulation versus cumulative COD load for various substrate concentrations during startup (Run 1)
Reactor A (▲), Reactor B (■) and Reactor C (●).

Reactors A, B and C, respectively. SRT for all reactors in Run 1 were in the range of 10–26 days (Fig. 5.10) which is greater than the doubling time of methanogenic bacteria. SRT in Reactor C were higher than for Reactor A. This is due to differences in HRT and the effect of floating biomass in Reactor C. For Run 2 similar results were observed for total biomass yield and biofilm biomass yield. Total biomass yields and biofilm yields (Table 5.1b) were 0.28, 0.16 and 0.11 g VSFS (g COD removed)$^{-1}$ and 0.031, 0.023 and 0.027 g VFS (g COD removed)$^{-1}$ for Reactors A, B and C respectively.

5.2.4 Microbial Activity

Figure 5.11 shows the distribution of methanogenic activity in the mixed liquor and biofilm during Run 1. These tests were not conducted for Run 2. As startup progressed the proportion of methanogenic activity present in the mixed liquor of all reactors decreased to negligible rates within 40–50 days of inoculation. (This activity does not take into account activity of the floating biomass in Reactor C). Methanogenic activity in the biofilm increased as startup progressed. Rates at which methanogenic activity increased appeared to be quite similar, however results indicate that final biofilm methanogenic activity in Reactor A, was higher than methanogenic activity for Reactors B and C treating more concentrated wastes. As reactors matured activity was

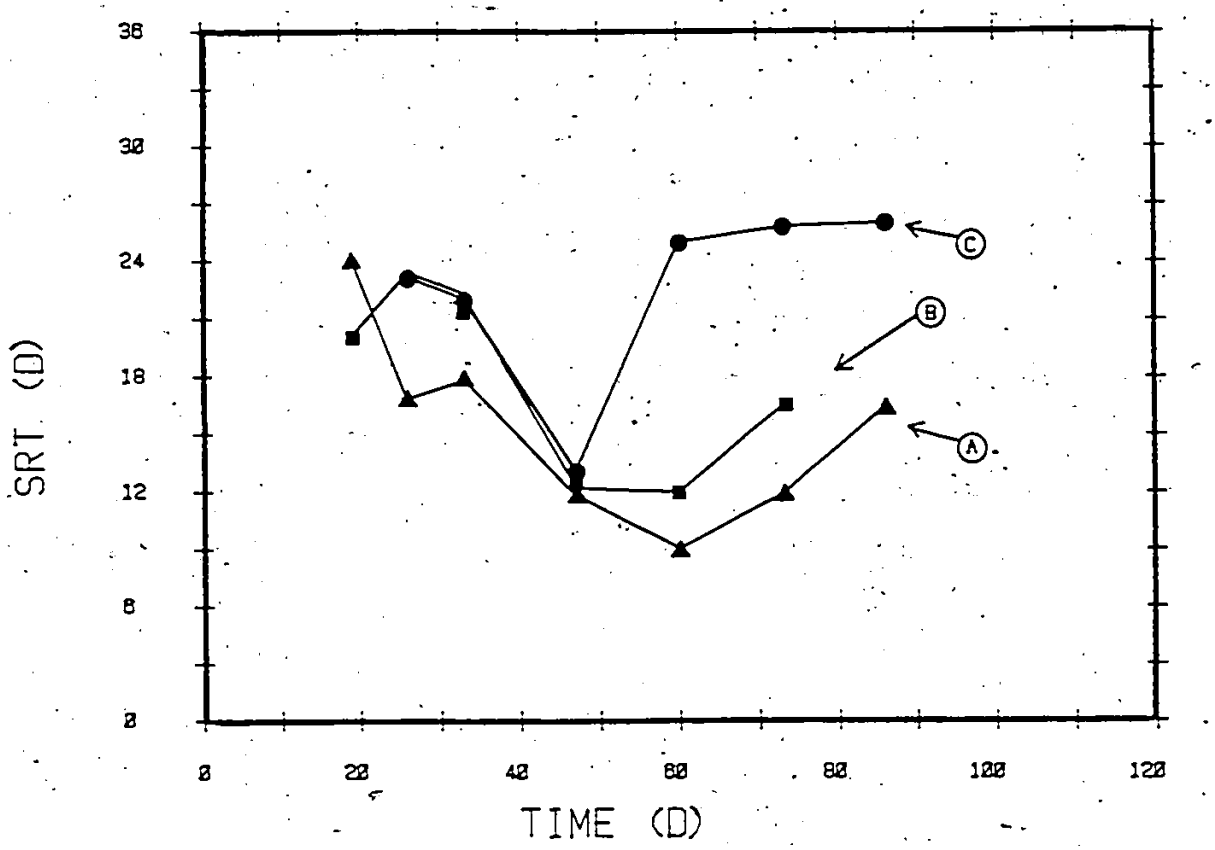

Figure 5.10 SRT versus time for various substrate concentrations during startup (Run 1).

dependent on the quantity of attached biomass. Assuming uniform biofilm distribution along the length of the support media, biofilm thicknesses ranged from 0-1.8 mm during startup. Batch activity tests indicated that specific methanogenic activity of all biofilms for an initial substrate concentration of 1000 mg acetate L^{-1} ranged between 0.6-1.4 g COD (g VFS)$^{-1}$ d^{-1} (Appendix F) and is discussed further in a later Section. Within the accuracy of the test, biofilm methanogenic activity was directly proportional to amount of biomass on the support media. It is possible for thicker biofilms that this would not be the case.

Although cumulative COD removal efficiencies in Runs 1 and 2 for Reactor A were lowest of the three reactors studied, total biomass yield, biofilm accumulation rate and biofilm yield were highest. Considering that the main objective of startup is development of a stable healthy biofilm, COD removal efficiency should not be an operational consideration.

Table 5.2 shows specific sucrose activity in the mixed liquor and biofilm during startup. Biofilm specific sucrose activity increased with increased influent waste strength. This indicated that the biofilm in Reactor A had a higher ratio of methane formers to acid formers compared to biofilms developed on more concentrated wastewater. Mixed liquor results for specific sucrose activity were reversed

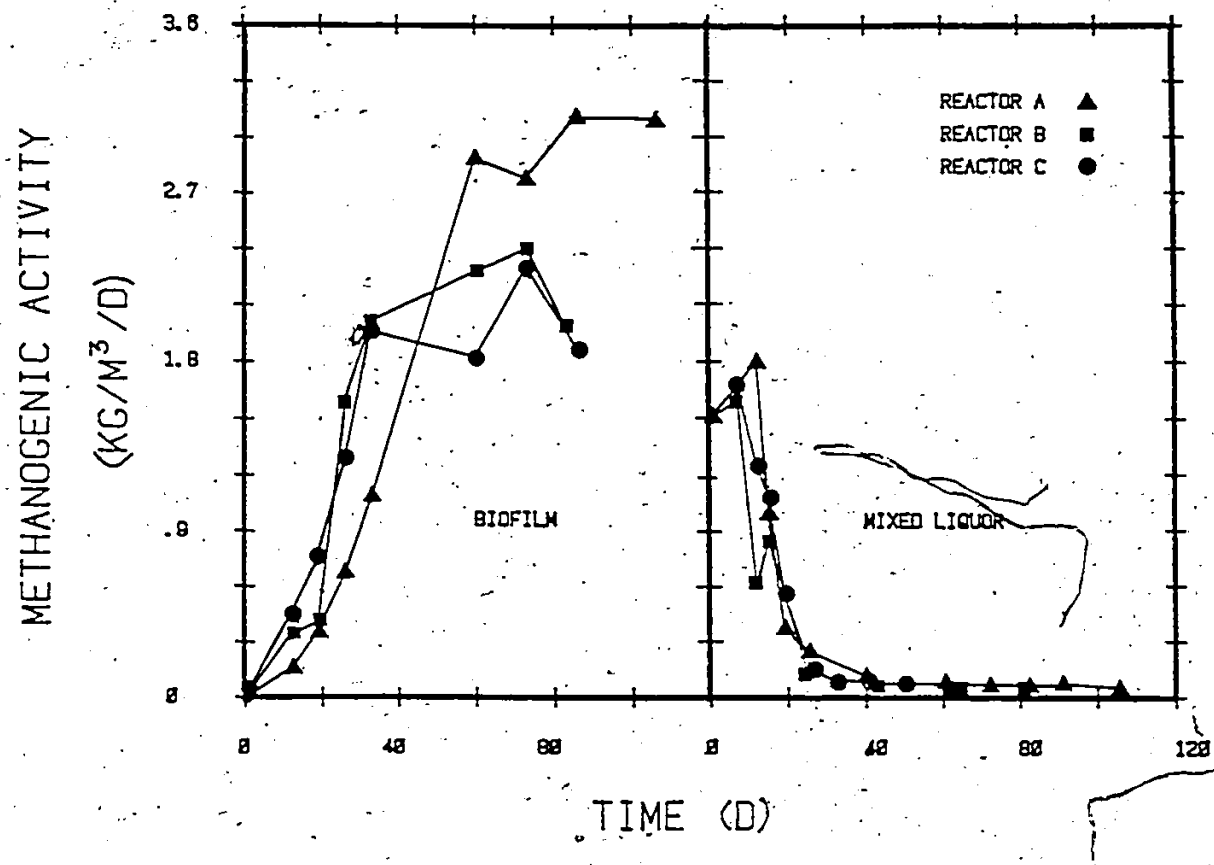

Figure 5.11 Distribution of methanogenic activity in DSFF reactors during startup (Run 1).

Table 5.2 Biofilm and Mixed Liquor Sucrose and Methanogenic Activity During Startup (Run 1)

Day	Reactor A	Reactor B	Reactor C
Biofilm specific sucrose activity (g COD(g VFS)$^{-1}$d^{-1})			
33	2.2	2.5	3.0
47	2.6	2.4	3.6
60	1.3	1.7	3.1
73	1.5	2.0	2.5
86	1.1		1.4
Mixed liquor specific sucrose activity (g COD(g VSS)$^{-1}$d^{-1})			
33	4.5	3.1	2.4
60	1.1	2.0	2.1
73	6.0	3.7	2.5
86	7.4	5.1	2.3
Biofilm specific methanogenic activity (g COD(g VFS)$^{-1}$d^{-1}			
33	0.7	1.5	1.7
60	1.5	1.0	1.2
73	1.1	1.1	1.4
86	1.1	0.9	0.9

indicating, for dilute wastewaters, a higher proportion of suspended biomass was made up of acidogens. In reactors treating concentrated sucrose wastes, suspended biomass had a higher percentage of methanogens. Biofilm methanogenic activity measurements also indicated these results. The trend was not as distinct, which reflects the slow growth rates of methanogenic bacteria.

Lower COD removal efficiency and higher growth yields associated with DSFF reactors started up with dilute wastewater are related to reactor HRT and growth rates of methane forming and acid forming bacteria. Reactors operating at

similar organic loading rates but with concentrated wastewater have longer HRT than reactors treating dilute wastewater. At HRT greater than 3-5 days some methanogenic bacteria are able to grow in the mixed liquor replacing those that are washed out. Waste stabilization is due to bacteria in the mixed liquor and biofilm (Reactor C). Substrate mass balances over CSTR demonstrate that for the same loading rate the efficiency of substrate removal increases as influent concentration (and consequently HRT) increases assuming that the same substrate removal constant applies to each case. Since the reactors studied here were CM a similar trend is reasonable. Furthermore, methanogenic bacteria in the mixed liquor are less affected by any diffusional resistance that might be associated with attached biomass.

Floating sludge that accumulated in Reactor C resulted from growth of methanogenic and acidogenic bacteria in the mixed liquor. The floating nature of the sludge was due to filamentous anaerobic bacteria with methanogenic activity and concomitant biogas production. Biogas became entrapped within the flocs causing flotation.

Reactors treating dilute wastewater at HRT less than 3-5 days have few methanogenic bacteria in the mixed liquor due to washout of these microorganisims. Only methanogens that are sloughed from the biofilm are found in the mixed liquor. During startup, biofilm sloughing is very small. Therefore, effectively all waste stabilization, particularly methanogenesis, in these reactors occurs in the biofilm.

With few filamentous anaerobic bacteria growing in the mixed liquor, accumulation of floating sludge was not found. At shorter HRT and with possible effects of diffusional resistance in the biofilm, COD removal efficiency is less than reactors treating concentrated wastewater at similar organic loading rates. Acid forming bacteria can grow in the mixed liquor at low HRT (Table 5.2).

Methanogens grow in the mixed liquor and biofilm of reactors treating concentrated wastewater but only grow in the biofilm of reactors treating dilute waste. For high strength wastewaters a portion of methanogenic substrate is consumed by methanogens in the mixed liquor leaving less substrate for methanogens in the biofilm. Therefore, concentration of methane formers in the biofilm of reactors treating concentrated wastewater would be less (*i.e.*, acid former concentration higher) than in reactors treating dilute wastewater at similar organic loading rates. From Tables 5.1a and b it is observed that reactors with lower influent COD concentration had lower COD removal efficiencies as discussed above, but total amounts of COD removed were greater in a shorter period of time because the total biofilm growth rates were higher allowing greater input of substrate. The net effect of a higher concentration of rate limiting methanogens in biofilms of reactors treating dilute wastewater combined with the loss of suspended methanogens in the effluent of reactors treating concentrated wastewater is a decrease in rate of

startup, stability and biofilm yield with an increase in influent concentration. The dynamic model to be presented later will demonstrate differences in relative microbial populations in the biofilm and mixed liquor with increased influent concentration.

Results indicate that it is advantageous to start reactors with a weak waste, which results in greater biofilm accumulation, higher methane former to acid former ratio in the biofilm and easier operational control. Once startup has been realized reactors can be switched to a more concentrated waste and operated at longer HRT to improve COD removal efficiency.

Downflow mode of operation and short HRT, in relation to the slow growth rates of methanogenic bacteria, makes DSFF reactor performance dependent on biomass attached to support media. Increased specific surface area has been shown to increase biomass concentration per unit reactor volume, with concomitant increased anaerobic reactor performance. However, it should be remembered that if specific surface area is too large there could be a decrease in reactor efficiency due to a decrease in effective reactor volume. Decrease in effective reactor volume results from biofilm accumulation that causes channel blockage (van den Berg and Lentz, 1979). In contrast to DSFF reactors, the effect of support surface area on the performance of upflow anaerobic filters has been shown to be of less importance than other media characteristics such as shape and void size

(Young and Dahab, 1982). Large plastic media, which had a surface area of 98 m^2 m^{-3}, provided better COD removal than did small plastic media which had a surface area of 138 m^2 m^{-3}. Improvement in anaerobic filter performance with larger media having a smaller surface area to volume ratio and larger void volume is due to the majority of biomass not being attached to support material but actually trapped within the interstitial spaces in the lower section of the filter. Media with a high void volume but capable of retaining biomass is most desirable for maximum anaerobic filter performance.

5.3 Steady State DSFF Reactor Operation

5.3.1 Summary of Steady State DSFF Reactor Performance

Summary data for each of the four substrate concentrations evaluated are presented in Table 5.3. Results are presented for effluent soluble and insoluble COD; VA; daily biogas production and composition; attached and suspended biomass concentrations; and mixed liquor pH and Eh. Each data point is the average of three measurements except for biofilm biomass concentration and biofilm thickness which are the average of 2 measurements. Steady state results are presented in Appendix 6.

Biofilm biomass measurements were not made at a 0.4 d HRT because of the limited number of removable biofilm sup-

Table 5.3. Data Summary for Steady State Reactor Operation

S	HRT	Organic loading rate	Effluent Soluble COD	COD removal	Effluent Insoluble COD	Biofilm VFS	Biofilm thickness	Biogas	Methane	pH
%	days	kg COD $m^{-3}d^{-1}$ (kg COD $m^{-3}d^{-1}$)	mg L^{-1}	%	mg L^{-1}	kg m^{-3} (kg m^{-2})	mm	L d^{-1}	%	
2	7	2.7 (0.0360)	800	96.0	1270	2.83 (0.0377)	0.84	35.0	57	7.5
0.25	4.4	0.57 (0.0076)	105	95.8	130	2.17 (0.0289)	0.64	4.9	80	7.6
0.50	4.4	1.20 (0.0160)	120	97.6	330	2.68 (0.0357)	0.79	14.0	62	7.6
1.0	4.0	2.80 (0.0373)	385	96.2	705	3.82 (0.0509)	1.13	36.8	60	7.5
2.0	4.0	4.80 (0.0640)	4000	80.0	1800	3.98 (0.0531)	1.18	57.7	54	7.2
0.25	2.0	1.27 (0.0169)	170	93.2	130	2.75 (0.0367)	0.81	10.9	76	7.4
0.5	2.0	2.66 (0.0355)	570	88.6	410	3.75 (0.0500)	1.11	34.0	54	7.1
1.0	2.0	5.33 (0.0707)	1330	86.7	460	5.20 (0.0693)	1.54	69.7	56	7.3
2.0	2.0	10.50 (0.1400)	8720	56.4	2670	6.94 (0.0925)	2.05	87.8	40	6.3
0.25	1.0	2.50 (0.0333)	295	90.2	205	3.19 (0.0425)	0.94	24.0	67	7.0
0.50	1.0	5.15 (0.0687)	1085	78.3	630	5.03 (0.0671)	1.49	46.3	53	6.9
1.0	1.0	9.76 (0.1301)	2400	75.4	950	8.44 (0.1125)	2.49	104.0	55	6.8
0.25	0.7	3.55 (0.0473)	515	79.4	145	3.46 (0.0461)	1.02	29.0	61	7.0
0.50	0.7	8.24 (0.1099)	2130	57.4	485	6.93 (0.0924)	2.05	74.0	44	6.8
1.0	0.7	14.60 (0.1947)	4090	59.1	1125	8.3 (0.1107)	2.45	117.0	45	6.8
0.25	0.5	4.70 (0.0627)	980	60.8	265	4.18 (0.0557)	1.23	30.8	56	6.7
0.50	0.5	10.17 (0.1356)	2400	52.0	490	7.87 (0.1049)	2.32	70.0	47	7.2
1.0	0.5	18.90 (0.2520)	4375	56.3	1330	8.71 (0.1161)	2.57	151.0	49	6.6
0.25	0.4	6.37 (0.0849)	1190	62.4	290	-	-	29.8	60	7.1

ports in the reactor. Organic loading rates, surface loading rates and HRT are based on a surface area to volume ratio of 75 m^2 m^{-3} and reactor liquid volume of 22.4 L, respectively. Liquid volume of the reactor and surface area to volume ratio takes into account volume occupied by support media but not volume occupied by biofilm. As an example, for a flow rate of 44.8 L d^{-1}, HRT is equal to reactor volume divided by flow rate or 22.4 L divided by 44.8 L d^{-1} which equals 0.50 days. Actual HRT would be slightly less than this since biofilm occupied a volume of the reactor.

5.3.2 Organic Carbon Balance

Organic carbon balances (Appendix D) were made for steady state operating conditions to provide additional support to experimental data by acting as a cross-check mechanism. The sum of the five columns (Table 5.4), soluble COD in effluent, insoluble COD in effluent, methane production, methane in effluent and accumulated COD is equal to total COD out of the reactor. This value is compared to total input COD and expressed as a ratio in the last column. Mean ratios of COD in to COD out were 1.06, 1.05, 1.00 and 1.01 for reactors treating 0.25, 0.5, 1.0 and 2.0 percent sucrose wastes, respectively. These results demonstrate good account of organic carbon going into and coming out of the DSFF reactor, and verify the reliability of experimental results. A sample carbon balance is given in Appendix D.

Table 5.4 Organic Carbon Balance for Steady State Reactor Operation

S_o %	HRT days	COD in g d^{-1}	Soluble COD out g d^{-1}	Insoluble COD out g d^{-1}	Methane production g COD d^{-1}	Methane in effluent g COD d^{-1}	Accumulated g COD d^{-1}	Total COD out g COD d^{-1}	Ratio $\frac{\text{COD in}}{\text{COD out}}$
2.0	7.0	60.48	2.56	4.06	50.73	0.30			
0.25	4.4	12.77	0.53	0.66	9.97	0.48			
0.50	4.1	26.88	0.66	1.80	22.07	0.51			
1.0	4.0	62.72	2.16	3.95	56.15	0.52			
2.0	4.0	107.52	22.40	10.08	79.23	0.52	1.14	113.3	0.95
0.25	2.0	28.45	1.90	1.46	21.07	1.05	0.58	26.1	1.09
0.50	2.0	59.58	6.38	4.59	46.69	1.05	1.06	59.8	0.97
1.0	2.0	118.72	14.90	5.15	99.25	1.05	1.37	121.7	0.98
2.0	2.0	235.20	97.66	29.90	89.31	1.05	2.95	220.9	1.06
0.25	1.0	56.00	6.61	4.59	40.89	2.10	0.39	54.6	1.02
0.50	1.0	115.36	24.30	14.11	62.40	2.10	1.13	104.0	1.10
1.0	1.0	218.62	55.10	21.28	145.45	2.10	2.87	226.8	0.96
0.25	0.7	79.52	16.48	4.67	44.98	3.00	0.24	69.4	1.14
0.50	0.7	184.58	68.16	15.52	82.80	3.00	1.64	171.1	1.07
1.0	0.7	327.04	130.88	36.00	133.88	3.00	-0.13	303.6	1.07
0.25	0.5	105.28	43.90	11.74	43.86	4.20	0.77	104.5	1.00
0.50	0.5	227.81	107.52	21.95	83.66	4.20	1.00	218.3	1.04
1.0	0.5	423.36	196.00	59.58	168.95	4.20	0.44	429.1	0.99
								Average	1.03

Table 5.5 shows a calculation similar to the above, in which COD removed is compared to methane produced. Total methane production (gaseous and dissolved) is compared to the methane equivalent of COD removed. Methane equivalent of COD removed was determined by multiplying the difference between influent and effluent soluble COD by the daily flow rate and a conversion factor. The conversion factor is discussed in Appendix D.

Results indicate that greater than 80 percent of soluble COD was recovered as methane. Net biological solids synthesis of DSFF reactors treating sucrose wastewater was low. This fact is further verified when compared with measured biomass yields (discussed later) and biomass yields determined during startup (Tables 5.1a and 5.1b).

5.3.3 General DSFF Reactor Performance

Anaerobic DSFF reactors successfully treated low and medium strength sucrose wastewater at high organic loading rates and short HRT. For all DSFF reactors operating at various steady state conditions, acetic, propionic and butyric acids were the main acids detected in the effluent and they were the major component of soluble effluent COD (Table 5.6). Periodic checks showed little or no sucrose in the effluent indicating that the balance of the soluble COD was either longer chain VA or other soluble microbial by products. DSFF reactors treating 0.25% and 0.5% sucrose

Table 5.5 Comparison of COD Removed to Methane Produced

S_o %	HRT days	COD in g d^{-1}	COD removed g d^{-1}	Methane equivalent of COD removed L d^{-1}	Total methane production L d^{-1}	Conversion of COD to methane %
2.0	7.0	60.48	57.92	20.3	17.8	88
0.25	4.4	12.77	12.23	4.2	3.9	86
0.50	4.1	26.88	26.22	9.1	7.9	86
1.0	4.0	62.72	60.56	21.2	19.9	94
2.0	4.0	107.52	85.12	29.7	27.9	94
0.25	2.0	28.45	26.54	9.2	7.7	78
0.50	2.0	59.58	53.20	18.6	16.7	90
1.0	2.0	118.72	103.82	36.3	35.1	97
2.0	2.0	235.20	137.54	48.9	31.6	66
0.25	1.0	56.00	49.39	17.2	15.1	87
0.50	1.0	115.36	91.06	31.6	22.8	71
1.0	1.0	218.62	163.52	57.7	51.6	90
0.25	0.7	79.52	63.04	22.0	16.8	76
0.50	0.7	184.58	116.42	40.7	29.9	73
1.0	0.7	327.04	196.16	68.6	47.9	70
0.25	0.5	105.28	61.38	21.5	16.8	78
0.50	0.5	227.81	120.29	42.1	30.7	73
1.0	0.5	423.36	227.36	79.6	60.5	76
0.25	0.4	142.7	76.04	26.6	17.7	67
					Average	81

wastewater were the most stable at all HRT's tested. Similar findings were made during startup. At HRT down to 0.5 days there was little accumulation of VA and pH remained above 6.7. With increasing influent waste concentration there was a decrease in reactor stability.

The reactor treating 2.0% sucrose wastewater was unstable and failed at an HRT of less than 2 days (10 kg COD m^{-3} d^{-1}; 0.133 kg COD m^{-2} d^{-1}). Instability was characterized by accumulation of longer chain VA in the mixed liquor and concomitant decrease in pH below 6.3 (Table 5.6). Because of the instability of this reactor only results recorded at HRT of 7.0 and 4.0 days are used for kinetic analysis. It has been reported that accumulation of propionic and butyric acids indicates that reactors are being operated under stress (Kennedy and van den Berg, 1982b; Kennedy et al., 1985). Guiot and van den Berg (1984) treating the same 2.0 % sucrose wastewater with an anaerobic UBF reactor also reported process instability and were unable to achieve significant rates of waste stabilization.

5.3.4 Effect of Hydraulic and Organic Loading Rate on COD Removal Efficiency

Effects of influent substrate concentration on COD removal efficiency of anaerobic DSFF reactor, compared to HRT and organic loading rate, are shown in Figs. 5.12 and 5.13. Substrate removal efficiency is a function of HRT and

Table 5.6 Characteristics of Soluble Effluent

S_o	HRT	Volatile acids, mg L^{-1}			Total volatile acids	Ratio of total volatile acids to soluble COD
%	days	acetic	propionic	butyric	mg COD L^{-1}	%
2.0	7.0	140	75	10	432	54
0.25	4.4	50	30	10	117	111
0.50	4.1	70	30	10	138	115
1.0	4.0	190	40	10	281	73
2.0	4.0	400	1400	100	2726	68
0.25	2.0	60	35	10	135	79
0.50	2.0	150	190	10	465	82
1.0	2.0	540	150	80	947	71
2.0	2.0	1385	3530	140	7070	81
0.25	1.0	135	65	10	260	88
0.50	1.0	205	280	50	733	68
1.0	1.0	915	275	120	1608	65
0.25	0.7	160	120	70	479	93
0.50	0.7	460	560	50	1428	67
1.0	0.7	880	370	820	2986	73
0.25	0.5	260	160	100	701	71
0.50	0.5	560	500	120	1571	65
1.0	0.5	1675	505	300	3093	71
0.25	0.4	325	140	-	--	-
					Average	77.5

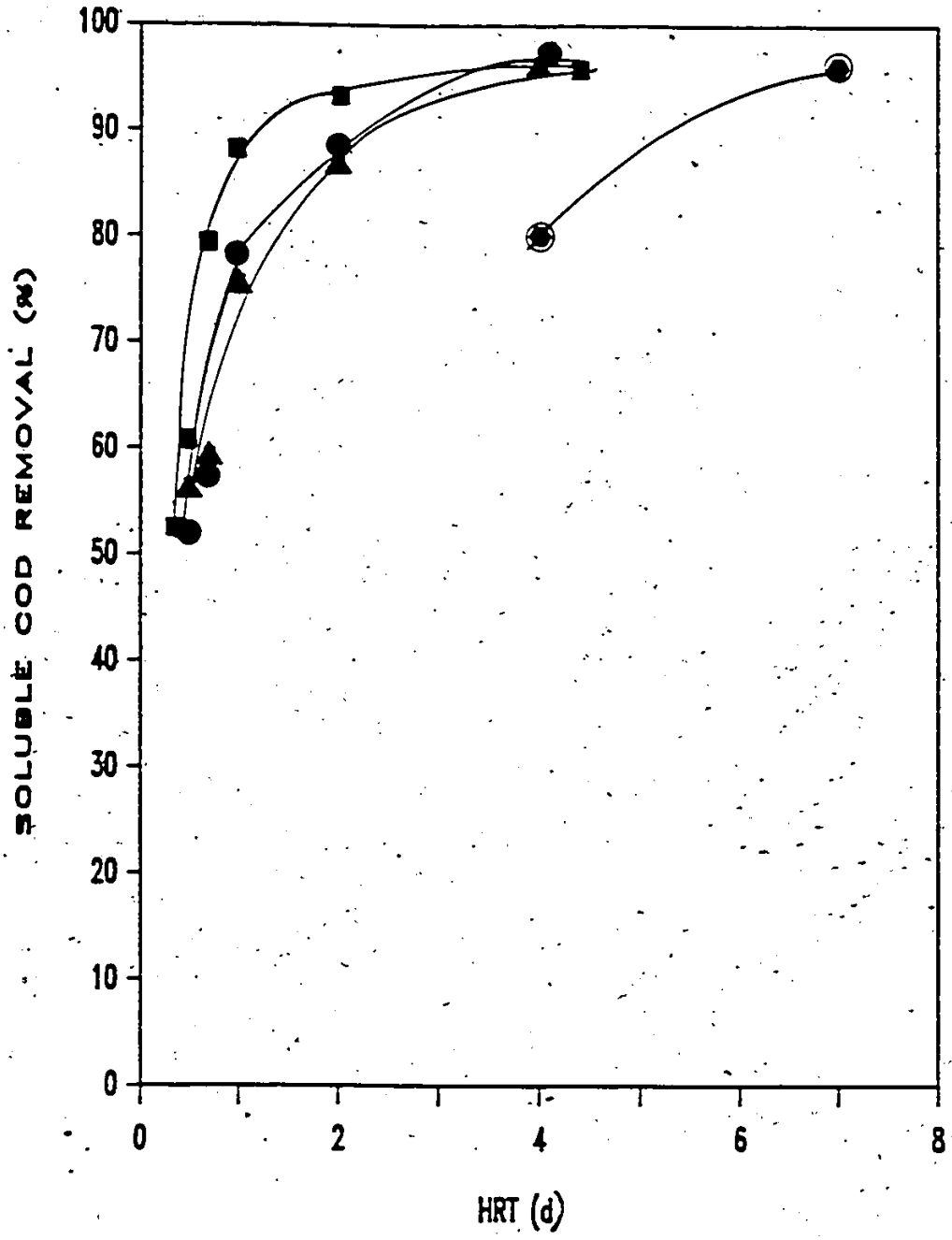

Figure 5.12 Soluble COD removal efficiency versus HRT, 2.5 g L^{-1} (■), 5.0 g L^{-1} (●), 10.0 g L^{-1} (▲) and 20 g L^{-1} (◉).

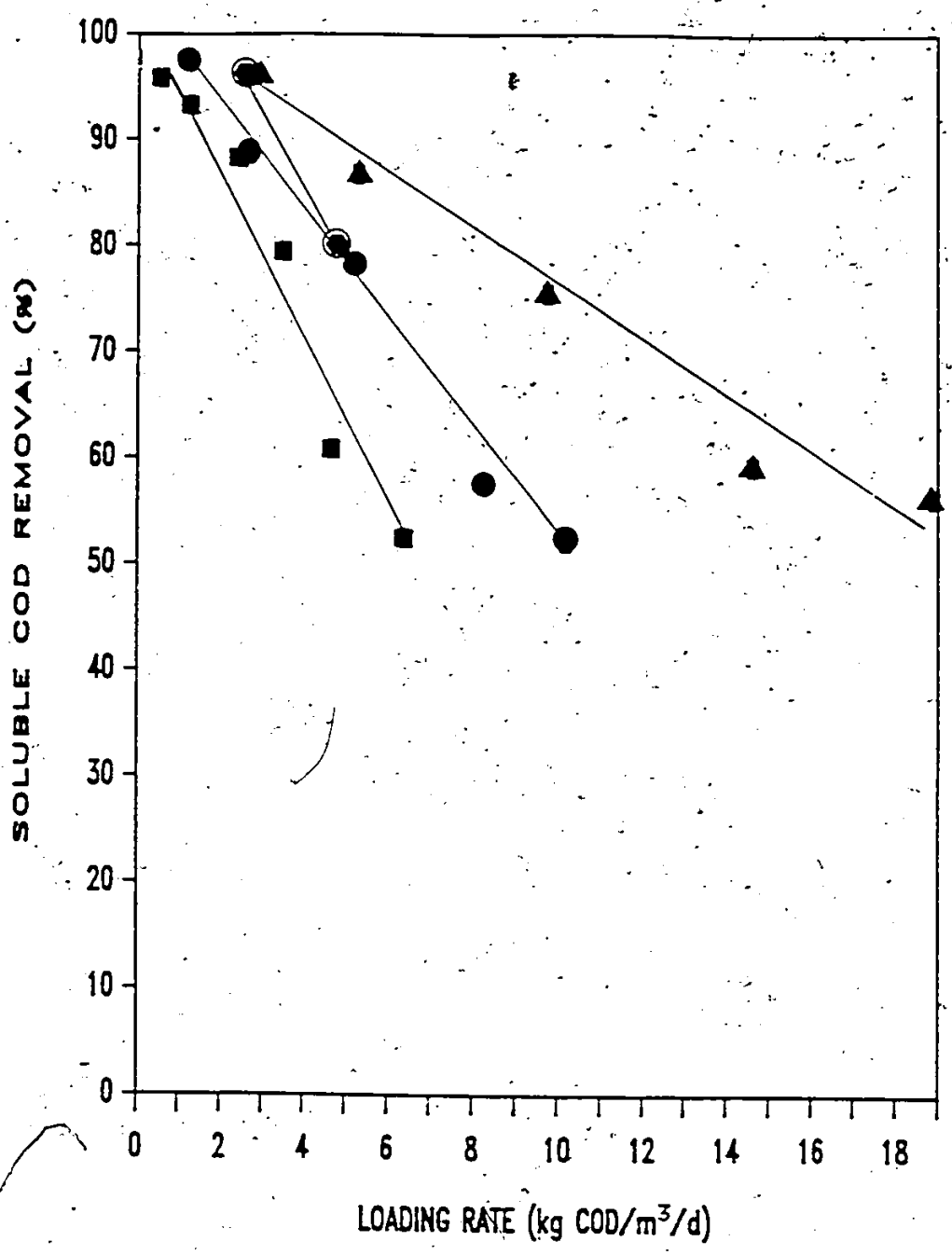

Figure 5.13 Soluble COD removal efficiency versus organic loading rate. 2.5 g L^{-1} (■), 5.0 g L^{-1} (●), 10.0 g L^{-1} (▲) and 20 g L^{-1} (●).

concomitant organic loading rate. It is important to note that for reactors treating 0.25, 0.5 and 1.0 % sucrose wastewater, COD removal efficiencies were in excess of 75 % at HRT as low as 1 day. A decrease in HRT from 1.0 to 0.5 days resulted in a 50 % decrease in soluble COD removal efficiency for the three reactors discussed above. At a 2 day HRT the reactor treating 2.0 % sucrose had a COD removal efficiency of 56%. However, in terms of organic loading, COD removal efficiency of the reactor treating 2.0 % sucrose wastewater was approximately the same as the other reactors at similar organic loading rates. It is important to mention that while the three DSFF reactors treating more dilute wastewaters were stable at all HRT tested the reactor treating 2.0 % sucrose waste was unstable. High sucrose concentration coupled with slight variations in flow rate often caused elevated VA concentrations (increased acidogenic biomass production) and low pH in the reactor. These conditions resulted in an inbalance between acidogenic and methanogenic bacterial species and concomitant reactor instability.

Total COD removal efficiency was only slightly less than soluble COD removal efficiency (Figs. 5.14 and 5.15). This reflected the low concentration of suspended biomass associated with DSFF reactors operated at short HRT.

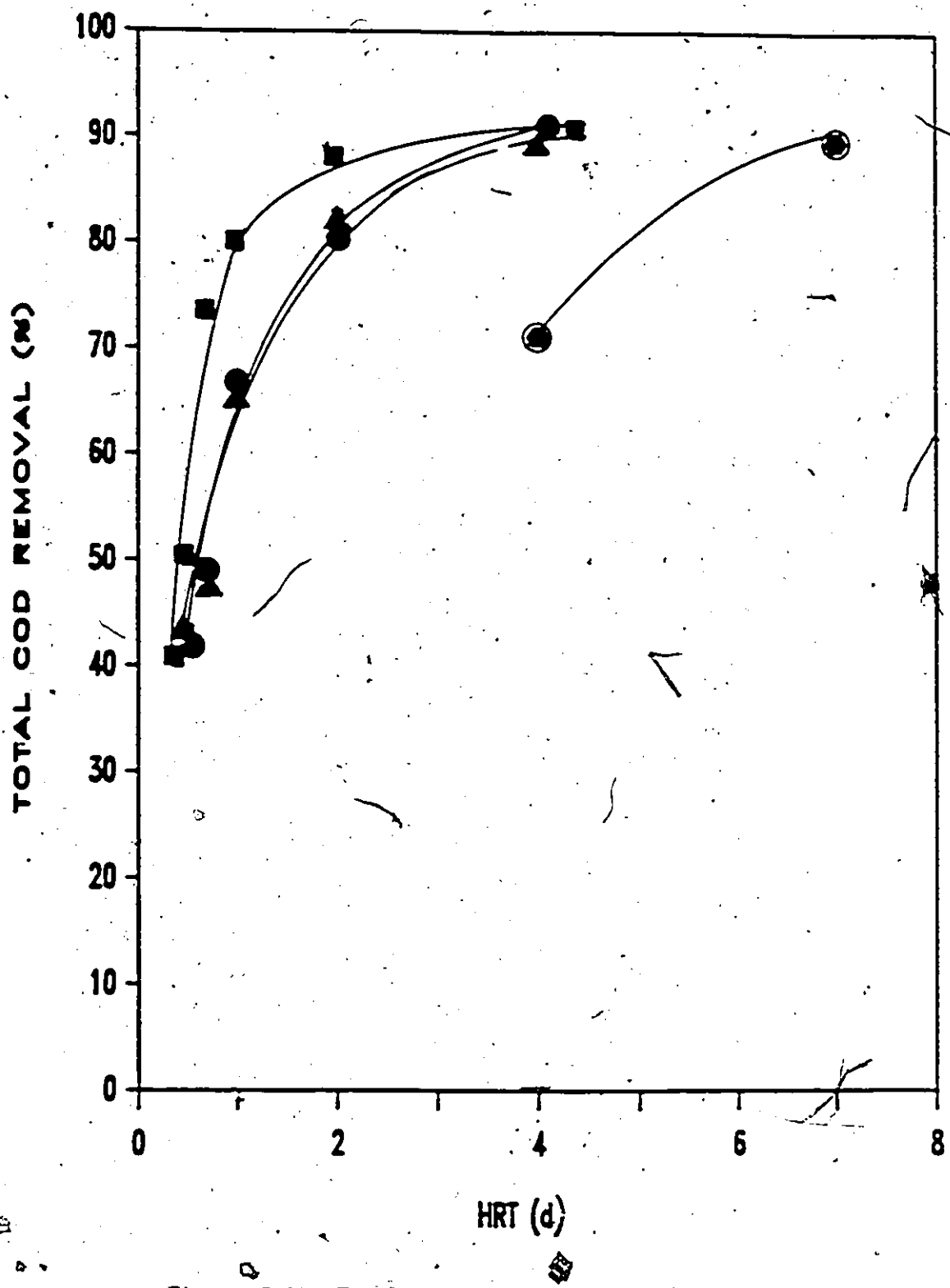

Figure 5.14 Total COD removal efficiency versus HRT, 2.5 g L^{-1} (■), 5.0 g L^{-1} (●), 10.0 g L^{-1} (▲) and 20 g L^{-1} (◉).

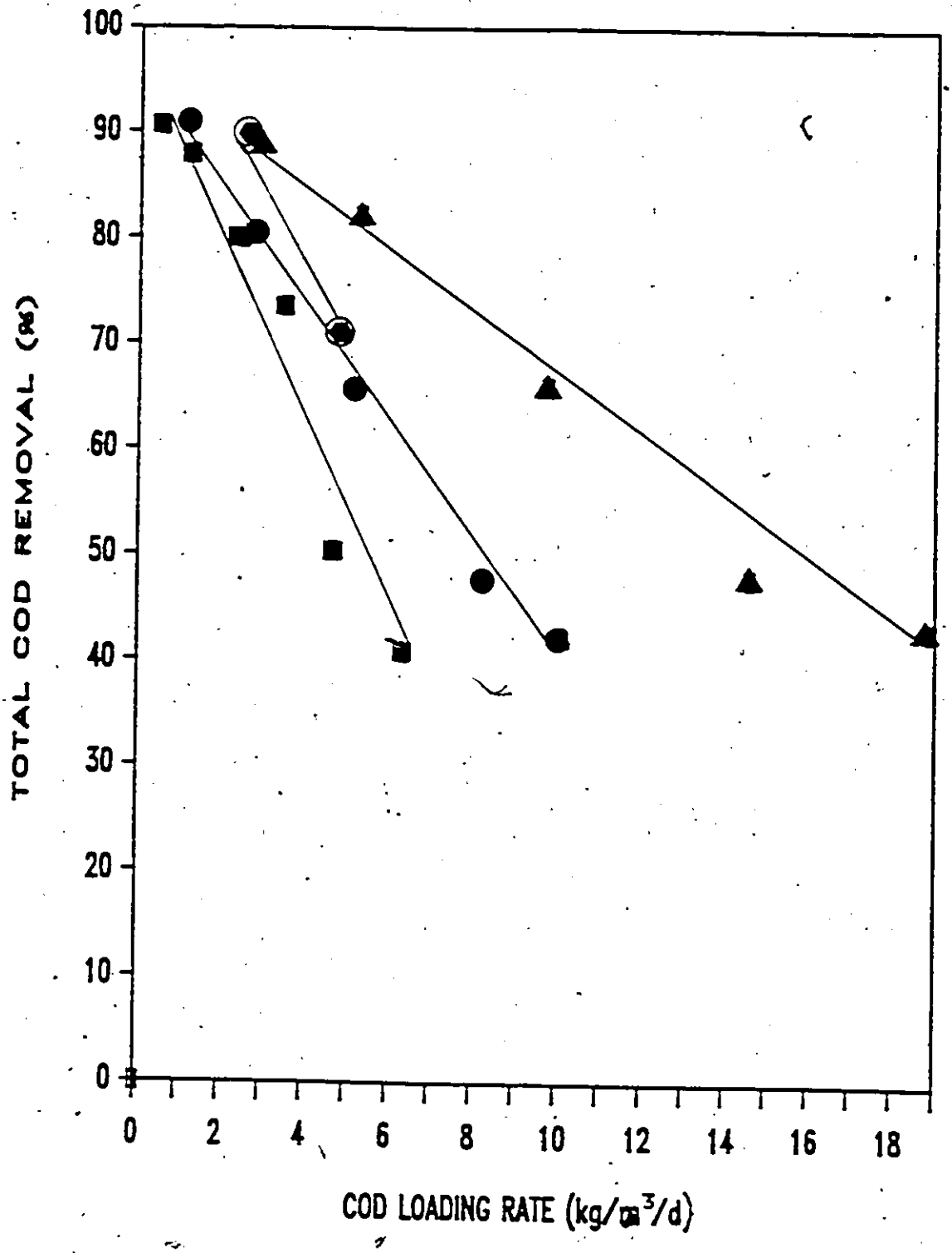

Figure 5.15 Total COD removal efficiency versus organic loading rate, 2.5 g L^{-1} (■), 5.0 g L^{-1} (●), 10.0 g L^{-1} (▲) and 20 g L^{-1} (◉).

5.3.5 COD Removal vs Reactor Height

DSFF reactors in this study were operated at a high recirculation rate to ensure complete mixed conditions (Appendix A). Figures 5.16a, b, c and d show soluble COD concentrations along reactor height at various HRT. Soluble COD removal was constant at any point for steady state conditions tested. Similar types of concentration profiles were obtained for VA concentrations. Insoluble COD reactor profiles also showed no significant suspended solids gradients existed in the mixed liquor and that there was little accumulation of biomass in the bottom of the reactor. There was no excess floating sludge which was characteristic of DSFF reactors started with sucrose wastewater at a concentration of 2.0 %. Absence of floating sludge at steady state is related to low operating HRT and has been discussed in a previous section. These results indicated CM behavior and supported DSFF reactor mixing studies discussed in Section 5.1 and Appendix A. The CM regime in a DSFF reactor contrasts with the plug flow (PF) pattern reported for conventional upflow anaerobic filters. In conventional filters, the majority of waste stabilization occurs in the bottom one-third of the reactor where most of the active biomass is located (Young and McCarty, 1969; Mueller and Mancini, 1975).

5.3.6 General Biomass Characteristics

Suspended biomass made up a small percentage of the total biomass within DSFF reactors (Table 5.7). An average

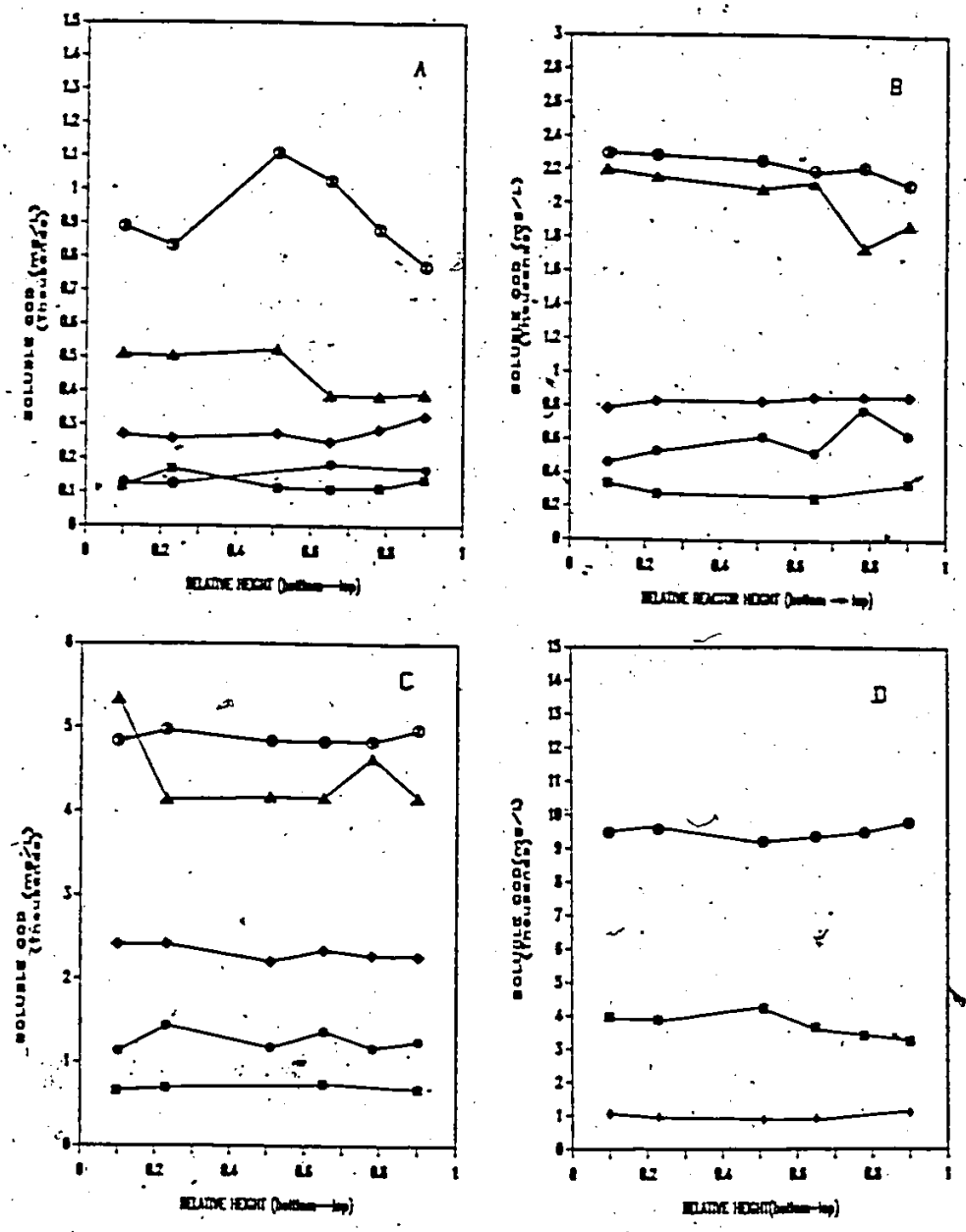

Figure 5.16 Mixed liquor soluble COD versus reactor height, 2.5 g L^{-1} (A), 5.0 g L^{-1} (B), 10.0 g L^{-1} (C) and 20 g L^{-1} (D), 7 d HRT (◆), 4 d HRT (■), 2 d HRT (●), 1 d HRT (◆), 0.7 d HRT (▲) and 0.5 d HRT (⊕).

Table 5.7 Suspended and Fixed Biomass for Steady State Reactor Operation

S_o	HRT	Suspended biomass	Attached biomass	Total biomass	Ratio of suspended to total biomass
%	days	kg VSS m^{-3}	kg VFS m^{-3}	kg VFS m^{-3}	%
2.0	7.0	0.89	2.83	3.72	24.0
0.25	4.4	0.09	2.17	2.26	4.0
0,50	4.1	0.23	2.68	2.91	8.0
1.0	4.0	0.49	3.82	4.32	11.5
2.0	4.0	1.26	3.98	5.25	24.2
0.25	2.0	0.09	2.75	2.84	3.2
0.50	2.0	0.28	3.75	4.04	7.1
1.0	2.0	0.32	5.20	5.52	5.9
2.0	2.0	1.88	6.94	8.82	21.3
0.25	1.0	0.14	3.19	3.33	4.3
0.50	1.0	0.44	5.03	5.47	8.1
1.0	1.0	0.66	8.44	9.11	7.3
0.25	0.7	0.10	3.46	3.56	2.9
0.50	0.7	0.34	6.93	7.27	4.7
1.0	0.7	0.79	8.30	9.09	8.7
0.25	0.5	0.18	4.18	4.36	4.2
0.50	0.5	0.34	7.87	8.22	4.2
1.0	0.5	0.93	8.71	9.65	9.7
				Average	8.6

value of 8.6 percent of all biomass in DSFF reactors was suspended biomass. In general, suspended biomass increased with increased waste strength and longer HRT. For DSFF reactors treating 0.25 and 2.0% sucrose wastewater, average VSS component of total reactor biomass was less than 5 percent and greater than 20 percent, respectively.

Suspended solids concentration in the effluent is often a measure of effluent quality. Figures 5.17a and b show effluent suspended solids for influent waste concentrations as a function of HRT and organic loading rate, respectively. Concentration of suspended solids in the effluent increased only slightly for large decreases in HRT and concomitant increased organic loading rates. Most effluent suspended solids concentrations were less than 1.8 kg COD m^{-3} (1.4 kg VSS m^{-3}). Low biomass suspended solids even at low HRT indicate that microbial washout is not a major problem.

Periodic checks of mixed liquor acidogenic and methanogenic activity showed little or no methanogenic activity for the majority of steady state conditions. Some methanogenic activity was found in the mixed liquor of the DSFF reactor treating 2.0 % sucrose at a 7 day HRT, this was not surprising since certain methanogenic bacteria have doubling times of less than 7 days (Wandrey and Aivasidis, 1984). Acidogenic activity was always found in the mixed liquor and varied between 2-8 g COD $(g\ VSS)^{-1}\ d^{-1}$. Low concentrations of suspended solids (biomass) and absence of methanogenic activity in the mixed liquor not only reflects the small

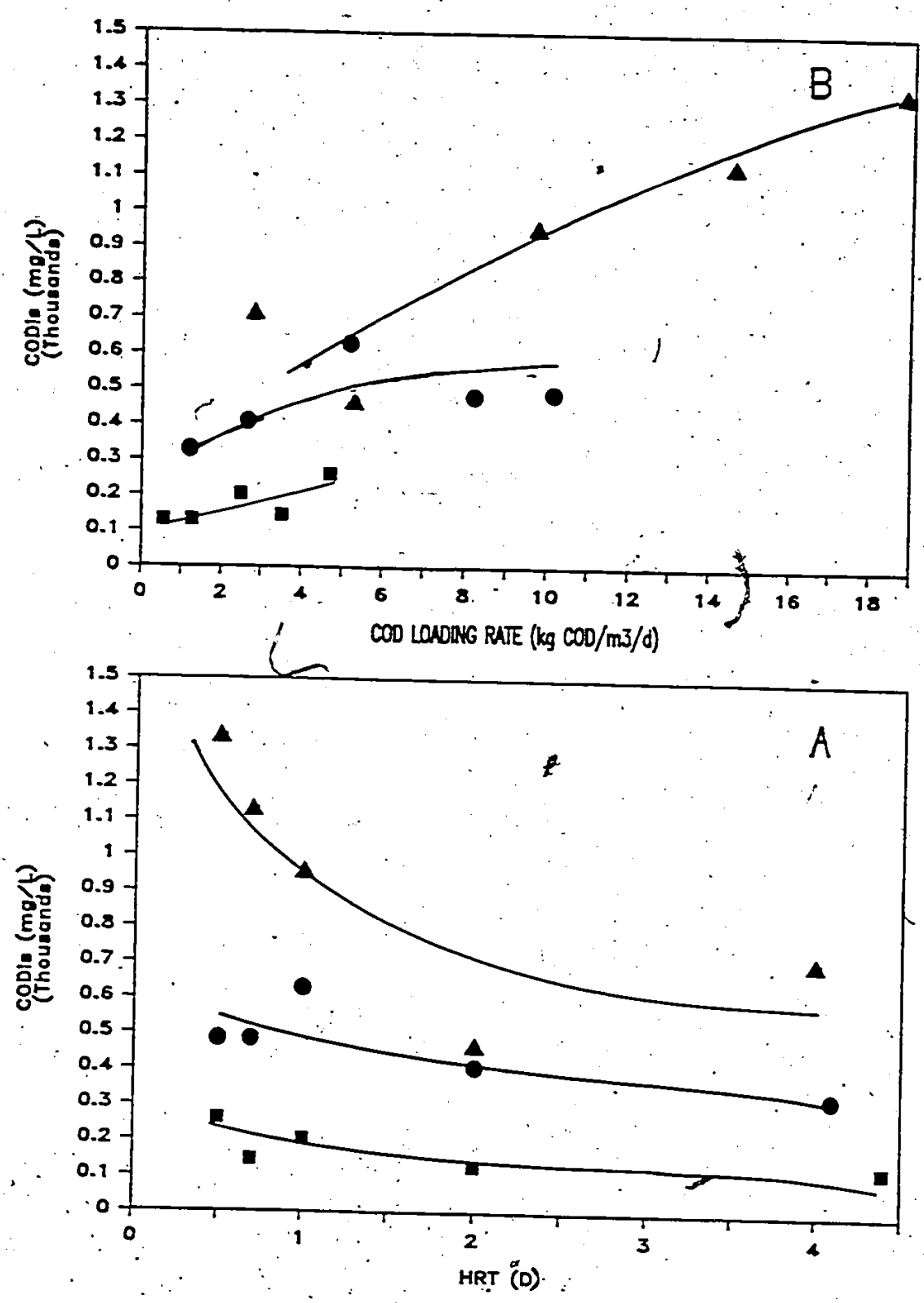

Figure 5.17 Effluent suspended solids versus HRT (A) or organic loading rate (B), 2.5 g L^{-1} (■), 5.0 g L^{-1} (●) and 10.0 g L^{-1} (▲).

biomass yield but also the importance of the biofilm for waste stabilization.

5.3.7 Effect of SRT on COD Removal Efficiency and Effluent Suspended Solids

SRT is a basic design parameter for biological waste treatment processes. Because of previous sampling problems related to the design of DSFF reactors it had been impossible to obtain reliable SRT data. This problem was overcome by using removable biofilm supports. Figure 5.18 is a plot of COD removal efficiency versus SRT. COD removal efficiency was related to SRT and relatively unaffected by influent waste strength and HRT. Maximum COD removal efficiency was achieved with SRT greater than 25 days. A curve based on SRT^{-1}, Eq. 3.53 and using kinetic constants determined for treatment of 0.5 % sucrose wastewater (discussed later) was compared with actual results. Measured results compare well with predicted values. The predictive curve indicates that at a SRT of approximately 9 days COD removal efficiency would be 0. At a SRT of less than 9 days methanogenic bacteria would be washed out of the reactor.

In a CSTR, HRT equals SRT. For DSFF reactors no information exists that shows a relationship between SRT and HRT. The empirical steady state model discussed in Chapter 3 relates COD removal efficiency and SRT to easily measured parameters such as HRT, influent waste strength and organic

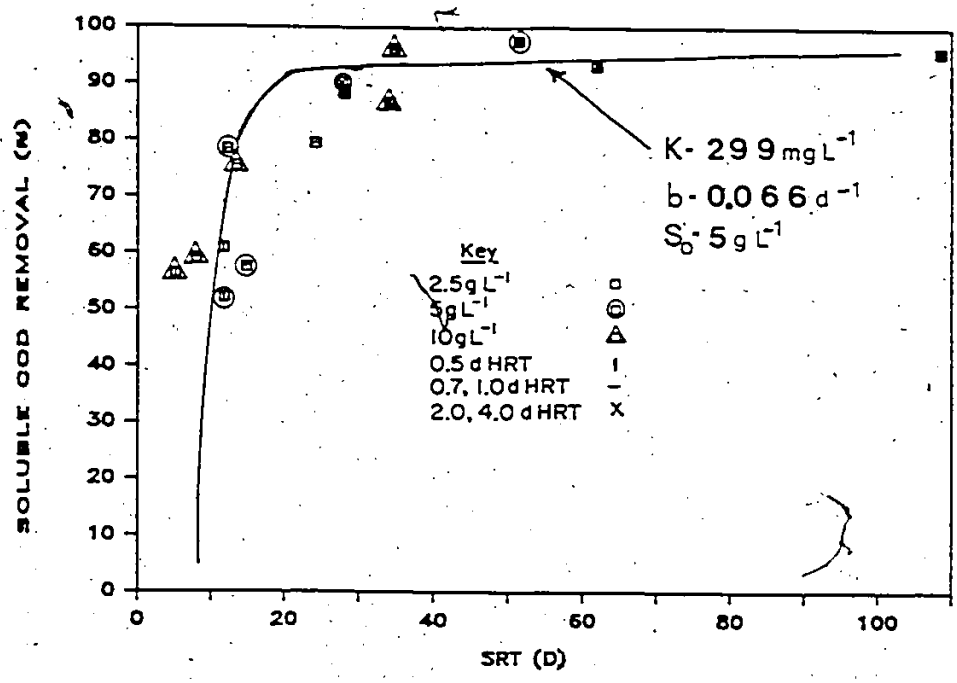

Figure 5.18 Measured and calculated soluble COD removal efficiency versus SRT.

loading rate. Determination of kinetic constants for this model are discussed later.

Figure 5.19 shows the relationship amoung SRT^{-1}, HRT and influent waste strength and insoluble effluent COD. Distinct trends are indicated for effluent TSS as a function of SRT, HRT and S_o. Knowing any 2 of the above parameters, Fig. 5.19 can be used to find the other parameters. For a given waste strength insoluble effluent COD concentration decreases with increasing SRT. For a given HRT insoluble COD concentration in the effluent increases with increasing waste strength while SRT decreases. Results from the reactor treating 2.0 % sucrose wastewater were not included because of the limited number of data points.

5.3.8 Biofilm Characteristics

Steady state biofilms that developed on NPP support material were zoogloeal biofilms. DSFF biofilms were thick (Table 5.3; Fig. 5.20) compared to biofilms found in anaerobic fluidized/expanded bed reactors which are about 15 microns thick (Switzenbaum, 1978). DSFF reactor biofilms were porous and filamentous with tentacle like appendages extending up to 1 cm into the mixed liquor surrounding the biofilm. Figure 5.21 shows many filaments of free floating yet attached biomass that produced a porous biofilm with extensive surface area. Visual inspection showed little diference between biofilms that developed during startup and steady state. Biofilms that developed in DSFF reactors

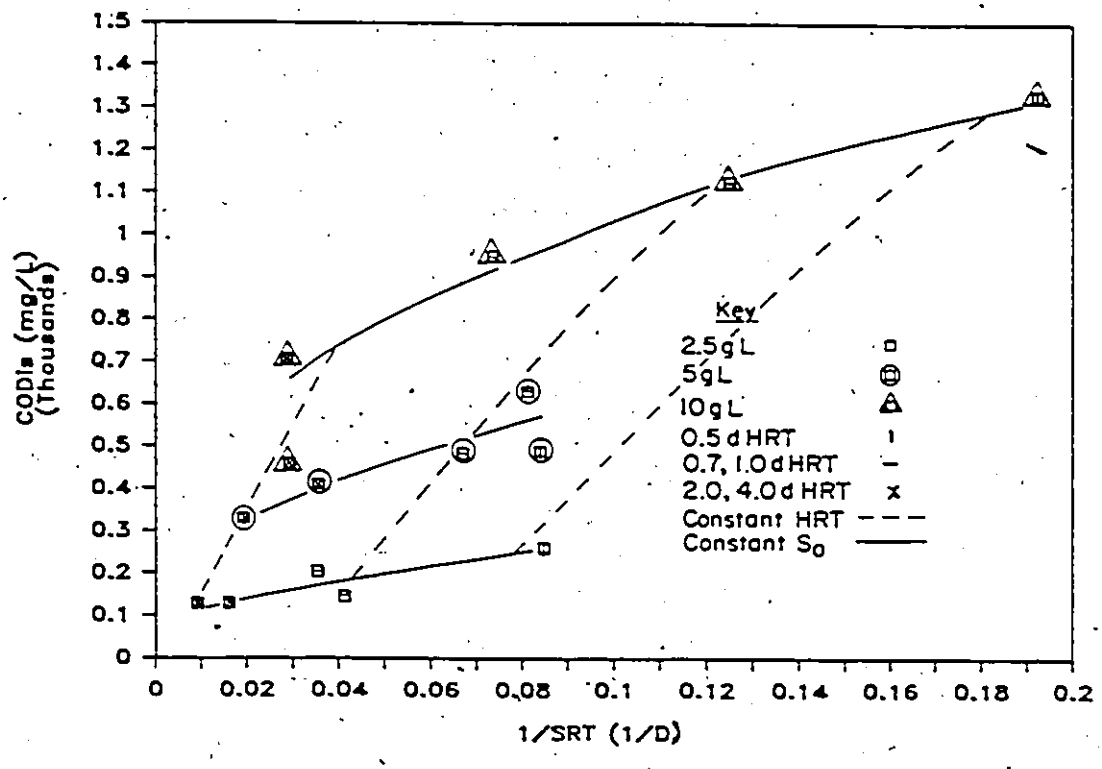

Figure 5.19 Effect of HRT, S_o and SRT^{-1} on insoluble effluent COD.

Figure 5.20 Photograph of mature anaerobic biofilms.

Figure 5.21 Photograph of gas bubble formation in mature biofilm.

COLOURED PICTURES
Images en couleur

during startup and steady state operation were 5-6 percent (w/v of biofilm) non-soluble solids of which 75-80 percent were volatile solids.

DSFF reactor methanogenic activity in the biofilm, biogas production and associated biofilm micromixing were observed to be intense in relation to HRT and slow reaction rates of anaerobic microbes. Formation of gas bubbles is readily observed in Fig. 5.21.

Microscopic observation of DSFF biofilms (Fig. 5.22a, magnification 95X) showed microbes attached both to individual polyester fibres and entrapped by the NPP support material. Further magnification (Fig. 5.22b, 2420X) shows bacteria characteristic of the genus *Methanothrix*.

Methanosarcina type bacteria were also observed but were not as numerous as *Methanothrix* type bacteria. Harvey (1984) reported that in DSFF reactors treating piggery wastewater the majority of bacteria in the biofilm were similar to those of the genus *Methanosarcina*. Differences in the methanogenic population which makes up the biofilm are due to differences in the waste or operating conditions.

Microscopic observation of microbes that make up good settling granular sludge in UASB reactors treating a variety of wastewaters have shown that they are mainly coccoid bacteria of the genus *Methanosarcina* (Lettinga *et al.*, 1980). As mentioned previously, attachment of filamentous and/or coccoid bacteria in fixed film reactors compared to mainly coccoid bacteria in UASB reactors would explain differences

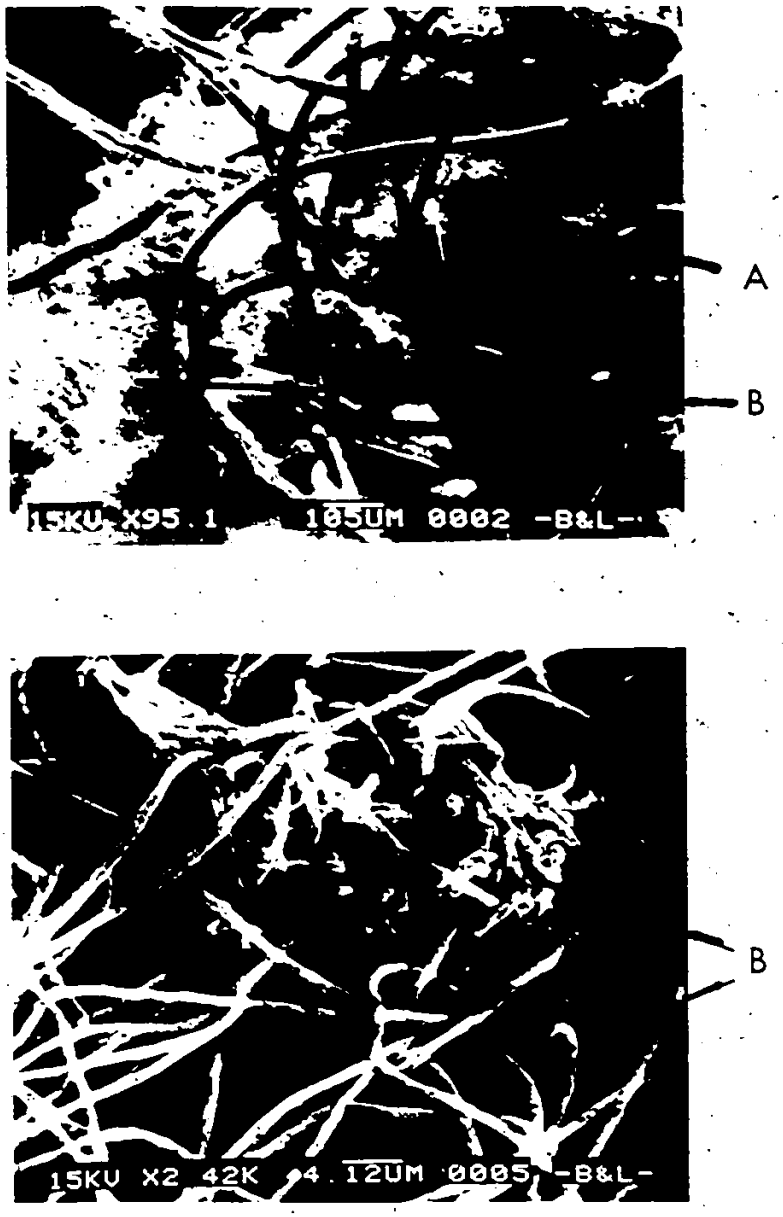

Figure 5.22 Electron micrographs of mature biofilms, NPP fibre (A), bacteria (B).

observed in startup and overall performance of these two reactor systems.

5.3.9 Biofilm Concentration and Thickness

The relationship between organic loading rate and DSFF reactor biofilm concentration is shown in Fig. 5.23. Biofilm biomass concentration (in terms of reactor liquid volume) increased linearly with increased organic loading rates up to 10 kg COD m^{-3} d^{-1} (0.133 kg COD m^{-2} d^{-1}) and was relatively unaffected by influent substrate concentration. At a loading rate of 10 kg COD m^{-3} d^{-1} a maximum biofilm concentration and maximum biofilm thickness of 8.7 kg VFS m^{-3} (0.116 kg VFS m^{-2}) and 2.6 mm respectively were obtained. At steady state loading rates higher than 10 kg COD m^{-3} d^{-1}, biofilm concentration levels off or at least the increase was very slow. Biofilm development during steady state DSFF reactor operation differed from that found for reactor startup. During startup, biofilm development was found to decrease with increased substrate concentration for reactors operated at similar organic loading rates. This difference in biofilm development is in part due to the startup protocol which limited VA accumulation in the reactor.

Figure 5.24 shows biofilm concentration for various steady state organic removal rates. Maximum biofilm concentration or a very low rate of increase in biofilm biomass concentration was achieved at a steady state organic removal rate of 7.5 kg COD m^{-3} d^{-1} (0.100 kg COD m^{-2} d^{-1}). This in-

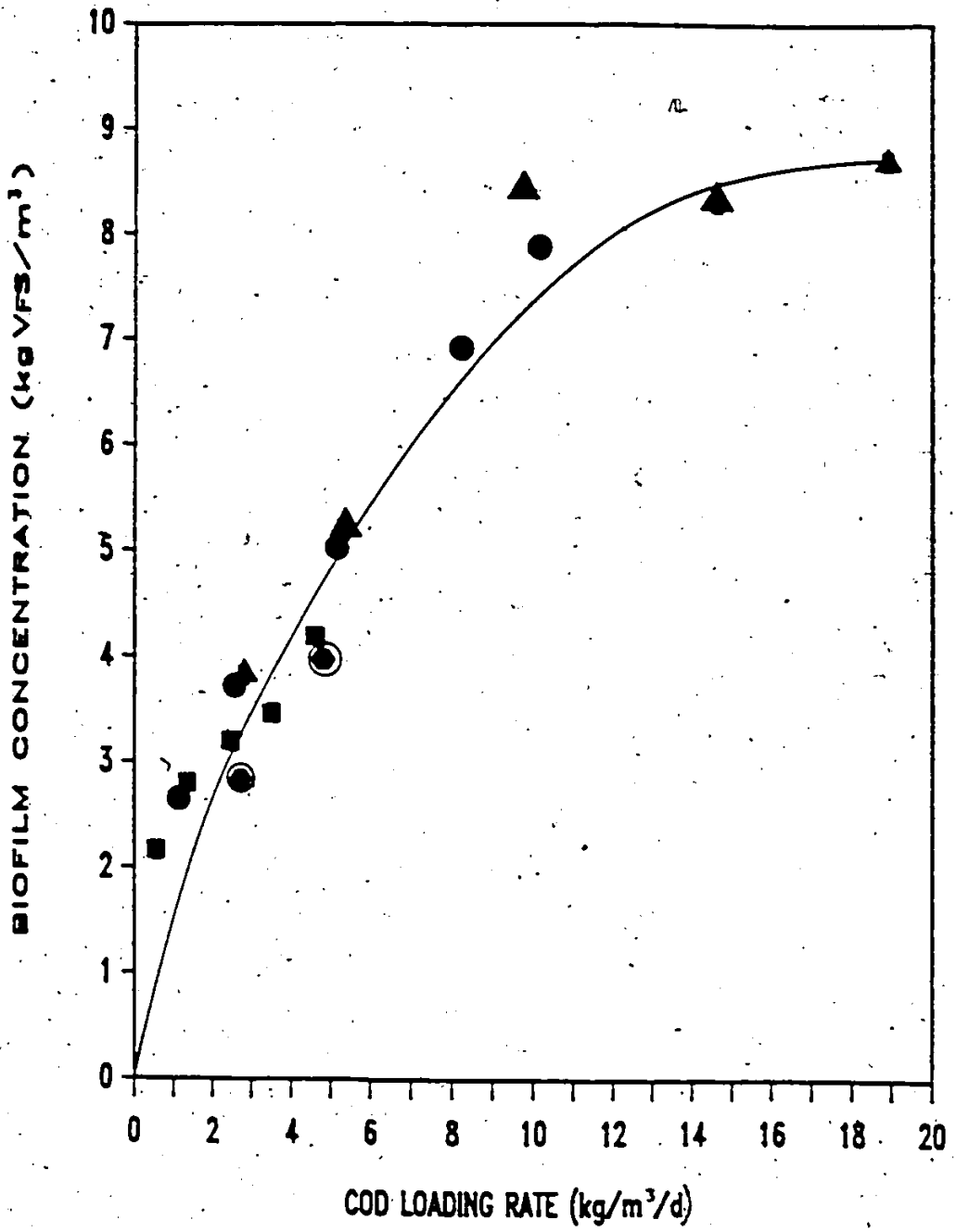

Figure 5.23 Biofilm concentration versus organic loading rate, 2.5 g L^{-1} (■), 5.0 g L^{-1} (●), 10.0 g L^{-1} (▲) and 20 g L^{-1} (◉).

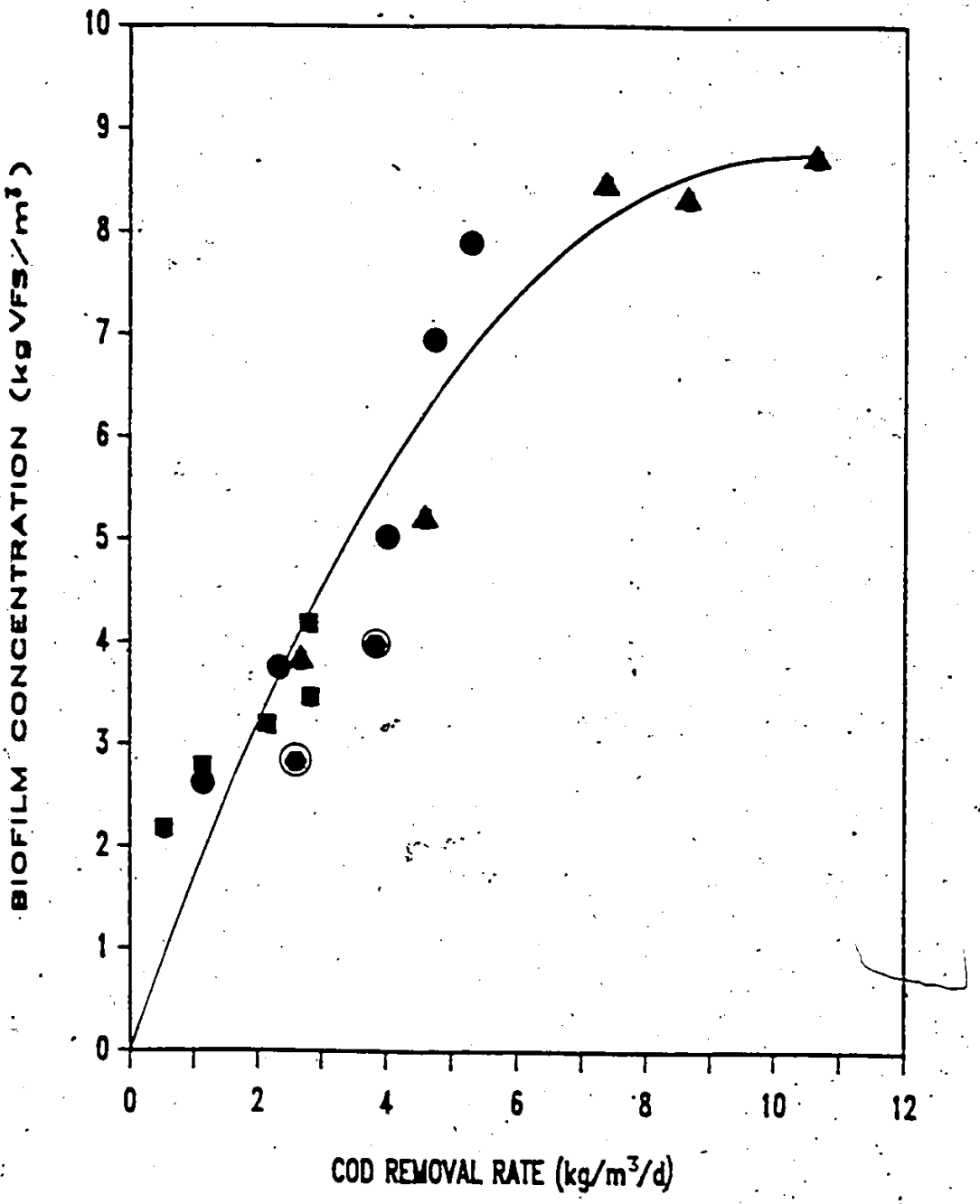

Figure 5.24 Biofilm concentration versus organic removal rate, 2.5 g L^{-1} (■), 5.0 g L^{-1} (●), 10.0 g L^{-1} (▲) and 20 g L^{-1} (◉).

dicates that a quasi- equilibrium was reached between biofilm and mixed liquor growth, attachment and biofilm sloughing. This situation corresponds to the final stage of aerobic biofilm development (Bryers and Characklis, 1981). Studies have indicated that when liquid velocity in reactor channels is sufficient, no significant plugging should occur (Samson *et al.*, 1984a). If this is the case, eventual plugging of reactor channels should not occur. In this study, high biofilm biomass concentrations (up to 8.7 kg biofilm VFS m^{-3}) coupled with extensive surface area, the porous nature of the biofilm and negligible methanogenic activity in the mixed liquor indicate that the biofilm is primarily responsible for waste stabilization. However, if a maximum biofilm concentration has been achieved, organic removal capacity of DSFF reactors is limited unless there is a change in the microbial population of the biofilm that would effect an increase in the specific substrate utilization rate.

Figure 5.25 shows effect of HRT on biofilm concentration at various steady state conditions. Reactor biofilm concentration and biofilm thickness increase with decreasing HRT and increasing waste strength. This behavior is similar to results reported for attached biomass in anaerobic expanded/fluidized beds (Switzenbaum and Jewell, 1980).

DSFF reactor biofilm concentration was less than reported for other advanced anaerobic reactors treating similar wastes at 35°C. Biomass concentrations in anaerobic ex-

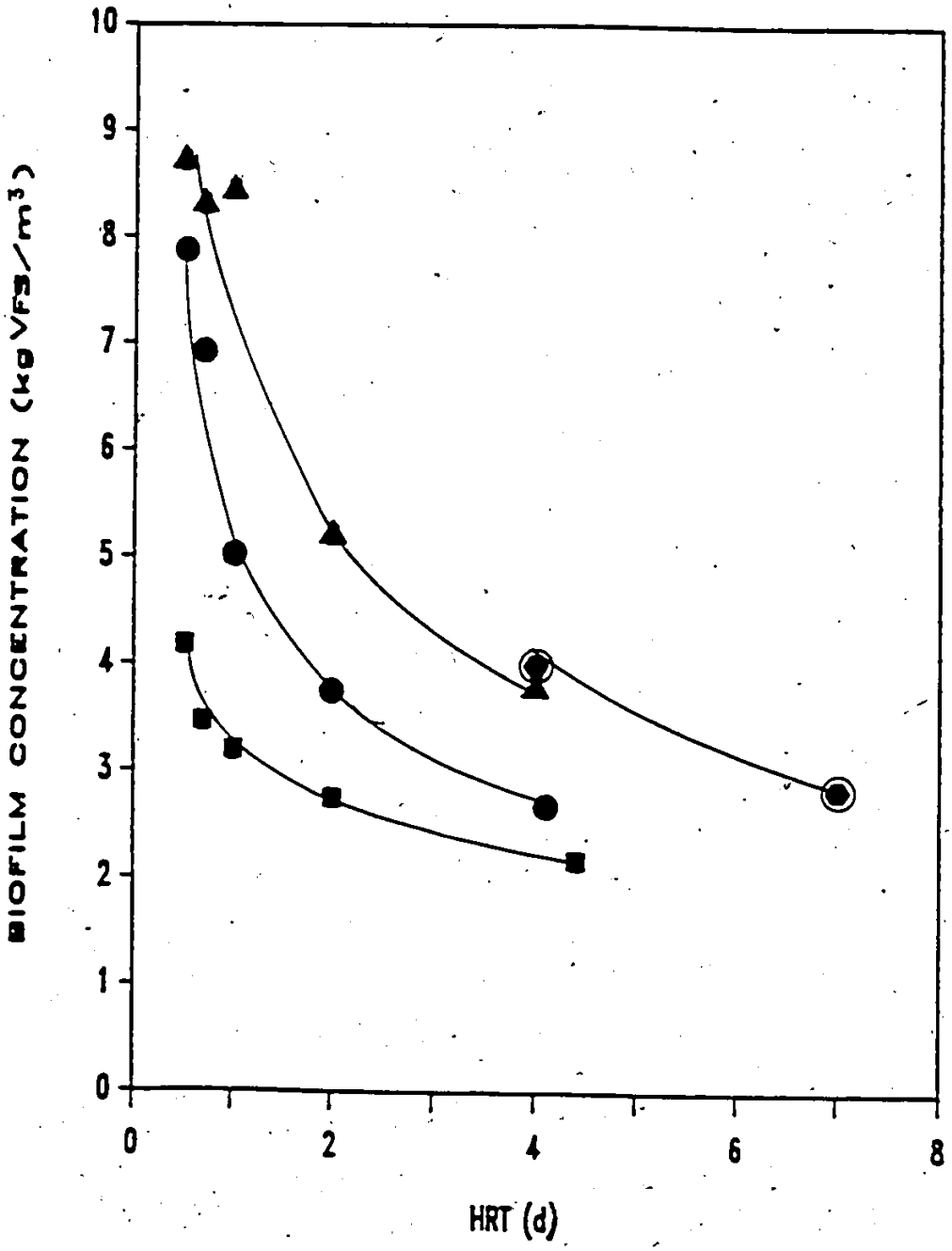

Figure 5.25 Biofilm concentration versus HRT, 2.5 g L^{-1} (■), 5.0 g L^{-1} (●), 10.0 g L^{-1} (▲) and 20 g L^{-1} (◉).

panded/fluidized beds (Switzenbaum and Jewell, 1980), upflow anaerobic filters (Dahab and Young, 1982), upflow anaerobic sludge blanket reactors (Lettinga *et.al.*, 1980) and combination upflow anaerobic blanket-filters (Guiot and van den Berg, 1984) of 40, 25, 30 and 30 kg VSS m^{-3} respectively, have been reported. Assuming that biomass of similar specific activity develops in each type of reactor (Table 5.8), the maximum waste stabilization capacity of DSFF reactors would be less than other advanced anaerobic reactors. However, biomass may still be accumulating in the DSFF reactor at a low rate (Fig. 5.24), and over an extended period of reactor operation biofilm concentration may increase resulting in a higher waste stabilization capacity. However, performance of DSFF reactors is quite satisfactory and they offer operational advantages* that have been discussed previously.

5.3.10 Biofilm Performance

Specific biofilm organic loading rates and specific biofilm substrate utilization rates, U_f, were obtained by dividing amount of substrate added per day and amount of substrate removed per day, respectively, by amount of biofilm biomass in the system (Table 5.9). The relationship between COD removal efficiency and specific biofilm loading rate is shown in Fig. 5.26. COD removal efficiency decreased with increased specific biofilm loading rate and was relatively unaffected by waste concentration. At a

Table 5.8 Comparison of specific utilization rate for anaerobic reactors treating carbohydrate wastewaters

Substrate	Reactor[a]	Operating Temperature °C	Specific rate $g^{COD}\ g^{VSS^{-1}}\ d^{-1}$	Reference
Sucrose	DSFF:(FG)	35	0.9-1.2	This study
Sucrose	Upflow sludge blanket filter; (SG)	27	1.0-1.2	Guiot and van den Berg (1984)
Dextrose/ Protein	Upflow filter; (FSG)	35	1.0	Mueller and Mancini (1975)
Sugar beets (soured)	Upflow sludge blanket;(SG)	30	0.6-0.9	Lettinga et al. (1980)
Sucrose	Expanded bed; (FG)	30	0.4-0.8	Switzenbaum and Jewell (1980)

a (FG) - fixed growth

(SG) - suspended growth

(FSG) - fixed and suspended growth

Table 5.9 Specific Substrate Loading and Substrate Removal Rates, SRT and u_o for Steady State Reactor Operation

S_o	HRT	Specific loading rate	Specific biofilm loading rate	U[a]	U_f[a]	SRT	u_o
%	days	kg COD(kg VSFS)$^{-1}$ d^{-1}	kg COD(kg VFS)$^{-1}$ d^{-1}	kg COD(kg VSFS)$^{-1}$ d^{-1}	kg COD(kg VFS)$^{-1}$ d^{-1}		
2	7.0	0.73	0.95	0.69	0.91	29.1	0.034
0.25	4.4	0.25	0.26	0.24	0.25	108.6	0.009
0.50	4.1	0.41	0.44	0.40	0.43	51.4	0.019
1.0	4.0	0.65	0.73	0.62	0.70	34.7	0.028
2.0	4.0	0.91	1.20	0.73	0.96	16.5	0.060
0.25	2.0	0.45	0.46	0.41	0.43	62.0	0.016
0.50	2.0	0.66	0.70	0.58	0.63	27.9	0.035
1.0	2.0	0.96	1.01	0.83	0.88	34.1	0.029
2.0	2.0	1.19	1.51	0.67	0.85	9.4	0.106
0.25	1.0	0.75	0.78	0.66	0.69	23.1	0.043
0.50	1.0	0.94	1.02	0.74	0.80	12.3	0.081
1.0	1.0	1.07	1.15	0.81	0.87	13.6	0.073
0.25	0.7	0.98	1.02	0.79	0.81	24.2	0.041
0.50	0.7	1.13	1.19	0.65	0.68	14.9	0.067
1.0	0.7	1.61	1.76	0.95	1.04	8.0	0.124
0.25	0.5	1.08	1.12	0.65	0.68	11.8	0.084
0.50	0.5	1.24	1.29	0.64	0.67	11.9	0.084
1.0	0.5	1.96	2.17	1.10	1.22	5.2	0.194

[a] U and U_f refer to specific substrate removal rate by total biomass and biofilm biomass, respectively.

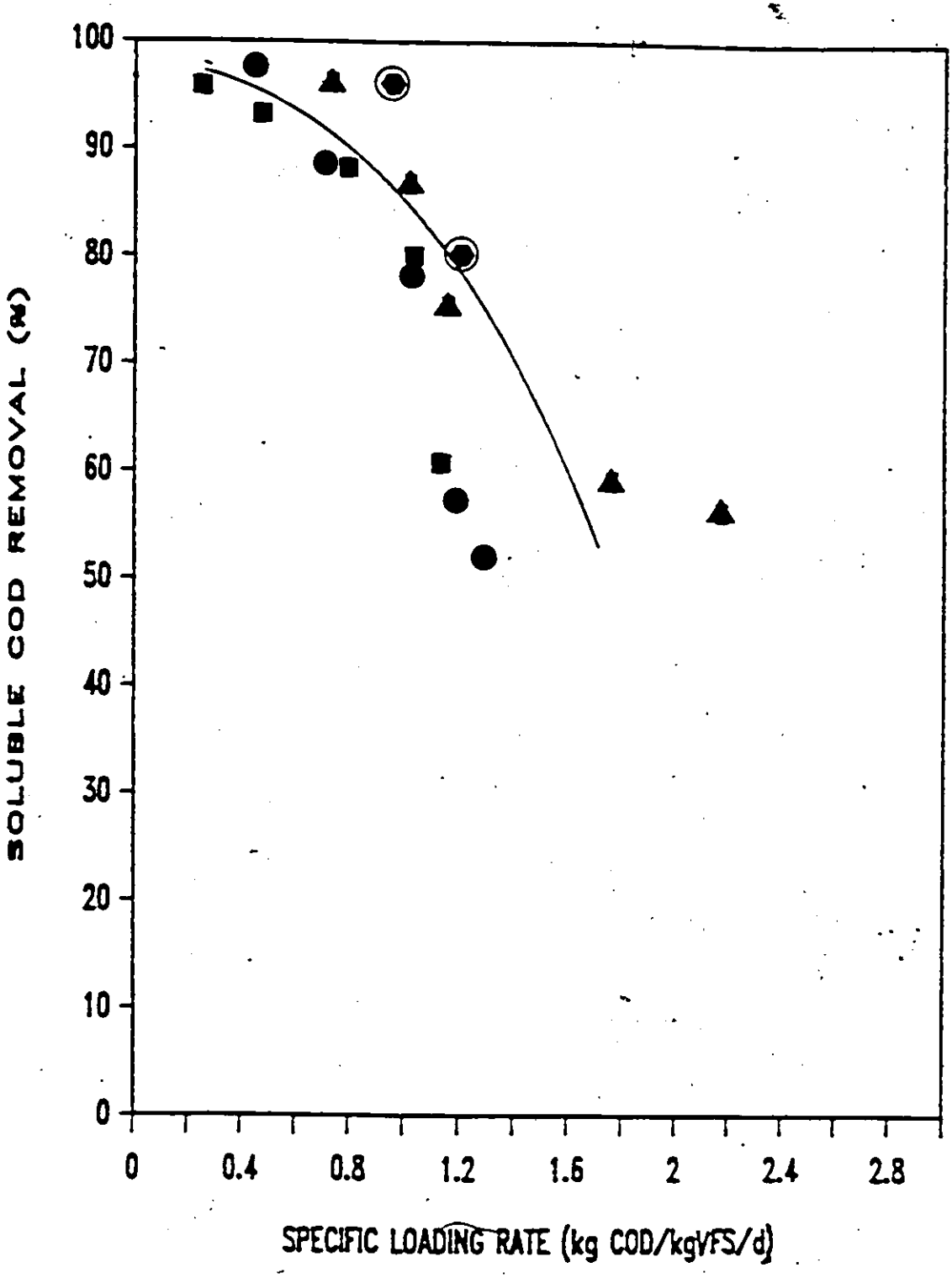

Figure 5.26 Soluble COD removal efficiency versus specific biofilm loading rate, 2.5 g L^{-1} (■), 5.0 g L^{-1} (●), 10.0 g L^{-1} (▲), and 20 g L^{-1} (◉).

specific biofilm loading rate of 1.0 kg COD (kg VFS)$^{-1}$ d^{-1} COD removal efficiencies were 80, 79, and 83 percent for reactors treating 2.5, 5.0 and 10 g L^{-1} sucrose wastewater, respectively. At loading rates greater than 1.0 kg COD (kg VFS)$^{-1}$ d^{-1} COD removal efficiency decreased rapidly. Comparison of specific biofilm loading and substrate removal rates to specific loading and substrate removal rates shows little difference indicating the small contribution of suspended biomass to waste stabilization (Table 5.9).

Figure 5.27 shows the relationship between specific biofilm loading rate and specific biofilm substrate removal rate. Specific biofilm substrate removal rate increased with increased specific biofilm loading rate. However, with increased specific biofilm loading, the measured specific biofilm substrate removal rate curve (curve B) diverges from the maximum COD removal curve (curve A) indicating a decrease in COD removal efficiency.

Figure 5.28 indicates that the specific biofilm substrate utilization rate increases with increasing volumetric organic loading rate. A maximum specific biofilm utilization rate of 0.9-1.2 kg COD (kg VFS)$^{-1}$ d^{-1} was obtained at a loading rate greater than 5 kg COD m^{-3} d^{-1} (0.066 kg COD m^{-2} d^{-1}). Figure 5.29 shows that the specific biofilm utilization rate increases with decreasing HRT and increasing wastewater concentration.

As discussed previously, Henze and Harremoes (1982) suggest that anaerobic biofilms become diffusion limited at

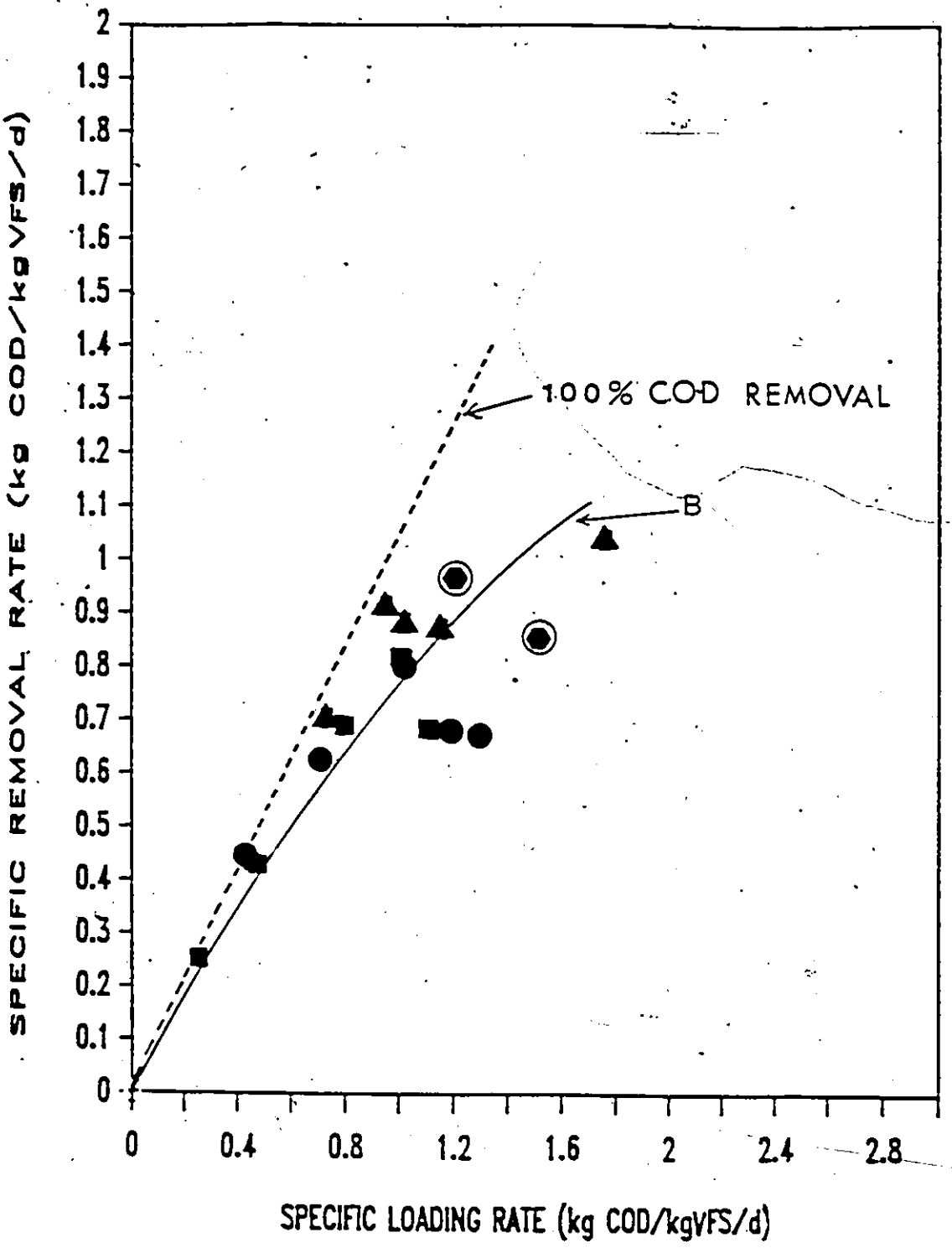

Figure 5.27 Specific biofilm substrate removal rate versus specific biofilm loading rate. 2.5 g L^{-1} (■), 5.0 g L^{-1} (●), 10.0 g L^{-1} (▲) and 20 g L^{-1} (◉).

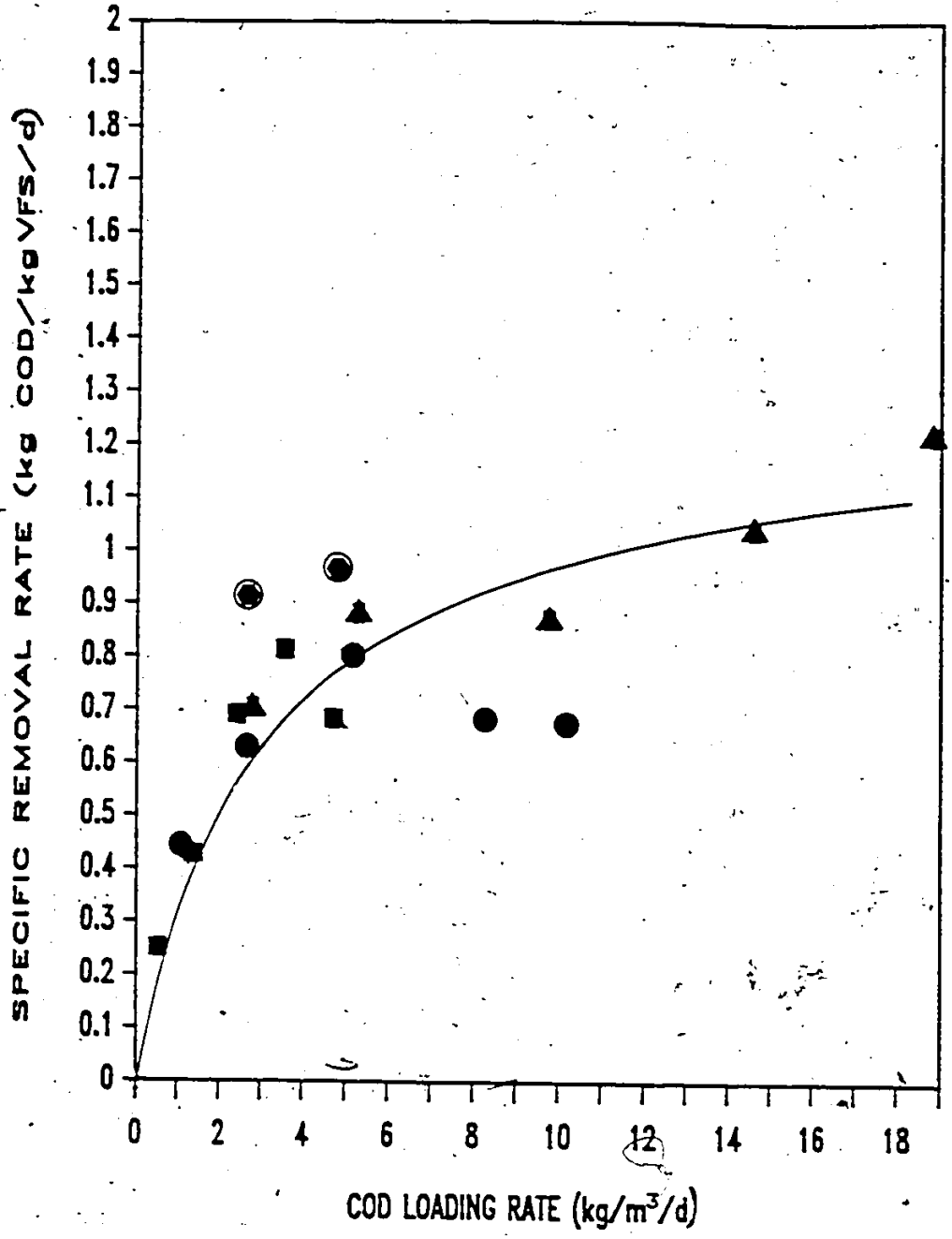

Figure 5.28 Specific biofilm substrate removal rate versus organic loading rate, 2.5 g L^{-1} (■), 5.0 g L^{-1} (●), 10.0 g L^{-1} (▲) and 20 g L^{-1} (◉).

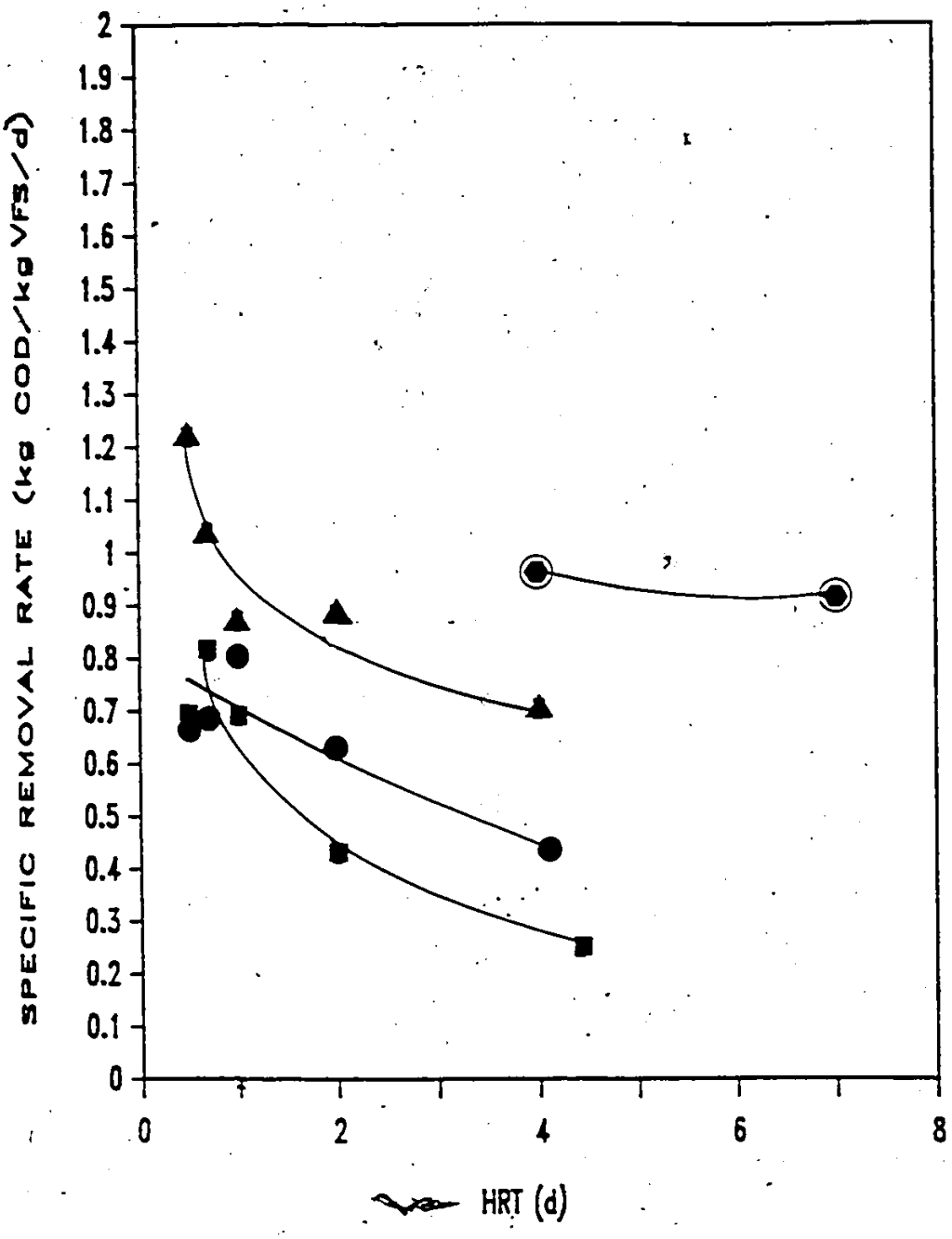

Figure 5.29 Specific biofilm substrate removal rate versus HRT, 2.5 g L^{-1} (■), 5.0 g L^{-1} (●), 10.0 g L^{-1} (▲) and 20 g L^{-1} (◉).

biofilm thicknesses of 1 mm or greater. On the other hand Williamson and McCarty (1976a, b) reported that anaerobic biofilms should not be diffusion limited at any thickness. Figure 5.30 shows the relationship between biofilm thickness and specific biofilm substrate removal rate. Biofilm substrate utilization rate increases with biofilm thickness, reaching a maximum at a thickness of 0.9 mm. When organic loading rates and reactor VA concentrations were low, biofilm thickness was less than 0.9 mm (Table 5.6). Under these conditions substrate concentration was less than the saturation coefficient, K. Therefore, substrate did not completely saturate the biofilm, as a result part of the biofilm was inactive. This results in the Monod type plot in Fig. 5.28. As biofilm thickness increased up to 2.6 mm, organic loading rates and mixed liquor VA concentrations were higher (Fig. 5.28; Table 5.6) and specific biofilm substrate removal rate remained constant. This indicates, that for thicknesses up to 2.6 mm the whole biofilm was active and that substrate completely penetrates the biofilm. Diffusional resistance was not serious, which is in agreement with results obtained by Kornegay and Andrews (1968). If the biofilm was not completely active or if a diffusion limitation existed there would have been a decrease in the specific biofilm activity with increased biofilm thickness.

In Table 5.8 biofilm substrate utilization rates found in the DSFF reactor are compared to other anaerobic systems treating carbohydrate wastewaters at 35°C. Little dif-

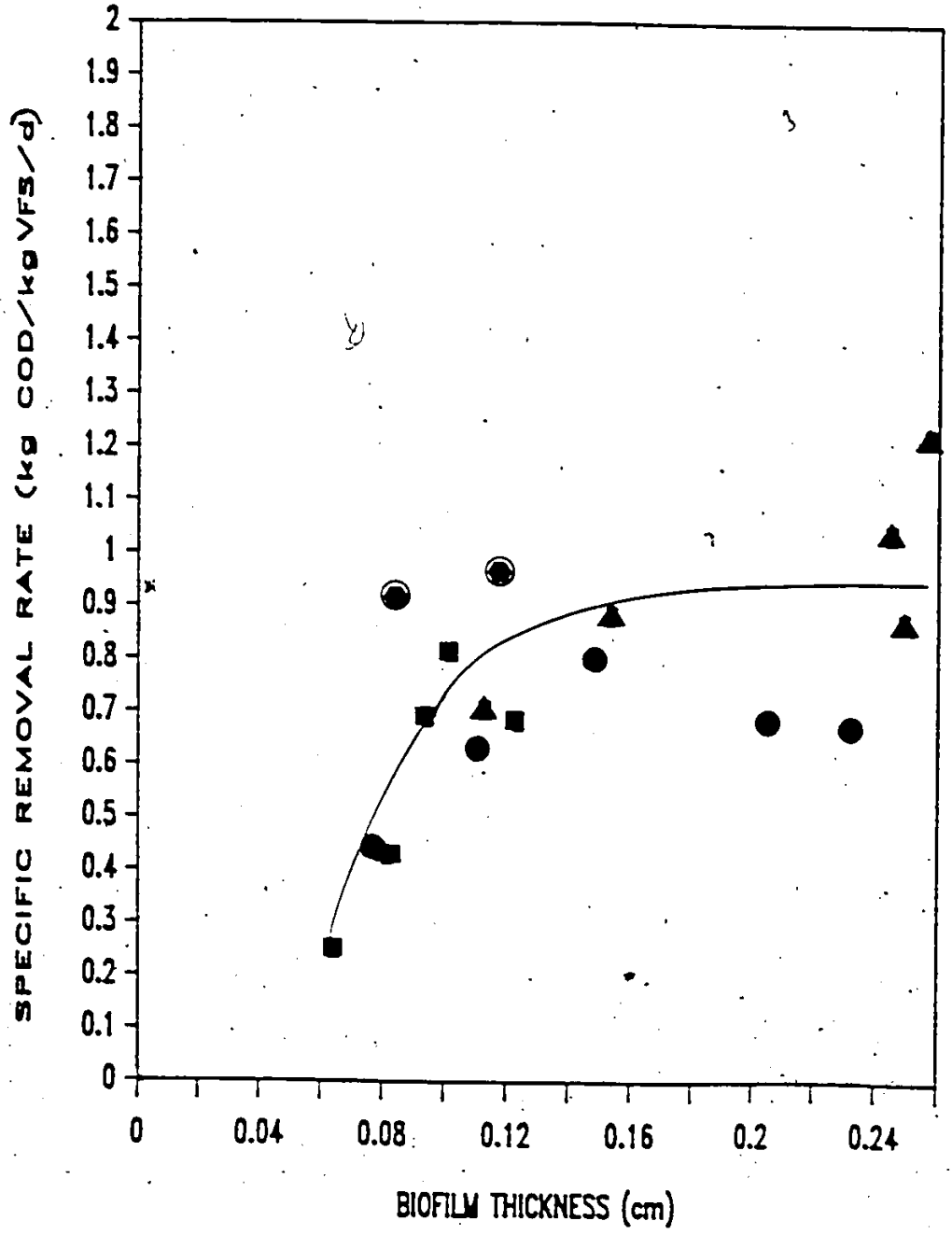

Figure 5.30 Specific biofilm substrate removal rate versus biofilm thickness, 2.5 g L^{-1} (■), 5.0 g L^{-1} (●), 10.0 g L^{-1} (▲) and 20 g L^{-1} ◉.

ference exists between suspended and attached biofilm reactor biomass. The porous nature of DSFF anaerobic biofilms with tentacle like appendages (increased surface area for microbial/substrate contact), lack of an electron donor, high K value of anaerobic bacteria (Williamson and McCarty, 1976a ,b), effects of sequential substrate utilization and disruption of the biofilm diffusion pattern caused by biogas micromixing all may be responsible for minimizing diffusion problems and increasing the active depth of anaerobic biofilms. It is also evident that high substrate removal rates in DSFF reactors are directly related to the amount of biofilm biomass.

5.4 Determination of Empirical Design Equation

Results presented in Sections 5.1 and 5.3 indicate that there were no obvious violations of the assumptions used in developing the empirical steady state DSFF model.

It is important to emphasize that waste stabilization in DSFF reactors operated at HRT of 4 days or less is primarily dependent on biofilm biomass. However, for the steady state empirical model development, kinetic parameters are based on total reactor biomass (Table 5.9).

5.4.1 Relationship Between HRT and SRT

The relationship between SRT and HRT for different influent wastewater concentrations is shown in Fig. 5.31 and summarized in Table 5.9. The inverse of the slope for each

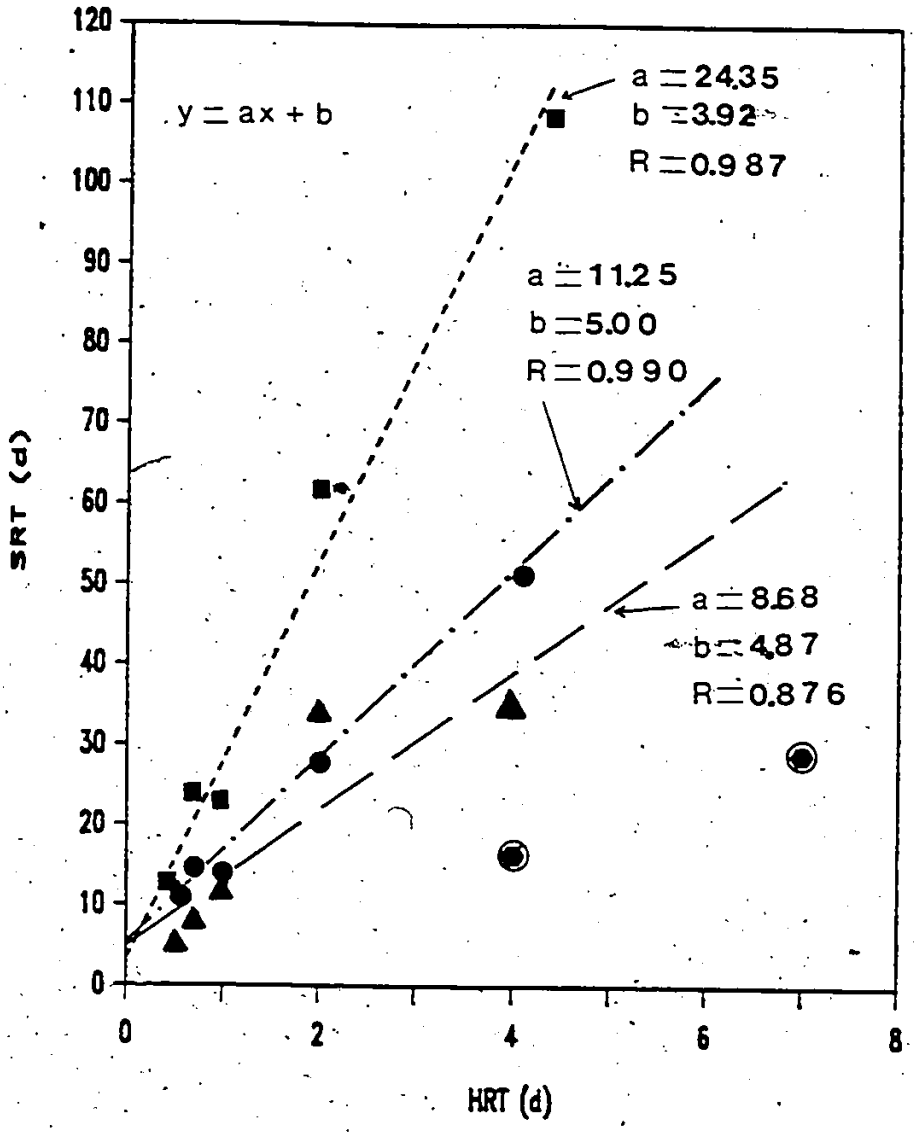

Figure 5.31 SRT versus HRT for steady state reactor operation. 2.5 g L^{-1} (■), 5.0 g L^{-1} (●), 10.0 g L^{-1} (▲) and 20 g L^{-1} ◉.

curve gives the washout factor, f (Eq. 3.52), for each substrate concentration tested.

Slopes of the curves in Fig. 5.31 indicate that there was an increase in the biomass washout factor with increasing influent wastewater concentration. Values of f were 0.041, 0.086 and 0.115 for 0.25, 0.5 and 1.0% sucrose wastewater respectively. The relationship between f, and influent feed concentration (Fig. 5.32) can be expressed by Eq. 5.1:

$$f = 0.012\ S_o \qquad 5.1$$

Substituting Eq. 5.1 into Eqs. 3.52, 3.53 and 3.54 permits u_m, E and X to be determined as a function of volumetric organic loading rate. Net specific growth rate, u_m, expressed in terms of organic loading rate can be written as Eq. 5.2. Figure 5.33 shows the relationship between measured and predicted (Eq. 5.2) values of volumetric organic loading rate and u_m for DSFF reactors used in this study.

$$u_m = 0.012\ \frac{S_o}{\theta_H} \qquad 5.2$$

Substrate removal efficiency, E (Eq. 3.53), expressed in terms of organic loading rate can be written as:

$$E = \left[1 - \left(\frac{K\ ((0.012\ S_o/\theta_H) + b)}{S_o\ (u_m - (0.012\ S_o/\theta_H) - b)}\right)\right] 100 \qquad 5.3$$

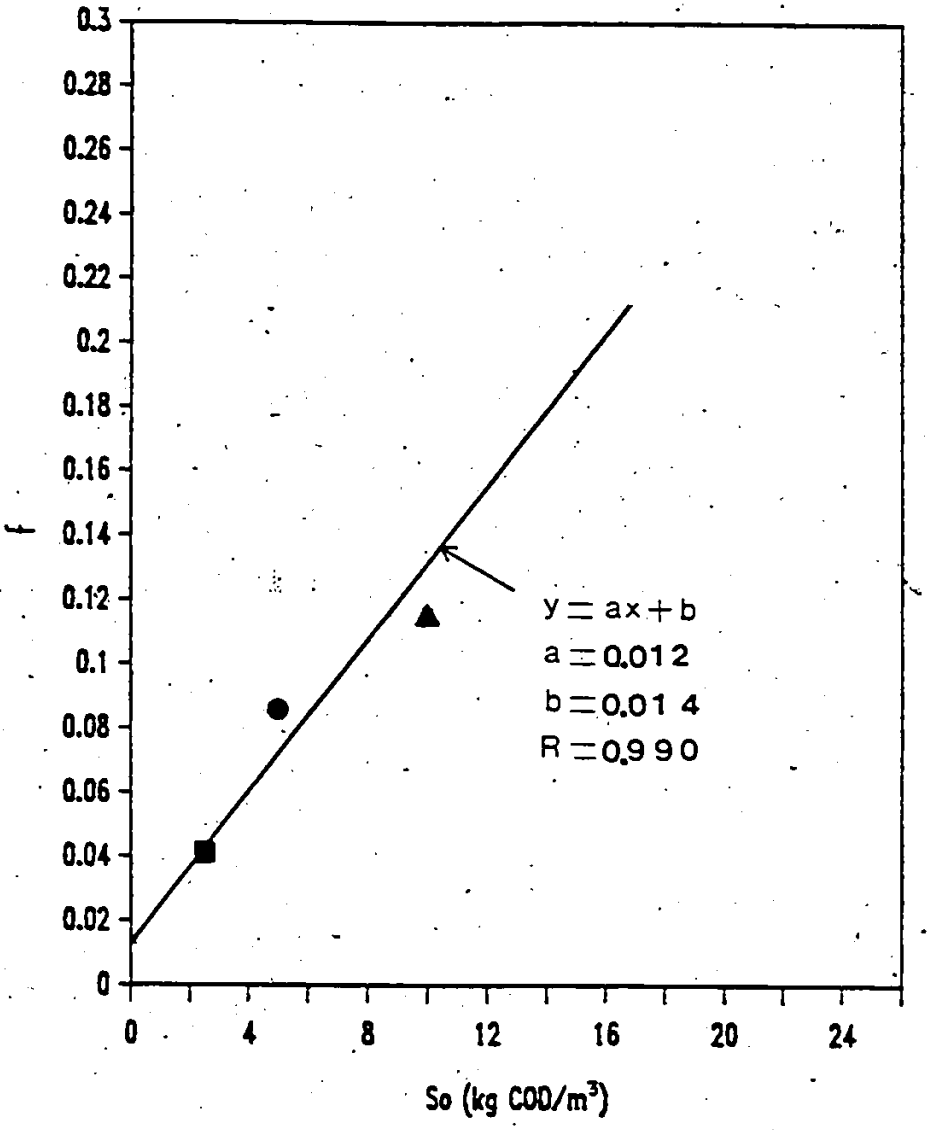

Figure 5.32 Influent substrate concentrations versus washout factor, f, 2.5 g L^{-1} (■), 5.0 g L^{-1} (●) and 10.0 g L^{-1} (▲).

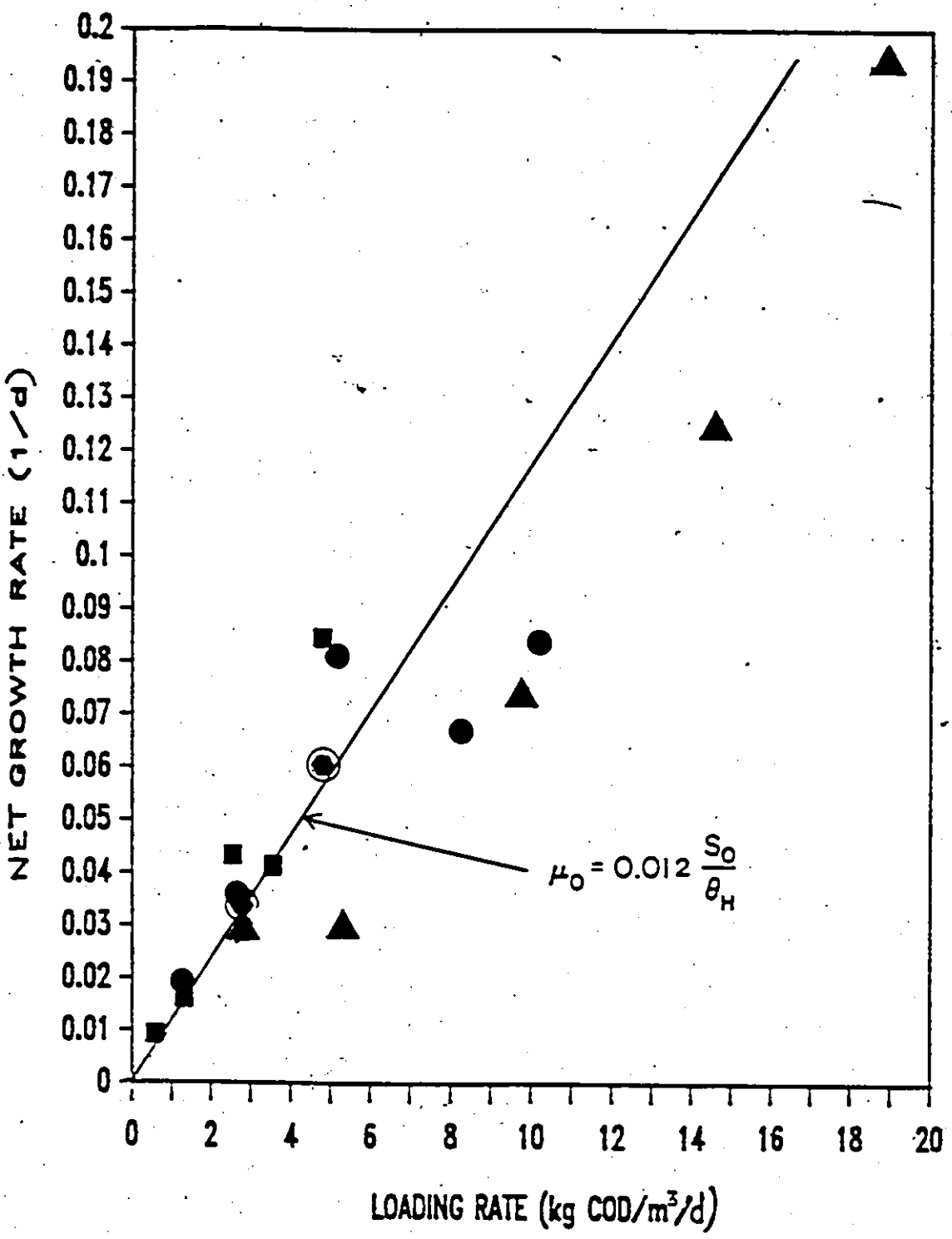

Figure 5.33 Organic loading rate versus net growth rate. 2.5 g L^{-1} (■), 5.0 g L^{-1} (●), 10.0 g L^{-1} (▲) and 20 g L^{-1} (●).

Reactor biomass concentration, X can be written as:

$$X = \frac{Y_M (S_o - S)}{(0.012 S_o/\theta_M) + b)\theta_M} \qquad 5.4$$

5.4.2 Determination of Kinetic Constants

Based on the assumption that non-biodegradable organic material in the reactors is negligible Y_M and b for each substrate concentration can be determined from the slope and intercept of a plot of U vs u_m (Eq. 3.50, Table 5.9). Both Y_M and b (Figs. 5.34a, b, c) increased with increasing influent waste concentration. Values of Y_M were 0.147, 0.205 and 0.362 and for b 0.033, 0.066 and 0.222 d^{-1} for influent waste strengths of 2.5, 5.0 and 10.0 g sucrose L^{-1}, respectively. Average values for Y_M and b were determined for all steady state data points and found to be 0.178 and 0.060 day^{-1} respectively. Parameters determined from the reactor treating 2.0 % sucrose waste water are suspect. Because of the limited number of data points no calculations were made for this reactor. Comparing COD removed to methane produced (Table 5.5) an average measured yield $Y_{M\,ave}$ can be formulated from the difference between COD removed and methane produced. This difference is assumed to be converted to biomass and hence is a measured yield. The value for average measured yield was 0.19, which compares well with the average calculated yield, $Y_{M\,ave}$ of 0.178. Good correlation between the two yield measurements further

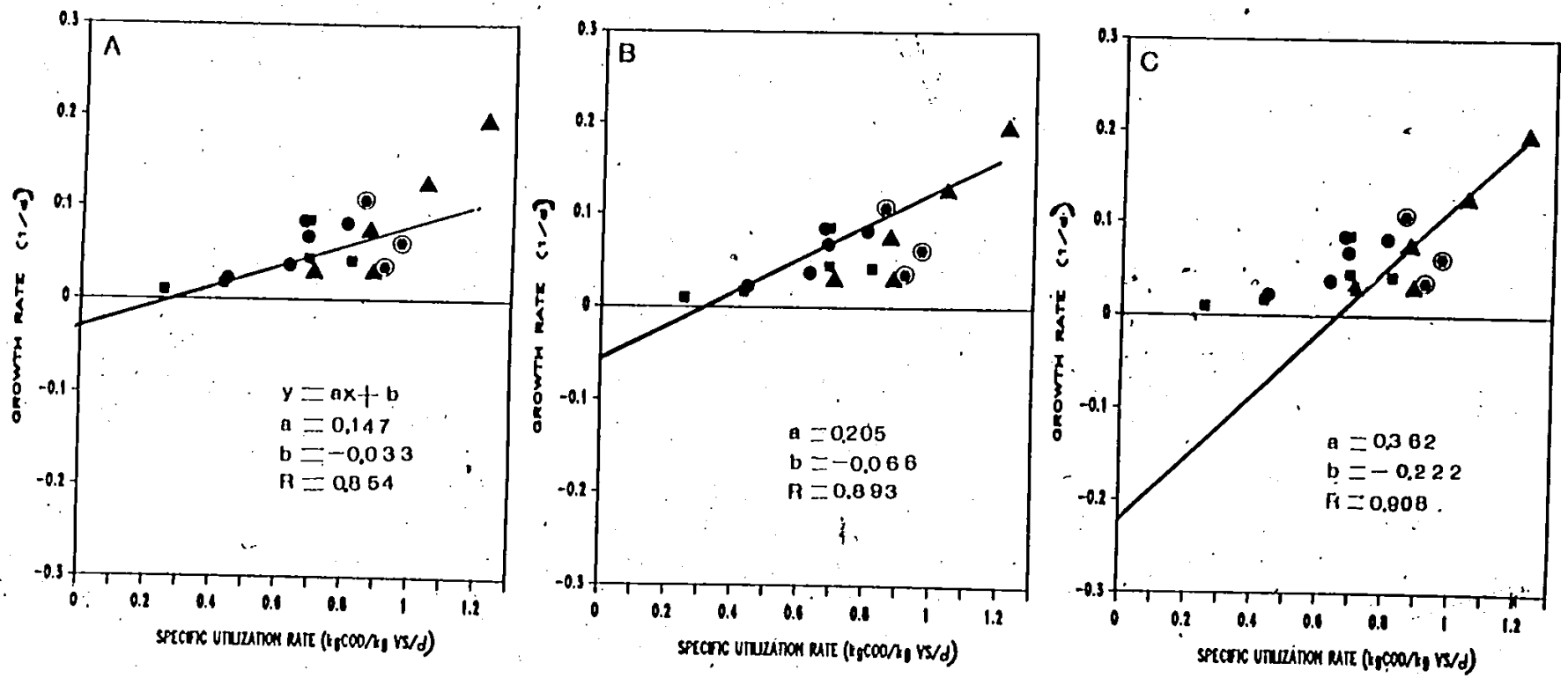

Figure 5.34 Specific utilization rate versus net growth rate 2.5 g L^{-1} (A), 5.0 g L^{-1} (B) and 10.0 g L^{-1} (C).

demonstrates low net synthesis of solids in anaerobic DSFF reactors which has practical engineering significance.

Since specific substrate utilization rate, U, is independent of influent waste strength (Fig. 5.26), k and K can be determined from a plot of Eq. 3.49 (Fig. 5.35; Table 5.8). Using linear regression analysis, values of K and k, based on soluble COD as limiting substrate, were determined to be 299 mg COD L^{-1} and 0.93 kg COD (kg VSFS)$^{-1}$ day^{-1} respectively. Substituting for k and Y_m in Eq. 3.51, u_m for each influent waste concentration can be determined. Values of u_m were 0.136, 0.190 and 0.335 d^{-1} for DSFF reactors treating 2.5, 5.0 and 10.0 g L^{-1} sucrose, respectively. Although u_m, increased with increased influent concentration net maximum specific growth rates for DSFF reactors were approximately the same. Net maximum specific growth rates were 0.103, 0.124 and 0.113 for reactors treating 2.5, 5.0 and 10.0 g L^{-1} sucrose wastewater, respectively.

5.4.3 Empirical Model Prediction

Predictive COD removal curves were calculated with Eq. 5.3 and compared with experimental results in Figs. 5.36a, b and c. Both experimental and predicted results for DSFF reactors treating 2.5, 5.0 and 10.0 g L^{-1} sucrose correlated well. Application of this predictive model to real situations is important in reactor design. Figure 5.37 compares measured biofilm concentrations with predicted values using Eq. 5.4. Predicted and measured values are very

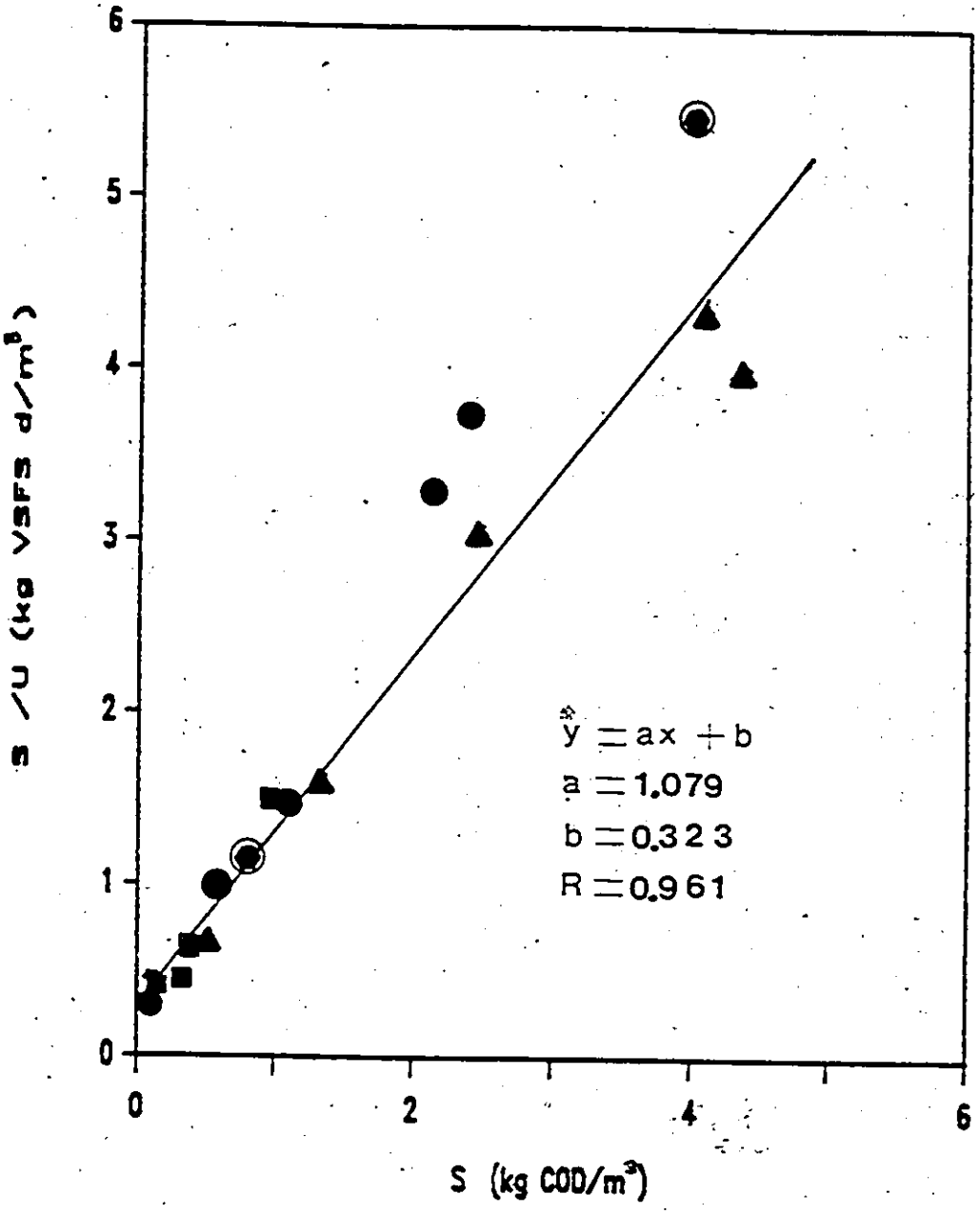

Figure 5.35 SeU^{-1} versus Se, 2.5 g L^{-1} (■), 5.0 g L^{-1} (●), 10.0 g L^{-1} (▲) and 20 g L^{-1} (◉).

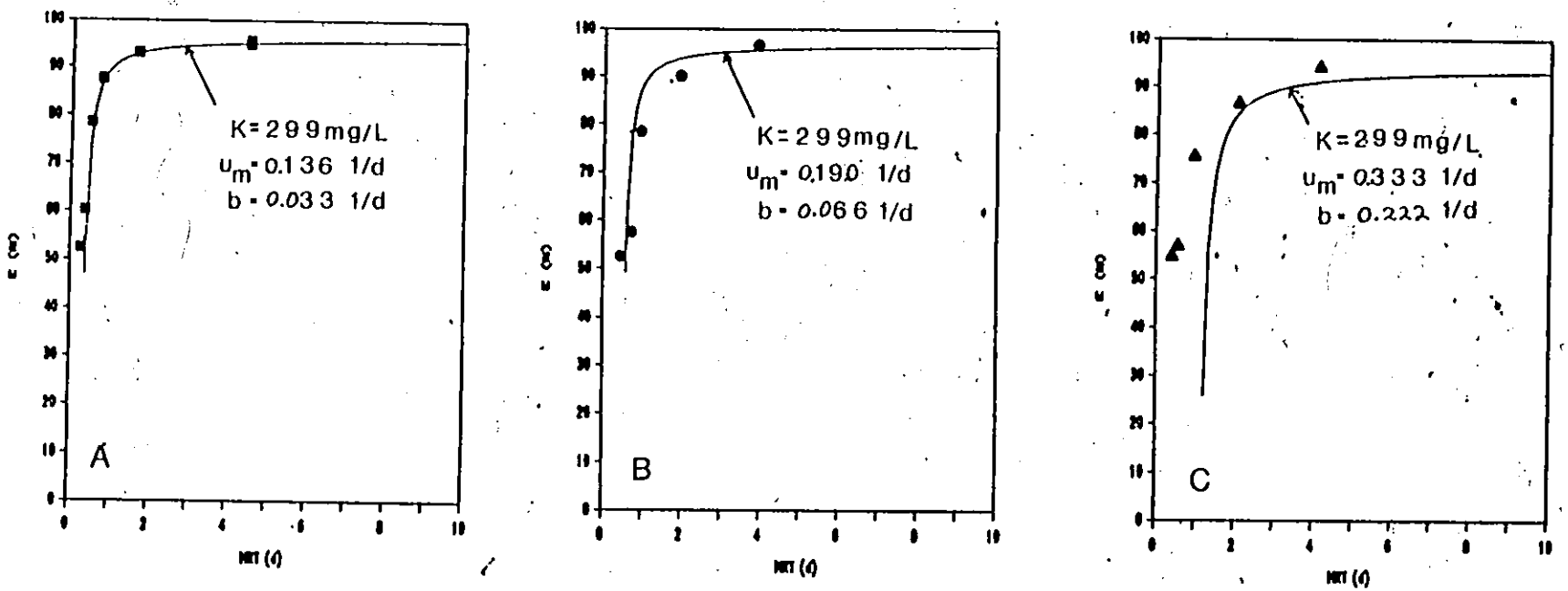

Figure 5.36 Comparison of experimental soluble COD removal efficiency with empirical model predictions, 2.5 g L^{-1} (A), 5.0 g L^{-1} (B) 10.0 g L^{-1} (C).

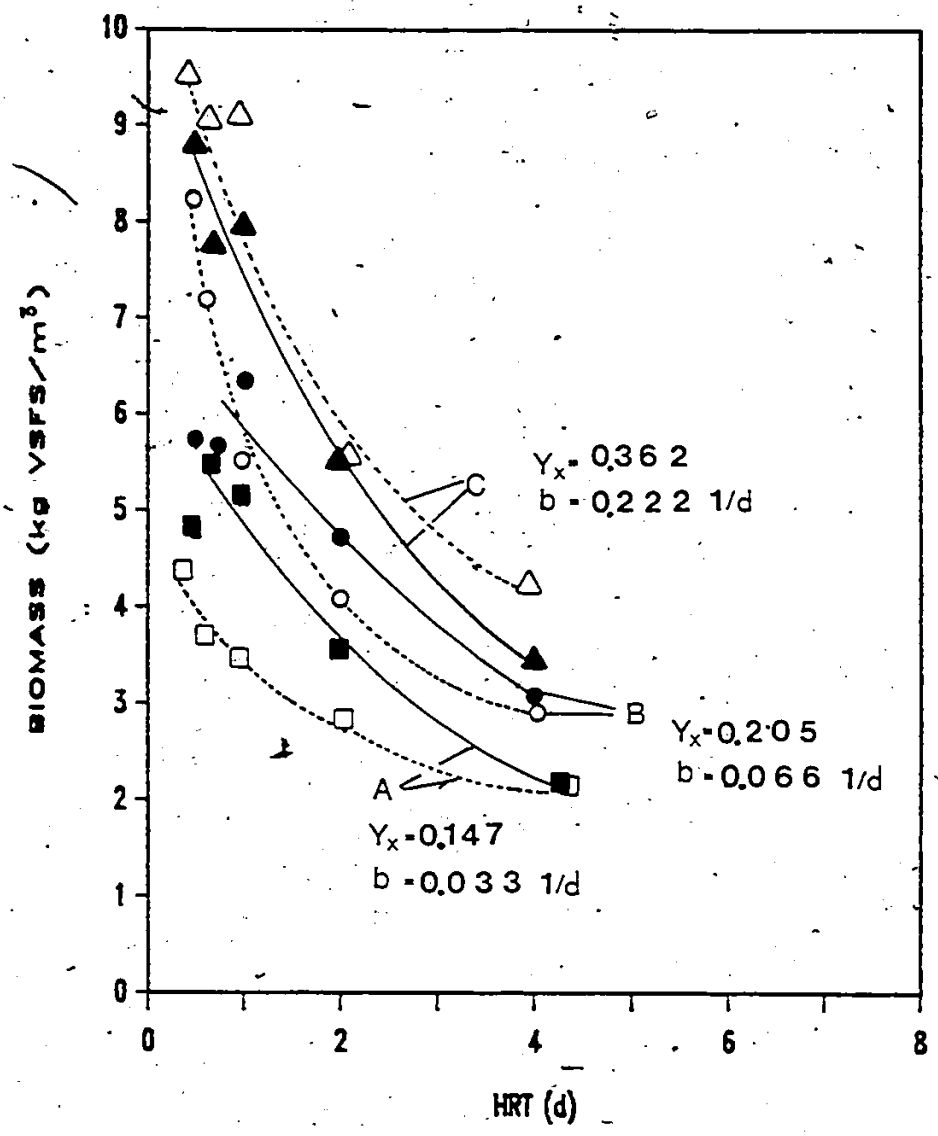

Figure 5.37 Comparison of experimental biomass concentration with empirical model predictions; measured, ----- 2.5 g L^{-1} (□), 5.0 g L^{-1} (○) and 10.0 g L^{-1} (△) predicted, 2.5 g L^{-1} (■), 5.0 g L^{-1} (●) and 10.0 g L^{-1} (▲).

close. Equations 5.2 and 5.3 can be used to predict reactor performance based either on SRT, HRT or LRT as demonstrated in this section and Section 5.3.7. Depending on the information available, the appropriate form of Eqs. 5.2 and 5.3 can be used.

5.4.4 Significance of Kinetic Constants

Values of various kinetic parameters determined for anaerobic DSFF reactors compare well to other immobilized and suspended anaerobic processes (Table 5.8). Small differences between values of k and K determined for biofilm and suspended growth processes indicate that effects of diffusional resistance in anaerobic biofilms are small. Hence, kinetic parameters obtained from an anaerobic biofilm should not differ significantly from those obtained from an anaerobic suspended growth system. These results are supported by kinetic constants obtained in batch tests and discussed in the next section.

Values of Y_x and b, when related to low values of u_o, indicate the importance of the anaerobic biofilm in DSFF reactors. Although there have been reports indicating that anaerobic filters and DSFF reactors can become plugged (Dahab and Young, 1982), low biomass yields, Y_x, and relatively large channels indicate that DSFF reactors could be operated for long periods of time without excess biomass accumulation and channel plugging.

A high K value allows substrate to penetrate thick anaerobic biofilms with minimal diffusional resistance (Williamson and McCarty, 1976a and b). Experimental evidence from this study has been presented that supports this. Increase in Y_m with increased influent waste concentration is the opposite of what occurred during startup of anaerobic DSFF reactors. During startup, Y_m decreased with increased waste strength. This phenomenon is due in part to operational restrictions placed on DSFF reactors during startup. During startup, mixed liquor VA concentrations were maintained within a range by controlling volumetric organic loading rate. For concentrated wastes this is a more restrictive condition in terms of microbial growth when compared to more dilute wastewaters. During steady state operation VA levels were not restricted and reactors achieved unrestricted steady state biomass yields.

Kinetic constants discussed above are calculated for total biomass in DSFF reactors operating at steady state. It is not known if these apparent kinetic constants would vary from intrinsic constants determined for biomass in suspension. It is also not known if kinetic constants determined during steady state apply to reactors during startup. The next section discusses results of batch biofilm activity tests conducted during startup and steady state reactor operation.

5.5 Apparent and Intrinsic Kinetic Constants

Diffusional limitations in immobilized enzyme systems and aerobic immobilized whole cell systems have been found to affect the half velocity constant, K and maximum specific reaction rate, k (Dewey *et al.*, 1984). On the other hand Williamson and McCarty (1976a, b) reported that values of k for nitrogen fixing biofilms did not vary greatly from those obtained with dispersed cultures. They did find that *Nitrobacter* biofilms made from cultures with differing k values exhibited a damping effect between a change in k and a change in substrate utilization rate. The damping effect, resulted from a decreased effective biofilm thickness, and, hence a smaller active mass of nitrifying bacteria when k increased.

Although steady state results obtained in this study (Section 5.3) indicated that anaerobic biofilms up to 2.6 mm in depth were completely active, no study has demonstrated the relationship between apparent and intrinsic kinetic constants k and K (Eq. 3.2). Additionally, because of the slow development of anaerobic biofilms it is important to know if kinetic parameters determined for mature biofilms are the same or different from those determined during startup. This fact is of particular importance in selecting constants for a mathematical model that describes startup or steady state reactor performance.

While methods have been suggested for determination of intrinsic kinetic constants for immobilized enzyme reactions (Hamilton *et al.*, 1974; Chen *et al.*, 1980; Lee *et al.*, 1984), no method has been applied to anaerobic biofilms. Since methanogenesis is rate limiting for easily degraded carbohydrate wastes, apparent kinetic constants can be determined in a series of batch biofilm activity tests using acetate as the limiting substrate. No tests were conducted to evaluate the effect of superficial liquid velocity on initial substrate utilization rates. However, Dewey *et al.* (1984) reported that for immobilized *Saccharomyces cerevisiae* operated at superficial liquid velocities similar to those used in these tests, the effect of external substrate diffusion was not significant, and reaction rate was controlled mainly by internal diffusion resistance.

During startup (Run 1) and steady state reactor operation, removable biofilms were transferred into batch activity test chambers and initial methanogenic reaction rates were determined as a function of acetate concentration (expressed as COD). Hanes plots (Appendix F) were used to estimate apparent kinetic parameters K and k for various biofilm thicknesses.

Apparent kinetic constants K and k were then plotted against apparent Thiele modulus, ϕ (Eq. 3.12a). The apparent Thiele modulus was determined by substituting apparent

or measured values of K, k, average biofilm thickness and biofilm concentration into Eq. 3.12a (Appendix F).

When ϕ equals zero, no internal diffusion limitations exist and intrinsic kinetic parameters can be determined. By fitting a curve to the data and extrapolating to ϕ equal to zero, intrinsic values of K and k can be estimated for startup and steady state reactor operation.

Figure 5.38 shows the relationship between apparent values of k and ϕ for startup and steady state biofilms, respectively. For startup and steady state biofilms, values of k ranged between 0.40-1.73 kg COD (kg VFS)$^{-1}$ d^{-1} and 0.80-1.67 kg COD (kg VFS)$^{-1}$ d^{-1}, respectively. Based on our experience with mixed anaerobic cultures treating carbohydrate wastewater the k value of 2.13 kg COD (kg VFS)$^{-1}$ d^{-1} is an outlier. Over the range of ϕ evaluated during steady state, apparent values of k did not indicate any positive or negative trends and remained relatively constant. Drawing the line of the the average of the data points and extrapolating to ϕ equal to zero the intrinsic value of k was approximately 1.2 kg COD (kg VFS)$^{-1}$ d^{-1} for steady state reactor operation. The steady state value of k determined from batch tests compares well with the value determined from continuous reactor operation.

Deposition on the biofilm of inert material or acid forming bacteria from the inoculum (low methanogenic activ-

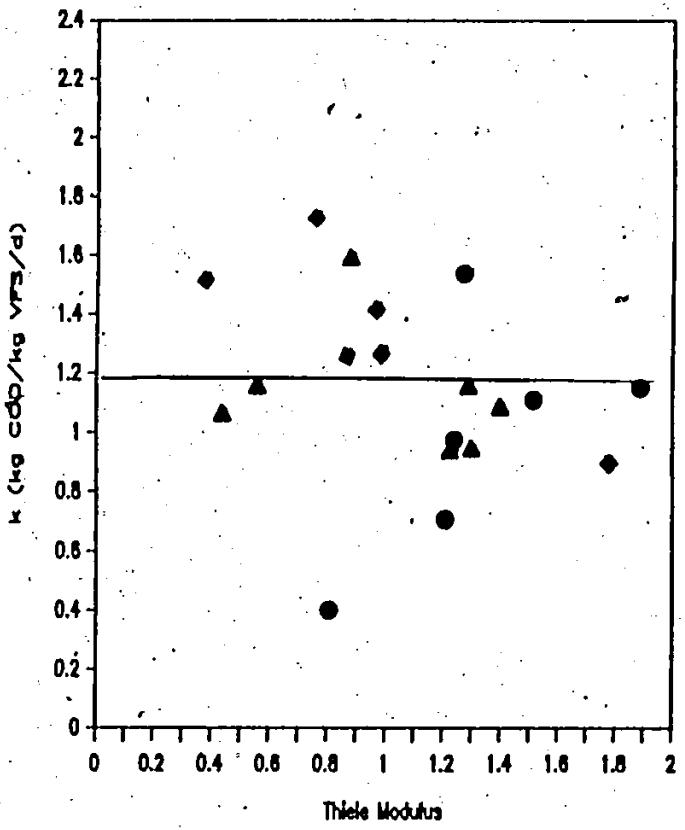

(A)

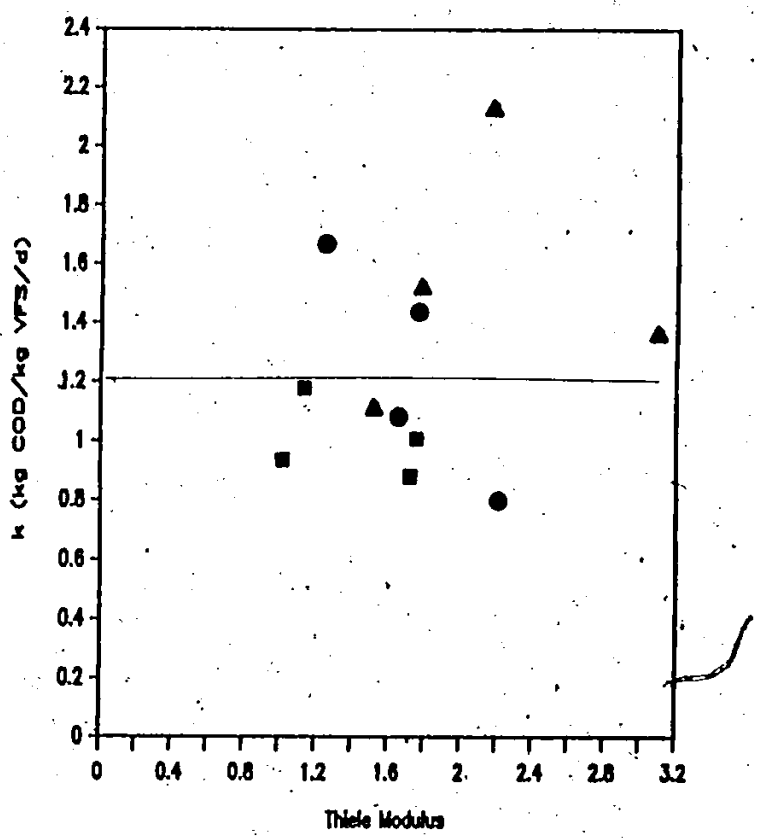

(B)

Figure 5.38 Apparent values of k versus apparent Theile modulus during startup, Run 1 (A) and steady state (B), 2.5 g L^{-1} (■), 5.0 g L^{-1} (●), 10.0 g L^{-1} (▲) and 20 g L^{-1} (◆).

ity), the startup protocol used to maintain VA concentrations and insufficient time for microbial adaptation effect the value of k during startup. For the first 40 days of startup there was considerable variation in values obtained for k. However, as the biofilm matured, variation in values of k decreased (Fig. 5.39). Similar to steady state, no specific positive or negative trend existed between apparent values of k and ϕ (Fig. 5.38).

Dewey *et al.*, (1984) reported that K was effected more by internal diffusion limitations than was k. Figure 5.40 shows the relationship between apparent values of K and ϕ for startup and steady state respectively. No relationship was indicated between apparent values of ϕ and K for startup and steady state. Since no relationship exists and k remained relatively constant, internal diffusion did not significantly affect the biofilm. Comparison of startup and steady state K values with those in the literature for conventional methanogenic sludges shows no great disparity which also indicates that internal diffusion limitations in DSFF biofilms are small. This may or may not be the case for biofilms in anaerobic fluidized beds which have been reported to be very dense (Switzenbaum, 1978) but quite thin (100 microns). Biofilm K values were within the range of K values associated with bacteria of the genera *Methanosarcina* and *Methanothrix* (Table 2.1)

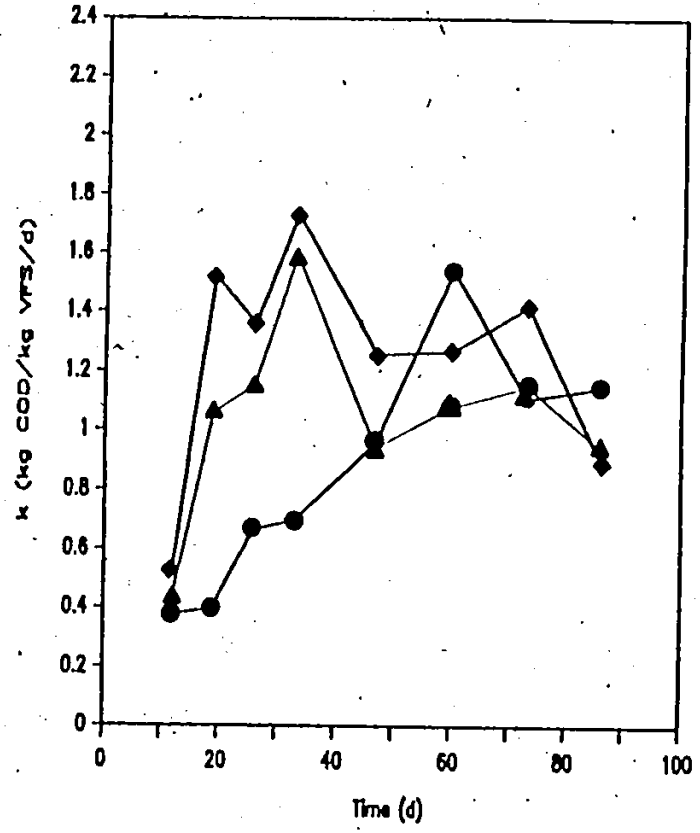

(A)

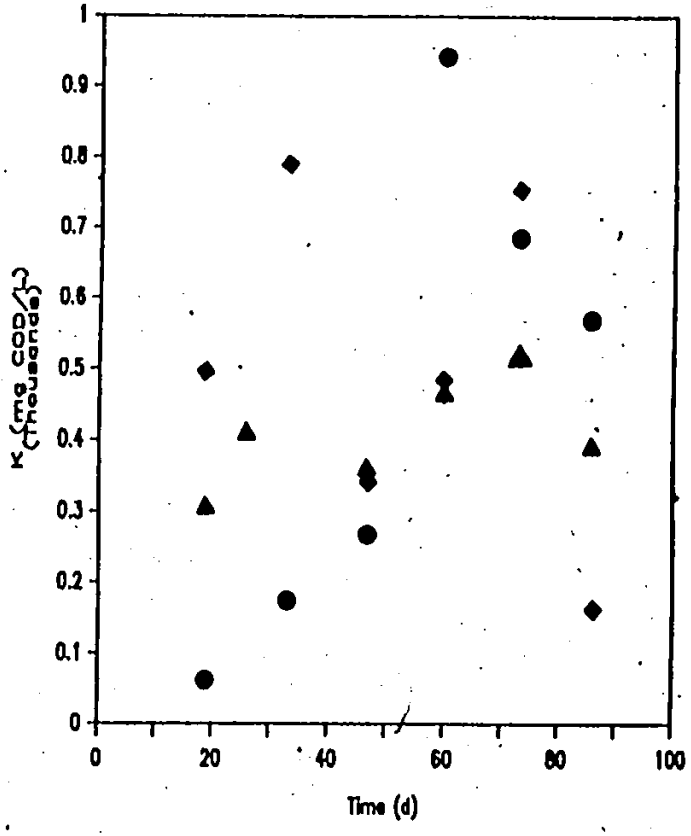

(B)

Figure 5.39 Apparent values of k (A) and K (B) during startup, Run 1. 5 g L^{-1} (●), 10 g L^{-1} (▲) and 20 g L^{-1} (◆).

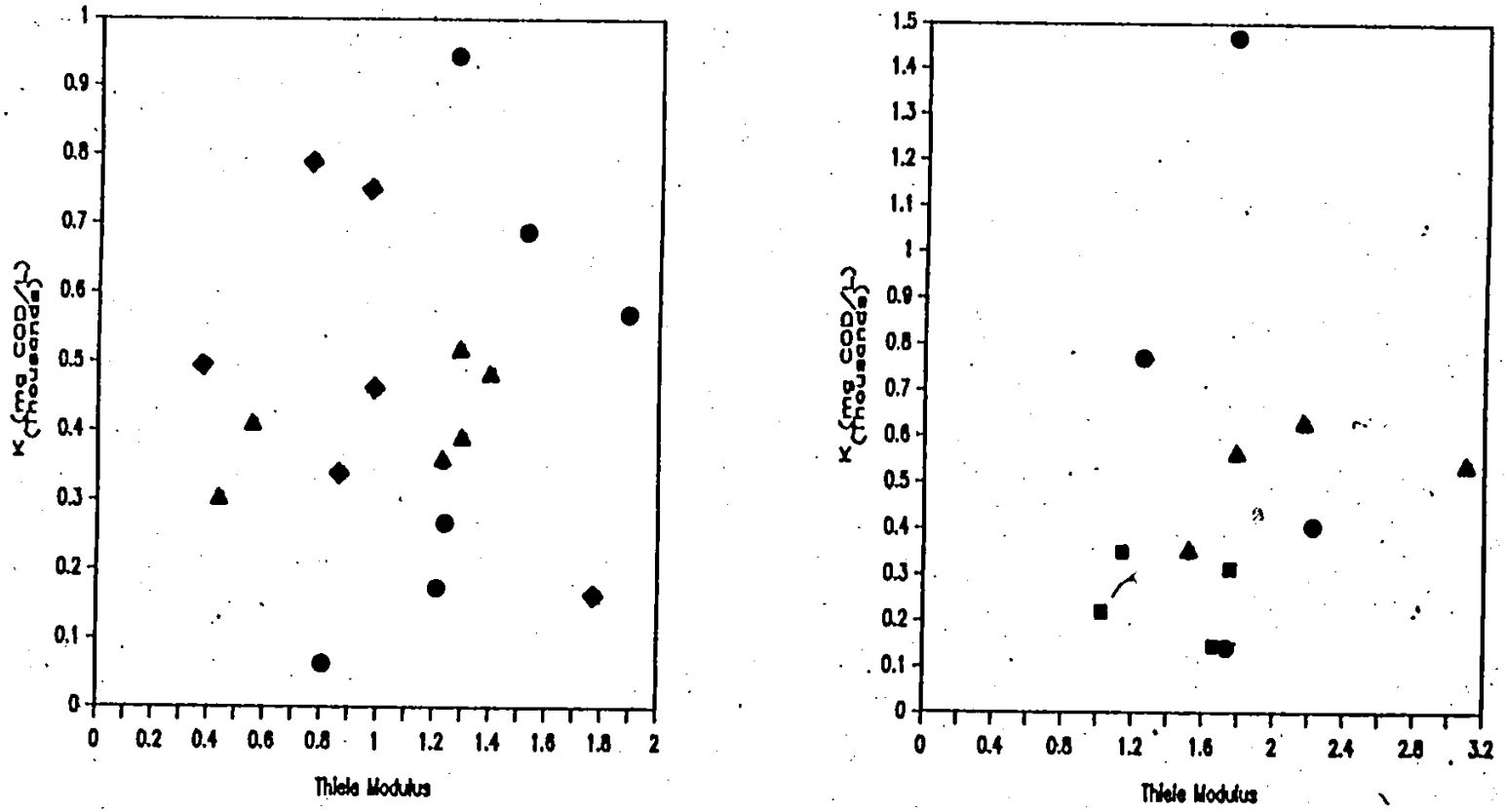

(A) (B)

Figure 5.40 Apparent values of K versus apparent Thiele modulus during startup, Run 1 (A) and steady state (B); 2.5 g L^{-1} (■)m 5 g L^{-1} (●)m 10 g L^{-1} (▲) and 20 g L^{-1} (◆).

There was a great deal of scatter for values of k and K obtained during the initial stages of startup. It is during startup that the greatest changes occur in the biofilm. It can be argued that as the biofilm matures there is a change in the types of methanogenic bacteria and/or relative proportions of methanogenic and acidogenic bacteria within the biofilm, and that changes in K as well as changes in k reflect this change in microbial population. Comparison of values of k and K during startup and steady state indicates that for carbohydrate wastewaters using the steady state values of these constants in a model describing startup would be adequate.

5.6 Application of Dynamic Model to DSFF Reactors

Simulations of DSFF reactor startup were made using the dynamic model developed in Chapter 3. The model was used to simulate the response of continuous flow cultures to changes in biomass attachment rates, biofilm detachment rates and substrate concentration. The model used daily flow rate data obtained during the experimental portion of the startup study. Kinetic constants and yield factors for acid forming and methane forming bacteria were obtained from pure or enrichment culture studies (Table 3.3). Values of kinetic constants used in the model can be found in the program listing (Appendix C). Kinetic constants for bacteria in the mixed liquor were the same as for bacteria in the biofilm.

Based on material presented previously the biofilm efficiency factor, E′, was set equal to 1. The model also assumed that no interactions between the two groups of bacteria occurs that will cause parameters to change from values associated with individual cultures of each group.

Using the daily flow rates for startup of Reactor A, (S_o = 5.0 g L^{-1}), Run 1 the dynamic model was used to simulate the effect of having A^* and D^* equal to 0.0. The values of the kinetic constants used in the model are found in lines 350-530 of the computer listing (Appendix C). Since the initial concentration of acid formers and methane formers on the biofilm was equal to 0 g L^{-1} the model simulates a CSTR. Under these conditions there is no biofilm accumulation and washout of the methanogenic bacteria occurs (Fig. 5.41a). The end result is process failure as shown by the increase in ratio of acetogenic to methanogenic bacteria in the reactor (Fig 5.41b).

Figures 5.42a, b and c and 5.42 A, B and C show the effect of varying A^* and D^* from 0.05 to 0.2 d^{-1} on the concentration of acetogenic and methanogenic bacteria, respectively in the mixed liquor and the biofilm. The model predicts a short exponential biofilm growth phase followed by a much longer period of linear growth. A similar trend was also reported in the experimental study. Depending on the values of A^* and D^* selected, the concentration of acid

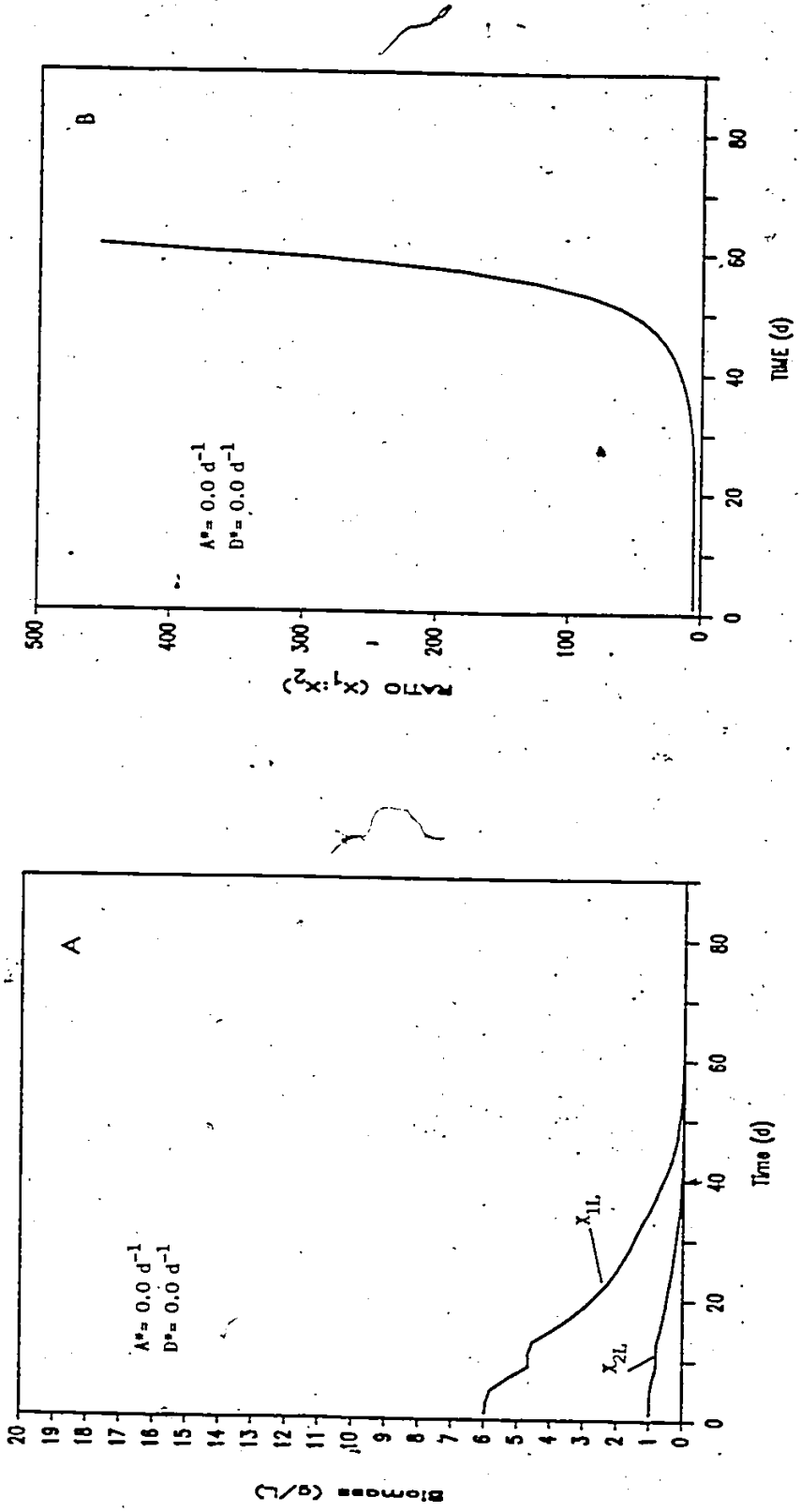

Figure 5.41 Biomass (A), and ratio of acid forming to methane forming bacteria (B) in a CSTR during startup (simulation).

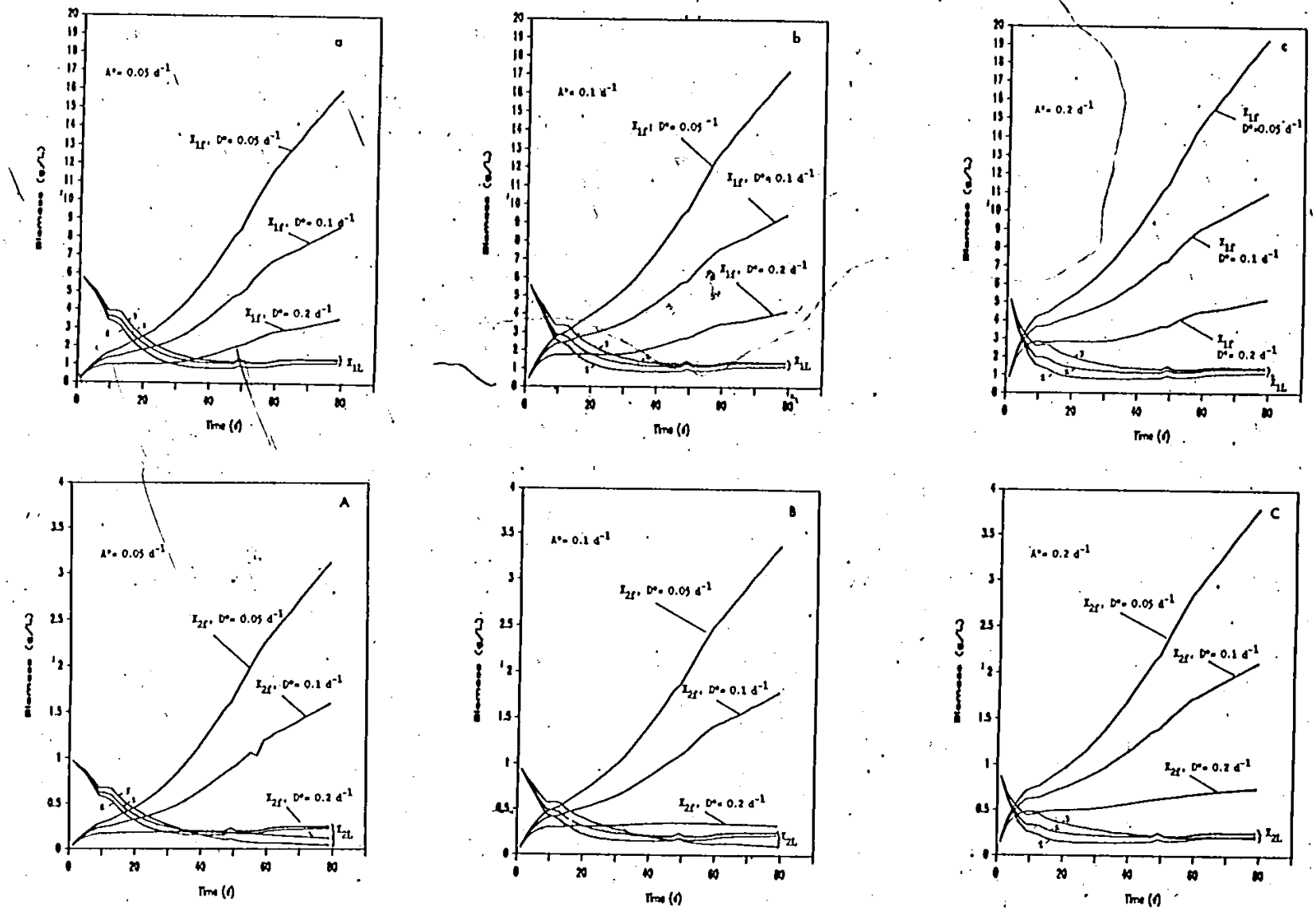

Figure 5.42 Effect of A* and D* on mixed liquor and biofilm acetogenic biomass concentration (a, b, c), and methanogenic biomass concentration (A, B, C), D* = 0.05 d^{-1} (1), D* = 0.1 d^{-1} (2) and D* = 0.2 d^{-1} (3).

formers or methane formers in the reactor biofilm could be changed significantly. Simulations with a high value of A^* and low value of D^* resulted in biofilm concentrations far beyond those achieved in DSFF reactors. Based on the parameter values used in the model, A^* and D^* values of 0.1-0.2 d^{-1} predicted biofilm concentrations similar to those achieved in the experimental study (Reactor A, Run 1).

Figures 5.43a, b and c and 5.43A, B and C show the ratio of acetogenic to methanogenic bacteria with respect to time in the reactor and biofilm respectively. The simulation predicts that the ratio of acetogenic bacteria to methanogenic bacteria in the mixed liquor and biofilm is between 5-6 to 1 when the reactor is stable. This indicates that the methanogens make up approximately 15-20 % of the biomass in the reactor. The measured k value during steady state operation was 0.93 kg COD kg $VSFS^{-1}$ d^{-1} and from batch methanogenic activity tests it ranged from 1-1.2 kg COD kg VFS^{-1} d^{-1}. Assuming from the simulation that methanogenic bacteria make up 20 % of the biomass in DSFF reactors the k value of the methanogenic bacteria in the reactor or biofilm would be approximately 4-6 kg COD kg $VSFS^{-1}$ d^{-1}. This value is similar to k values reported for pure or enriched methanogenic cultures (Table 3.3).

Experimental techniques are not advanced enough to physically differentiate the quantity of methane forming and

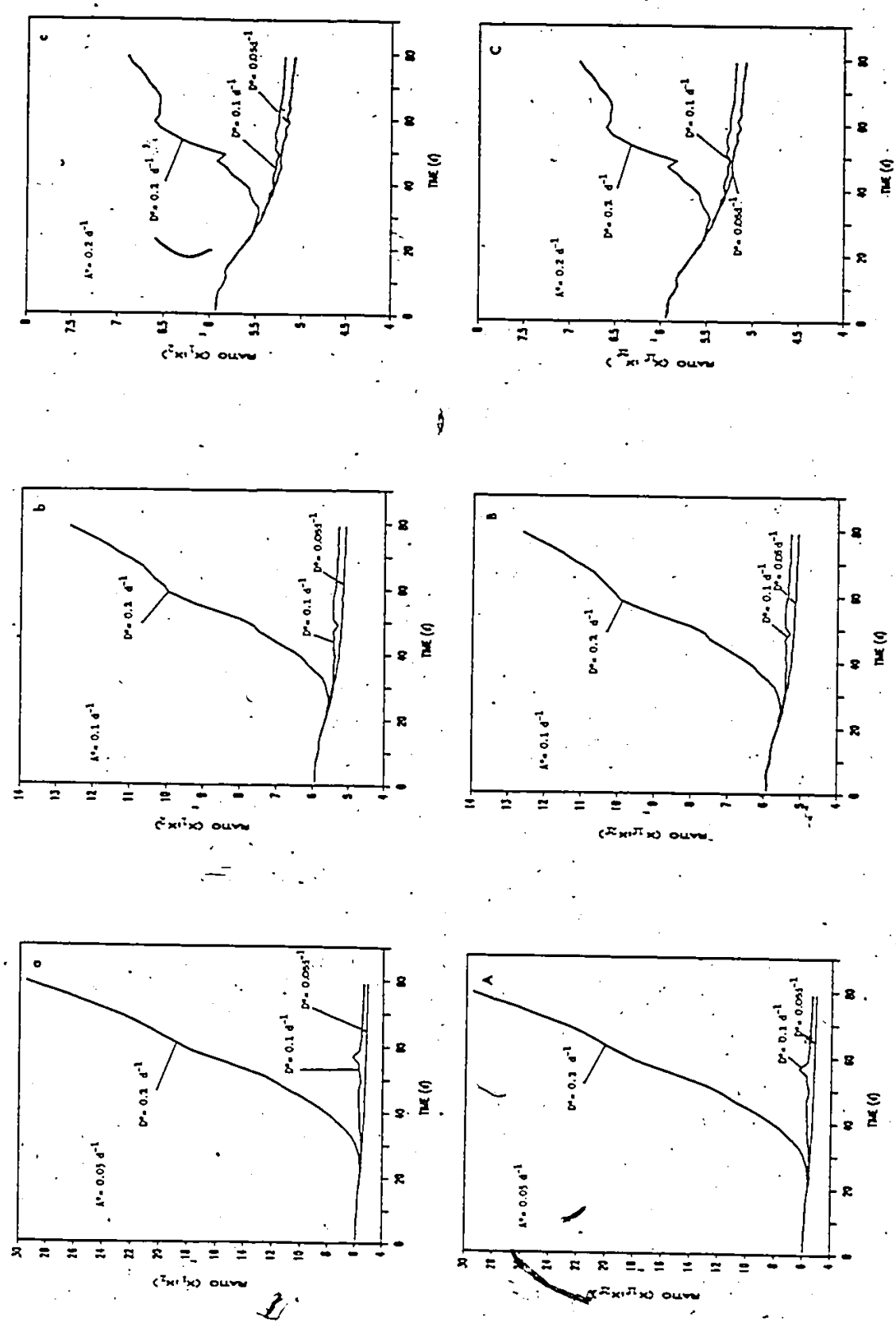

Figure 5.43 Effect of A* and D* on ratio of acetogenic bacteria to methanogenic bacteria in the reactor (a, b, c) and biofilm (A, B, C).

acid forming bacteria that coexist in DSFF reactors. However, the simulation ratio of acetogenic to methanogenic bacteria of 5-6 to 1, coupled with experimental measurements of k and K values reported for pure and enrichment cultures indicate that the model can be used to predict the relative proportion and concentration of these bacteria in the mixed liquor and biofilm.

As DSFF reactors become unstable the ratio of acetogenic bacteria to methanogenic bacteria increases indicating that acid forming bacteria are becoming more predominate in the reactor. Instability associated with this increase in acid formers results in increased accumulation of VA (Fig. 5.44). As discussed in previous sections accumulation of VA is a sign of reactor stress and instability. When the ratio of acid formers to methane formers remains between 5 and 6, VA remain relatively low. Comparing simulated biomass and substrate concentration information from Fig. 5.42, Fig. 5.44 and Fig. 5.45 with experimental results shown in Figs. 5.1 and 5.8, indicates that A^* and D^* values of 0.1-0.2 d^{-1} give the best fit to the startup data.

Results in Appendix C show biomass and substrate concentrations for startup of Reactor B (S_o = 10 g L^{-1}), Run 1, based on A^* and D^* values of 0.0 d^{-1} and 0.1-0.2 d^{-1}. With A^* and D^* equal to 0.0 the simulation predicts that the

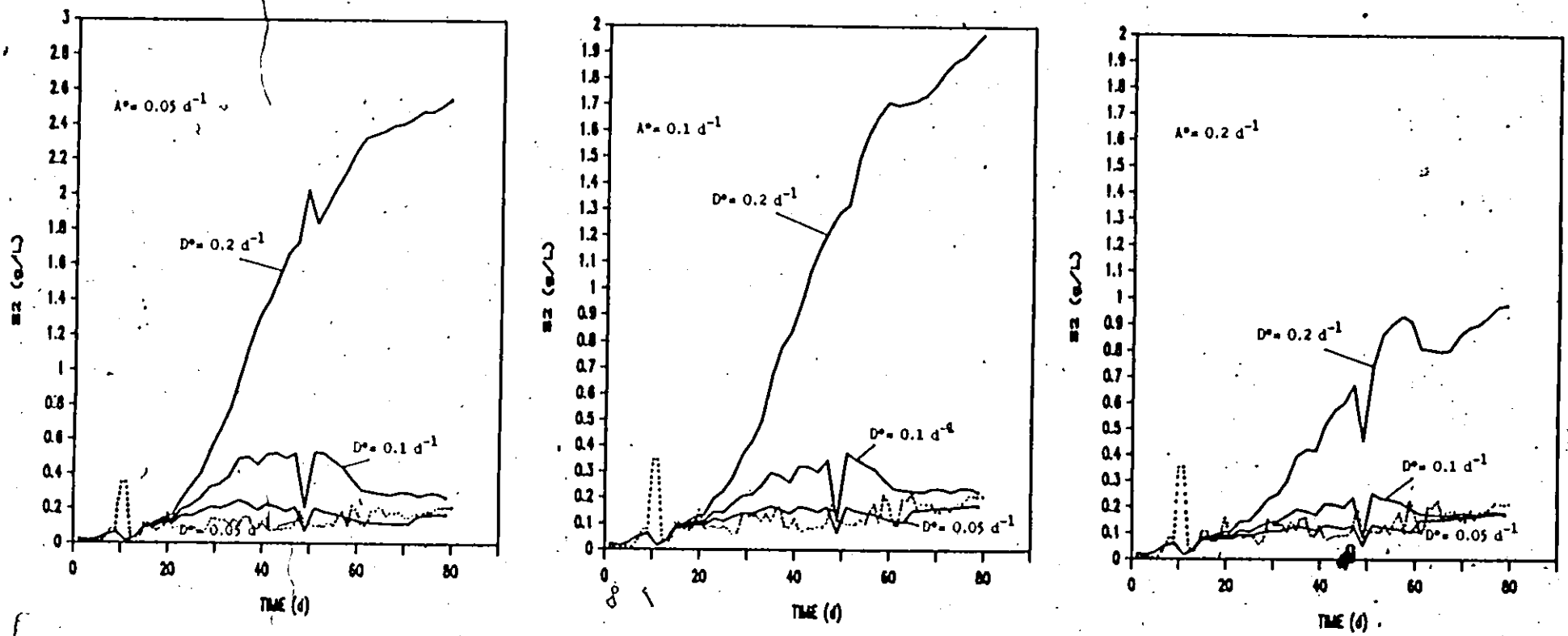

Figure 5.44 Effect of A* and D* on intermediate substrate concentration during startup, simulated (——), measured (•••).

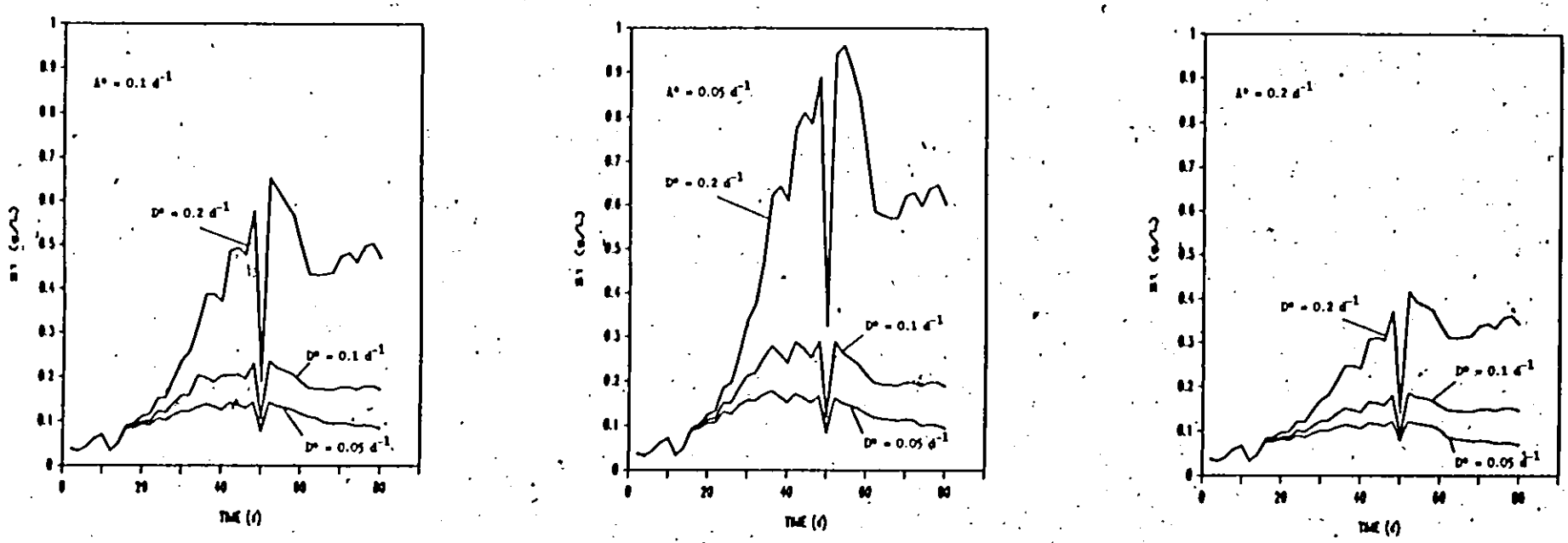

Figure 5.45 Effect of A* and D* on primary substrate concentration during startup.

reactor will fail due to microbial washout. Based on A^* 0.1 d^{-1} and D^* of 0.2 d^{-1} the simulation shows relatively good agreement with biomass concentrations and substrate concentrations reported in Figs. 5.1 and 5.8.

The model also has the capability to simulate step changes in substrate concentration, step changes in flow rate and steady state reactor operation. Even though the model has several limitations, it should be useful in guiding experimentation and investigating the effect of different control actions and design procedures on the dynamics of the DSFF process. Undoubtedly the model will require modification as more experimental data are obtained and more comparisons are made between simulation results and experimental operation.

6. CONCLUSIONS

A theoretical development of sequential substrate utilization in biofilms was developed. The model showed that production of intermediate substrate in a biofilm enhances conversion of primary substrate to ultimate product. Concomitant improvement of the biofilm effectiveness factor is proportional to the ß modulus. For some anaerobic fermentations a significant change in the effectiveness factor may apply which could lead to erroneous results if production of intermediate substrate in the biofilm is not taken into account.

Modified anaerobic DSFF reactors fitted with removable biofilm supports were used to evaluate startup and steady state reactor operation. For startup total biomass and biofilm yields were higher and rates of biofilm accumulation faster for treatment of lower strength wastes. It is advantageous to start fixed film reactors with a weak waste that results in greater biofilm accumulation and easier operational control. It was also concluded that organic loading of fixed film reactors can be increased while volatile acid concentrations are maintained between 200-1500 mg L^{-1}. This assumes that the wastes are well buffered and reactor pH is maintained in an optimum range (6.8-7.6). This conclusion differs from that reported for the startup of UASB reactors. For UASB reactors volatile acid

concentrations should be negligible before implementing increases in the organic loading rate.

Steady state operation of anaerobic DSFF reactors has shown that the high concentration of biomass retained in the biofilm permits successful treatment of low to medium strength carbohydrate wastewater at high organic loading rates and short HRT. DSFF reactors do not retain as much biomass as other advanced reactors and connot achieve as high organic loading rates and removal rates. During steady state operation biofilm concentration increased with increased organic loading rate and decreased HRT reaching a maximum of 8.7 kg VFSm^{-3} (0.116 kg VFS m^{-2}) at a loading rate of 10 kg COD m^{-3} d^{-1} (0.133 kg COD m^{-2} d^{-1}).

For reactors treating different concentrations of wastewater SRT could be described as a function of the HRT or LRT. Both HRT and LRT are easily measured and important design criteria. A steady state empirical model and kinetic coefficients based on this fact were developed to predict COD removal efficiency and biomass concentration in DSFF reactors. The model gave a good fit to the data.

Activity tests made during startup and steady state operation showed that the majority of methanogenic activity was located in the biofilm. Maximum biofilm substrate utilization rates were not influenced by the film thickness and were similar to rates reported for suspended growth systems treating similar wastes. Plots of k and K versus ϕ indicated that for ϕ values between 0-3.1, apparent kinetic con-

stants were the same as intrinsic constants. The biofilm was completely active and substrate penetrated the complete depth of the biofilm. For anaerobic biofilms on NPP support material of up to 2.6 mm in thickness, internal diffusional resistance is negligible.

A dynamic model for DSFF reactors based on mass balances of the acid forming and methane forming bacteria in the liquid and biofilm phases was developed. Assuming that the reactor pH remained in an optimum range and no inhibition occured the model described startup of DSFF reactors. Based on the kinetic constants and yield factors used to describe acetogenic and methanogenic bacteria growing in the mixed liquor and biofilm, attachment rates and detachment rates of 0.1-0.2 d^{-1} best described startup reactor performance. The simulation also indicated that under stable operating conditions the methanogenic bacteria make up approximately 15-20 % of the total reactor or biofilm biomass.

7. Future Studies

The following topics are suggested as possible subjects for further investigation:

1. Determine the effect of different control strategies on startup.
2. Develop techniques to separate and quantify acetogenic and methanogenic bacteria coexisting in a single reactor.
3. Incorporate substrate diffusion across the liquid boundary layer in the sequential substrate utilization model.
4. Conduct further experiments to provide information for modification or verification of parameters used in the dynamic model.
5. Use the dynamic model to simulate different control actions.
6. Refine the dynamic model to incorporate an inhibition factor.
7. Conduct research to find ways of attaching viable organisms to support material thus shortening startup time.

REFERENCES

Ackman, R.G. 1972. Porous polymer bead packing and formic acid vapour in GLC of volatile fatty acids. J. Chromatogr. Sci., 10, 560.

Andrews, J.F. 1969. Dynamic model of the anaerobic digestion process. J. San. Eng. Div., Proc. ASCE., 95, 95.

Andrews, J.F. and S.P. Graef. 1971. Dynamic modeling and simulation of the anaerobic digestion process. Anaerobic Biological Treatment Processes, Adv. in Chemistry Series, 105, 126.

APHA, Standard Methods for the Examination of Water and Wastewater. 1971. 13th edition, American Public Health Assoc. Inc, New York, N.Y.

Atkinson, B. 1974. *Biochemical Reactors*. Pion Ltd., London.

Atkinson, B. and I.S. Daoud. 1968. The analogy between micro-biological reactions and heterogenous catalysis. Trans. Inst. Chem. Eng., 46, T19.

Atkinson, B. and I.J. Davies. 1972. The complete mixed microbial film fermenter: a method of overcoming washout in continuous culture. Trans. Inst. Chem. Eng. 50, 208.

Atkinson, B. and I.J. Davies. 1974a. The overall rate of substrate uptake (reaction) by microbial films: Part I-A biological rate equation. Trans. Inst. Chem. Eng., 52, 248.

Atkinson, B. and H.W. Fowler. 1974b. The significance of microbial film in fermenters. Adv. in Biochem. Eng., T.K. Ghose et al. Vol. 3.

Atkinson, B. and S.Y. How. 1974c. The overall rate of substrate uptake (reaction) by microbial films: Part II-Effect of concentration and thickness with mixed microbial films. Trans. Inst. Chem. Eng., 52, 260.

Bachman, A., V.L. Beard and P.L. McCarty. 1983. Performance characteristics of the anaerobic baffled reactor. Third Int. Symp. on Anaerobic Digestion, Boston, Aug 14-19.

Balch, W.E. and R.S. Wolfe. 1979a. Specificity and biological distribution of Coenzyme M (2-mercaptoethanesulfonic acid). J. Bacteriol. 137, 256.

Balch, W.E. and R.S. Wolfe. 1979b. Transport of Coenzyme M (2-mercaptoethanesulfonic acid) in *Methanobacterium ruminantium*. J. Bacteriol. 137, 264.

Balch, W.E., G.E. Fox, L.J. Magrum, C.R. Woese and R.S. Wolfe. 1979. Methanogens: reevaluation of a unique biological group. Microbiol. Rev., 43, 260.

Balch, W.E., S. Schoberth, S. Tawner and R.S. Wolfe. 1977. An ancient divergence among the bacteria. J. of Molec. Evolution 9, 305.

Balmer, R.G. 1974. Anaerobic treatment of dairy waste using a fiber wall reactor. M.S. Thesis, Purdue University, Indiana.

Bischoff, K.B. 1965. Effectiveness factor for general reaction rate forms. Am. Inst. Chem. Eng. J. 11, 351.

Bochem, H.P., S.M. Schoberth, B. Sprey. 1982. Thermophilic biomethanation of acetic acid: morphology and ultrastructure of a granular consortium. Can. J. Microbiol. 28, 500.

Bryant, M.P. 1979. Microbial methane production: theoretical aspects. J. Animal Sci. 48, 193.

Bryant, M.P., B.C. McBride and R.S. Wolfe. 1968. Hydrogen-oxidizing methane bacteria. J. of Bacteriol. 95(3), 1118.

Bryant, M.P., E.A. Wolin, M.J. Wolin and R.S. Wolfe. 1967. *Methanobacillus omeliamskii*, a symbiotic association of two species of bacteria. Arch. Microbiol. 59, 20.

Bryers, J.D. 1984. Biofilm formation and chemostat dynamics: pure and mixed cultures. Biotech. Bioeng. 26, 748.

Bryers, J. and W.G. Characklis. 1981. Early fouling biofilm formation in turbulent flow system: overall kinetics. Wat. Res. 15, 483.

Bryers, J. and W.G. Characklis. 1982. Processes governing primary biofilm formation. Biotech. Bioeng. 26, 2451.

Buhr, H.O. and J.F. Andrews. 1977. The thermophilic anaerobic digestion process. Wat. Res. 2, 129.

Carnahan, B. 1969. *Applied Numeric Methods*. J. Wiley & Sons, Ltd., Toronto.

Characklis, W.G. 1981. Fouling biofilm development; a process analysis. Biotech. Bioeng. 23, 1923.

Characklis, W.G. 1973. Attached microbial growth-1. Attachment and growth. Wat. Res. 7, 1113.

Cheeseman, P., A. Toms-Wood and R.S. Wolfe. 1971. Isolation and properties of fluorescent compound factor 420, from *Methanobacterium* strain M.O.H. Bacteriol. 112, 527.

Chen, K.C., K. Suga and H. Taguchi. 1980. Intrinsic kinetic constants of immobilized enzyme system. J. Ferment. Technol. 58, 439.

Christensen, D.R. and P.L. McCarty. 1975. Multi-process biological treatment model. J.WPCF. 47, 2652.

Cohen, A., A.M. Breure and G. van Andel. 1980. Influence of phase separation on the anaerobic digestion of glucose-I maximum COD-turnover rate during continuous operation. Wat. Res. 14, 1439.

Copp, G.H. and K.J. Kennedy. 1983. Support materials for downflow stationary fixed film (DSFF) methanogenic reactors. J. Ferment. Technol. 61(3), 333.

Dahab, M.F. and J.C. Young. 1982. Retention and distribution of biological solids in fixed-bed anaerobic filters. First Int. Conf. Fixed Film Biol. Proc., Ohio, April 20.

Dawson , K.A. 1980. Inhibition by hydrogen on a continuous culture of an anaerobic oxalate-degrading population. Written communication.

DeWalle, F.B. and E.S.K. Chian. 1976. Kinetics of substrate removal in completely mixed anaerobic filters. Biotech. Bioeng. 18, 1275.

Dewey, D.Y.R., H.S. Kim and H. Taguchi. 1984. Intrinsic fermentation kinetic parameters of immobilized yeast cells. J. Ferment. Technol. 62(3), 255.

De Zeeuw, W. and G. Lettinga. 1981. Acclimation of digested sewage sludge during start-up of an upflow anaerobic sludge blanket (UASB) reactor. Proc. 35th Purdue Ind. Waste Conf., Purdue Univ., Lafayette, Indiana, 39.

Duarte, A.C. 1980. Studies on inhibition modeling in anaerobic digesters. Ph>D. Thesis, Univ. of Newcastle upon Tyne, England.

Duff, S.J.B., and K.J. Kennedy. 1982. Effect of organic and hydraulic overloading on thermophilic anaerobic fixed film reactors. Biotech. Letters 4(12), 815.

Duff, S.J.B., and K.J. Kennedy. 1983. Effect of effluent recirculation on startup and steady state operation of the DSFF reactor. Biotech. Lett. 5, 317.

Ferry, J.G. and R.S. Wolfe. 1976. Anaerobic degradation of benzoate to methane by a microbial consortium. Arch. Microbiol. 107, 33.

Ghosh, S. and F.G. Pohland. 1974. Kinetics of substrate assimilation and product formation in anaerobic digestion. J. WPCF. 46, 748.

Ghosh, S., J.R. Conrad and D.L. Kloss. 1975. Anaerobic acidogenesis of wastewater sludge. J. WPCF. 47, 30.

Gill, M. 1978. Study of the kinetic response of an anaerobic reactor with fibre panels. Ph.D. Thesis, Univ. of Purdue, Indiana.

Grady, C.P.L., and H. Lim. 1980. *Biological Wastewater Treatment: Theory and Application.* Marcel Dekker, Inc. New York, N.Y.

Graef, S.P. and J.F. Andrews. 1974. Stability and control of anaerobic digestion. J. WPCF. 46(4),666.

Guiot, S.R. and L. van den Berg. 1984. Performance and biomass retention of an upflow anaerobic reactor combining a sludge blanket and a filter. Biotech. Lett. 6(3), 161.

Hall, E.R. 1982. Biomass retention and mixing characteristics in fixed film and suspended growth anaerobic reactors. Proc. IAWPR Spec. Sem. on Anaerobic Treatment of Wastewater in Fixed Film Reactors. Copenhagen, Denmark, Pergamon Press, Oxford, U.K. 371.

Hamilton, B.K., C.R. Gardner and C.K. Colton. 1974. Effect of diffusional limitations on Lineweaver-Burk plots for immobilized enzymes. Am. Inst. Chem. Eng. 20(3), 503.

Hartman, L. 1967. Influence of turbulence on the activity of bacterial slimes. J. WPCF. 39, 958.

Harvey, M. 1984. Anaerobic digestion of swine waste using downflow stationary fixed film digesters. M.A.Sc. Thesis, Univ. of Guelph, Guelph, Ont.

Henze, M. and P. Harremoes. 1982. Review paper: Anaerobic treatment of wastewater in fixed-film reactors. Proc. IAWPR Spec. Sem. on Anaerobic Treatment of Wastewater in Fixed Film Reactors. Copenhagen, Denmark. Pergamon Press, Oxford, U.K., 1.

Herbert, D. 1963. Some principles of continuous culture: Recent progress in Microbiology. 7th Int. Cong. in Microbiol.

Heukelekian, H. 1956. Slime formation in polluted waters

II. Factors affecting slime growth. Sew. Ind. Waste 28, 78.

Hobson, P.N., S. Bousfield and R. Summers. 1974. Anaerobic digestion of organic matter. Crit. Rev. in Environ. Control 4, 109.

Howell, J.A. and B. Atkinson. 1976a. Influence of oxygen and substrate concentrations on the ideal film thickness and the maximum overall substrate uptake rate in microbial fermenters. Biotech. Bioeng. 17, 15.

Howell, J.A. and B. Atkinson. 1976b. Sloughing of microbial film in trickling filters. Wat. Res. 10, 307.

Howell, J.A., C.T. Chi and U. Pawlowsky. 1972. Effect of wall growth on scale-up problems and dynamic operating characteristics of the biological reactor. Biotech Bioeng. 14, 253.

Hulshoff Pol, L. W., W.J. de Zeeuw, C.T. Velzeboer and G. Lettinga. 1982. Granulation in UASB-reactors. Proc. IAWPR Spec. Sem. on Anaerobic Treatment of Wastewater using Fixed Film Reactors. Copenhagen, Denmark. Pergamon Press, Oxford, U.K. 305.

Huser, B.A. 1981. Methanbildung aus Acetat. Thesis, Swiss Federal Inst. of Tech. Nr 6750 (In German).

Huser, B.A., K. Wuhrmann and A.J.B. Zehnder. 1982. *Methanothrix soehngenii* gen. nov. sp. nov., a new acetotrophic non-hydrogen-oxidizing methane bacterium. Arch. Microbiol. 132, 1.

Iannotti, E.L. 1973. Glucose fermentation products of *Ruminococcus albus* grown in continuous culture with *Vibrio suocimogenes* Changes caused by interspecies transfer of H_2. J. of Bacteriol. 114(3), 1231.

Jewell, W.J., M.S. Switzenbaum and J.W. Morris. 1981. Municipal wastewater treatment with the anaerobic attached microbial film expanded bed process. J. WPCF. 53(4), 482.

Kandler, O. 1979. Cell-wall structure of methane producing bacteria. Naturwissenschaften 66, 95.

Kandler, O. and H. Hippe. 1977. Lack of peptidoglycan in the cell walls of *Methanosarcina barkeri*. Arch. Microbiol. 113, 57.

Kandler, O. and H. Konig. 1978. Chemical composition of peptidoglycan-free cell walls of methanogenic bacterial Arch. Microbiol. 118(2), 141.

Kaspar, H.F. and K. Wuhrmann. 1978. Kinetic parameters and relative turnover of some important catabolic reactions in digesting sludge. Appl Environ. Microbiol. 36, 1.

Kennedy, K.J. and L. van den Berg. 1985. Anaerobic downflow stationary fixed film reactors. Comp. Biotech. Inpress.

Kennedy, K.J. and L. van den Berg. 1981. Effects of temperature and overloading on the performance of anaerobic fixed film reactors. Proc. 36th Purdue Ind. Waste Conf., Purdue University, Lafayette, Indiana. 678.

Kennedy, K.J. and L. van den Berg. 1982a. Anaerobic digestion of piggery waste using a stationary fixed film reactor. Agr. Wastes 4, 151.

Kennedy, K.J. and L. van den Berg. 1982b. Stability and performance of anaerobic fixed film reactors during hydraulic overloading at 10 to 35 °C. Wat. Res. 16, 1391.

Kennedy, K.J. and L. van den Berg. 1982c. Continuous vs slug loading of downflow stationary fixed film reactors digesting piggery waste. Biotechnol. Lett. 4(2), 137.

Kennedy, K.J. and L. van den Berg. 1982d. Thermophilic downflow stationary fixed film reactors for methane production from bean blanching waste. Biotechnol. Lett. 4(3), 171.

Kennedy, K.J. and L. van den Berg. 1982e. Effect of height on the performance of anaerobic downflow stationary fixed film (DSFF) reactors treating bean blanching waste. Proc. 37th Purdue Ind. Waste Conf. Purdue Univ., Lafayette, Indiana. 71.

Kennedy, K.J., M. Muzar and G.H. Copp. 1985. Stability and performance of mesophilic anaerobic fixed film reactors during organic overloading. Biotech. Bioeng. 27, 86.

Kennedy, K.J., L. van den Berg and W.D. Murray. 1981. Advanced fixed film reactors from microbial production of methane from waste. Proc. 2nd World Congress Chem Eng., Montreal, Que. 317.

Kirsch, E.J., and R.M. Sykes. 1971. Anaerobic digestion in biological waste treatment. Prog. Ind. Microbiol 9, 155.

Kirsop, B.H. 1982. *Methanogenesis*, CRC Crit. Rev. in Biotechnol. 1, 109.

Kleinstreuer, C. and T. Poweigha. 1982. Dynamic simulator for anaerobic digestion processes. Biotech. Bioeng. 26, 1941.

Knetchel, R.J. 1977. A more economical method for the determination of chemical oxygen demand. Water and Waste Eng. 14(4), 25.

Konig, H. and K.O. Stetter. 1982. Isolation and characterization of *Methanobys tindarius*, sp. nov., a coccoid methanogen growing only on methanol-ethyl-amines. Zbl. Bakt. Hyp., I. Abt. orig. C, ????.

Kornegay, B.H. and J.F. Andrews. 1968. Kinetics of fixed film biological reactors. J. WPCF. 40, R460.

Lee, G.K., R.A. Lesch and P.S. Reilly. 1984. Intrinsic immobolized enzyme kinetics. Biotech and Bioeng. 23, 487.

Lehninger, A.L. 1975. *Biochemistry*. Worth Publishers Inc. New York, N. Y..

Lawrence, A.L. and P.L. McCarty. 1969. Kinetics of methane fermentation in anaerobic treatment. J. WPCF 41(2), R1.

Lettinga, G. 1979. Direct anaerobic treatment handles wastes effectively. Ind. Wastes, 25, 18.

Lettinga, G., S.W. Hobma, L.W. Hulshoff Pol, W. de Zeeuw, P. de Jong, P. Grin and R. Roersma. 1982. Design, operation and economy of anaerobic treatment. Proc. IAWPR Spec. Seminar on Anaerobic Treatment of Wastewater in Fixed Film Reactors. Copenhagen, Denmark. Pergamon Press, Oxford, U.K. 283.

Lettinga, G., T., van der Geest and S.W. Hobma. 1979. Anaerobic treatment of methanobic wastes. Wat. Res. 13, 725.

Lettinga, G., A.F. van Velsen, S.W. Hobma, W. de Zeeuw and A. Klapwijk. 1980. Use of the Upflow Sludge Blanket (USB) Reactor Concept for Biological Wastewater Treatment, Especially for Anaerobic Treatment. Biotech. Bioeng. 22, 699.

Levenspiel, O. 1972. *Chemical Reaction Engineering, 2nd Ed.* J. Wiley and Son, New York, N.Y..

Lo, K.V., A.J. Whitehead and P.H. Liao. 1984. Methane production from screened dairy manure using a fixed film reactor. Agr. Wastes 9, 175.

Maat, D. 1983. Design, construction and operation of a full scale donwflow fixed film reactor using hog waste substrate. 5th Bioenergy R. and D. seminar , Ottawa, Canada, Mar. 26-28.

Mah, R.A. 1980. Isolation and characterization of *Methanococcus mazei*. Current Microbiol. 3, 312.

Mah, R.A., M.R. Smigh and L. Baresi. 1978. Studies on an acetate-fermenting strain of *Methanosarcina*. Appl. Environ. Microbiol. 35, 1174.

Mah, R.A., D.M. Ward, L. Baresi and T.L. Glass. 1977. Biogenesis of methane. Ann. Rev. Microbiol. 31, 309.

Massey, M.L. and F.G. Pohland. 1978. Phase separation of anaerobic stabilization by kinetic controls. J. WPCF. 50, 2204.

McBride, B.C. and R.S. Wolfe. 1971. A new coenzyme of methyl transfer coenzyme M. Biochem. 10, 2317.

Mehta, K.B. and N.W. LeRoux. 1974. Effect of wall growth on continuous biological oxidation of ferrous iron. Biotech. Bioeng. 16, 559.

Monod, J. 1949. The growth of bacterial cultures. Ann. Rev. Microbiol. 3, 371.

Mueller, J.A. and J.L. Mancini. 1975. Anaerobic filter kinetics and applications. Proc. 20th Purdue Ind. Waste Conf., Purdue Univ., Lafayette, Indiana. 423.

Murray, W.D. and L. van den Berg. 1982. Effect of nickel, cobalt and molybdenum on the performance of methanogenic fixed film reactors. Appl. Environ. Microbiol. 42, 502.

Ohwaki, K. and R.E. Hungate. 1977. Hydrogen utilization by *Clostridia* in Sewage Sludge. Appl. and Environ. Microbiol. 33(6), 1270.

Patel, G.B. 1985. Characterization and nutritional properties of *Methanothrix concillii* sp. nov., a mesophilic aceticlastic methanogen. Can. J. Microbiol. Inpress.

Patel, G.B. and B.J. Agnew. 1981. A simple apparatus for measuring the Eh of anaerobic media. Can. J. Microbiol. 27(8), 853.

Perry, R.H. and C.C. Chilton (Eds.). 1973. *Chemical Engineers Handbook*. 5th Ed. McGraw-Hill Book Co., Toronto, Ont.

Pretorius, W.A. 1972. The effect of formate on the growth of acetate utilizing methanogenic bacteria. Wat. Res. 6(10), 1213.

Rich, L.G. 1963. *Unit Processes of Sanitary Engineering*. J. Wiley and Sons (Ed.), New York, New York.

Rittmann, B.E. and P.L. McCarty. 1980a. Model of steady-state-biofilm kinetics. Biotech. Bioeng. 22, 2343.

Rittmann, B.E. and P.L. McCarty. 1980b. Evaluation of steady-state-biofilm kinetic. Biotech. Bioeng. 22, 2357.

Rose, C.S. and S.J. Pirt. 1981. Conversion of glucose to fatty acids and methane, roles of two mycoplasmal agents. J. Bacteriol. 147, 248.

Samson, R., L. van den Berg and K.J. Kennedy. 1984a. Influence of continuous vs non-continuous channels on mixing characteristics and performance of anaerobic downflow stationary fixed film (DSFF) reactors before and during waste treatment. Proc. 39th Purdue Ind. Waste Conf., Purdue Univ. Lafayette, Indiana. (in press).

Samson, R., L. van den Berg and K.J. Kennedy. 1985. Mixing characteristics of anaerobic downflow stationary fixed film (DSFF) reactors. Biotech. Bioeng. 27, 10.

Samson, R., R. Peters, C. Hade and B. van den Berg. 1984b. Dairy waste treatment using industrial scale fixed film and upflow sludge bed anaerobic digesters: design and startup experience. Proc. 39th Purdue Ind. Waste Conf., Purdue Univ., Lafayette, Indiana. (in press).

Schillinger, M.S. 1975. Treatment and digestion of antibiotic fermentation wastes using a fiber wall bioreactor. M.S. Thesis, Purdue Univ. Lafayette, Indiana.

Schoberth, S.M. 1977. Acetic acid from H_2 and CO_2. Arch. Microbiol. 114, 143.

Schoberth, S.M. 1982. Methanogenic flow and their metabolic routes. Advances en degestion anaerobica. Mircera, Mexico. Oct. 25-27. 1.

Shapiro, S. and R.S. Wolfe. 1980. Methyl CoM, an intermediate in methanogenic dissimilation of C_1 compounds by *Methanosarcina barkeri*. J. Bacteriol. ???.

Shea, T.G., W.A. Pretorius, R.D. Gole and E.A. Pearson., 1968. Kinetics of hydrogen assimilation in the methane fermentation. Wat. Res. 2, 833.

Smith, M.R. and R.A. Mah. 1980. Growth and methanogenesis by *Methanosarcina* strain 227 on acetate and methanol. Appl. Environ. Microbiol. 39, 993.

Smith, M.R., S.H. Zinder and R.A. Mah. 1980. Microbial methanogenesis from acetate. Proc. Biochem. 5, 34.

Speece, R.E. 1981. Fundamentals of the anaerobic digestion of municipal and industrial wastes. Proc. Sem. on Anaerobic Wastewater Treatment and Energy Recovery. Duncan, Lagnese and Assoc., Inc. Pittsburgh, Pennsylvania. 1.

Stetter, K.O., M. Thomm, J. Winter, G. Wildgrubber and S. Wanderl. 1981. *Methanothermus fervidus*, sp. nov., A novel extremely thermophilic methanogen isolated from an icelandic hot spring Zbl. Bkt. Hyg., I. Abt. Orig. C2, 166.

Stevens, T.G. and L. van den Berg. 1981. Anaerobic treatment of food processing wastes using a fixed-film reactor. Proc. 36th Purdue Ind. Waste Conf., Purdue Univ., Lafayette, Indiana. 224.

Switzenbaum, M.S. 1978. The anaerobic attached film expanded bed reactor for the treatment of dilute organic wastes. Ph.D. Thesis, Cornell Univ., U.S.A.

Switzenbaum, M.S. and W.J. Jewell. 1980. Anaerobic attached film expanded bed reactor treatment. J. WPCF. 52, 1953.

Szendry, M.L. 1983a. Bacardi Corporation digestion process for stabilizing run distillery wastes and producing methane. Proc. 7th. Sym. Energy from Biomass and Waste, Orlando, Florida. Jan. 11-13. 976.

Szendry, M.L. 1983b. Startup and operation of the Bacardi Corporation anaerobic filter. Proc. 3rd. Int. Anaerobic Digestion Conf. Boston, Massachusettes. Aug. 12-14.

Thiele, E.W. 1939. Relation between catalytic activity and size of a particle. Ind. Eng. Chem. 31, 916.

Toerien, D.F., P.G. Thiele and W.A. Pretorius. 1970. Substrate flow in anaerobic digestion. 5th Int. Conf. on Water Pollution Res., San Francisco, California.

Topiwala, H.H. and G. Hamer. 1971. Effect of wall growth on steady-state continuous cultures. Biotech. Bioeng. 13, 919.

Trudell, M. 1983. Treatment of high strength acidic organic wastewater. M.A.Sc. Univ. of Western Ontario, London, Ont.

Trulear, M.G. and W.G. Characklis. 1982. Dynamics of biofilm processes. J. WPCF. 54(9), 1288.

Tzeng, S.F., R.S. Wolfe and M.P. Bryant. 1975. Factor 420 dependent pyridine nucleotide - linked hydrogenase system of *Methanobacterium ruminantium*. J. Bacteriol. 121, 154.

van den Berg, L. 1977. Effect of temperature on growth and activity of a methanogenic culture utilizing acetate. Can. J. Microbiol. 23, 898.

van den Berg, L. and K.J. Kennedy. 1981a. Support materials for stationary fixed film reactors for high-rate methanogenic fermentations. Biotechnol Lett. 3(4), 165.

van den Berg, L. and K.J. Kennedy. 1981b. Potential use of anaerobic processes for industrial waste treatment. Sem. on Anaerobic Waste Water Treatment and Energy Recovery. Pittsburg, Pennsylvania.

van den Berg, L. and K.J. Kennedy. 1982a. Comparison between intermittent and continuous loading of stationary fixed film reactors for methane production from wastes. J. Chem. Technol. Biotechnol. 32, 427.

van den Berg, L. and K.J. Kennedy. 1982b. Effect of substrate composition on methane production rates of downflow stationary fixed film reactors. Proc. 7th Symp. "Energy from Biomass and Waste". Bonavista, Florida. 401.

van den Berg, L. and K.J. Kennedy. 1982c. Dairy waste treatment with anaerobic stationary fixed film reactors. Proc. IAWPR Spec. Sem. on Anaerobic Treatment of Waste Water in Fixed Film Reactors. Copenhagen, Denmark. Pergamon Press, Oxford, U.K. 229.

van den Berg, L. and K.J. Kennedy. 1982d. Performance characteristics of anaerobic downflow stationary fixed film reactors. Proc. 1st. Int. Conf. of Fixed Film Biological Processes. 1414.

van den Berg, L. and K.J. Kennedy. 1983. Comparison of advanced anaerobic reactors. 3rd. Int. Conf. on Anaerobic Degestion. Boston, Massachusettes. 71.

van den Berg, L. and C.P. Lentz. 1979. Comparison between up and downflow anaerobic fixed film reactors of varying surface to volume ratios for the treatment of bean blanching waste. Proc. 34th Purdue Ind. Waste Conf., Purdue Univ., Lafayette, Indiana. 319.

van den Berg, L. and C.P. Lentz. 1980. Effects of film area-to-volume ratio, film support, height and direction of flow on performance of methanogenic fixed film reactors. Proc. U.S. Dept. of Energy Workshop/Seminar on Anaerobic Filters. Howey-in-the-Hills, Florida. Jan. 9-10. 1.

van den Berg, L., K.J. Kennedy and M.F. Hamoda. 1981. Effects of type of waste on performance of anaerobic fixed film and upflow sludge bed reactors. Proc. 36th Purdue Ind. Waste Conf., Purdue University, Lafayette, Indiana. 686.

van Huyssteen, J.J. 1967. Gas chromatographic separation of anaerobic digester gases using porous polymer. Wat. Res. 1, 237.

van Velsen, A.F.M. 1977. Anaerobic digestion of piggery waste. I. The influence of detention time and manure concentration. Neth. J. Agr. Sci. 25, 151-169.

Wandrey, C., and A. Aivasidis. 1984. Continuous anaerobic digestion with *Methanosarcina barkeri*. Annals N.Y. Academy of Sci. 2, 241.

Weldgruber, G., M. Thomm, H. Konig, K. Ober, T. Ricchiuto and K.O. Stetter. 1982. *Methanoplanus limicola*, a plate-shaped methanogen representing the *Methanoplanaceae*. Arch. Microbiol. 132, 31.

Williamson, K. and P.L. McCarty. 1976a. A model of substrate utilization by bacterial films. J. WPCF. 48, 9.

Williamson, K. and P.L. McCarty. 1976b. Verification studies of the biofilm model for bacterial substrate utilization. J. WPCF. 48, 281.

Wilkinson, J.F. 1978. Methanogenic bacteria-new primary kingdom. Nature 271(5647), 707.

Wolfe, R.S. 1971. Microbial formation of methane. Adv. Microbiol. Physiol. 6, 107.

Wolfe, R.S. 1979a. Methanogenesis. Int. Rev. Biochem., Microbial Biochem. 21, 270.

Wolfe, R.S. 1979b. Methanogens: a surprising microbial group. Antonie van Leeuwenhoek 45, 353.

Wolfe, R.S. 1980. Respiration in methanogenic bacteria. *Diversity of Bacterial Respiratory Systems*. Vol. 1. C.J. Knowles (Ed.) CRC Press, Boca Raton. 161.

Wolin, M.J. 1974a. Interactions between the bacterial species of the rumen. Proc. 4th Int. Symp. on Ruminant Physiol. I.W. McDonald (Ed.) Univ. of New England.

Wolin, M.J. 1974b. Metabolic interactions among intestinal microorganisms. Am. J. Clinical Nutrition 27(10), 1320.

Young, J.C. 1967. Anaerobic wastewater treatment using the anaerobic filter. Ph.D. Thesis, Stanford Univ., Stanford, California.

Young, J.C. 1980. Performance of anaerobic filters under transient loading and operating conditions. Proc. U.S.

Dept. of Energy Workshop/Seminar on Anaerobic Filters. Howey-in-the-Hills, Florida. Jan. 9-10. 159.

Young, J.C., and M.F. Dahab. 1982. Effect of media design on the performance of fixed bed anaerobic filters. Proc. IAWPR Spec. Sem. on Anaerobic Treatment of Waste Water in Fixed Film Reactors. Copenhagen, Denmark. Pergamon Press, Oxford, U.K. 321.

Young, J.C. and P.L. McCarty. 1969. The anaerobic filter for waste treatment. J. WPCF. 41(5), 160.

Zehnder, A.J., Ingvansen, K. and T. Marti. 1982. Microbiology of methanogens including taxonomy. 2nd Int. Symp. on Anaerobic Digestion, Travemunde, Germany. Elsevier/North Holland Biomedical Press, The Netherlands. 45.

Zehnder, A.J. and K Wuhrmann. 1977. Physiology of a *Methanobacterium* Strain AZ. Arch. Microbiol. 111, 199.

Zehnder, A.J., B. Huser, T.D. Brock and K. Wuhrmann. 1980. Characterization of an acetate decarboxylating non-hydrogen-oxidizing methane bacterium. Arch. Microbiol. 124, 1.

Zeikus, J.G. 1977. The biology of methanogenic bacteria. Bacteriol. Rev. 41, 514.

Zeikus, J.G. 1975. Bacterial methanogenesis: acetate as a methane precursor in pure culture. Arch. Microbiol. 104(2), 129.

Zinder, S.H. 1984. Microbiology of anaerobic conversion of organic wastes to methane: recent developments. ASM News 50, 294.

Zinder, S.H. and R.A. Mah. 1979. Isolation and characterization of a thermophilic strain of *Methanosarcina* unable to use H_2-CO_2 for methanogenesis. Appl. Environ. Microbiol. 38, 996.

Zinder, S.H., S.C. Cardwell, T. Anguish and M. Lee. 1984. Methanogenesis in a thermophilic (58°C) anaerobic digestor: *Methanothrix* sp. as an important aceticlastic methanogen. Appl. Environ. Microbiol. 796.

Zoetemeyer, R.J. 1982. Acidogenesis of soluble carbohydrate containing wastewaters. Ph.D. Thesis, Univ. of Amsterdam.

APPENDIX A

A.1 Mixing Study Results

An ideal completely mixed reactor was assumed (mixed liquor) for material balances and model development. Any departure from reactor ideality was determined by accepted stimulus-response tracer methods (see methods; Levenspiel, 1972).

Stimulus-response studies for the DSFF reactor system were carried out at HRT of 0.9, 3.0 and 15.0 days. Results obtained were compared with the tracer curve for a complete mixed reactor, which is described by Eq. A.1:

$$\ln \frac{C}{C_o} = \frac{t}{t_d} \qquad \text{A.1}$$

where C = measured concentration of tracer, DPM mL^{-1}
C_o = initial tracer concentration, DPM mL^{-1}
t = time, h
t_d = mean hydraulic residence time, h

Results plotted in Figure A.1 indicate no discernible deviation of the experimental tracer response from theoretical predictions. Results at the two extemes of HRT tested indicated no large differences; indicating ideal mixing throughout the operating range tested. In all mixing tests, tracer recovery was in excess of 90 percent.

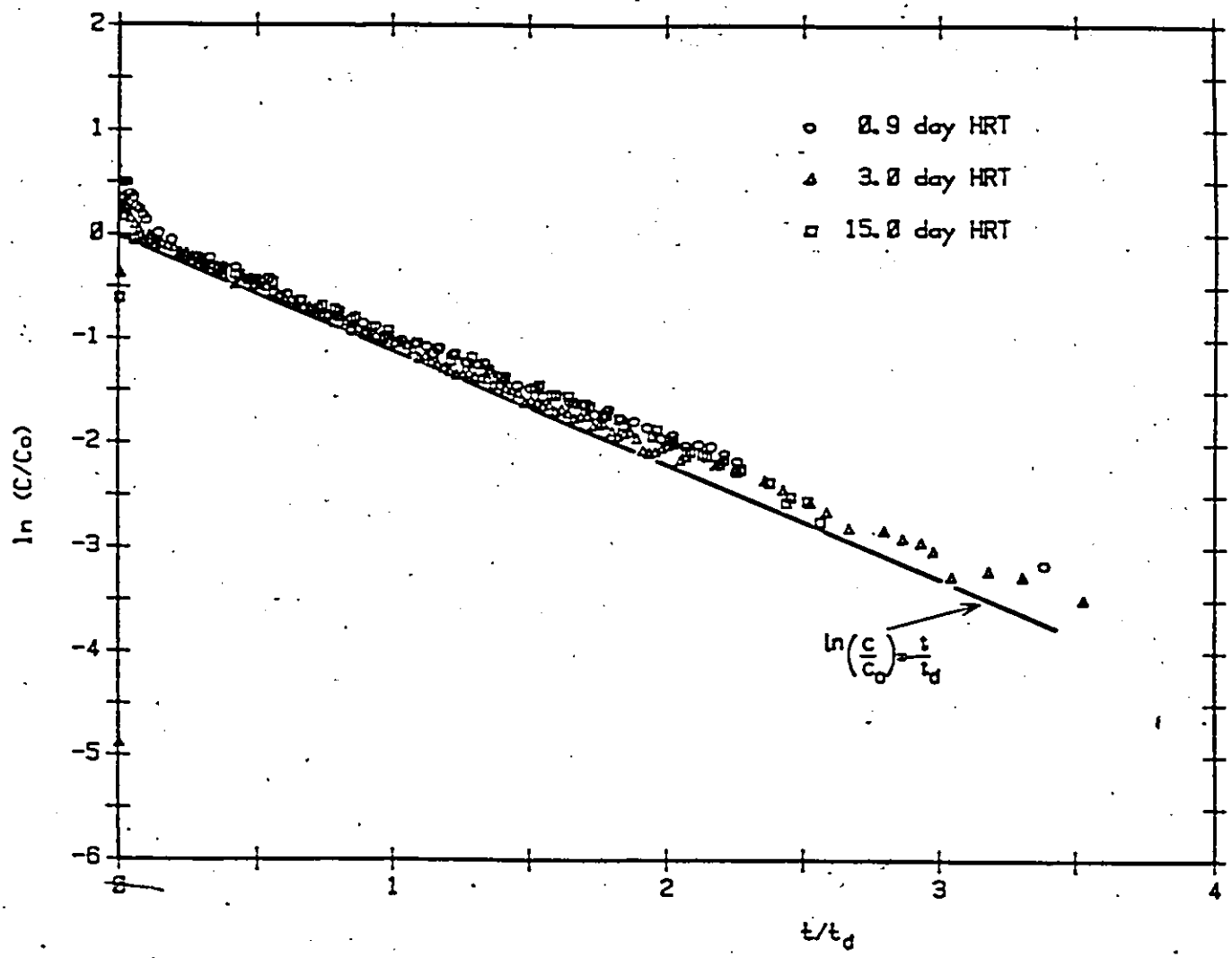

Figure A.1 Tritium tracer curves for DSFF reactors operating at different HRT.

```
      C
      C     DIFFUSION PROGRAM ***** FP4S9 *****
      C
      C     PROGRAM OWNED BY R.DROSTE AND K.KENNEDY
      C
      C     THIS  PROGRAM SOLVES THE DIFFUSION EQUATION FOR TWO SUBSTRATES
      C     WITH CONVERSION IN THE BIOFILM
      C
            IMPLICIT REAL*8 (A-H,O-Z)
            DIMENSION SAVEY(4),PHI(4),F(4),SETA(4)
            DIMENSION ZETA2(201),DZETA2(201),ZZ(201),ZETA1(201)
            DIMENSION ETA(2,10),DZETA1(201)
            DIMENSION V1A(40),V2A(40),V3A(40),DZET(40),ZET(40),EFF(40)
      C
            NEQ=4
            KK=1
            H=0.00500
      C
      C     KAPPA1 = 0.1, THIELE = 0.2  READ COMPLETE SET OF INPUT VALUES
      C
            DTH1=0.500
            VKAP1=0.1D0
            TH1=0.2D0
            DO 30 L=1,40
         30 READ(1,601) V1A(L),V2A(L),V3A(L),EFF(L),DZET(L),ZET(L)
      C
      C
            DO 60 L=1,40
            LL=L
            V1 = V1A(LL)
            V2 = V2A(LL)
            IF(DABS(VKAP1-V1).LT.0.01D0.AND.DABS(TH1-V2).LT.0.0100) GO TO 120
         60 CONTINUE
            GO TO 990
      C
        120 CONTINUE
            EFF1=EFF(LL)
            DZETA0=DZET(LL)
            ZETA1(1)=ZET(LL)
            TH51=TH1*TH1
            BK1=DSQRT(2.0D0*VKAP1-2.0D0*DLOG(1.0D0+VKAP1))
            THM1=((TH1*VKAP1)/(1.0D0+VKAP1))/BK1
      C
            WRITE(5,500) VKAP1,TH1,THM1,EFF1,DZETA0
            WRITE(5,502)
      C
      C     KAPPA2 = 0.1   THIELE2 = 0.2
      C     DELTA=THIELE2=0.5
```

```
FP459    04/17/84 13:48:38

      C
            JJ = 1
            DTH2=0.500
            VKAP2=0.100
            TH2=0.200
        170 IT=1
      C
        190 IHS2=TH2*TH2
            BK2=DSQRT(2.0D0*VKAP2-2.0D0*DLOG(1.0D0+VKAP2))
      C
      C       THM2 = MODIFIED THIELE 2
      C
            IHM2=(TH2*VKAP2)/(1.0D0+VKAP2)/BK2
            YMOD=0.200
            IY=1
      C
            DO 670 IK=1,40
            LL=IK
            V1 = V1A(LL)
            V2 = V2A(LL)
            IF(DABS(VKAP2-V1).LT.0.0100.AND.DABS(TH2-V2).LT.0.0100)GO TO 680
        670 CONTINUE
            GO TO 995
      C
        680 CONTINUE
            EFF2=EFF(LL)
            DZETN=DZET(LL)
            ZETT = ZET(LL)
      C
            WRITE(5,503) VKAP2,TH2,THM2,EFF2,DZEIN
      C
      C     FINDING BLEFT FOR DIFFERENT KAPPA2 AND THIELE2 VALUES
      C
        230 M=0
            HG=YMOD*IHS1*ZETA1(1)/IHS2/(1.0D0+VKAP1*ZETA1(1))
            BLEFT=HG/(1.0D0-HG*VKAP2)
      C
            IF(ZET1.GT.BLEFT) BLEFT = ZET1
            IF(BLEFT.GT.0.7D0) BLEFT = 0.7D0
            BRITE = 10.0D0*BLEFT
            IF(BRITE.GT.1.4D0) BRITE = 1.4D0
      C
        330 ITER=1
      C
        400 I=1
            SETA(1)=ZETA1(1)
            SETA(2)=0.0D0
            SETA(3)=(BLEFT+BRITE)*0.5D0
            SETA(4)=0.0D0
            BNEWR=SETA(3)
            BNEWL=BNEWR
            Z=0.0D0
        440 ZETA1(I)=SETA(I)
```

```
FP459    ,04/17/84 13:48:38

   10400          DZETA1(I)=SETA(2)
   10500          ZETA2(I)=SETA(3)
   10600          Z7(I)=Z
   10700          DZETA2(I)=SETA(4)
   10800  C
   10900          IF(ZETA2(I).GE.0.0D0) GO TO 460
   11000          BLEFT = 1.000000000001D0*ZETA2(I)
   11100          M = 0
   11200          GO TO 400
   11300  C
   11400  C       CALL RUNGE-KUTTA SUBROUTINE
   11500  C
   11600     460  CALL ES363A(SAVEY,SETA,NEQ,F,PHI,H,Z,LRUNGE,M)
   11700          IF(LRUNGE.EQ.0) GO TO 540
   11800          FF=YMOD*THS1*SETA(1)/(1.0D0+VKAP1*SETA(1))
   11900          F(1)=SETA(2)
   12000          F(2)=THS1*SETA(1)/(1.0D0+VKAP1*SETA(1))
   12100          F(3)=SETA(4)
   12200          F(4)=(THS2*SETA(3))/(1.0D0+VKAP2*SETA(3))-FF
   12300          GO TO 460
   12400  C
   12500     540  I=I+1
   12600          IF(Z.LE.1.0D0) GO TO 440
   12700          D=1.0D0-ZETA2(I-1)
   12800          IF(DABS(D).LE.0.00200) GO TO 610
   12900          IF(D.GT.0.0D0) BLEFT=BNEWL
   13000          IF(D.LE.0.0D0) BRITE=BNEWR
   13100          ITER=ITER+1
   13200          IF(ITER.LE.75) GO TO 400
   13300  C
   13400          WRITE(5,506) YMOD
   13500          IF(IY.EQ.1) ETA(1,II) = 0.00
   13600          ETA(2,II) = 0.00
   13700          GO TO 800
   13800  C
   13900     610  EFF4=DZETA2(201)*(1.0D0+VKAP2)/THS2
   14000          EFF3=(YMOD*DZETA0+DZETA2(201))/DZEIN
   14100          ETA(IY,II)=EFF3
   14200          WRITE(5,504) YMOD,EFF4,EFF3,DZETA2(201),ITER
   14300          WRITE(5,505) (ZETA2(N),N=1,201,20)
   14400  C
   14500          IF(YMOD.LT.0.1500) GO TO 800
   14600          YMOD=0.1D0
   14700          IY=2
   14800          GO TO 230
   14900  C
   15000     800  TH2=TH2+DTH2
   15100          II=II+1
   15200          IF(II.EQ.11) GO TO 810
   15300          GO TO 190
   15400  C
   15500  C       OUTPUT ETA
   15600  C
```

```
FP459    04/17/84 13:48:38

 15700      810 WRITE(6,510) VKAP1,TH1,THM1,VKAP2
 15800          WRITE(6,509)(EIA(1,II),II=1,10),(EIA(2,II),II=1,10)
 15900    C
 16000    C       SETING THIELE2,KAPPA2 AND DELTA THIELE2 VALUES
 16100    C
 16200      830 IF(JJ.GT.1) GO TO 850
 16300          TH2=0.400
 16400          DTH2=0.600
 16500          VKAP2=1.000
 16600          JJ=JJ+1
 16700          GO TO 170
 16800      850 IF(JJ.GT.2) GO TO 870
 16900          TH2=1.500
 17000          DTH2=1.500
 17100          VKAP2=10.000
 17200          JJ=JJ+1
 17300          GO TO 170
 17400      870 IF(JJ.GT.3) GO TO 890
 17500          TH2=7.000
 17600          DTH2=4.000
 17700          VKAP2=100.000
 17800          JJ=JJ+1
 17900          GO TO 170
 18000    C
 18100    C       SETING THIELE1,KAPPA1 AND DELTA THIELE1 VALUES
 18200    C
 18300      890 KK=KK+1
 18400          IF(KK.EQ.41) GO TO 1240
 18500          TH1=TH1+DTH1
 18600          IF(KK.EQ.11) GO TO 960
 18700          IF(KK.EQ.21) GO TO 970
 18800          IF(KK.EQ.31) GO TO 980
 18900          GO TO 60
 19000      960 TH1=0.400
 19100          DTH1=0.600
 19200          VKAP1=1.000
 19300          GO TO 60
 19400      970 TH1=1.500
 19500          DTH1=1.500
 19600          VKAP1=10.000
 19700          GO TO 60
 19800      980 TH1=7.000
 19900          DTH1=4.000
 20000          VKAP1=100.000
 20100          GO TO 60
 20200    C
 20300      990 WRITE (3,701)
 20400          GO TO 1240
 20500      995 WRITE (3,702)
 20600    C
 20700     1240 STOP
 20800    C
 20900      600 FORMAT('1'/' KAPPA1=',F7.2,3X,'THIELE1=',F8.2,3X,'MOD THIELE1 =
```

```
FP459    04/17/84 13:48:38

 21000          1=',F10.6,4X,'EFF1 =',F7.4,4X,'DZETA0 =',F8.5 ///)
 21100      502 FORMAT(' KAPPA2',4X,'IHIELE2',4X,'MOD IHIELE2',5X,'EFF2',
 21200         1 6X,'DZEIN'/ 74X,'YMOD',7X,'EFF4',9X,'EFF3',5X,'DZETA2(201)',4X,
 21300         2 'ITER')
 21400      503 FORMAT(/ 1X,F7.2,4X,F6.2,5X,F10.6,4X,F7.4,3X,F8.6)
 21500      504 FORMAT(73X,F5.2,3(4X,F9.6),6X,I2)
 21600      505 FORMAT(' ZETA2: ',11(1:3X))
 21700      506 FORMAT(73X,F5.2,44X,'>75')
 21800      509 FORMAT(10D13.4)
 21900      518 FORMAT(//2X,'KAPPA1 =',F8.3,'  IHIELE1 = ',F8.3,' MOD IHIELE1 =
 22000         1',F8.3,'  KAPPA2 = ',F8.3 /)
 22100      601 FORMAT(6D13.4)
 22200      701 FORMAT(///2X,'****-ERROR-AT-SEARCH-LOOP-130'-//)
 22300      702 FORMAT(/// 2X,'**** ERROR AT SEARCH LOOP 670' //)
 22400      C
 22500          END
```

```
  100   C      RUNGE-KUTTA SUBROUTINE
  200   C
  300         SUBROUTINE FS363A(SAVEY,Y,NEQ,F,PHI,H,X,LRUNGE,M)
  400         IMPLICIT REAL*8 (A-H,O-Z)
  500         DIMENSION Y(4),PHI(4),F(4),SAVEY(4)
  600         M=M+1
  700         GO TO (860,880,960,1020,1090),M
  800     860 LRUNGE=1
  900         RETURN
 1000     880 DO 920 J=1,NEQ
 1100         SAVEY(J)=Y(J)
 1200         PHI(J)=F(J)
 1300         Y(J)=SAVEY(J)+0.5D0*H*F(J)
 1400     920 CONTINUE
 1500         X=X+0.5D0*H
 1600         LRUNGE=1
 1700         RETURN
 1800     960 DO 990 J=1,NEQ
 1900         PHI(J)=PHI(J)+2.0D0*F(J)
 2000         Y(J)=SAVEY(J)+0.5D0*H*F(J)
 2100     990 CONTINUE
 2200         LRUNGE=1
 2300         RETURN
 2400    1020 DO 1050 J=1,NEQ
 2500         PHI(J)=PHI(J)+2.0D0*F(J)
 2600         Y(J)=SAVEY(J)+H*F(J)
 2700    1050 CONTINUE
 2800         X=X+0.5D0*H
 2900         LRUNGE=1
 3000         RETURN
 3100    1090 DO 1110 J=1,NEQ
 3200         Y(J)=SAVEY(J)+(PHI(J)+F(J))*H/6.0D0
 3300    1110 CONTINUE
 3400         LRUNGE=0
 3500         M=0
 3600         RETURN
 3700         END
```

APPENDIX C

```
10 RESTORE
20 CLS:PRINT:PRINT:PRINT
30 PRINT "              DYNAMIC SIMULATION PROGRAM FOR ANAEROBIC DSFF REACTOR "
40 PRINT "              ************************************************"
50 REM
60 REM PROGRAM OWNED BY K. KENNEDY AND R. DROSTE
70 REM
80 REM DSFF SIMULATION WITH ACID FORMER AND METHANE FORMERS DIFFERENTIATED IN T
HE MIXED LIQUOR AND BIOFILM
90 REM
100 REM AT OR ATT = ATTACHMENT RATE
110 REM DAT OR DATT = DETACHMENT RATE
120 REM FQQ = FLOW RATE DATA STARTUP RUN 1 REACTOR A
130 REM
140 DIM AT(4),DAT(4),FQQ(79)
150 REM
160 REM COMPOSITION OF MICROORGANISMS C6H1206, (ANDREWS AND GRAEF, 1972)
170 REM Y(1) & YP(1) = ACID FORMERS IN MIXED LIQUOR, MOLES/L
180 REM Y(2) & YP(2) = ACID FORMERS ON BIOFILM, MOLES/L
190 REM Y(3) & YP(3) = METHANE FORMERS IN MIXED LIQUOR, MOLES/L
200 REM Y(4) & YP(4) = METHANE FORMERS ON BIOFILM, MOLES/L
210 REM Y(5) & YP(5) = PRIMARY SUBSTRATE (C6H1206), MOLES/L
220 REM Y(6) & YP(6) = INTERMEDIATE SUBSTRATE (ACETIC ACID), MOLES/L
230 REM
240 DIM Y(6),YP(6),SAVEY(6),PHI(6),F(6),YX(6)
250 AT(1)=0:AT(2)=.05:AT(3)=.1:AT(4)=.2:DAT(1)=0:DAT(2)=.05:DAT(3)=.1
260 FSA=.027777:FXA=0:FXM=0:FSM=1E-11:DAT(4)=.2:FQQ(1)=.4:FQQ(2)=.4:FQQ(3)=.001:
FQQ(4)=.001:FQQ(5)=.8:FQQ(6)=1.4:FQQ(7)=2.1:FQQ(8)=2.5
270 FQQ(9)=2.5:FQQ(10)=.001:FQQ(11)=.001:FQQ(12)=.001:FQQ(13)=1.2:FQQ(14)=2.5:FQ
Q(15)=3.3:FQQ(16)=3.3:FQQ(17)=3.4:FQQ(18)=3.4:FQQ(19)=3.8
280 FQQ(20)=3.9:FQQ(21)=3.8:FQQ(22)=4.7:FQQ(23)=4.7:FQQ(24)=5.6:FQQ(25)=4.6:FQQ(
26)=5.3:FQQ(27)=5.5:FQQ(28)=6.1:FQQ(29)=6.2:FQQ(30)=6.2
290 FQQ(31)=6.5:FQQ(32)=6.5:FQQ(33)=7.4:FQQ(34)=8.2:FQQ(35)=8.3:FQQ(36)=8.399999
:FQQ(37)=8.399999:FQQ(38)=8.399999:FQQ(39)=8.399999:FQQ(40)=9.3
300 FQQ(41)=10!:FQQ(42)=9.8:FQQ(43)=10.3:FQQ(44)=10.3:FQQ(45)=10.4:FQQ(46)=10.4:
FQQ(47)=12!:FQQ(48)=12.3:FQQ(49)=6!:FQQ(50)=13.2
310 FQQ(51)=13.2:FQQ(52)=13.2:FQQ(53)=13.2:FQQ(54)=13.2:FQQ(55)=13.5:FQQ(56)=13.
6:FQQ(57)=13.7:FQQ(58)=13.4:FQQ(59)=13.3:FQQ(60)=12!
320 FQQ(61)=12.8:FQQ(62)=13!:FQQ(63)=12.9:FQQ(64)=12.9:FQQ(65)=13.1:FQQ(66)=13.2
:FQQ(67)=13.3:FQQ(68)=14!:FQQ(69)=14!:FQQ(70)=14.3
330 FQQ(71)=14.3:FQQ(72)=14.4:FQQ(73)=14.2:FQQ(74)=14.5:FQQ(75)=15!:FQQ(76)=15!:
FQQ(77)=15.3:FQQ(78)=15.3:FQQ(79)=15!
340 REM
350 REM UMAXA = MAXIMUM SPECIFIC GROWTH RATE OF ACID FORMERS
360 REM UMAXM = MAXIMUM SPECIFIC GROWTH RATE OF METHANE FORMERS
370 REM HKSA = SATURATION COEFF. FOR ACID FORMERS
380 REM HKSM = SATURATION COEFF. FOR METHANE FORMERS
390 REM HKDA = DECAY RATE OF ACID FORMERS
400 REM HKDM = DECAY RATE OF METHANE FORMERS
410 REM GROWTH CONSTANTS IN BIOFILM AND MIXED LIQUOR WERE THE SAME
420 REM
430   UMAXA = .333: UMAXM = .195: HKSA = .00133: HKSM = .0025: HKDA = .04: HKDM
= .02
440 REM
450 REM VOL = REACTOR VOLUME,L
460 REM YXAS = YIELD OF ACID FORMERS FROM SUBSTRATE, MOLE/MOLE
470 REM YXAM = YIELD OF METHAE FORMERS FROM SUBSTRATE, MOLE/MOLE
480 REM H = TIME INCREMENT
```

```
500 REM FREQ = PRINTOUT FREQUENCY
510 REM EFF = BIOFILM EFFICIENCY FACTOR
520 REM
530  VOL = 37.4: YXAS = .3: YXMA = .033: H = .05: YXAAS = (1-YXAS)*3
540 FREQ = 20:EFF = 1!
550 DEFINT I-M:LPRINT CHR$(15) : WIDTH "LPT1:",132
560 NEQ = 6
570 FOR T = 1 TO 4
580 DATT = DAT(T)
590 FOR U = 1 TO 4
600 ATT = AT(U)
610 Y(1) = .0333: Y(2) = 0: Y(3) = .00555: Y(4) = 0: Y(5) = .0015: Y(6) =.0016
620 X=1
630 LPRINT USING "FXA     = ##.#####^^^^  M/L ";FXA;
640 LPRINT USING "          FXM     = ##.#####^^^^   M/L";FXM
650 LPRINT USING "FSA     = ##.#####^^^^   M/L";FSA;
660 LPRINT USING "          FSM     = ##.#####^^^^   M/L";FSM
670 LPRINT USING "ATT     = ##.####    1/DAY ";ATT;
680 LPRINT USING "          DATT    = ##.####    1/DAY ";DATT
690 LPRINT USING "UMAXM    = ##.####    1/DAY";UMAXM;
700 LPRINT USING  "          UMAXA     = ##.####    1/DAY";UMAXA
710 LPRINT USING  "HKDA      = ##.####    1/DAY";HKDA;
720 LPRINT USING  "          HKDM      = ##.####    1/DAY";HKDM
730 LPRINT USING  "HKSA      = ##.######    M/L";HKSA;
740 LPRINT USING  "          HKSM      = ##.######    M/L";HKSM
750 LPRINT USING  "YXAS      = ##.####    M/M";YXAS;
760 LPRINT USING  "            YXMA      = ##.####    M/M";YXMA
770 LPRINT USING "VOL        = ##.##      L   ";VOL;
780 LPRINT USING "           HRT       = ##.###     D   ";HRT
790 LPRINT USING  "YXAAS     = ##.####    M/M";YXAAS;
800 LPRINT USING  "            EFF       = ##.####       ";EFF:LPRINT:LPRINT:ICOUNT
 = 0
810 REM
820 REM SPECIFIC GROWTH RATE OF ACID FORMERS = UA
830 REM SPECIFIC GROWTH RATE OF METHANE FORMERS = UM
840 REM METHANE PRODUCTION RATE = QCH4
850 REM
860 LPRINT "  T          FQ          XAS          XAF          XMS          XMF
 SA          SM          UA          UM          QCH4"
870 LPRINT "  D          L/D         G/L          G/L          G/L          G/L
G/L         G/L         1/D         1/D         G/L/D    "
880 LPRINT "================================================================
================================================="
890 UA =(UMAXA*Y(5)/(HKSA+Y(5)))*EFF
900 UM =(UMAXM*Y(6)/(HKSM+Y(6)))*EFF
910 YX(1) = Y(1)*180
920  YX(2) = Y(2)*180
930  YX(3) = Y(3)*180
940  YX(4) = Y(4)*180
950  YX(5) = Y(5)*180
960  YX(6) = Y(6)*60
970 LPRINT USING ".###^^^^    ";X,FQ,YX(1),YX(2),YX(3),YX(4),YX(5),YX(6),UA;
980 LPRINT USING ".###^^^^";UM
990 FOR V = 1 TO 79
1000 FQ = FQQ(V)
1010 HRT =VOL/FQ
1020 M=0
1030 REM CALL RUNGE-KUTTA SUBROUTINE
1040 REM
1050 GOSUB 1350
1060 IF LRUNGE <> 1 GOTO 1190
1070 REM COMPUTE INTERMEDIATE VALUES
1080 YP(1) = (FQ/VOL*(FXA-Y(1)))+(UA-HKDA)*Y(1)-ATT*Y(1)+DATT*Y(2)
1090 YP(2) = (ATT*Y(1))-(DATT*Y(2))+((UA-HKDA)*Y(2))
1100 YP(3) = (FQ/VOL*(FXM-Y(3)))+(UM-HKDM)*Y(3)-ATT*Y(3)+DATT*Y(4)
1110 YP(4) = (ATT*Y(3))-(DATT*Y(4))+(UM-HKDM)*Y(4)
```

```
1120 IF Y(5) <= 0 THEN Y(5) = 0
1130 YP(5) = (FQ/VOL*(FSA-Y(5)))-(UA-HKDA)*Y(1)/YXAS-(UA-HKDA)*Y(2)/YXAS
1140 IF Y(6) <= 0 THEN Y(6) = 0
1150 YP(6) = (FQ/VOL*(FSM-Y(6)))-(UM-HKDM)*Y(3)/YXMA-(UM-HKDM)*Y(4)/YXMA+(UA-HKD
A)*Y(1)/YXAS*YXAAS+(UA-HKDA)*Y(2)/YXAS*YXAAS
1160 UA =(UMAXA*Y(5)/(HKSA+Y(5)))*EFF
1170 UM =(UMAXM*Y(6)/(HKSM+Y(6)))*EFF
1180 GOTO 1050
1190 ICOUNT = ICOUNT + 1
1200 REM
1210 REM PRINT RESULTS OR RECALL RUNGE-KUTTA SUBROUTINE
1220 REM
1230 IF ICOUNT <> FREQ GOTO 1020
1240 ICOUNT = 0
1250 QCH4 = (FQ/VOL*FSA*180)-((180*Y(5))+(60*Y(6))+(Y(1)*180-YX(1))+(Y(2)*180-YX
(2))+(Y(3)*180-YX(3))+(Y(4)*180-YX(4)))*FQ/VOL
1260 YX(1) = Y(1)*180
1270 YX(2) = Y(2)*180
1280 YX(3) = Y(3)*180
1290 YX(4) = Y(4)*180
1300 YX(5) = Y(5)*180
1310 YX(6) = Y(6)*60
1320 LPRINT USING ".###^^^^    ";X,FQ,YX(1),YX(2),YX(3),YX(4),YX(5),YX(6),UA,UM,Q
CH4
1330 NEXT V,U,T
1340 REM ================================================================
1350 REM RUNGE-KUTTA SUBROUTINE
1360 M = M+1
1370 ON M GOTO 1380,1400,1480,1540,1610
1380 LRUNGE = 1
1390 RETURN
1400 FOR J = 1 TO NEQ
1410 SAVEY(J) = Y(J)
1420 PHI(J) = YP(J)
1430 Y(J) = SAVEY(J)+.5*H*YP(J)
1440 NEXT J
1450 X = X+.5*H
1460 LRUNGE = 1
1470 RETURN
1480 FOR J = 1 TO NEQ
1490 PHI(J) = PHI(J)+2!*YP(J)
1500 Y(J) = SAVEY(J)+.5*H*YP(J)
1510 NEXT J
1520 LRUNGE = 1
1530 RETURN
1540 FOR J = 1 TO NEQ
1550 PHI(J) = PHI(J)+2!*YP(J)
1560 Y(J) = SAVEY(J)+H*YP(J)
1570 NEXT J
1580 X = X+.5*H
1590 LRUNGE = 1
1600 RETURN
1610 FOR J = 1 TO NEQ
1620 Y(J) = SAVEY(J)+(PHI(J)+F(J))*H/6
1630 NEXT J
1640 LRUNGE = 0
1650 M = 0
1660 RETURN
1670 END
```

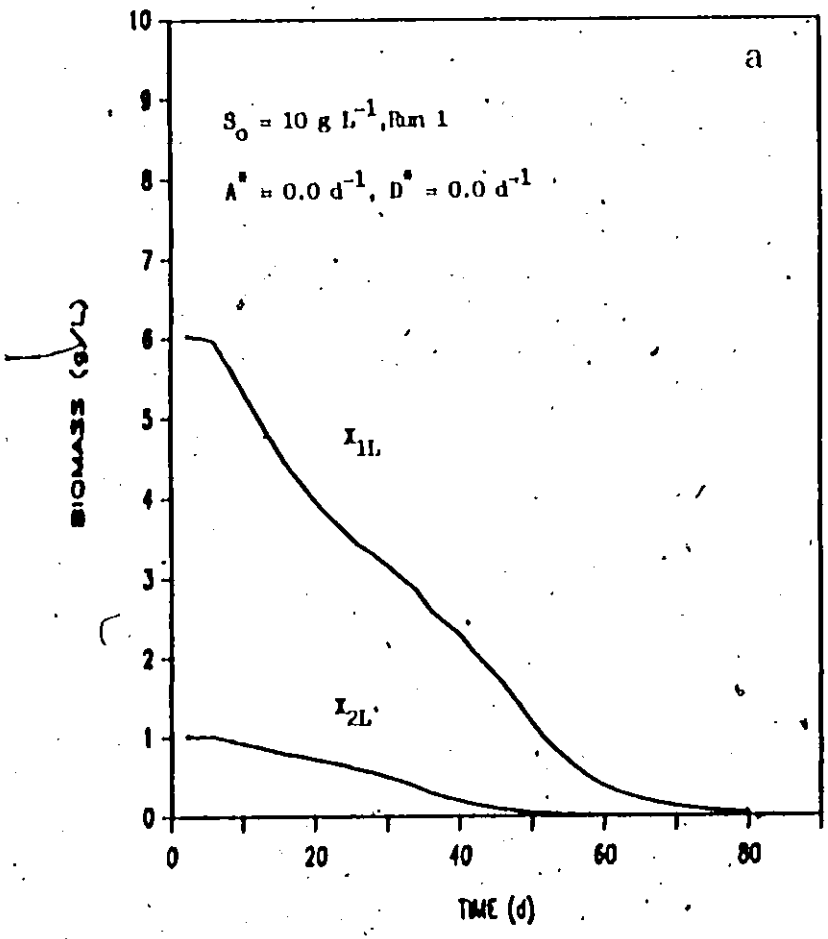

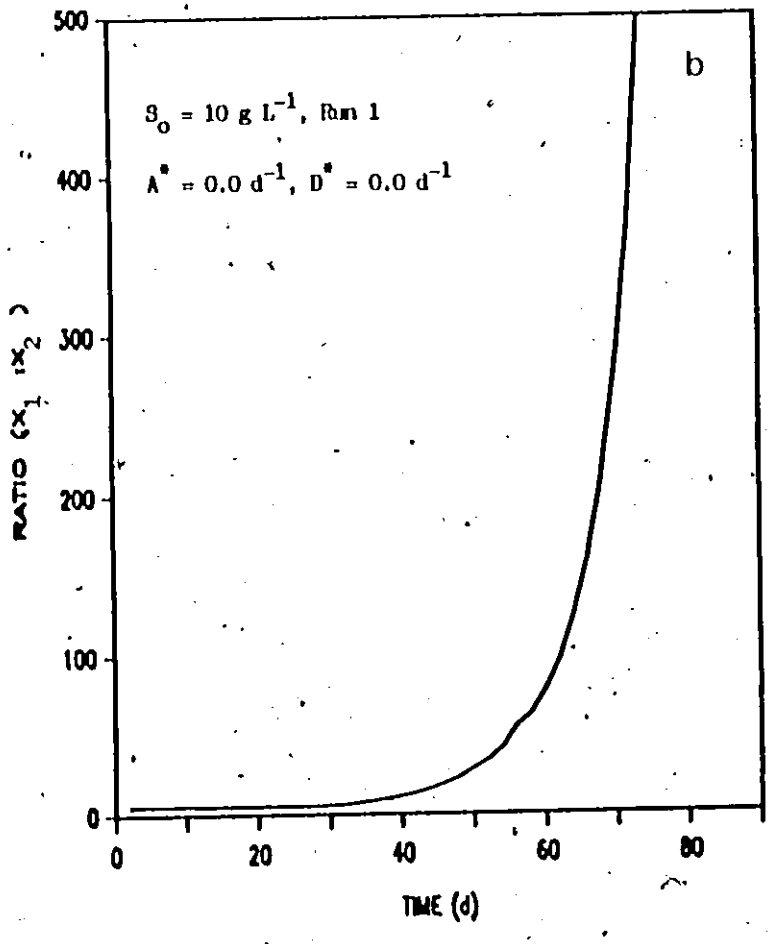

Figure C.1 Simulated biomass concentrations (a) and ratio of acid formers to methane formers (b) for S_o = 10 g L^{-1}; Run 1; A^* = 0.1 d^{-1}; D^* = 0.2 d^{-1}.

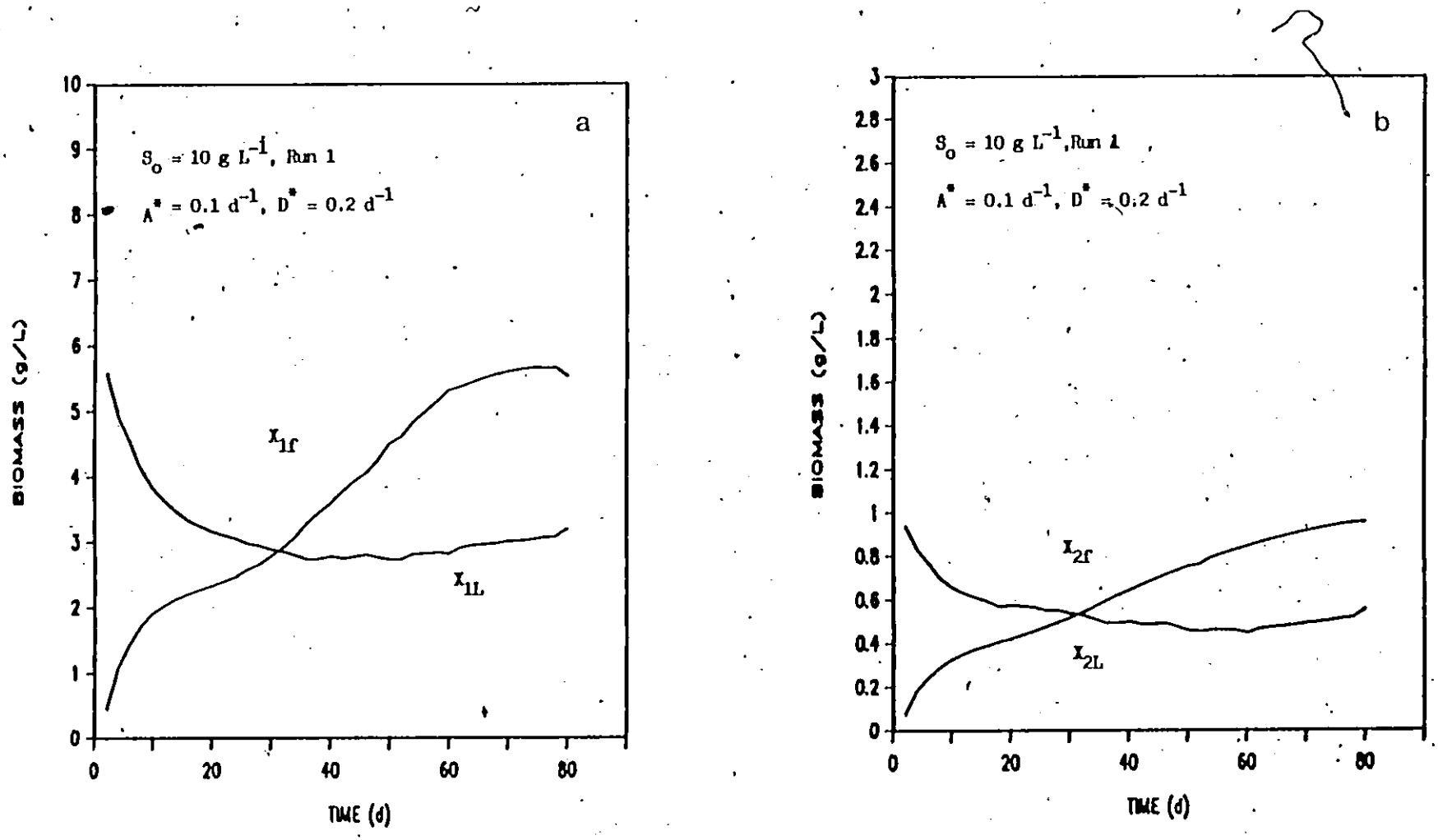

Figure C.2 Simulated mixed liquor (a) and biofilm (b) biomass concentrations for S_o = 10 g L^{-1}; Run 1; A^* = 0.1 d^{-1}; D^* = 0.2 d^{-1}.

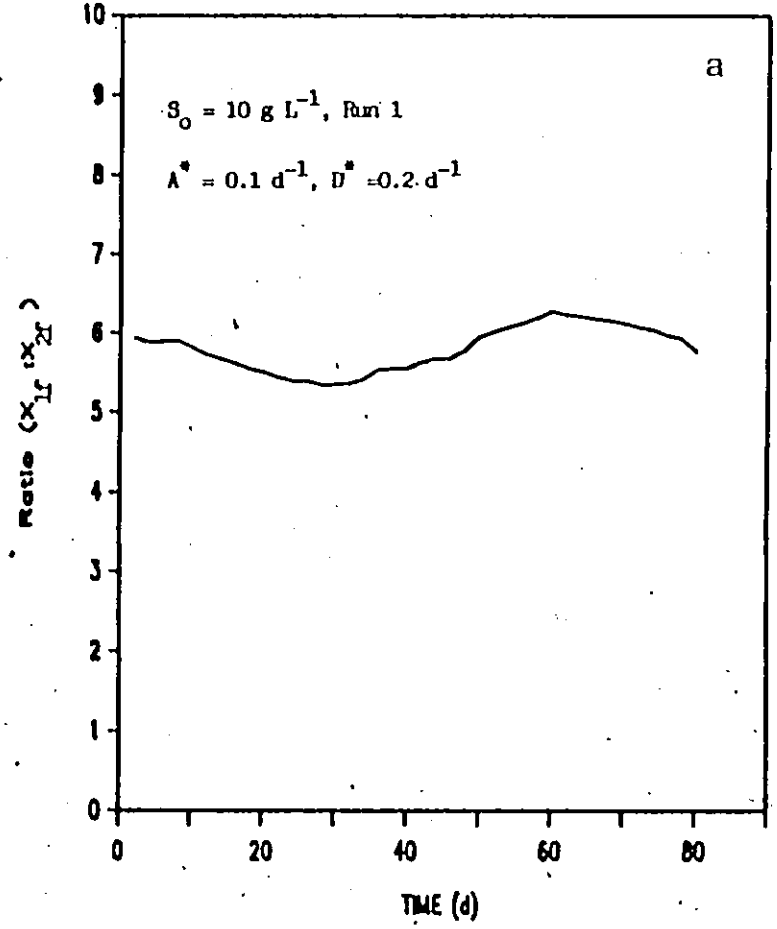

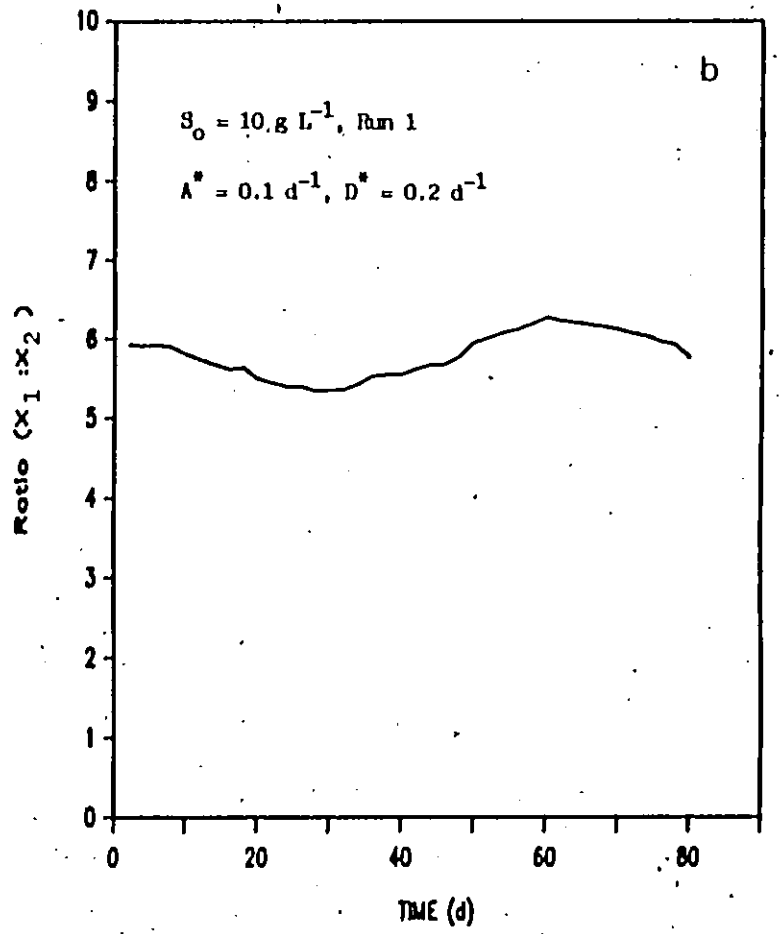

Figure C.3 Simulated ratio of acid formers to methane formers in the biofilm (a) and reactor (b) for S_o = 10 g L^{-1}; Run 1; A^* = 0.1 d^{-1}; D^* = 0.2 d^{-1}.

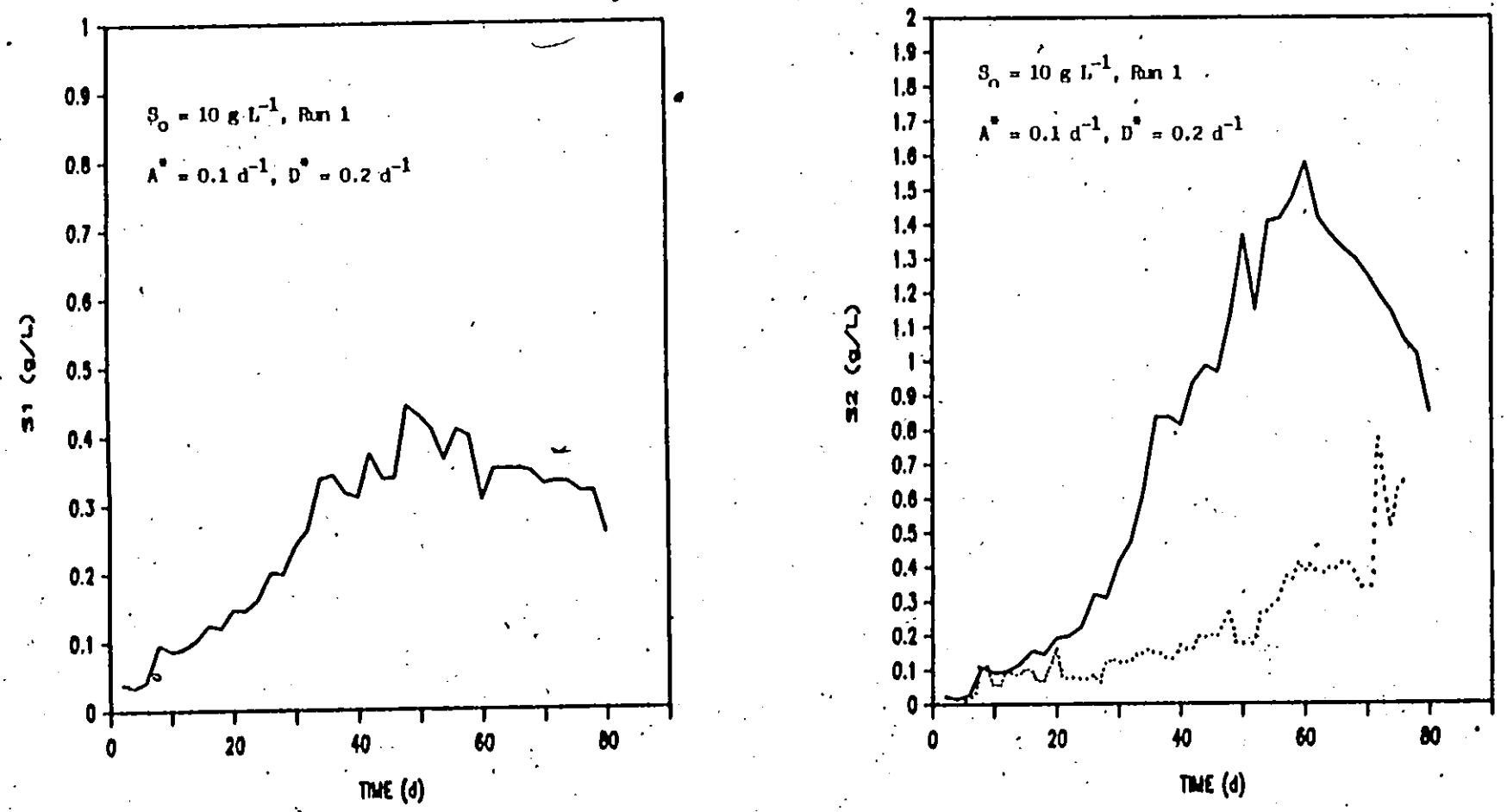

Figure C.4 Simulated primary (S1) and intermediate (S2) substrate concentrations in reactor for S_o = 10 g L^{-1}; Run 1; A^* = 0.1 d^{-1}; D^* = 0.2 d^{-1}, simulated (——), measured (····).

APPENDIX D

D1. Organic Carbon Mass Balance

Organic carbon mass balances were made during startup and steady state reactor operation. Organic carbon mass balances are useful because they give additional support to experimental data by acting as a cross-check mechanism. DSFF reactors behaved similar to a CSTR in terms of mixed liquor COD and it was assumed that biofilm samples were representative of the whole biofilm.

Mass balances on organic carbon during steady state DSFF reactor operation were assessed in the following manner: carbon in = soluble carbon (COD) in the effluent + insoluble carbon in the effluent + gaseous methane production + methane dissolved in the effluent + accumulated organic carbon in the DSFF reactor (biomass).

"Carbon in" was calculated by multiplying the influent COD concentration by the flow rate. "Carbon in" is expressed as g COD d^{-1} as are all other entries. "Soluble effluent carbon" and "insoluble effluent carbon" are the products of soluble COD and insoluble COD multiplied times the flow rate, respectively. "Gaseous methane production" was calculated by multiplying daily gas production by the percentage of methane as determined by gas chromatography, and then converting this quantity to its COD equivalent.

Methane can be converted to a COD equivalent by the relationship that at 0°C and one atmosphere, one gram of COD is equivalent to 350 mL of methane. This relationship can be further modified for temperature effects by the following gas law relationship between temperature and gas volume.

$$V_{stp} = V_t \frac{T_{stp}}{T_K}$$

where V_{stp} = Gas volume at standard temperature (0°C) and pressure (1 atm.)

V_t = Gas volume at operating temperature.

T_{stp} = Standard temperature in degrees Kelvin.

T_K = Temperature in degrees Kelvin.

Using the above relationship, one gram of soluble COD is equivalent to 394 mL of methane at 35°C assuming a standard pressure of one atmosphere.

"Methane in the effluent" describes rate of loss of dissolved methane in the effluent stream. The rate of loss of dissolved methane is the product of methane solubility at 35 °C and one atmosphere (0.032 L of methane (stp)L^{-1} of effluent; Switzenbaum, 1978) and waste flow in litres per day. This assumes that effluent is saturated with methane in solution. The volume of dissolved gas is then converted to its COD equivalent.

"Accumulated organic carbon" accounts for solids accumulating in the reactor. This was determined measuring the

difference between successive biofilm biomass measurements and then dividing by the number of days ,between measurements.

The sum of the five previously mentioned columns is equal to the "total carbon out" and is compared to "total carbon in".

Carbon balances during DSFF reactor startup were determined similarly to the above except that a daily cumulative mass balance was made.

A sample organic carbon balance calculation follows:

Organic carbon balance equation:

Carbon in = soluble carbon in effluent + insoluble carbon in effluent + gaseous methane production + methane dissolved in effluent + accumulated carbon in the DSFF reactor

EXAMPLE DATA: HRT = 0.7 d, S_o = 2.5 g L^{-1} COD

1. Carbon in : multiply influent substrate concentration by flow rate.

   2.5 g L^{-1} COD x 32 L d^{-1} = 80 g COD d^{-1}

2. Soluble carbon in effluent : multiply soluble effluent COD concentration by flow rate.

   0.515 g L^{-1} COD x 32 L d^{-1} = 16.5 g COD d^{-1}

3. Insoluble carbon in effluent: multiply soluble effluent COD by flow rate.

0.146 g L^{-1} COD x 32 L d^{-1} = 4.7 g COD d^{-1}

4. Gaseous methane production: multiply amount of gas produced by percent of methane; then convert to COD equivalent.

   29.0 L gas d^{-1} x 61 % methane = 17.7 L methane d^{-1}

   17.7 L methane d^{-1} = 44.9 g COD d^{-1}

   (1 gram COD equals 394 mL of methane)

5. Methane dissolved in effluent: multiply dissolved methane concentration by flow rate, effluent is saturated with dissolved methane at aconcentration of 32.8 mL methane L^{-1}

   0.0328 L methane L^{-1} x 32.8 L d^{-1} = 1.05 L methane (stp) d^{-1}

   1.05 L methane (stp) d^{-1} / 0.35 L methane g COD^{-1} = 3.0 g COD d^{-1}

6. Accumulated carbon in DSFF reactor: difference between two successive biofilm biomass measurements; then convert to COD equivalent

   at HRT = 1 d, S_o = 2.5 g COD L^{-1}, biomass = 3.19 g VFS L^{-1}; at HRT = 0.7 d, S_o = 2.5 g COD L^{-1}, biomass = 3.46 g VFS L^{-1}

   Difference = 0.27g VFS L^{-1}

   0.27 g VFS.L^{-1} x 1.42 g COD g VFS^{-1} x 22.4 L / 36 d = 0.24 g COD d^{-1}

Total COD in = #1 = 80 g COD d^{-1}

Total COD out = #2 + #3 + #4 + #5 + #6

= 16.5 + 4.7 + 45.0 + 3.0 + 0.24 = 69.4

Ratio In/Out = 80.0/69.4 = 1.14

APPENDIX E

E1. Determination of Biofilm Thickness

	TFS[1] g cm^{-3} biofilm	VFS[1] g cm^{-3} biofilm
	0.0515	0.0400
	0.0486	0.0363
	0.0441	0.0314
	0.0500	0.0383
	0.0620	0.0478
	0.0682	0.0527
	0.0600	0.0446
	0.0496	0.0382
	0.0543	0.0460
	0.0562	0.0428
	0.0676	0.0510
	0.0728	0.0578
	0.0577	0.4558
	0.0552	0.0428
average	0.0558	0.0443
standard deviation	0.0062	0.0048

[1] Based on 30 ml biofilm sample.

Biofilm thickness was calculated based on the average volatile solids mass per unit volume of biofilm. A sample calculation follows:

EXAMPLE DATA: HRT = 0.7 days, S_o = 2.5 g L^{-1} sucrose

Biofilm thickness = reactor VFS concentration divided by average volatile solids mass per unit volume of biofilm divided by reactor surface area to volume ratio.

L_f = 3.28 kg VFS m^{-3} / 44.3 kg VFS m^{-3} / 75 $m^2 m^{-3}$

L_f = 0.00097 m

APPENDIX F

F1. Measurement of Biofilm Methanogenic Activity During Startup

Time	Initial removal rate	Initial substrate concentration	Correlation coefficient
d	g acetate $L^{-1}d^{-1}$	g acetate L^{-1}	
		REACTOR A	
12	0.250	1.292	0.976
		k = 0.38 gCOD $gVFS^{-1}d^{-1}$	
19	0.170	0.051	0.997
	0.219	0.096	0.997
	0.278	0.135	0.995
	0.371	0.258	0.991
	0.380	1.280	0.998
		k = 0.40 gCOD $gVFS^{-1}d^{-1}$	
		K = 0.061 gCOD L^{-1}	
		Correlation coefficient = 0.999	
		ϕ' = 0.81	
26	0.667	1.342	0.991
		k = 0.67 gCOD $gVFS^{-1}d^{-1}$	
33	0.336	0.055	0.992
	0.409	0.093	0.989
	0.439	0.127	0.994
	0.823	0.241	0.991
	1.072	1.417	0.999
		k = 0.70 gCOD $gVFS^{-1}d^{-1}$	
		K = 0.173 gCOD L^{-1}	
		Correlation coefficient = 0.997	
		ϕ' = 1.21	
47	0.0460	0.051	0.990
	0.558	0.102	0.993
	0.623	0.141	0.993
	0.878	0.257	0.995
	1.644	1.379	0.979
		k = 0.96 gCOD $gVFS^{-1}d^{-1}$	
		K = 0.267 gCOD L^{-1}	
		Correlation coefficient = 0.994	
		ϕ' = 1.24	
60	0.323	0.052	0.991
	0.461	0.099	0.990
	0.602	0.135	0.998

	0.914	0.250	0.992
	2.832	1.305	0.997

k = 1.54 gCOD gVFS^{-1}d^{-1}
K = 0.945 gCOD L^{-1}
Correlation coefficient = 0.975
ϕ' = 1.27

73	0.392	0.045	0.994
	0.482	0.091	0.990
	0.647	0.128	0.986
	0.884	0.236	0.996
	2.802	1.390	0.984

k = 1.11 gCOD gVFS^{-1}d^{-1}
K = 0.687 gCOD L^{-1}
Correlation coefficient = 0.966
ϕ' = 0.1.52

86	0.432	0.049	0.994
	0.568	0.098	0.997
	1.048	0.137	0.996
	1.635	0.253	0.994
	3.330	1.335	0.985

k = 1.15 gCOD gVFS^{-1}d^{-1}
K = 0.569 gCOD L^{-1}
Correlation coefficient = 0.983
ϕ' = 1.89

REACTOR B

12	0.348	1.302	0.986

k = 0.43 gCOD gVFS^{-1}d^{-1}

19	0.164	0.024	0.996
	0.173	0.053	0.930
	0.246	0.097	0.969
	0.088	0.134	0.961
	0.388	0.260	0.991
	0.648	1.336	0.995

k = 1.06 gCOD gVFS^{-1}d^{-1}
K = 0.303 gCOD L^{-1}
Correlation coefficient = 0.922
ϕ' = 0.44

26	0.212	0.057	0.945
	0.222	0.081	0.998
	0.239	0.116	0.992
	0.403	0.193	0.990
	1.525	1.407	0.962

k = 1.15 gCOD gVFS^{-1}d^{-1}
K = 0.409 gCOD L^{-1}
Correlation coefficient = 0.956
ϕ' = 0.56

33	0.216	0.031	0.993
	0.274	0.063	0.985
	0.187	0.093	0.968
	0.312	0.109	0.985
	0.621	0.241	0.985
	2.049	1.309	0.998

$k = 1.59$ gCOD $gVFS^{-1}d^{-1}$
$K = 1.112$ gCOD L^{-1}
Correlation coefficient = 0.764
$\phi' = 0.88$

47	0.233	0.026	0.985
	0.377	0.044	0.990
	0.353	0.060	0.992
	0.405	0.082	0.997
	0.435	0.131	0.993
	0.727	0.220	0.974

$k = 0.94$ gCOD $gVFS^{-1}d^{-1}$
$K = 0.356$ gCOD L^{-1}
Correlation coefficient = 0.966
$\phi' = 1.23$

60	0.204	0.026	0.990
	0.332	0.042	0.944
	0.521	0.097	0.998
	0.524	0.128	0.994
	2.340	1.234	0.997

$k = 1.08$ gCOD $gVFS^{-1}d^{-1}$
$K = 0.483$ gCOD L^{-1}
Correlation coefficient = 0.977
$\phi' = 1.40$

73	0.232	0.024	0.986
	0.340	0.041	0.994
	0.396	0.068	0.995
	0.488	0.092	0.995
	0.490	0.128	0.992
	0.779	0.258	0.980
	2.330	1.392	0.987

$k = 1.15$ gCOD $gVFS^{-1}d^{-1}$
$K = 0.518$ gCOD L^{-1}
Correlation coefficient = 0.945
$\phi' = 1.29$

86	0.274	0.023	0.998
	0.338	0.041	0.996
	0.378	0.090	0.998
	0.524	0.137	0.991
	0.828	0.240	0.971
	1.905	1.244	0.909

$k = 0.94$ gCOD $gVFS^{-1}d^{-1}$
$K = 0.390$ gCOD L^{-1}
Correlation coefficient = 0.962
$\phi' = 1.30$

REACTOR C

12	0.448	1.265	0.994
		$k = 0.53$ gCOD $gVFS^{-1}d^{-1}$	
19	0.120	0.050	0.997
	0.209	0.107	0.989
	0.229	0.148	0.978
	0.319	0.271	0.991
	0.768	1.364	0.991
		$k = 1.52$ gCOD $gVFS^{-1}d^{-1}$	
		$K = 0.496$ gCOD L^{-1}	
	Correlation coefficient = 0.987		
		$\phi' = 0.38$	
26	1.281	1.406	0.998
		$k = 1.36$ gCOD $gVFS^{-1}d^{-1}$	
33	0.354	0.050	0.994
	0.411	0.100	0.997
	0.361	0.121	0.992
	0.395	0.249	0.997
	1.840	1.417	0.989
		$k = 1.73$ gCOD $gVFS^{-1}d^{-1}$	
		$K = 0.791$ gCOD L^{-1}	
	Correlation coefficient = 0.811		
		$\phi' = 0.76$	
47	0.320	0.049	0.993
	0.420	0.068	0.999
	0.448	0.122	0.994
	0.580	0.237	0.998
	1.524	1.665	0.976
		$k = 1.26$ gCOD $gVFS^{-1}d^{-1}$	
		$K = 0.340$ gCOD L^{-1}	
	Correlation coefficient = 0.987		
		$\phi' = 0.87$	
60	0.320	0.049	0.996
	0.524	0.076	0.992
	0.446	0.127	0.993
	0.625	0.248	0.995
	1.788	1.305	0.997
		$k = 1.27$ gCOD $gVFS^{-1}d^{-1}$	
		$K = 0.462$ gCOD L^{-1}	
	Correlation coefficient = 0.953		
		$\phi' = 0.99$	
73	0.408	0.066	0.994
	0.510	0.122	0.993
	0.718	0.146	0.989
	0.479	0.251	0.999

	2.190	1.411	0.993

$k = 1.42$ gCOD $gVFS^{-1}d^{-1}$
$K = 0.754$ gCOD L^{-1}
Correlation coefficient = 0.867
$\phi' = 0.97$

86	0.761	0.048	0.987
	0.918	0.073	0.887
	0.788	0.128	0.998
	1.032	0.240	0.994
	1.890	1.475	0.992

$k = 0.90$ gCOD $gVFS^{-1}d^{-1}$
$K = 0.163$ gCOD L^{-1}
Correlation coefficient = 0.993
$\phi' = 1.78$

F2. Measurement of Biofilm Methanogenic Activity During Steady State

HRT	Initial removal rate	Initial substrate concentration	Correlation coefficient
d	g acetate $L^{-1}d^{-1}$	g acetate L^{-1}	
	REACTOR 1 (2.5 g L^{-1} sucrose)		
4.4	0.340	0.042	0.950
	0.396	0.072	0.993
	0.600	0.186	0.993
	0.712	0.392	0.995
	0.876	0.582	0.987
	1.200	0.888	0.979

$k = 0.94$ gCOD $gVFS^{-1}d^{-1}$
$K = 0.221$ gCOD L^{-1}
Correlation coefficient = 0.959
$\phi' = 1.03$

2.0	0.370	0.060	0.991
	0.588	0.148	0.994
	1.134	0.326	0.998
	1.243	0.565	0.982
	1.604	0.921	0.921

$k = 1.18$ gCOD $gVFS^{-1}d^{-1}$
$K = 0.349$ gCOD L^{-1}
Correlation coefficient = 0.986
$\phi' = 1.14$

1.0	1.92	0.780	0.960
0.7	0.528	0.040	0.975
	0.744	0.111	0.995

	0.800	0.155	0.999
	1.353	0.341	0.994
	1.410	0.596	0.990

$k = 0.88$ gCOD $gVFS^{-1}d^{-1}$
$K = 0.145$ gCOD L^{-1}
Correlation coefficient = 0.986
$\phi' = 1.72$

0.5	0.754	0.144	0.995
	1.128	0.159	0.993
	1.248	0.311	0.992
	1.800	0.350	0.999
	1.764	0.875	0.999

$k = 1.01$ gCOD $gVFS^{-1}d^{-1}$
$K = 0.314$ gCOD L^{-1}
Correlation coefficient = 0.959
$\phi' = 1.76$

REACTOR 2 (5.0 g L^{-1} sucrose)

4.1	0.500	0.045	0.972
	1.02	0.093	0.985
	1.26	0.187	0.975
	1.08	0.377	0.992
	1.481	0.637	0.996
	1.760	0.963	0.995

$k = 1.08$ gCOD $gVFS^{-1}d^{-1}$
$K = 0.144$ gCOD L^{-1}
Correlation coefficient = 0.975
$\phi' = 1.66$

2.0	0.310	0.039	0.991
	0.460	0.100	0.990
	0.740	0.205	0.998
	1.330	0.396	0.997
	2.160	0.691	0.986
	3.403	1.113	0.989

$k = 1.67$ gCOD $gVFS^{-1}d^{-1}$
$K = 0.770$ gCOD L^{-1}
Correlation coefficient = 0.827
$\phi' = 1.25$

1.0	3.210	0.760	0.994

0.7	0.910	0.042	0.988
	1.000	0.140	0.990
	0.930	0.214	0.995
	1.450	0.401	0.994
	2.760	0.681	0.993

$k = 0.80$ gCOD $gVFS^{-1}d^{-1}$
$K = 0.405$ gCOD L^{-1}
Correlation coefficient = 0.781

$\phi' = 2.22$

0.5	0.63	0.087	0.996
	0.95	0.215	0.991
	1.13	0.318	0.999
	1.46	0.401	0.998
	2.42	0.655	0.996
	3.16	0.920	0.996

$k = 1.44$ gCOD $gVFS^{-1}d^{-1}$
$K = 1.469$ gCOD L^{-1}
Correlation coefficient = 0.723
$\phi' = 1.76$

REACTOR 3 (10 g L^{-1} sucrose)

4.0	0.979	0.085	0.997
	0.588	0.058	0.965
	0.867	0.148	0.975
	1.188	0.315	0.996
	3.768	0.580	0.949
	6.192	1.153	0.987

$k = 1.11$ gCOD $gVFS^{-1}d^{-1}$
$K = 0.350$ gCOD L^{-1}
Correlation coefficient = 0.914
$\phi' = 1.52$

2.0	1.152	0.115	0.988
	1.728	0.200	0.984
	4.200	0.646	0.991
	4.632	1.162	0.994

$k = 2.13$ gCOD $gVFS^{-1}d^{-1}$
$K = 0.626$ gCOD L^{-1}
Correlation coefficient = 0.986
$\phi' = 2.17$

1.0	2.088	0.905	0.997

0.7	0.192	0.046	0.999
	0.475	0.132	0.995
	0.548	0.156	0.990
	1.646	0.653	0.997

$k = 0.89$ gCOD $gVFS^{-1}d^{-1}$
$K = 0.345$ gCOD L^{-1}
Correlation coefficient = 0.993
$\phi' = 1.78$

0.5	0.619	0.179	0.944
	3.120	0.316	0.991
	4.201	0.590	0.984
	5.632	1.140	0.933

$k = 1.36$ gCOD $gVFS^{-1}d^{-1}$
$K_s = 0.536$ gCOD L^{-1}

Correlation coefficient = 0.998
$\phi' = 3.10$

REACTOR 4 (20 g L^{-1} sucrose)

7.0	0.192	0.040	0.999
	0.400	0.083	0.992
	0.528	0.178	0.996
	0.876	0.448	0.989
	0.364	0.643	0.938
	1.267	0.949	0.990

$k = 0.65$ gCOD $gVFS^{-1}d^{-1}$
$K = 0.237$ gCOD L^{-1}
Correlation coefficient = 0.643
$\phi' = 0.86$

4.0	0.436	0.062	0.982
	0.357	0.089	0.995
	0.588	0.181	0.997
	0.960	0.357	0.988
	0.871	0.580	0.995
	0.976	0.951	0.999

$k = 0.56$ gCOD $gVFS^{-1}d^{-1}$
$K = 0.146$ gCOD L^{-1}
Correlation coefficient = 0.989
$\phi' = 1.40$

F3. Measurement of Mixed Liquor Methanogenic Activity During Startup

Time	Initial removal rate	Initial substrate concentration	Correlation coefficient	k
d	g acetate $L^{-1}d^{-1}$	g acetate L^{-1}		*

REACTOR A

7	1.768	1.597	0.974	0.36
	1.811	1.670	0.988	0.45
11	1.989	1.924	0.938	0.55
	1.846	1.748	0.971	0.47
14	1.128	1.132	0.982	0.31
	0.727	1.454	0.999	0.13
18	0.272	1.499	0.976	0.37

	0.548	1.680	0.990	0.43
25	0.202	1.617	0.980	0.22
	0.405	1.701	0.985	0.36
32	0.013	1.790	0.808	0.02
	0.010	1.630	0.887	0.02
39	less than 0.02 g acetate L^{-1} d^{-1}			
46	less than 0.02 g acetate L^{-1} d^{-1}			
59	less than 0.02 g acetate L^{-1} d^{-1}			
72	less than 0.02 g acetate L^{-1} d^{-1}			
85	less than 0.02 g acetate L^{-1} d^{-1}			

* gCOD $gVSS^{-1}$ d^{-1}

REACTOR B

7	1.560	1.565	0.949	0.48
	1.608	1.600	0.949	0.43
11	0.655	1.853	0.943	0.45
	0.434	1.419	0.952	0.39
14	0.873	1.579	0.998	0.43
	1.488	1.435	0.996	0.75
18	0.784	1.621	0.988	0.66
	0.808	1.539	0.966	0.59
25	0.076	1.695	0.848	0.20
	0.093	1.846	0.863	0.22
32	0.011	1.832	0.831	0.02
	0.021	1.624	0.877	0.03
39	less than 0.02 g acetate L^{-1} d^{-1}			
46	less than 0.02 g acetate L^{-1} d^{-1}			
59	less than 0.02 g acetate L^{-1} d^{-1}			
72	less than 0.02 g acetate L^{-1} d^{-1}			
85	less than 0.02 g acetate L^{-1} d^{-1}			

REACTOR C

7	1.665	1.638	0.994	0.41
	1.809	1.816	0.999	0.45
11	1.192	1.740	0.989	0.47
	1.528	1.740	0.999	0.53
14	1.060	1.559	0.999	0.56
	1.135	1.733	0.996	0.61
18	0.518	1.681	0.987	0.37
	0.404	1.726	0.996	0.35
25	0.082	1.814	0.961	0.08
	0.144	2.048	0.881	0.15
32	0.039	1.952	0.824	0.05
	0.087	1.785	0.887	0.07
39	less than 0.02 g acetate L^{-1} d^{-1}			
46	less than 0.02 g acetate L^{-1} d^{-1}			
59	less than 0.02 g acetate L^{-1} d^{-1}			
72	less than 0.02 g acetate L^{-1} d^{-1}			
85	less than 0.02 g acetate L^{-1} d^{-1}			

Acidogenic and methanogenic mixed liquor and biofilm activity were evaluated based on the volumetric removal rate of sucrose and acetate respectively. The degradation curves were determined using least-squares linear regression. The slope of the curves represents the volumetric acetate or sucrose removal rate, expressed as g L^{-1} d^{-1}. The intercept determines the initial substrate concentration, expressed as g L^{-1}. The corresponding correlation coefficient is calculated. Maximum specific substrate utilization rates, k, and half velocity coefficients, K, were determined by using Eq. 3.49 and least squares linear regression. Both k and K

are expressed in terms of substrate COD. The corresponding correlation coefficient is also calculated. In some cases only k was determined. In these situations it was assumed that S in Eq. 3.48 was much larger than K and that U was independent of S, following zero order kinetics. Therefore U equals k.

Values of ϕ' were calculated by substituting the measured values of k, K and L_f into Eq. 3.12a. The diffusivity is assumed to be 80 % of the value reported for water. A sample calculation follows:

Steady state HRT 2.0 days; S_o = 5 g L^{-1} sucrose

1. A removable biofilm was placed in the activity test chamber (surface area to volume ratio, 50 m^2m^{-3}). Volumetric acetate removal rates were determined for different runs at various initial substrate concentrations.

Initial removal rate	Initial substrate concentration	Correlation coefficient
g acetate $L^{-1}d^{-1}$	g acetate L^{-1}	
0.31	0.039	0.991
0.46	0.100	0.990
0.74	0.205	0.998
1.33	0.396	0.997
2.16	0.691	0.986
3.40	1.113	0.989

2. Based on a 50 m^2m^{-3} surface area to volume ratio the biomass concentration is:

gVFS L^{-1} = 4.00 gVFS L^{-1} x (50 m^2m^{-3} / 75 m^2m^{-3})

Biomass concentration = 2.60 gVFS L^{-1}

3. To determine specific substrate utilization rate, U, divide volumetric substrate utilization by biomass concentration for each initial substate concentration.

U = 3.40 g acetate L^{-1} d^{-1} / 2.6 g VFS L^{-1}

= 1.307 g acetate g VFS^{-1} d^{-1}

4. Determine the value of S/U for each initial substrate concentration.

S/U = 1.113 g acetate L^{-1} / 1.307 g acetate g VFS^{-1} d^{-1}

= 0.851 g VFS d L^{-1}

S	U	S/U
g acetate L^{-1}	g acetate g VFS^{-1} d-1	g VFS d L^{-1}
0.039	0.119	0.327
0.100	0.177	0.565
0.205	0.285	0.719
0.396	0.511	0.774
0.691	0.830	0.832
1.113	1.307	0.851

5. Make a plot of S vs S/U.

5a) Slope = k^{-1} = 0.637

k = 1.56 g acetate g VFS^{-1} d

1 g acetate = 1.065 g COD.

Therefore k = 1.56 g acetate g VFS^{-1} d^{-1} x (1.065 g COD g $acetate^{-1}$) = 1.67 g COD g VFS^{-1} d^{-1}.

5b) Intercept = K k^{-1} = 0.461

K = 0.461 x 1.67

= 0.770 g COD L^{-1}.

5c) Correlation coefficient = 0.827

6. The apparent Thiele modulus, ϕ', is calculated from Eq. 3.21a.

$$\phi' = \left(\frac{1.67 \times 44.3 \times 0.122^2}{1.03 \times 0.80\ 0.770}\right)^{0.5}$$

$$= 1.25$$

APPENDIX G

G1. STEADY STATE REACTOR 1 So = 2.5 g/L sucrose

HRT d	DURATION d		CODs mg/L	CODis mg/L	VA acetic mg/L	VA propionic mg/L	VA butyric mg/L	BIOGAS L/d	METHANE %	BIOFILM BIOMASS g VFS/L	pH	Eh mV
4.4	39		105	100	55	35	10	5.0	77	2.30	7.6	-354
			105	165	55	35	10	4.8	80	2.04		
			110	125	40	20	10	4.8	82			
		average	106.7	130.0	50.0	30.0	10.0	4.9	79.7	2.17		
		std	2.36	26.77	7.07	7.07	0.00	0.09	2.05			
2.0	32		195	150	65	40	10	11.9	74	2.58	7.4	-350
			160	150	60	35	10	11.4	76	2.92		
			155	90	55	30	10	9.5	78			
		average	170.0	130.0	60.0	35.0	10.0	10.9	76.0	2.75		
		std	17.80	28.28	4.08	4.08	4.71	1.03	1.63			
1.0	36		260	200	145	50	10	25.8	71	3.33	7.1	-315
			280	200	85	60	10	21.6	67	3.05		
			345	215	175	80	10	24.6	65			
		average	295.0	205.0	135.0	63.3	10.0	24.0	67.7	3.19		
		std	36.29	7.07	37.42	12.47	0.00	1.77	2.49			
0.7	37		580	160	185	130	60	28.0	60	3.28	7	-330
			520	175	150	125	100	27.5	60	3.63		
			445	105	145	105	45	31.6	62			
		average	515.0	146.7	160.0	120.0	68.3	29.0	60.7	3.46		
		std	55.23	30.09	17.80	10.80	23.21	1.83	0.94			
0.5	30		1160	345	255	140	120	28.1	60	4.55	6.7	-340
			905	300	250	165	90	29.8	55	3.81		
			870	135	270	180	90	34.5	53			
		average	978.3	260.0	258.3	161.7	100.0	30.8	56.0	4.18		
		std	129.25	90.28	8.50	16.50	14.14	2.71	2.94			
0.4	17		1250	140	250	80		24.8	58		7.1	
			1350	505	310	135		30.9	59			
			970	225	415	205		33.7	62			
		average	787.7	290.0	325.0	140.0		29.8	59.7			
		std	160.83	155.94	68.19	51.15		3.72	1.70			

APPENDIX G

G2. STEADY STATE REACTOR 2 So = 5.0 g/L sucrose

HRT d	DURATION d		CODs mg/L	CODis mg/L	VA acetic mg/L	VA propionic mg/L	VA butyric mg/L	BIOGAS L/d	METHANE %	BIOFILM BIOMASS g VFS/L	pH	Eh mV
4.1	39		135	490	60	10	10	13.5	59	2.83	7.6	-350
			110	250	75	40	10	14.2	64	2.53		
			110	250	75	40	10	14.7	64			
		average	118.3	330.0	70.0	30.0	10.0	14.1	62.3	2.68		
		std	11.79	113.14	7.07	14.14	0.00	0.49	2.36			
2.0	32		575	380	145	180	10	30.9	54	4.00	7.1	-340
			625	405	145	200	10	36.8	54	3.50		
			510	435	160	195	10	34.4	54			
		average	570.0	406.7	150.0	191.7	10.0	34.0	54.0	3.75		
		std	47.08	22.48	7.07	8.50	4.71	2.42	0.00			
1.0	36		1130	730	220	330	70	45.0	54	4.10	6.9	-320
			1020	570	235	305	50	48.0	53	5.97		
			1105	590	165	200	30	46.0	52			
		average	1085.0	630.0	206.7	278.3	50.0	46.3	53.0	5.035		
		std	47.08	71.18	30.09	56.32	16.33	1.25	0.82			
0.7	37		2155	660	455	530	70	76.0	44	7.40	6.8	-340
			2085	415	435	540	70	76.5	43	6.43		
			2150	380	495	610	70	69.6	44			
		average	2130.0	485.0	461.7	560.0	70.0	74.0	43.7	6.92		
		std	31.89	124.57	24.94	35.59	0.00	3.14	0.47			
0.5	30		2655	480	520	530	130	72.5	47	8.37	7.2	-320
			2290	555	585	490	95	69.3	47	7.37		
			2255	440	520	480	135	68.2	47			
		average	2400.0	491.7	541.7	500.0	120.0	70.0	47.0	7.87		
		std	180.88	47.67	30.64	21.60	17.80	1.82	0.00			

APPENDIX G

G3. STEADY STATE REACTOR 3 So = 10.0 g/L sucrose

HRT d	DURATION d		CODs mg/L	CODis mg/L	VA acetic mg/L	VA propionic mg/L	VA butyric mg/L	BIOGAS L/d	METHANE %	BIOFILM BIOMASS g VFS/L	pH	Eh mV
4.0	39		380	750	215	40	10	36.6	61	4.03	7.5	-282
			420	640	215	40	10	30.7	57	3.60		
			350	720	140	45	10	43.0	61			
		average	383.3	703.3	190.0	41.7	10.0	36.8	59.7	3.815		
		std	20.67	46.43	35.36	2.36	0.00	5.02	1.89			
2.0	32		1345	580	475	130	90	73.5	56	5.54	7.3	-320
			1335	505	560	145	90	65.9	56	4.85		
			1310	350	585	170	70	69.6	56			
		average	1330.0	461.7	540.0	148.3	83.3	69.7	56.0	5.195		
		std	14.72	79.62	47.08	16.50	38.59	3.10	0.00			
1.0	36		2650	830	920	290	130	108.0	55	5.55	6.8	-330
			2450	750	940	260	90	99.2	56	4.51		
			2280	1030	890	265	140	104.9	54			
		average	2460.0	870.0	916.7	271.7	120.0	104.0	55.0	5.03		
		std	151.22	117.76	20.55	13.12	21.60	3.64	0,82			
0.7	37		4650	490	845	405	605	118.0	43	7.75	6.8	-320
			5140	695	950	420	595	112.0	43	8.85		
			2480	2190	845	280	480	121.0	47			
		average	4090.0	1125.0	880.0	368.3	560.0	117.0	44.3	8.30		
		std	1155.88	757.70	49.50	62.76	56.72	3.74	1.89			
0.5	30		4170	1250	1270	355	230	147.0	40	9.20	6.6	-320
			4585	1525	1260	405	345	160.2	43	8.21		
			4375	1210	1450	460	325	145.8	49			
		average	4376.7	1328.3	1326.7	406.7	300.0	151.0	44.0	8.705		
		std	169.43	140.02	87.31	42.88	50.17	6.52	3.74			

1 COD and VA values rounded to nearest 5 mg/L

APPENDIX G

G4. STEADY STATE REACTOR 4 So = 20.0 g/L sucrose

HRT d	DURATION d		CODs mg/L	CODis mg/L	VA acetic mg/L	VA propionic mg/L	VA butyric mg/L	BIOGAS L/d	METHANE %	BIOFILM BIOMASS g VFS/L	pH	Eh mV
7.0	39		970	1400	140	225	10	33.0	58	2.46	7.5	-344
			695	975	120	175	10	34.2	58	3.20		
			735	1435	165	125	10	38.0	56			
		average	800.0	1270.0	141.7	175.0	10.0	35.1	57.3	2.83		
		std	121.31	209.09	18.41	40.82	0.00	2.13	0.94			
4.0	32		4250	1595	480	1450	80	59.0	52	3.30	7.2	-340
			3960	2010	420	1440	145	55.6	53	4.65		
			3785	1790	300	1305	80	58.5	57			
		average	3998.3	1798.3	400.0	1398.3	101.7	57.7	54.0	3.975		
		std	191.76	169.53	74.83	66.12	59.30	1.50	2.16			
2.0	36		8660	2930	1530	3610	130	88.0	40	6.63	6.3	-340
			9400	2300	1320	3530	140	83.0	39	8.25		
			8100	2780	1305	3450	150	92.2	40			
		average	8720.0	2670.0	1385.0	3530.0	140.0	87.7	39.7	7.44		
		std	532.42	268.70	102.71	65.32	8.16	3.76	0.47			
1.0		Reactor failed a 1.0 d HRT. Final VA reading shown.			3970	4815	410					

1 COD and VA values rounded to nearest 5 mg/L